A Straight-in Approach to Flight Dynamics

Motions in Two Spatial Dimensions

1. B SHAYAK

2. SARTHAK GIRDHAR, SUNANDAN MALVIYA

Equal second authorship : SUNANDAN and SARTHAK contributed equally and may be listed in any order in any place where this Article is cited

SHAYAK : Department of Mechanical Engineering, University of Maryland, College Park – 20742, Maryland, USA. Corresponding author. Email : sbhatta4@umd.edu, shayak.2015@iitkalumni.org ORCID : 0000-0003-2502-2268

SUNANDAN : Department of Physics, Indian Institute of Science Education and Research Bhopal, Bhopal Bypass Road, Bhauri, Bhopal – 462066, Madhya Pradesh, India. Email : sunandan21@iiserb.ac.in

SARTHAK : Department of Physics, Indian Institute of Technology Bombay, Powai, Mumbai – 400076, Maharashtra, India. Email : 215120026@iitb.ac.in

Monday May Day 2023

----- o -----

Keywords. Explicit nonlinear equation of motion Equilibria, stability, characteristics Flight simulations Analysis of manoeuvres Analysis and prevention of accidents and incidents

Word counts. Grand total – 103927

---- o ---- o ---- o ---- ---- o ---- o ---- o ----

ABSTRACT

In this Article we present a new approach to flight dynamics which unifies the perspectives and requirements of the aerospace engineer and the pilot. In the process, we also present a comprehensive course on aviation to non-specialists who are fascinated by flying and possess the mathematical training to understand it quantitatively. We begin with a Chapter describing the components of an aircraft as well as the basics of navigation and communication. In the next Chapter we use the principles of classical mechanics, combined with the momentum theory of lift and drag, to derive a closed-form nonlinear dynamical model of an aircraft. Restricting ourselves for conceptual and technical simplicity to motions in two spatial dimensions, we treat separately the planes of pitch, yaw and bank, writing a sixth order system in each plane. Among these, the pitch plane equations are of the greatest significance. In the following Chapter we analyse the model equations to obtain the modes of motion and their stabilities as well as pilot-induced oscillations. We also introduce the characteristic curves, which are plots of fixed point or steady state solutions as one or more parameters are varied. This prepares us for the climactic Chapter in which we use the model to construct a flight simulator and demonstrate a variety of manoeuvres including takeoff, landing, vertical loops, coordinated turns and flight with non-functional control surfaces. Extensive calculation and discussion show us how to maximize safety during each phase of flight, and set the simulation results against the backdrop of actual aviation accidents and incidents. Overall, the model-based simulations combine the theoretical approach of the engineer with the hands-on approach of the pilot; this combination should enhance pilots' technical training and can potentially improve aviation safety by mitigating accidents and incidents. We hope that our work may prove as useful for the university as it does for the flying school; if in addition it opens for the eager explorer the portals to the fascinating world of aviation, then our mission in writing this Article will be wholly accomplished.

---- o ----

TABLE OF CONTENTS

We have opted for quite detailed Section headings, so that a glance through the contents can give you an idea of the topics which we will cover. We have further implemented the entire Table of Contents as bookmarks in the pdf – please use those for easy navigation.

Title 1
Abstract 2
Table of contents 3
List of symbols 6
List of abbreviations and acronyms 8
Numbering conventions 10
Copyright and other statements 10

Chapter 1 : Aims and Scope

O. This Chapter has no Subdivisions 12
§01 The Literature 12
§02 Flight dynamics Quiz 14
§03 Outline, novelty, learning objectives and prerequisite requirements 18
§04 Presentation style, change of narrative voice 20

Chapter 2 : Aviation, Navigation and Communication

A. Aircraft components, operating variables and units 21
§05 Primary components of an aircraft 21
§06 Additional components 29
§07 Operational quantities, system of units 30
§08 Types of pilot, roles of the two pilots 35
§09 Environmental impact of aviation 35
B. Introduction to navigation 36
§10 VFR or visual flight rules – course maintenance 36
§11 VFR – departures and arrivals 37
§12 IFR or instrument flight rules – course maintenance 38
§13 IFR – departures and arrivals 41
§14 STAR and SID example – John F Kennedy International Airport 44
C. Rudiments of communication 49
§15 Spelling alphabet, airport and airline codes 49
§16 Good communication practices 51

Chapter 3 : The Aircraft Dynamic Model

A. Axes and angles, lift and drag 54
§17 Axis and angle conventions – full treatment 54
§18 Axis and angle conventions – simplified treatment 56
§19 Different theories of lift 59
§20 Momentum theory of lift, drag 61
§21 Aerodynamic stall 66
B. Pitch plane equations of motion 67
§22 Geometry, variables and parameters 67
§23 The horizontal tail or elevator (stabilator) 67
§24 Forces and torques 70
§25 The xyz model 73

§26 The qdo model . . . 73
§27 The space vector model . . . 74
§28 Interpretation of the space vector model . . . 74
§29 Model in some special situations . . . 76
C. Yaw and banking plane equations of motion . . . 78
§30 Yaw plane equations of motion . . . 78
§31 Banking plane equations of motion . . . 80
D. Chapter conclusion . . . 81
§32 Limitations of yaw and banking plane models, concluding remarks to Chapter 3 . 81

Chapter 4 : Stability and Characteristic Curves

O. This Chapter has no Subdivisions . . . 82
§33 Static stability, difference between one- and two-piece tails, CM position limits . 82
§34 Modes of motion and their stabilities . . . 84
§35 Pilot-induced oscillation . . . 89
§36 Characteristic curves and their interpretation, normal and reversed command . . 93

Chapter 5 : Flight Simulations

A. The Academic flight simulator . . . 100
§37 Description of the simulator . . . 100
§38 Characterization of the short period and phugoid modes . . . 101
§39 Structure of the following Subdivisions . . . 103
B. Takeoff . . . 105
§40 Description . . . 105
§41 Planning – calculation of the V-speeds . . . 105
§42 Execution . . . 109
§43 Further discussion, accidents and incidents . . . 113
C. Immelmann turn . . . 116
§44 Immelmann turn . . . 116
D. Landing . . . 120
§45 Description . . . 120
§46 Planning – calculation of the approach and flare . . . 121
§47 Execution . . . 124
§48 Perfecting the approach – velocity ratio . . . 128
§49 Types of flare, bounce and shimmy . . . 133
§50 Further discussion, accidents and incidents . . . 140
E. Coordinated turns . . . 144
§51 Turn coordination . . . 144
F. Simple stall . . . 148
§52 Approach to the stall . . . 148
§53 Stall . . . 151
§54 Recovery from stall . . . 153
§55 Further discussion, accidents and incidents . . . 155
G. Banking plane dynamics . . . 161
§56 Why don’t we feel a banked turn ? . . . 161
§57 Further discussion . . . 163
H. Pugachev cobra . . . 164
§58 Description . . . 164
§59 Design of the aircraft . . . 165
§60 Execution . . . 166

J. Elevator fault 168
§61 Description 168
§62 Planning – basics of approach and flare 169
§63 Planning – calculation of waypoints on the flight path 172
§64 Execution 176
§65 Further discussion, accidents and incidents 181
K. Chapter conclusion 183
§66 Concluding remarks to Chapter 5 183

Chapter 6 : Conclusion and Future Directions

O. This Chapter has no Subdivisions 185
§67 Summary of contributions 185
§68 Future directions 186
§69 Conclusion 188
Answers to the quiz questions 189
References 190

LIST OF SYMBOLS

$\dot{a}$	—	da/dt (a is any variable)
B	—	The centre of mass of the aircraft
C	—	The centre of pressure of the wings
C	—	The nonstall drag constant of the aircraft
C_1	—	The additional drag constant in stall
C_D	—	The coefficient of lift in Literature theories of flight dynamics
C_L	—	The coefficient of drag in Literature theories of flight dynamics
C_m	—	The coefficient of elevator moment in Literature theories flight dynamics
C_w	—	The drag constant
$\mathcal{C}$	—	A damping coefficient
d	—	The direct axis, running from the tail to the nose
d_1	—	The signed d-axis distance from the centre of mass to the wings' centre of pressure
$\bar{d_1}$	—	The negative of d_1
d_2	—	The signed d-axis distance from the centre of mass to the elevator
$\bar{d_2}$	—	The negative of d_2
d_3	—	The signed d-axis distance from the centre of mass to the point of action of stall drag
E	—	The tail
f_{ex}	—	An external force applied to provide a centripetal acceleration
f_p	—	The force applied at the elevator
$\bar{f_p}$	—	The negative of f_p
f_w	—	The force applied at the rudder
g	—	The acceleration due to gravity
h	—	The signed o-axis distance from the centre of the mass to the line of action of the thrust
$\bar{h}$	—	The negative of h
I	—	The moment of inertia of the aircraft about the quadrature axis
I_r	—	The moment of inertia of the aircraft about the direct axis
I_w	—	The moment of inertia of the aircraft about the orthogonal axis
j	—	The imaginary unit $\sqrt{-1}$
k	—	A spring constant
K_C	—	The lift constant of the wings
k_E	—	The lift constant of the elevator
k_R	—	The lift constant of the rudder
k_S	—	The lift constant of the vertical stabilizer
m	—	The mass of the aircraft
o	—	The orthogonal axis, vertical when the aircraft is horizontal
q	—	The quadrature axis, perpendicular to the direct axis and in the plane of the wings
q_1	—	The signed q-axis distance from the centre of mass to the centre of pressure of the wing
S	—	A distance
t	—	The time
$\mathbf{U}$	—	The velocity vector of the wind (or an airflow) relative to the ground frame
$\mathbf{V}$	—	The velocity vector of the aircraft relative to the ground frame
V	—	The ground speed
$\mathbf{V}_E$	—	The velocity vector of the tail relative to the ground frame
w	—	The signed q-axis distance from the centre of mass to the line of action of the thrust
x	—	One of three axes in the ground frame, in the horizontal plane
y	—	The second of three axes in the ground frame, in the horizontal plane
z	—	The last of three axes in the ground frame, directed vertical
α	—	The angle of attack
α_E	—	The angle of attack of the elevator
$\bar{\alpha_E}$	—	The negative of α_E

α_S	—	The stall angle of attack
Δ	—	An increment
δ	—	The deflection of the horizontal stabilizer
$\overline{\delta}$	—	The negative of δ
ε	—	A parameter in the momentum theory of lift
Γ	—	The damping constant for quadrature axis rotational motions
Γ_r	—	The damping constant for direct axis rotational motions
Γ_w	—	The damping constant for orthogonal axis rotational motions
γ	—	The camber of the wings
λ	—	An eigenvalue or a root
φ	—	The angle of yaw made by the aircraft
φ_E	—	The angle of yaw made by the rudder
θ	—	The angle of pitch made by the aircraft
θ_E	—	The angle of pitch made by the horizontal tail
ψ	—	The angle of bank made by the aircraft
τ	—	EITHER torque OR a time delay or interval
ω	—	The angular velocity of the aircraft in the pitch plane
ξ	—	The angle of azimuth made by the aircraft's trajectory
η	—	The angle of elevation made by the aircraft's trajectory

LIST OF ABBREVIATIONS AND ACRONYMS

AC	—	Aerodynamic centre
APU	—	Auxiliary power unit
ATC	—	Air traffic control
ATPL	—	Air transport pilot’s licence
ATS	—	Air traffic service
CAD	—	Computer aided design
CM	—	Centre of mass
CP	—	Centre of pressure
CPL	—	Commercial pilot’s licence
CVR	—	Cockpit voice recorder
DDE	—	Delay differential equation
DME	—	Distance measuring equipment
EPR	—	Engine pressure ratio
F###	—	Flight level ### (where # denotes a digit)
FADEC	—	Full authority digital engine control
FBW	—	Fly-by-wire
FDR	—	Flight data recorder
GA	—	General aviation
GPS	—	Global positioning system
GPU	—	Ground power unit
IATA	—	International Air Travel Agency
ICAO	—	International Civil Aviation Organization
IFR	—	Instrument flight rules
IMC	—	Instrument meteorological conditions
ILS	—	Instrument landing system
L/D	—	Lift-to-drag ratio
LHS	—	Left hand side
MCAS	—	Maneuvering (sic) characteristics augmentation system (on Boeing 737 MAX)
MSL	—	Mean sea level
MTOW	—	Maximum takeoff weight
N1	—	Rotation rate of the low pressure rotor
OEW	—	Operating empty weight
PAPI	—	Precision approach path indicator
PPL	—	Private pilot’s licence
RHS	—	Right hand side
RNAV	—	Area navigation
RVSM	—	Reduced vertical separation minima
SID	—	Standard instrument departure
STAR	—	Standard terminal arrival route
TCAS	—	Traffic collision avoidance system
TOGA	—	Takeoff / go-around
UAV	—	Unmanned air vehicle
V_1	—	The takeoff decision speed
V_2	—	The best climb gradient speed
V_{mca}	—	The minimum controllable speed in air
V_{mcg}	—	The minimum controllable speed on ground
V_{mu}	—	The minimum unstick speed
V_r	—	The rotation speed
V_{ref}	—	The landing speed
V_s	—	The stall speed

V_z/V	—	The ratio of climb or descent rate to ground speed
VFR	—	Visual flight rules
VGSI	—	Visual glideslope indicator
VOR	—	Very high frequency omnidirectional range

NUMBERING CONVENTIONS

This Article is composed of six Chapters numbered 1 to 6. The longer Chapters are broken up into Subdivisions labelled as A, B, C etc. Each equation, figure, table and reference has a four-character identifier, of the form NL–NN where "N" denotes a number and "L" a letter. The first two characters refer to the Chapter and Subdivision while the last two to the number within the Subdivision. If a Chapter has no Subdivisions, we use the letter "O" in the second place. Thus, the twenty second equation in Subdivision 3B has the identifier 3B–22. Within the concerned Subdivision however, we omit the first two characters and use only the last two characters to refer to the object. Thus, in Subdivision 3B itself, the equation 3B–22 will be referred to as plain "22". For your convenience, we provide the Subdivision number on the top of each page. For equations, we write the identifier within parentheses, for references within box brackets, for figures we precede the identifier by the word "Fig." and for tables we precede the identifier by the word "Table". Subdivisions are further broken up into Sections – the numbers of these run continuously since their succession presents a plot-line which runs across Subdivision and Chapter boundaries.

COPYRIGHT AND OTHER STATEMENTS

This Article represents original research done by us authors. It is free to download, read, share, distribute and use for non-commercial purposes. Please however make sure to cite this Article if you use any results contained herein, in any forum including but not limited to academic publications, websites and training materials. At this time, codes are available on demand. To access them, please email any of us stating the reason why you are asking for access. We will comply with the request after assessing its legitimacy. For the following two commercial uses of the content of this Article – (*a*) implementation of a cockpit instrument based on results obtained herein, and (*b*) incorporation of the material in the curriculum of for-profit educational institutions – please contact us via email. All other commercial uses of this Article in whole or in part, including but not limited to sale of printed copies at a price above the printing cost, and sale of flight simulators based on equations derived herein, are unconditionally prohibited.

We have not been funded by any individual or any agency, public or private, to undertake this study. As such, the question of competing interests does not arise. It is a fact that aircraft are manufactured by a tiny handful of corporations and sold for profit to a larger handful of corporations who operate them again for profit. An Article on aviation which makes no reference to commercial manufacturers and airlines will not be realistic. In all our mentions of commercial entities relating to aviation, nowhere do we state, intend to state, or imply a preference for any one entity vis-a-vis a competitor. In our discussions of aviation safety, we have referred to a small sample of aviation accidents which have occurred in the past few decades. This sample has been picked arbitrarily from the database of historical accidents of each type. Our act of selection does not intend to state or imply that the airlines or aircraft models mentioned in this context are less safe than airlines or models which have not been mentioned. If in future we receive funding for extension of this study, then we will mention in this space the name of the funding agency and the manner if any in which the funder has influenced the contents of the Article.

---- o ----

"Now, wait a minute. A story goes with it."

– THOMAS WILHELM KOERNER, "Fourier Analysis"
himself quoting DAMON RUNYON

"And now, folks, we tell a story."

– RICHARD STOLTZMAN, referring to WOLFGANG AMADEUS
MOZART's Trio for clarinet, viola and piano, K498

1

AIMS AND SCOPE

Like many prefatory Chapters, this one is partly intended for readers who are familiar with aircraft dynamics and are evaluating our Article in comparison with Literature items. Hence, we have freely used technical concepts and jargon here. If you are new to the subject and find this confusing or overwhelming, then please go ahead to Chapter 2 and come back here only later. If on the other hand you are willing to suspend your non-understanding and get a summary of our objective and outline, then you are welcome to continue with what follows.

§01 **The Literature.** There are three classes of audience for any work on aircraft dynamics. First is the aerospace professionals in academia and industry who work on research and development of aircraft and aircraft systems. Second is the pilots who actually fly the aircraft and the flight instructors who train them to do so. Third is the students and faculty of academic institutions, not formally trained in aerospace engineering, who are nonetheless fascinated by aviation and are in a position to understand the subject quantitatively. Existing literature on flight dynamics presents widely disparate portrayals of the subject to the first two audiences, while almost completely neglecting the third.

The largest amount of academic work on flight dynamics caters to aerospace engineers in a university setting. The first item of this class was “Stability in Aviation” written by the British applied mathematician GEORGE BRYAN in 1911 [01]; the technical content appears nearly verbatim in modern textbooks on the subject, a few of which we shall list shortly. In these works, two broad approaches can be distinguished. The first is a top-down approach as given by BRYAN himself and emulated countless times [02-09]. This begins with the equations of motion of the aircraft in three spatial dimensions. On the left hand side (LHS) these equations feature the standard Newtonian terms for translational and rotational acceleration. On the right hand side (RHS) they involve functions such as lift coefficient $C_L(\ldots..)$, drag coefficient $C_D(\ldots..)$, and control surface force or torque $C_m(\ldots..)$ where the arguments include velocity, pitch, angle of attack, control surface deflection and optionally other variables as well. These equations are then linearized, the suitable derivatives of the unknown functions taken from tables of experimental or numerical data, and the modes of motion determined together with their stabilities. Among these modes are short period, phugoid and Dutch roll.

The second approach to academic flight dynamics is bottom-up [10-20], starting from theoretical treatments of lift and drag. These are followed by a discussion of the aircraft’s performance, such as the power curves and the runway lengths required for takeoff and landing. Subsequently introducing the concepts of stability and control, the bottom-up approach goes on to the equations of motion first in two and then in three dimensions. These equations have the same structure as in the top-down approach, and lead to the same linearized analysis of the normal modes. In easier bottom-up treatments, the presentation concludes part way into the approach. Of course, top-down and bottom-up is a simple classification scheme and not every work on flight dynamics can be thrown into this or that bin. Nevertheless, the patterns fit a large amount of the university-centric aircraft dynamics literature. A feature common to these treatments is the absence of concepts and jargon associated with flight operations – it is not unusual to find cursory or zero references to the pilot and how s/he actually flies the airplane. Concurrently, jargon related to operation of aircraft is also absent.

In the case of BRYAN’s pioneering work, this absence is easy to understand. When he wrote it, aircraft had been in existence for all of eight years. Let him explain it in his own words : “There seems a general desire on the part of many writers to minimize the dangers of instability or defective stability and to attribute accidents to other causes. But in reading the accounts of accidents, both fatal and otherwise,

that appear every few days in the daily papers, it is difficult to avoid coming to the conclusion that much of this loss of life and damage could be avoided by a systematic study of stability and certain other problems regarding the motion of airplanes particularized in this book." At that time, it was of the essence to prevent the plane from falling out of the sky; mathematically perfecting takeoffs and landings were luxuries that one could ill-afford. The absence of this topic from subsequent works, written when aviation was a mature field, can perhaps be attributed to jumping onto the BRYAN bandwagon. Indeed, a couple of mathematical errors made by BRYAN had to wait for a century before being corrected, by N ANANTHKRISHNAN and colleagues [19-21].

A smaller amount of literature on flight dynamics caters to those who will use it practically i.e. the pilots. The pioneering work here is by WOLFGANG LANGEWIESCHE, who published his book "Stick and Rudder" (in English) in 1944 [22]. Subsequent works [23-29] follow his cue to a greater or lesser extent. The mathematical level in these works is vastly simpler than in those intended for engineers. The treatment is more practical, with frequent references to the control actions needed by the pilot. Operational jargon is also introduced. Despite the practical slant, the reduced dependence on mathematics ends up restricting the scope of the treatment. As one example of this, consider the discussion of "the airplane's gaits" by LANGEWIESCHE himself – six of the eight 'gaits' he mentions are in fact different cases of the same steady state pitch plane motion. Sometimes, the prescriptions of the required pilot actions – for instance the technique of the landing flare – appear like given facts rather than logical consequences of the dynamics. Detailed analyses of individual flight phases or manoeuvres, such as the simulation of a takeoff for a particular aircraft, remain outside the scope of such works. Pilots learn these nitty-gritties only after completing the on-ground training and stepping inside the simulator or the cockpit behind the flight instructor.

Just as we looked at BRYAN's own view of the topic, let's also look at LANGEWIESCHE's. "What is wrong with the theory of flight, from the pilot's point of view, is not that it is theory. What's wrong is that it is the theory of the wrong thing – it usually becomes a theory of building the airplane rather than of flying it. It goes deeply – much too deeply for the pilot's needs – into the theory of aerodynamics; it even gives the pilot a formula by which to calculate his lift. But it neglects those phases of flight that interest the pilot most." The theory which LANGEWIESCHE was referring to was still BRYAN's theory of stability, which indeed caters to aircraft design rather than operation for reasons that we've seen before. LANGEWIESCHE presents his own intuitive and entirely qualitative treatment of flight dynamics, going as far as one can go without taking recourse to mathematical equations. In the absence of a later theory of the flight phases that interest the pilot most, later authors have also towed the LANGEWIESCHE line.

As for the non-specialist student or faculty who is enthusiastic about aviation and wants to learn about it in a technical way, neither of the above classes of work is particularly suitable. Materials aimed at engineers either presuppose knowledge of the elements of an aircraft on the reader's part or cover it in a very short space. Materials aimed at pilots appear too non-technical and obsessed with vocabulary or phraseology. One resource which tries to cater to this audience is the NASA Glenn article series on aviation [30]. Although these materials are excellent, they cater primarily to high school students and are liable to be found elementary by someone wishing for a more in-depth treatment. A lot of practical knowledge regarding planes and flying can also be found on websites and discussion forums maintained by aviation enthusiasts; the majority of this knowledge tends to be qualitative in character.

To better illustrate the divergent perspectives of the university and flight school aircraft dynamics curriculum, we give in the next Section a 20-question quiz on the subject. The first ten questions relate to basic aspects of aircraft operation which are bread and butter for pilots but might be unfamiliar to students of even an advanced theoretical course. The next ten questions relate to more advanced aspects of operation which pilots learn from experience in the air but not (at least routinely) as part of ground training. These questions draw on the syllabus of the theoretical course, but might still be outside its scope on account of the way it is presented. Of course, we don't include meaningless questions, such asking the engineer whether the ICAO code for the letter W is wander, whiskey, winglet or wombat, or asking the pilot whether the stability of the aircraft is determined by the D'Alambertian, Hessian, Jacobian or Wronskian.

§02 **Flight dynamics Quiz.** Here is the Quiz which highlights the difference between flight dynamics from the engineers' and pilots' viewpoints.

QUIZ

This Quiz contains 20 questions. Each question has four answer choices out of which only one is correct. Wherever necessary or appropriate, assume an aircraft with performance and handling characteristics similar to a modern passenger airliner. Assume further that the autopilot and autothrottle are inactive, unless explicitly stated otherwise in the question.

Q01 The picture alongside shows a photograph of an aircraft. Assuming that there is no distortion of pitch, the aircraft has been captured



A. Shortly after takeoff
B. During cruise
C. Shortly before landing
D. Cannot be determined from the information given

Q02 Which of the following describes the conventional position of the centre of mass of the aircraft with respect to the centre of pressure of the wings ?

A. The centre of mass is forward of the centre of pressure
B. The centre of mass is aft of the centre of pressure
C. The centre of mass is coincident with the centre of pressure
D. The centre of mass changes position during different phases of flight

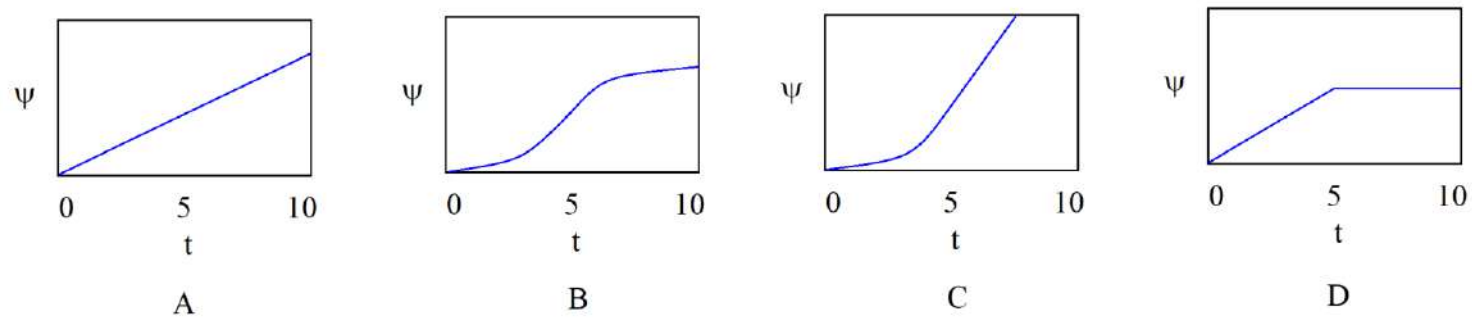
Q03 On a breezy day in New York City, the wind is blowing from the South-East. If wind is the only factor determining the traffic flow, which of the following runway allocations will be in place at John F Kennedy International Airport ?

A. 13L for arrivals, 13R for departures
B. 13L for arrivals, 31L for departures
C. 31R for arrivals, 13R for departures
D. 31R for arrivals, 31L for departures

Q04 If an aircraft enters a stall, the recovery procedure involves applying

A. Idle thrust and nose-down elevator input
B. Idle thrust and nose-up elevator input
C. Full thrust and nose-down elevator input
D. Full thrust and nose-up elevator input

Q05 With the aircraft at zero bank, the starboard aileron is extended for five seconds and then retracted. Which of the following is the closest approximation to the bank angle ψ as a function of time t ?



Q06 A typical thrust-to-weight ratio (TOGA/MTOW) is

A. 10 percent
B. 25 percent
C. 60 percent
D. 100 percent

Q07 Assuming that there are no knock-on equipment failures, which of the following technical malfunctions occurring at 15,000 ft of altitude is most likely to result in an accident ?

A. One out of two engines fails
B. The elevator and stabilizer trim fail
C. The vertical stabilizer and rudder are shorn off
D. An explosion blows a 6 ft diameter hole in the fuselage

Q08 For a particular departure, the onboard computer calculates a takeoff thrust of 92 percent N1 when the runway is dry. Due to a rainstorm, the runway contains standing water when the takeoff clearance is actually received. The most likely thrust setting (percent N1) to be used for the takeoff is

A. 76
B. 88
C. 92
D. 104

Q09 Your friend lives 10 km away from an airport, directly under the flight path. At which of the following altitudes are incoming aircraft most likely to be while overflying her house ?

A. 1200 ft
B. 1800 ft
C. 2600 ft
D. 3600 ft

Q10 During a landing, the runway threshold is passed at a radio altitude of 50 ft. If the flare is executed skilfully, then the distance between the threshold and the touchdown point will be closest to which of the following values ?

A. 200 m
B. 400 m
C. 800 m
D. 1400 m

Q11 After crossing V_1 during the takeoff run, the pilots realize that the flap setting is lower than the planned value. Which of the following steps should they take to maximize the safety of the departure ?

A. Rotate at a lower speed and use a lower initial climb gradient
B. Rotate at a lower speed and use a higher initial climb gradient
C. Rotate at a higher speed and use a lower initial climb gradient
D. Rotate at a higher speed and use a higher initial climb gradient

Q12 At a busy airport, ATC is asking for expedited arrival. The landing configuration of flaps and undercarriage is selected at the beginning of the final approach. If V_{ref} is to be attained at or before runway threshold and spoilers are not be used during the approach, then the maximum speed permitted at the beginning of the approach is given by

A. The speed on the power curve corresponding to approach configuration, cruise thrust and level flight
B. The speed on the power curve corresponding to approach configuration, approach thrust and glideslope descent
C. The speed on the power curve corresponding to approach configuration, glideslope descent and maximum L/D
D. The desired maximum speed cannot be determined using the power curve alone

Q13 Considering one particular long-haul flight, during which of the following times is the lift generated by the wings likely to be the maximum ?

A. The initial 3000 ft per minute climb from takeoff to 1000 ft altitude
B. The 120^o turn at 1500 ft altitude from departure runway track onto assigned outbound radial
C. The 180^o turn at 2000 ft altitude onto final approach at the destination airport
D. The question cannot be answered basis the information given

Q14 During a 465 km/hr (250 kts) climb, a hydraulics failure causes the horizontal stabilizer to jam and the elevator to float freely. Which of the following difficulties will the pilot face in controlling the aircraft ?

A. Unintentional coupling between speed and pitch
B. Low pitch rate

C. Excessive speed near ground
D. All of the above

Q15 A pilot performs an extended turn by applying the suitable bank input and zero rudder input. Which of the following holds true ?

A. There is zero sideslip throughout the turn
B. There is small and approximately constant sideslip throughout the turn
C. There is progressively increasing sideslip throughout the turn
D. There is transient sideslip during the entry to and exit from the turn but none during the bulk of the turn

Q16 In the absence of unforced errors by the pilot, which of the following situations is most likely to become dangerous ?

A. Takeoff in steady tailwind
B. Takeoff in gusty headwind
C. Landing in steady tailwind
D. Landing in gusty headwind

Q17 For a particular flight, the onboard computer has calculated V_1 and V_r, with V_1 strictly less than V_r, based on full-length departure from the runway. After receiving takeoff clearance, the pilots use an intersection departure from the same runway without adjusting the thrust level or the flap setting. Which of the following will hold true for the revised departure ?

A. V_1 will decrease and V_r will decrease
B. V_1 will decrease and V_r will remain same
C. V_1 will remain same and V_r will decrease
D. V_1 will remain same and V_r will remain same

Q18 A malfunction causes an aircraft to lose all flight instruments other than airspeed indicator while flying in instrument meteorological conditions. Assuming no other traffic in the vicinity of the stricken aircraft, the phenomenon most likely to cause an accident is

A. Fuel exhaustion
B. Loss of control
C. Spiral dive
D. Stall

Q19 An aircraft is in a trimmed condition when the pilot applies a given push/pull force on the stick. If the fly-by-wire is programmed to simulate hydraulic activation of the elevator, then which of the following will be the closest approximation of reality ?

A. The pitch rate will be proportional to the square root of the force applied by the pilot
B. The pitch rate will be proportional to the force applied by the pilot
C. The pitch rate will be proportional to the square of the force applied by the pilot
D. The pitch rate will increase with time while the force is maintained

Q20 In an aircraft, the phugoid oscillations are increasing in amplitude despite the pilots' applying what appear to be appropriate elevator inputs. Which of the following control measures is indicated ?

A. Increase thrust, trim for a higher airspeed and reduce the amplitude of elevator input
B. Extend spoilers and optionally undercarriage to increase the damping
C. Increase the amplitude of elevator input
D. Initiate a banked turn

That we shall be answering all these questions *quantitatively*, through analysis and simulation of a dynamic model for the aircraft's motions, gives you an excellent idea of the scope and contents of this Article. You will see that a lot of the questions, especially in the latter half, feature safety considerations – technical malfunctions, control compromise, wrong decisions made by pilot etc. This is no accident, since improving safety standards is a problem of paramount interest in aviation. The particular aspect of safety we address in this Article is accidents and incidents which can be averted with good flying technique. We will solve the Quiz questions in the body of the Article, taking on each question after we have covered all the relevant theory. For this reason, the solutions will not appear in the order that the questions have been posed. For your convenience though, we include the answers alone on a separate page between the last line of content and the References.

§03 **Outline, novelty, learning objectives and prerequisite requirements.** Here we describe how we will realize our intention of creating a unified treatment which caters to engineers, aviators as well as technically trained air-laymen. As in the Quiz, the representative aircraft throughout this Article will be a modern passenger airliner. In Chapter 2 we will give a detailed description of such an aircraft and its components. We will also introduce the elements of navigation and communication. This material will familiarize the engineer with the operational aspects and the pilot with the engineering aspects of aviation. It will also enable the student or professor with no aerospace background to get a mental picture of the stage on which the subsequent action takes place. Chapter 3 will feature the derivation of the aircraft dynamic model. We shall treat separately the pitch, yaw and banking planes, with the first of these being by far of the greatest significance. The LHS or left hand side of our equations of motion will be conventional. For the RHS or right hand side however, we will use a particular theory of lift and drag – the momentum theory in this case – and combine it with models of the wings and control surfaces to obtain closed form expressions for all aerodynamic forces and torques. This will lead to an explicit sixth order nonlinear model in each plane. In Chapter 4, we will obtain the fixed points of the pitch plane equations of motion and determine their stability. This exercise will lead to the short period and phugoid modes, and pilot-induced oscillations. We shall also find and plot the characteristic curves of the aircraft i.e. equilibrium quintuplets of speed, elevation, pitch, thrust and elevator force. Then, in Chapter 5, we will use the model equations to construct the academic flight simulator, and use this simulator to demonstrate the behaviour of the aircraft during flight phases and manoeuvres such as takeoff, landing, Pugachev cobra, stall recovery and coordinated turns. For those manoeuvres which are relevant to civil aviation, we will discuss how to best achieve the manoeuvre objectives and how to maximize safety. We will put our simulation results into the context of actual aviation accidents and incidents from the modern aviation age, to give you a first-hand feel for the connection between theoretical understanding of the dynamics and practical airmanship technique.

To the best of our knowledge, the explicit nonlinear dynamical model of the aircraft which we derive in this Article is the first of its kind. A dynamical systems approach to aircraft motions is rare to begin with, although this was pursued with great enthusiasm in a spate of papers published in the Philosophical Transactions of the Royal Society in 1998 [31-39] and can also be found in some other works [19,20,40]. In each of these works, the equation RHS is obtained by numerical interpolation or continuation from an experimentally obtained data table. While this approach works well for obtaining bifuractions and other mathematical features of the equations, physically it is less insightful. Inclusion of simulation results in academic flight dynamics work is again rare, with some examples being Refs. [07,20,41]. Once again, the equations used in these simulators have data-table RHSes and as a result, intuition into the airplane's motions has not been developed. The synergy of theory and practice which we achieve here, the mathematical bridge between BRYAN and LANGEWIESCHE, is, again in our considered opinion of which we would welcome correction if necessary, without precedent in aerospace Literature.

As the subtitle and abstract make clear, this Article will deal with two-dimensional motions only. This indicates all motions in which two of three Euler angles (yaw, pitch or bank) are identically zero throughout. In a future sequel Article, we shall take on the case of general motions. Why this separation into two Articles ? This is because, in our experience, planar mechanics is a subject which many find intuitive and easy to understand while three-dimensional mechanics is not. This may have something to do with the fact that planar free-body diagrams can be drawn while three-dimensional ones cannot (in the true sense – the forces and torques would exit the plane of the paper). Since intuition is one of the pillars of our approach to flight dynamics, we have elected to proceed as far as possible while relying on its support. Many realistic aircraft manoeuvres, such as takeoff, landing and the others considered in Chapter 5, are in fact primarily two-dimensional, operating in the pitch plane. When out of plane modes are stable, as they usually are for passenger airliners, they remain negligible or at worst small throughout such manoeuvres. We can understand them far more thoroughly if we treat them within the framework of a two-dimensional model instead of as a special case of a three-dimensional model. There are of course many manoeuvres which are quintessentially three-dimensional, such as a climbing turn, crosswind landing, or operation with a failed engine. We have no regret in deferring these to the three-dimensional sequel. Of necessity, that will be something of a mathematical tour de force, featuring a twelfth order equation in five angle variables (azimuth, elevation, yaw, pitch, bank) and three more angle parameters (sweep, camber and dihedral of the wings). Before coming to those, it will help everyone to get a feel for the aircraft through an understanding of these easier motions.

Regarding prerequisite, Chapter 3 requires classical mechanics at the level of a demanding introductory course or relaxed second course at typical universities. An appropriate text supplying the relevant mechanics might be any of Refs. [42-44]. While formulating the axis and angle convention in its full generality, we will use elementary Euler angles, in particular the theory of representing a composite rotation as a chain of three successive rotations. If you are familiar with this topic, then that will be a plus; nevertheless, we will also present a simpler alternative treatment which avoids this prior knowledge at the expense of a little mathematical imprecision. Chapter 4 requires knowledge of linearized stability analysis of a high-order nonlinear system – this is perhaps the ruling prerequisite of the entire Article. One Section of this Chapter also features a delay differential equation but for that analysis we have treated a key fact as a given and worked out the rest from the ground up. Chapter 5 requires facility with manipulating linear differential equations, a skill typically provided by the first compulsory course in the subject; appropriate materials for covering this prerequisite should be Refs. [45-47].

In a university setting, the entire Article (together with some supplementations which we will discuss in §68) will be suitable for the bulk or the totality of an advanced undergraduate or introductory graduate course on flight dynamics. For an advanced graduate course, this material will need to be supplemented by some stuff on three-dimensional motions. For the timebeing, this can be taken from any conventional text on flight dynamics, for example the ones cited in §01; after our sequel is written, the supplement may be drawn from there. Currently though we are not sure of how difficult this sequel will turn out to be; it may end up being suitable only for a very specialized audience. In an aviation academy, we have no idea regarding how much of this Article can be covered and in what timeframe; this is because of our own

current unfamiliarity with such academies and their curricula. As and when we can rectify this deficiency, we will provide an estimate.

§04 **Presentation style, change of narrative voice.** In the rest of this Article minus its concluding Chapter, we have elected to present the material in the style of a lecture course or a textbook. That is, we start from aircraft fundamentals and lead up to our results as gradually as possible, showing all intermediate steps and elaborating all the pieces of logic involved. A more concise presentation, which some may find more appropriate for the exposition of novel results, will alienate our work to non-aerospace-engineers as well as to all students, specialized or otherwise. Simultaneously, we place significant emphasis on the Figures – there are numerous illustrations of aircraft components, a plethora of graphs of simulator inputs and outputs, as well as several combined diagrams showing aircraft trajectory and attitude during manoeuvres. We include scale diagrams (using a CAD model), schematic drawings and hybrids of the two, whichever we feel to be the most appropriate in context. Our hope is that a heavily illustrated presentation will facilitate short-term understanding as well as improve long-term retention of results, an aspect which is particularly important for pilots in training. Finally, we shall implement a change of narrative voice in the following four Chapters. This is that we shall switch to the first person singular to refer to the authors alone while reserving the first person plural for the authors and readers combined. This style mimics any one author presenting the material at a lecture, and draws an important distinction as the following examples show. "*We* shall use the convention that the z-axis points vertically upwards, and add a minus sign to φ" – here, the lecturer as well as the audience use this convention. On the other hand, "*I* find the convention where z points vertically downwards to be unnecessarily counter-intuitive; it is so much easier to add on a minus sign to φ" – here, only the lecturer dislikes the sign convention on z and prefers to trade the minus with φ, and it is upto the individual audience members to agree or disagree with this preference. We assume that our audience is a student of a university or aviation academy.

The issue of narrative style in academic work was succinctly put by Sir BRIAN PIPPARD in the introduction to his book on Vibrations [48]. Quoting verbatim, "Already I have shown an unbecoming personal touch in revealing my aims and aspirations. It is time to disappear from the scene. But though, following custom, *I* [italics in the original] adopt the cloak of invisibility and simultaneously cease to acknowledge the existence of *You*, my reader, there will still be found, as *We*, the assumption of collaboration between writer and reader without which a book might as well remain unwritten." Forty years ago, Sir BRIAN's convention was customary. Today, when stylistic conventions are more flexible, an all-encompassing "we" on works with more than one author often tends to blot out the distinction between authors and readers together and authors alone. Here, we take recourse to the first person singular (rather than the passive voice or third person options) to preserve this distinction while not appearing stilted or artificial.

It is a fact that, despite being an intensely technical subject, aviation – unlike say the theory of functions of a complex variable – enjoys an appeal transcending the boundaries of science, engineering and mathematics. To the extent possible, we have attempted in this Article to preserve or even enhance this appeal. Thus, even though we go full strength on mathematical rigour, we place at least equal emphasis on the concepts behind the symbols and the implications of the results. The graphs and equations notwithstanding, this Article proceeds in a single arc from the first pictures of the wings and tail to the final simulation of a heroic landing in next-to-impossible conditions. Our hope is that, in addition to creating practical and academic value, we have also arranged for some entertaining reading.

---- o ----

2

AVIATION, NAVIGATION AND COMMUNICATION

This Chapter familiarizes you with the aircraft and its operation, starting from scratch. We first take a look at the components of a jetliner, then at the basics of navigation and finally the rudiments of communication. If our Article were a novel or a play, then this would be where the characters are introduced and the locale described, setting the scene for the action proper to take place. If on the other hand our Article were a certain kind of musical piece, then this would be the slow introduction and the next three Chapters the allegro. The Chapter title is adapted from the piloting catchphrase "aviate, navigate, communicate" which refers to the pilot's priorities when an aircraft malfunctions – first, keep the plane in air, second, make sure the plane is going where you want it to go, and third, maintain communication with air traffic control and other aircraft in the vicinity.

A. AIRCRAFT COMPONENTS, OPERATING VARIABLES AND UNITS

§05 **Primary components of an aircraft.** In this Section we look at the components of an aircraft which are most important for keeping it aloft. For each component I will include a brief, qualitative description of its function. Depending on your familiarity with the material, you are welcome to skim or skip the entire Section.

In the upcoming Figure we can see an isometric view of an aircraft. In this Figure – as well as in the rest of this Article – we shall consider an aircraft similar in structure to a modern jetliner such as an Airbus A320 or a Boeing 777. This is because such a structure is shared by the vast majority of aircraft today. Note that this Figure, and the subsequent equations and simulations, do not feature any actual aircraft but a fictitious aircraft which looks like a real one and has parameter values similar to a real one. In what follows, we shall call this aircraft "Our Plane". Owing to a technicality which I shall clarify in a couple of pages, the aircraft we see below is actually not Our Plane but Our Plane Prime. Whenever we see Our Plane or Our Plane Prime, it will be a computer-aided-design (CAD) model which I have created using the free software Blender. The use of a CAD model rather than a simple drawing ensures mathematical consistency among all views of the whole aircraft as well as individual components.

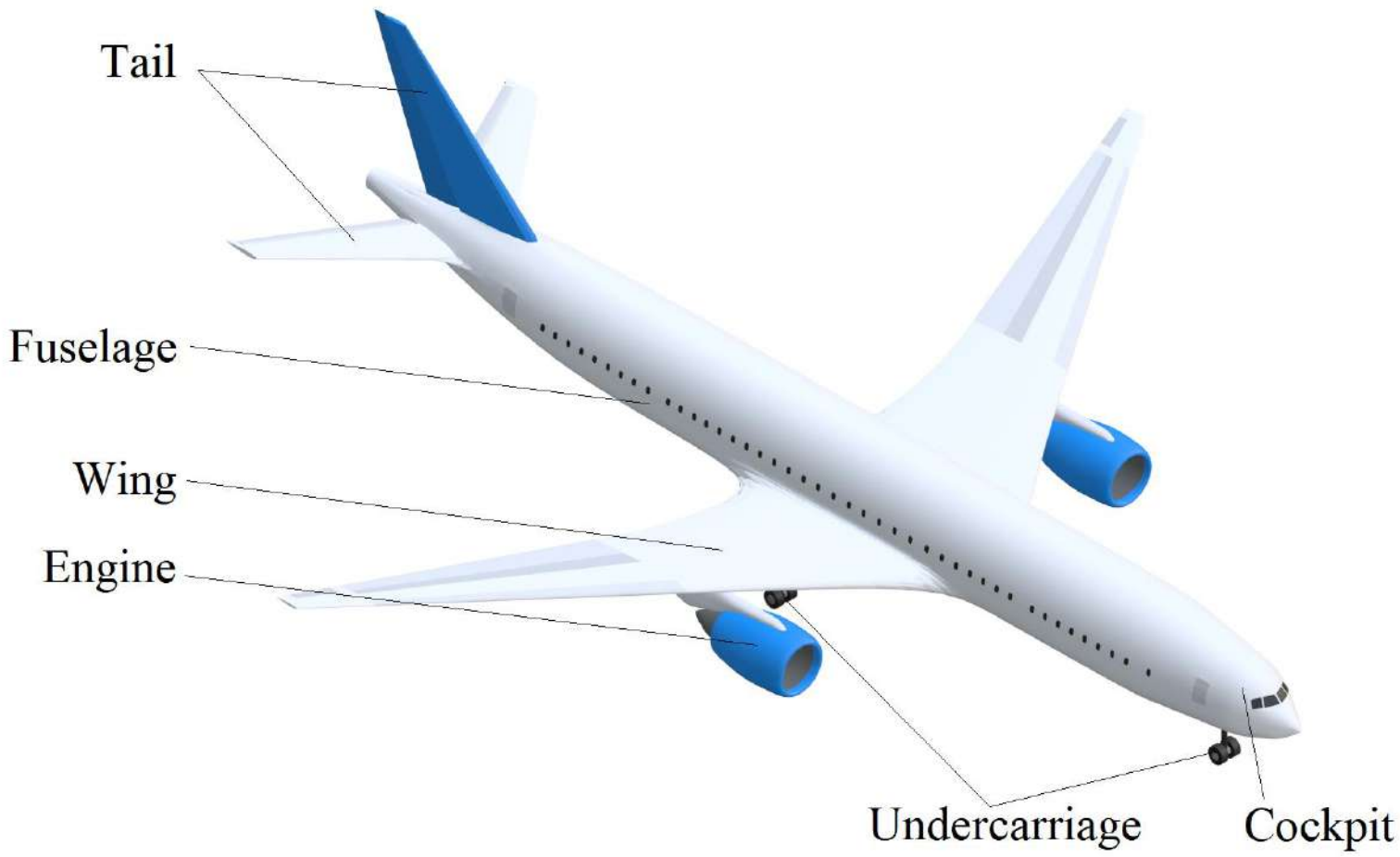


Figure 01 : *Isometric view of Our Plane Prime.*

Just the drawing of the plane has 74 different objects; now imagine the number of components in the real thing.

Since our model will be derived for Our Plane, the equations will be most directly applicable to modern jetliners. With cosmetic changes (change in parameter values and hence in the operating speeds etc), they will also become applicable to smaller aircraft like the propeller planes which people fly for fun. The same modeling principles will apply to less conventional configurations such as the delta wing of Concorde or the custom-built designs of unmanned air vehicles (UAV) with immobile wings – deriving the actual equations themselves will be a little more work. All these planes, to which our model applies directly or indirectly, are **fixed wing aircraft**. The primary aerodynamic elements of these aircraft are **airfoils*** – bodies designed to generate lift when placed in moving air – and these airfoils are fixed to the aircraft. The other category of aircraft is moving-wing, such as helicopters, quadcopter drones and UAV with flapping wings. Here, lift comes from rotating or oscillating airfoils and our model will not be applicable to these as is. To derive their dynamic models, we'll need to account for the forces and torques on moving wings, but that is suitable for another Article.

* In some words, there is a choice between a prefix of "air-" and a prefix of "aero-". Here I shall go with "air-" as it sounds more modernistic and more in tune with words such as aircraft and airport. In general, British English users prefer "aero-" while American English users prefer "air-". Sometimes however, only one of the two forms is standard, as in "aerodynamics" and "airport" (it's called "aeroport" in French). And the two prefixes mean completely different things when applied to the word "space". The word "airport" – a port (for ships) here applied to aircraft – is just one example of naval terminology being adapted to the sky. The Bangla word for airport, বিমানবন্দর (bimanbandar), is a verbatim translation, as is perhaps to be expected. The Hindi word, हवाईअड्डा (hawaaiadda), however literally translates as "a place where aircraft can sit and converse". Such are the vagaries of language, but that's appropriate for another Article.

Throughout this Article, I will use boxes like this to make parenthetical points which shouldn't distract from the flow of the main text but are nonetheless interesting in their own right. A star in the main text near the box will indicate the exact location where the box links up.

The scope of the model over, let's come back to Our Plane. The direction from the tail to the nose is called **forward** (not a surprise) and the reverse direction is called **aft**. Facing forward, the left side is called **port** while the right side is called **starboard**. Note that port and starboard are always defined this way – they don't change if the observer happens to be facing the aircraft from the front. This nomenclature

eliminates confusion between left and right for different observers*. There are three rotational motions of an aircraft. To visualize them, consider an aircraft which is initially horizontal. **Yaw** is a rotation which causes the nose to move rightwards and the tail leftwards, or vice versa. A bus or car turning on a level road performs a yaw motion. **Pitch** is a rotation which causes the nose to move up and the tail to move down or vice versa. A bus or car transitioning from level road to a flyover performs a pitch motion. Finally, **bank** is a rotation which causes the port wingtip to move up and the starboard wingtip to move down or vice versa. A bus or car travelling along a road with a cross-slope from one sidewalk to the other has a nonzero bank angle. These are informal definitions of the three rotations – for a completely rigorous treatment see §17-18.

* How many of us have not felt a momentary confusion in the metro railway when the motorman (or recorded voice) announces "doors opening on the right" and we happen to be sitting facing the rear.

Now for a summary of the main components of the plane.

► **Fuselage :** This is the body of the aircraft, equivalent to the chassis of a road vehicle or the frame of a railway locomotive. Note that "fuselage" is the only acceptable term for this component. It is non-aerodynamic, in the sense that the air flowing past the fuselage is not intended to exert any force on it (in reality, it does exert a drag force, but that is unwanted and aircraft designers take great pains to minimize it). The fuselage of course is where we sit; jetliners are classified as narrow-body if the passenger cabin has one aisle and as wide-body if the cabin has two.

► **Cockpit :** This is the area in front of the aircraft where the pilots sit and control the aircraft. We shall look at the cockpit in detail later in this Section.

► **Wings :** These are the primary lift-generating surfaces of the aircraft. Wings are airfoils, having several sub-components, which we shall look at later in this Section.

► **Tail :** This consists of two horizontal elements and one vertical element. Like the wings, these elements are airfoils. Although their lift is smaller than that of the wings, the torque of this lift is significant and the tail has an invaluable contribution to the aircraft's overall motion. The tail is also called "empennage". Once again, the tail is made up of more than one significant component; we zoom in on the sub-assembly later in this Section.

► **Engines :** These generate the forward force which makes the aircraft move; this force is usually called the **thrust**. Most airliner engines are fitted with thrust reversers which enable the thrust to act backwards while on the ground; reverse thrusting contributes to the plane's deceleration following touchdown. In a multi-engine aircraft, engines are always numbered from left to right.

► **Undercarriage :** This refers to the wheels on which the aircraft rests when it is on the ground. All modern airliners have a *tricycle undercarriage* with a single pair of wheels near the nose, dead on the centreline (axis of symmetry of the fuselage), and one or more wheel pairs further aft, some distance to port and starboard of centreline. The former are called nose wheels while the latter are called main wheels. We can see the wheels on Our Plane Prime below.

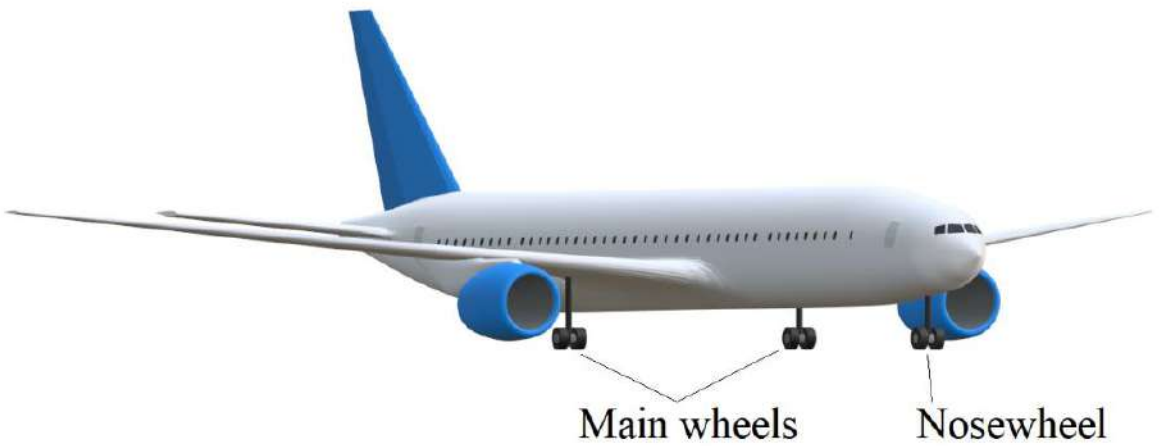


Figure 02 : *Our Plane Prime viewed from the front and right.*

Our Plane (Prime) has two main wheels (one pair) on starboard and two on port. This is consistent with the dimensions which I will later attribute to it. The number of main wheels increases with increasing size of the aircraft – on an Airbus A320 or Boeing 737 there are only four main wheels as in Our Plane, on Boeing 777 there are 12 while on Airbus A380 there are 20. The undercarriage is also referred to as the landing gear*, sometimes contracted to just "gear". At taxi speeds, the undercarriage achieves control over the direction of the plane's motion, just as in a bus or a car. The disk brakes attached to the wheels are the primary source of deceleration after the aircraft lands. Though intended to be non-aerodynamic, practically the undercarriage is an enormous source of drag; it is retracted immediately following takeoff and extended again before or during the final approach to landing.

* "Undercarriage" is the British word and "landing gear" the American. Since the wheels do not possess gears, the former is the more appropriate. If "undercarriage" feels too long to pronounce, just say "wheels".

Now we will look at the sub-parts of the major components.

Wing

The components here serve to change the shape of the wing i.e. its properties as an airfoil.

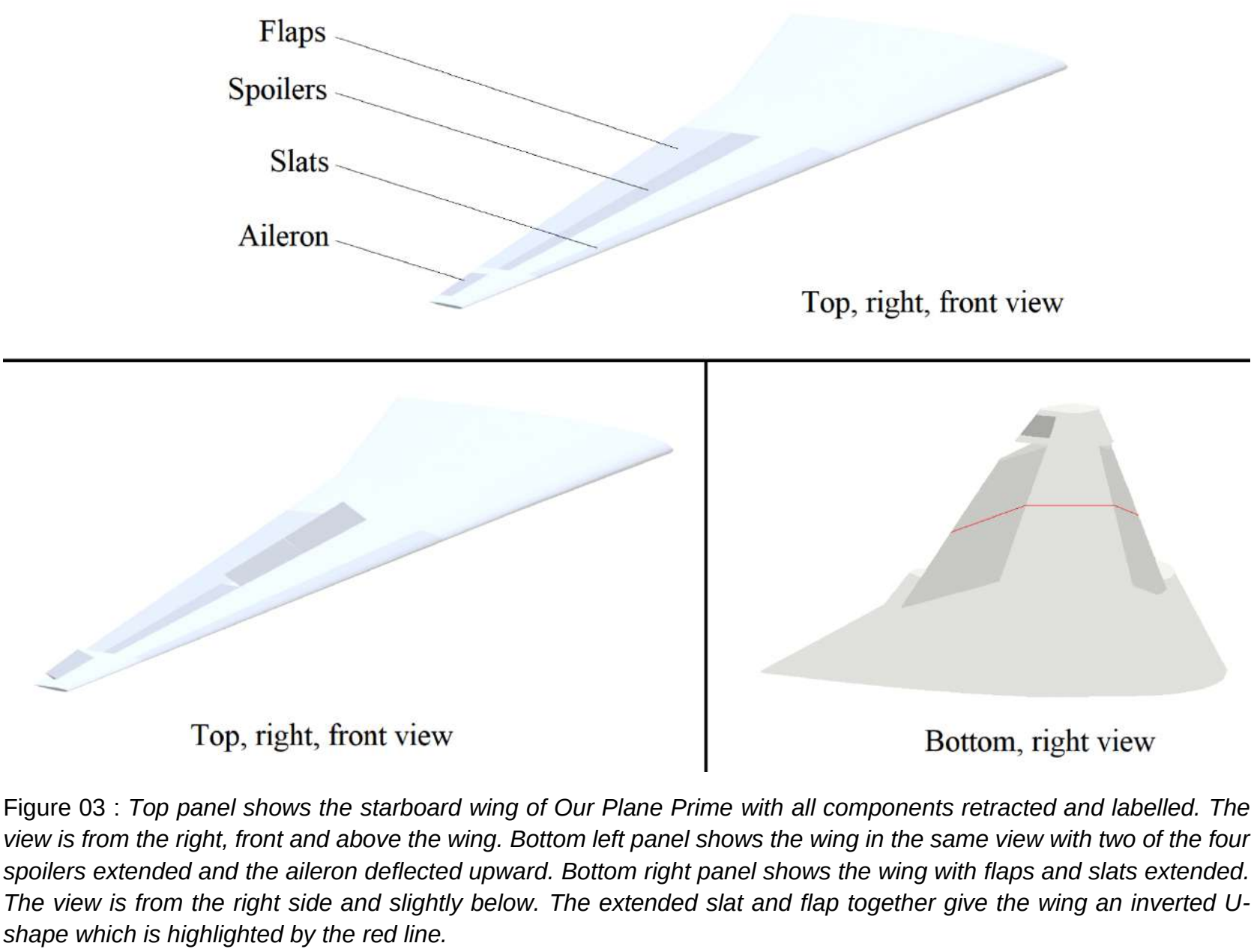


Figure 03 : *Top panel shows the starboard wing of Our Plane Prime with all components retracted and labelled. The view is from the right, front and above the wing. Bottom left panel shows the wing in the same view with two of the four spoilers extended and the aileron deflected upward. Bottom right panel shows the wing with flaps and slats extended. The view is from the right side and slightly below. The extended slat and flap together give the wing an inverted U-shape which is highlighted by the red line.*

Let's look at the descriptions of these components.

► **Flaps :** When extended, the flaps come out of the aft side of the wing and deflect downwards, as in the bottom right panel of Fig. 03. They generate increased lift at low speeds. They also generate extra drag, so they are used only during the low-speed phases of flight i.e. takeoff and landing.

► **Slats :** Like flaps, these are lift-augmenting devices; they are located on the forward side of the wing rather than the aft side. When extended, they deflect downward like the flaps. Once again, their

primary use is during takeoff and landing. You can see from Fig. 03 that when both flaps and slats are extended, the wing acquires a curved shape from front to back like an inverted "U". We shall have more to say on this in §19. The wing surface area also becomes larger when the flaps and slats are extended.

► **Spoilers :** When extended, they protrude from the main wing surface, presenting a rectangular obstruction to the oncoming airflow. These reduce lift and increase drag. In the air they are extended to slow down the aircraft and increase the descent rate. Sometimes, they also augment the ailerons to achieve banking. Spoiler extension in air is at max partial, never full. After landing, when the plane is at high speed on the runway, spoilers are extended fully to reduce lift and increase the deceleration rate.

► **Ailerons :** When deflected upward, ailerons protrude from the wing surface like spoilers; when deflected downward, they create an inverted U like flaps. Typically, ailerons work in tandem, deflecting upward on one wing and downward on the other so that the lift of one wing decreases and that of the other increases. This gives rise to a banking moment with the wing with less lift dipping below the one with more lift. Since planes bank for turns, the primary function of the ailerons is to achieve turns.

This list is of course the tip of the iceberg; it excludes the pylons for mounting engines, pipes for transferring fuel, servomotors for controlling the various surfaces etc. My purpose here is not to describe the aircraft in its full glory but to give you an idea of those components which are the most relevant for constructing its dynamic model and understanding its primary flight behaviour. ■

Tail

Hands up those who didn't know that the tail assembly had a horizontal component as well. Although it looks dwarfish compared to the wings, the horizontal tail is almost equally important for steady flight; if it shears off midair, the result is a pilot's worst nightmare (Subdivision 5J). Below we see the tail and its components.

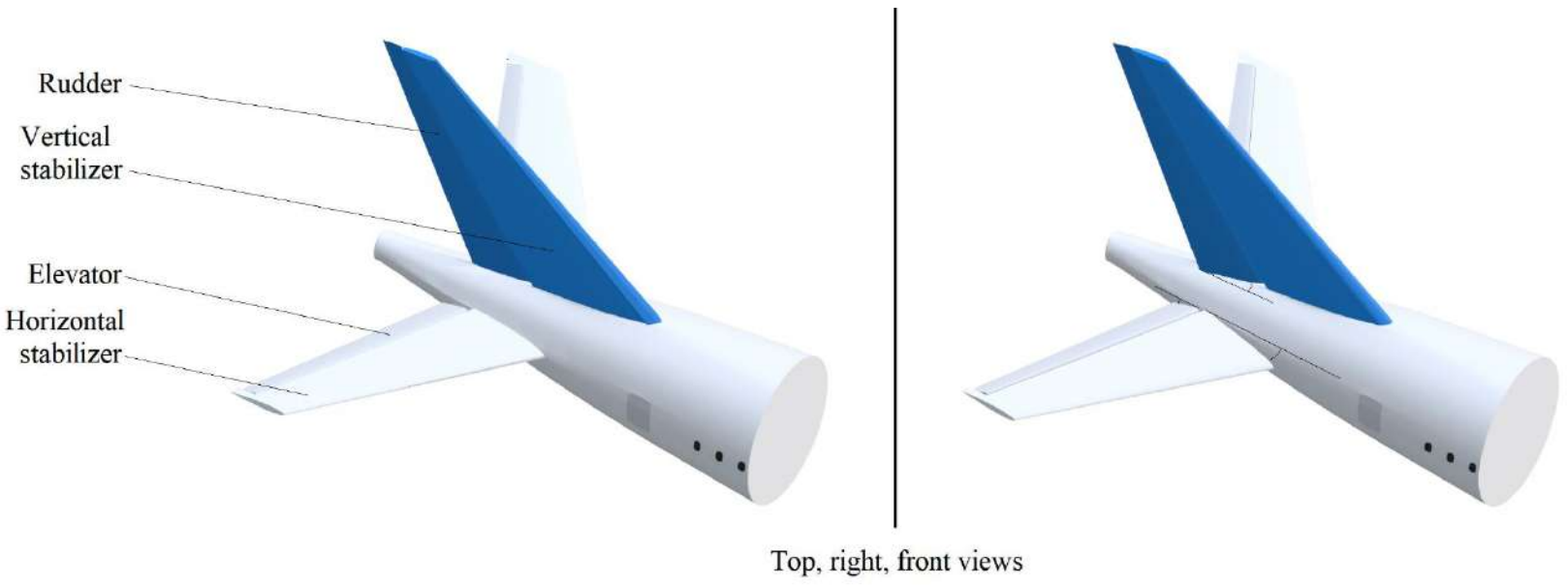


Figure 04 : *Left panel shows the tail with all components straight or minimally deflected. Right panel shows the horizontal stabilizer deflected downwards, the elevator deflected upwards and the rudder deflected to the port side (which causes the plane to yaw to the right).*

Now for the descriptions.

► **Horizontal stabilizer :** This is an airfoil or mini-wing at the back of the aircraft, fixed or quasi-fixed to the fuselage. In smaller aircraft, it is fixed rigidly, making a constant angle of deflection with the fuselage. In most modern jetliners, this deflection can be changed by the pilot (within reasonable limits). Even so, it generally stays constant over extended periods, and, when changes are commanded, the rate of change is slow. The deflection of a movable stabilizer is also called **trim**. Typically, the lift of the stabilizer acts *downwards* during normal flight; it acts together with the wing lift to achieve torque equilibrium of the whole aircraft and stabilize it in pitch.

► **Elevator :** Yet another airfoil, usually smaller than the horizontal stabilizer and located just aft of it. Unlike the stabilizer, the elevator is highly mobile. Its deflection is controlled by the pilot and can be changed rapidly. Doing so changes the pitch angle and climb/descent rate of the aircraft.

► **Vertical stabilizer :** Equivalent of the horizontal stabilizer, this is an airfoil fixed to the rear of the fuselage in the vertical plane. Its lift, acting laterally, stabilizes the aircraft in yaw. Unlike the horizontal stabilizer however, this item is generally not movable, even in the most sophisticated aircraft.

► **Rudder :** Equivalent of the elevator, it is mobile and influences the yaw angle of the aircraft.

In some aircraft, the horizontal stabilizer and elevator are merged to form a single movable surface called a **stabilator** or all-moving tail. In this case, the horizontal tail has the size of a horizontal stabilizer and the mobility of an elevator. We see this element in the below Figure. Aircraft with stabilators range from Piper Cherokee at one end of the performance spectrum to Concorde at the other.

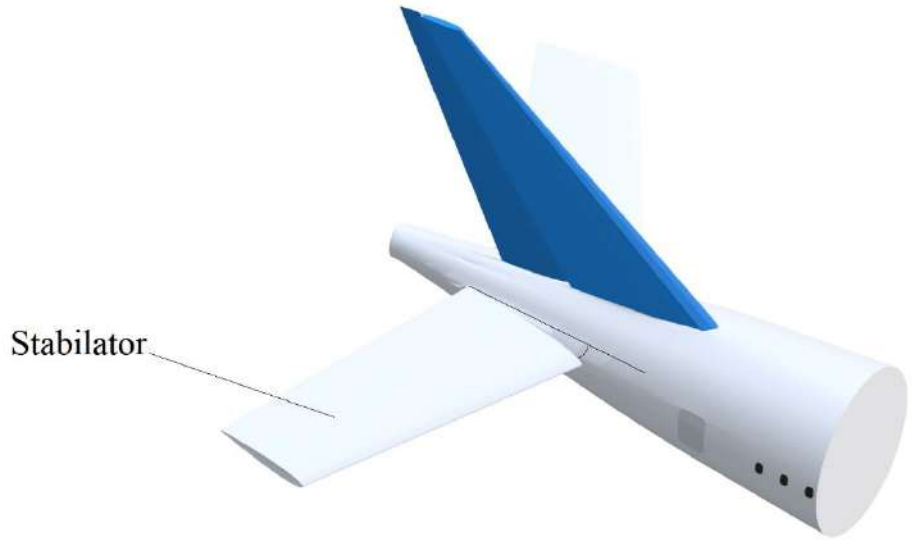


Figure 05 : *A stabilator and its deflection.*

While developing the aircraft dynamic model, it will be most convenient for us to assume that the aircraft has a stabilator rather than two separate tail elements. This assumption will reduce the number of terms in the equations while not compromising generality. Hence, Our Plane will include a stabilator. This is why the aircraft of Figs. 01-04 was Our Plane Prime – it has a two-piece tail while Our Plane proper has a one-piece tail. The primed form was necessary for the visuals; now that they are done with, it has no further use. All subsequent aircraft figures will actually show Our Plane. ■

Cockpit

Finally, we have the cockpit. This has two kinds of apparatus – control devices (called the **flight controls**) and measurement devices (called the **flight instruments**). A modern cockpit has several hundred devices of each kind as we can see in the below Figure, taken from Ref. [01].



Figure 06 : *A picture of a cockpit with salient parts labelled. The aircraft is a Bombardier C-Series, later known as Airbus A220. The image [01] carries appropriate permissions for this usage. I did not find a picture of a 'more standard' airliner cockpit which can be used as a demonstration and also carries the suitable permissions.*

Cockpits are designed so that both the pilot sitting on the left and the one on the right have equal access to all controls and instruments. This is achieved by central position and/or duplication as we can see in the Figure above (for instance, there are two sticks and two attitude indicators while the thrust levers and direction indicator are located centrally).

Below is a list of the cockpit components which are the most relevant for everyday flight operations and also for modeling such operations. First let's look at the controls. Note that all jetliners of today are **fly-by-wire** (FBW), which means that the link between a cockpit control and the component it affects is electronic instead of mechanical. Concorde was the first aircraft equipped with this technology.

- **Throttles or thrust levers :** These regulate the thrust developed by the engines – there are as many levers as there are engines. Pushing the levers forward increases thrust. The maximum permissible thrust setting is called TOGA or takeoff, go-around (aborted landing); the minimum possible setting at which the engine keeps running is called ground idle while the minimum permitted in flight is called flight idle. Flight idle is higher than ground idle; the exact setting is determined by the time taken for the engines to ramp up to TOGA thrust in the event of a sudden emergency. In fly-by-wire aircraft, engines are controlled by a software called FADEC or full authority digital engine control. The position of the thrust lever is transmitted to the FADEC and that selects a thrust level which is compatible with the pilot's command as well as the engine's performance limitations. In non-FBW aircraft, the throttle directly controls the fuel flow rate.

- **Control column, yoke or sidestick :** This is the primary flight control instrument apart from the thrust levers. A yoke is a large pole coming out of the floor of the aircraft, directly in front of the pilot, with a handlebar pivoted to the top. Boeing aircraft use this instrument. Sidestick is a full-motion joystick mounted to the pilot's one side, as in Fig. 06. Airbus aircraft use this instrument. Both have the same functionality, achieving control over the elevator and ailerons. Pulling the yoke or sidestick stick

backwards causes the aircraft nose to pitch up while pushing it forwards causes the nose to pitch down. Rotating the yoke's handlebar counterclockwise or moving the sidestick leftwards causes the plane to bank counterclockwise facing forward, which leads to the aircraft entering a left turn. The opposite lateral motion of the device causes the plane to bank clockwise facing forward, which leads to a starboard turn. In what follows, we shall refer to this instrument as the "stick", irrespective of implementation. As with the throttles, in fly-by-wire systems the relation between the stick position and the elevator/aileron deflection is electronic; in non-FBW aircraft, the connections are mechanical (hydraulic), about which we shall see more in §23.

- **Trim wheel :** The trim wheel controls the deflection of the movable horizontal stabilizer. In tails where the stabilizer is fixed, the trim wheel controls a fixed non-zero deflection of the elevator itself.
- **Rudder pedals :** These control the deflection of the rudder. Pushing the left pedal causes the aircraft's nose to move leftwards and vice versa.
- **Autopilot :** This is a software which automatically regulates the engine thrust as well as the control surface deflections to generate the flight trajectory which has been entered into the computer beforehand. It does all the work which the pilot would have had to do in its absence, so much so that the aircraft can fly while the pilots sleep. The bulk of a modern passenger flight takes place under autopilot, with the pilots flying manually only for a short while after takeoff and a short while prior to landing.
- **Autothrottle :** This is a software which automatically regulates the engine thrust only. Thus, if the autothrottle is commanded to generate a 2000 feet per minute climb, it will provide the requisite thrust; however, whether or not the climb will actually be achieved will depend on whether the pilot provides the correct stick inputs.

  Now we take a look at the instruments.

- **Attitude indicator :** This displays the pitch and bank angles of the aircraft relative to the vertical and horizontal at the aircraft's current location. In the absence of this instrument, these angles are inferred by looking at the horizon; for this reason, attitude indicator is also called artificial horizon.
- **Airspeed indicator :** Airspeed is defined as the speed (magnitude of velocity vector) of the aircraft with respect to the surrounding air; its indicator is one of the most vital displays in the cockpit. It is not a tautology to say that the airspeed indicator displays the indicated airspeed; why this is so you'll see in §07.
- **Climb rate indicator :** This shows the rate of climb or descent which the aircraft is performing.
- **Altimeter :** This displays the aircraft's altitude above mean sea level. The default altimeter in an aircraft is a pressure altimeter; in addition, most modern jetliners have a radio altimeter which measures the altitude above the ground which the plane is overflying. We'll see more about altimeters in §07.

Over and above this, there are myriad displays which provide more detailed information, for example angle of attack sensors, navigational instruments, fault diagnostic displays and the like. In the flight simulator we shall implement such instruments as are realistic and are most appropriate for each manoeuvre under consideration. ■

Let us take this opportunity to formally define the word "manoeuvre" in the context of this Article. A **flight manoeuvre*** is a condition in which the aircraft is subjected to temporary or transient linear and/or angular accelerations resulting from displacement of the controls relative to their equilibrium positions [1O–08].

* The word is derived from the root "man-" or "hand", as in "manual" and "manicure", plus the word "oeuvre" or "work", as in "a writer's oeuvre" or "hors d'oeuvre" (literally "outside the work", i.e. not part of the regular courses in the meal). Hence, "manoeuvre" literally means "a work of the hand", and this is the etymologically consistent way of spelling it, as against "maneuver".

For modeling the aircraft's motions, this is about all we need. A good few other components are however interesting enough in their own right; even if they don't enter the equations, they give us a better picture of the technological marvel which a jetliner is. Let's look at some of those now.

§06 **Additional components.** We start with some details about the engine. For almost all aircraft, the engine is a turbomachine, a device which works using moving air. To explain its operation in a nearly trivialized way, it has three components – compressor, combustor and turbine. The compressor is rotary and serves to compresses the air entering the engine. The combustor mixes the pressurized air with fuel and ignites it. The ignition causes the air to expand dramatically and shoot out the back of the engine at great speed. The turbine is mounted in this airstream and develops a torque. It is mechanically connected to the compressor (mounted on the same shaft) so that its torque keeps the compressor spinning. The combination of compressor and turbine is called a rotor or a spool. Most engines have two rotors nested inside each other, so that from front to back one encounters compressor no. 1, compressor no. 2, combustion chamber, turbine no. 2 and then turbine no. 1. Some engines have three rotors. In a dual rotor engine, the no. 1 rotor is called low pressure rotor while the no. 2 rotor is called high pressure rotor; in a triple rotor engine, the three are called low, intermediate and high pressure rotors. Typically, higher pressure rotors spin faster – reference values are 2000-5000 rpm for the low pressure rotor and 10,000-20,000 rpm for the high pressure one.

In a turbojet, the rotors are all, with the thrust coming from the speeding gases. In a turbofan, the low pressure rotor is connected to a medium-sized, multi-bladed, ducted fan in front of the engine. This fan provides most of the thrust. In both these engines, reverse thrust works by redirecting the exhaust gases and fan air out of the jet in a forward-facing direction. In a turboprop, the gases generated by the rotors turn another turbine which is connected to a large, unducted fan with few blades (the propeller). Reverse thrust works by changing the angle of the propeller blades. Concorde had turbojets, all modern jetliners have turbofans while propeller planes have turboprops; only the smallest recreational aircraft ("flying cars") have internal combustion engines like road vehicles. Each compressor and turbine in a jet engine has multiple rows of blades – each such row is called a stage. The dual rotor General Electric GE90 has 1+4 (1 for fan) stages on the low pressure compressor, 9 stages in the high pressure compressor, 2 stages in the high pressure turbine and 6 stages in the low pressure turbine; the triple rotor Rolls Royce Trent 900 has 1 (fan), 8, 6, 1, 1 and 5 stages from front to back.

The engines also provide the electricity on board the aircraft. A modern airliner has a huge number of gadgets running on electricity – in the cockpit we have all the instruments and controls, and in the passenger cabin we have the air conditioning, cabin lights, food/drink heaters and in-flight entertainment systems, just to name a few. The total electrical power consumption of a Boeing 777 is approximately 300 horsepower [02]. All this electricity comes from generators mounted inside the engines, usually connected via gears to the high-pressure rotor. When the aircraft is on the ground with the engines off, the power can come from either one of two sources. One is a separate mini-engine on board the plane, called **APU or auxiliary power unit**, which can also be switched on during flight, should the need arise. The other is **GPU or ground power unit**, a device which supplies electricity at the desired voltage and frequency via a cable connecting to the aircraft.

Now let's look at some other components. Humans are not designed for survival at the low atmospheric pressures encountered above 15,000 ft or so of altitude, and certainly not at the typical cruising altitudes (30,000 ft or more). Hence, the cabin is **pressurized** during flight, usually to an equivalent altitude of 8000 ft (the Boeing 787 cabin is rated for a pressure of 6000 ft). The cargo hold is pressurized as well. In most jetliners, the pressurization as well as air conditioning are achieved by extracting compressed air from near the final stages of the compressors in the jets. This air is called **bleed air**. Boeing 787 dispenses with bleed air but instead compresses outside air using electrically-powered compressors. The fuselage of a jetliner is designed to withstand a significant pressure difference between inside and outside. At the front and back, it is sealed by circular structures called **pressure bulkheads**. If a hole develops anywhere in the fuselage, or the bulkhead fails, the pressure in the fuselage drops suddenly and sharply. This is the situation which the cabin crews refer to in the sentence on "in case of a drop in cabin pressure ….." during the flight

safety briefing prior to departure. Needless to say, if this really happens, oxygen masks drop down from the ceiling and you should pull the mask over your nose and mouth and breathe normally. Simultaneously, the pilot performs an emergency descent to 8000 ft or lower so that the masks are not required any longer. The doors of the aircraft are designed to open inwards and remain pinned to the fuselage if the internal pressure exceeds the external one; for this reason, they cannot be opened inflight by an unruly or fractional-witted passenger.

Fly-by-wire is very different from autopilot, even though both deal with cockpit electronics and automation. While autopilot actually flies the aircraft itself, fly-by-wire merely helps the pilot to fly it manually. Fly-by-wire systems typically have **normal** and **alternate control laws**. Normal control law remains valid when the aircraft is fully functional, and is a specification of the relations between the input at the cockpit control and the output at the control surface (for instance, the position of the stick and the deflection of the elevator). Normal law automatically prevents exceedance of the aircraft's design, performance and other limits. Alternate laws kick in where there are systemic failures and malfunctions. The type and nature of these laws depends on the aircraft as well as the malfunction which has occurred; a detailed discussion of this will become too specialized and is outside the scope here.

The **black boxes** refer to two devices called the flight data recorder (FDR) and the cockpit voice recorder (CVR). Flight data recorder keeps a record of all the control inputs made by the pilots, the dynamical variables such as speed, altitude etc as well as other factors like outside temperature and pressure during the flight. The data are sampled many times per second, and FDR can store time traces of 15 hours or more. CVR records all sounds made in the cockpit, practically the pilots' communications with each other and over the radio, as well as alarms and warning sounds. For privacy protection, CVR usually stores data of two hours and not more. When an aircraft crashes, it is recovery of the FDR and CVR and analysis of the stored data which enables the investigators to piece together what happened to the ill-fated flight.

For night-time operations, aircraft come equipped with lots of lights. A steady green light at the starboard wingtip, a steady red at the port wingtip and a steady white at the tail constitute the navigation lights which enable other pilots and ground observers to estimate the position and orientation of the aircraft. They are kept on throughout. Flashing red beacon lights on the top and bottom of the fuselage warn ground personnel that the engines are on; they are kept on whenever the engines are running. Flashing bright white strobe lights on the aft side of the wings near the tips attract attention of other pilots, and are used near airports, where traffic is more dense. Taxi lights, runway turnoff lights and landing lights are steady, medium to extremely intense yellow lights mounted on the fuselage, illuminating the ground. Usually, a night-time arrival first appears in the distance as a bright yellow speck – that's the landing light. Logo lights are mounted on the horizontal stabilizer and illuminate the airline's logo which is generally painted on the vertical stabilizer.

§07

Operational quantities, system of units. Here we look at the scientific quantities related to aircraft operation, such as mass, speed, thrust etc. For each quantity I will also specify the units we shall use in this version of the Article. In the longer run, it is my hope to have parallel versions in different sets of units, for example all SI, all aviation, Imperial Units etc. But until such versions exist, this combination – the most intuitive one in my view – is what we'll have to make do with.

The issue of units presents us with a choice because air transport uses a mixture of SI and non-SI units, while scientific calculation uses mostly SI units (there are some exceptions in engineering disciplines in the USA). Here, we shall *perform all calculations in SI*. That way, we won't have to keep track of dimensions of individual quantities; if everything entering the calculation is SI, everything exiting it will be SI as well. While *reporting or plotting answers* however, we shall use a mixture of SI and non-SI, to achieve at least partial alignment with the piloting community, as well as maximize intuition. I give the details of this mixture below.

Mass

We shall use the *kilogram* exclusively. The masses involved in aviation are typically thousands of kilograms, so we shall report them in tons, where one ton denotes exactly one thousand kilograms. To

develop intuition regarding airplane mass, I list in Table 01 below the masses of some of the most common airliners today. The data is taken from Wikipedia [03].

Aircraft	Minimum mass (tons)	Maximum mass (tons)
Boeing 737-800	41	78
Airbus A321	49	94
Boeing 757-200	58	116
Concorde	79	185
Airbus A350-900	140	283
Boeing 777-300ER	168	352
Boeing 747-400	187	413
Airbus A380-800	285	575

Table 01 : *Minimum and maximum masses of some modern airliners.*

The minimum mass I've listed here is what is called the **OEW or operating empty weight** – what the plane weighs without passengers and just enough fuel to make it off the ground and back. The maximum mass of Table 1 is the **MTOW or maximum takeoff weight** – the highest permissible mass which the plane can have and still takeoff safely. MTOW operation usually occurs when an aircraft performs a flight at the limit of its range (fuel tanks fully filled) and with maximum passenger capacity. The Boeing 777-300ERs operated by Air India for nonstop flights between India and USA typically take off close to MTOW.

The jargons OEW and MTOW also reveal a convention in aviation – use of the word "weight" to mean "mass". This convention is so deep-seated that I will appear insufferably pedantic if I don't give in to it. At the same time, there will be occasions when "weight" will really refer to $-mg\hat{\mathbf{z}}$ rather than m. The meaning will always be clear from context. Moreover, to avoid confusion, I will (*a*) use "mass" whenever there is a question of potential ambiguity, and (*b*) completely refrain from measuring forces in gravitational units (see Force later in this Section). ■

Horizontal distance and dimensions

For horizontal distance we shall use *metres* (short distance) and *kilometres* (longer distance) exclusively. For aircraft dimensions, metres will be our preferred unit. Because feet (ft) are still very popular for measuring human heights and dimensions of houses, and because the dimensions of an aircraft are comparable to these in value, I shall occasionally give the feet equivalent of the aircraft dimension also. A typical runway length is 3000 m; primary runways at the largest airports are generally 4000 m or longer. Representative aircraft range is 5500 km for a Boeing 737 (600 to 900 series) to 18,000 km for an Airbus A350-900 ULR. Representative aircraft dimensions are 38 m (125 ft) length and 36 m (118 ft) wingspan for an Airbus A320 and 74 m (242 ft) length and 65 m (213 ft) wingspan for a Boeing 777-300ER.

It is near-universal practice in air transport to measure distances in nautical miles (NM, capitalization essential to avoid confusion with nanometre) where 1 NM equals 1852 metres exactly. These are generally referred to as "miles", with "nautical" being implicit (note that 1 NM corresponds to about 1·15 statute or road miles). In the olden days of aviation, the use of nautical miles aided navigation since 1 NM due north-south corresponds to exactly one minute of latitude while 1 NM due east-west corresponds to $\sec\theta$ minutes of longitude where θ is the latitude. Since latitudes and longitudes of the source and destination were known precisely, while the plane's instantaneous position in the sky was not, pilots often flew directly along the cardinal directions and used the distance travelled to keep track of their (approximate) current coordinates. Today, when radar and global positioning system (GPS) give the position of each plane correct to a few centimetres, the nautical mile no longer has relevance. Airline companies also love the nautical mile because, measured in this unit, the distance flown by a passenger and hence the reward points added to his/her account work out to the smallest value. **ICAO or International Civil Aviation Organization**, a supranational entity in charge of regulating aviation worldwide, recommends using kilometres for distance [04] but the recommendation is non-binding. For this Article, I have gone with kilometre since (*a*) it is familiar to a much wider audience, myself included and (*b*) it is the ICAO future recommendation, so I'm not entirely violating an aviation convention. The approximate conversion factor is 9/5 while

converting from NM to km and 5/9 the other way around (same as the Centigrade-Fahrenheit conversion); this incurs a 3 percent error which is acceptable for most practical purposes. ■

Vertical distance

There are two words which denote vertical distance – "altitude" refers to the vertical distance between the aircraft and mean sea level (MSL) while "height" refers to the distance between the aircraft and the ground which it is overflying. For reporting both, we shall use *feet*. One foot is defined as 0·3048 metres exactly; the simpler conversion 3 metres for 10 feet (NOT 1 metre for 3 feet!) is accurate to 1·5 percent. Foot is the primary choice for measuring altitude in worldwide aviation and, unlike the nautical mile, it has relevance today. If two cruising airliners are at the same horizontal location, then the minimum vertical separation between them such that they don't interfere aerodynamically with each other works out to be close to but less than 1000 feet. Hence, 1000 feet of vertical separation between co-located airliners achieves safety without wasting space, and aircraft are required to cruise at altitudes which are exact multiples of 1000 feet. Under the **RVSM or reduced vertical separation minima** scheme, aircraft whose velocity have a westward component must fly at even thousands of feet while aircraft whose velocity have an eastward component must fly at odd thousands (if you haven't already, next time you fly as a passenger check that this is holding true). Cruising altitudes are also known as **flight levels**, in which case they are designated by the letter "F" or the word "FL" followed by the altitude divided by 100; thus the altitude of 8500 feet (not a bona fide cruising location but can be used for initiating a course change etc) is called F085 or FL 085 and the altitude of 31,000 feet is called F310 or FL 310.

Vertical distance can be measured using three types of altimeters. GPS altimeter measures the altitude above MSL. Radio altimeter measures the height above the underlying ground. Finally, pressure altimeter measures the outside atmospheric pressure and converts it to altitude. This is the type of altimeter which is mandatory to be installed on all aircraft and used during flight. By law, aircraft cannot set altitude using GPS or radio altimeters. Now, to convert pressure to altitude above MSL, the altimeter needs a value of pressure at MSL. This baseline pressure is inputted by the pilot. When close to the ground i.e. during takeoff and landing, the pilot must input the value obtained from the origin or destination airport. Thus, during these parts of the flight, the pressure altimeter shows the aircraft's true altitude. At higher altitudes however, the pilot must input as MSL pressure the fixed value 101·325 kPa or 1·01325 bars corresponding to the international standard atmosphere, never mind what the actual MSL pressure is at the location which the aircraft is overflying. This means that the altitude as per the pressure altimeter may not be the true (i.e. GPS) altitude of the aircraft. For instance, the standard atmosphere features a pressure of 22·600 kPa at 36,000 ft. Now, suppose the aircraft is flying through a region where the MSL pressure is actually 104 kPa and 22·6 kPa is hit at 37,200 ft. Then, the plane with altimeter set for 36,000 ft based on standard atmosphere will actually be at 37,200 ft MSL while passing this region. This is alright since the purpose of altimeter is not to ensure flight at an exact number of feet above ground but to ensure vertical separation between aircraft, and, at least in the cruising altitudes, a pressure altimeter always reports a lower pressure for a higher altitude. The altitude at which the pilot must reset the altimeter to shift between local baseline and standard atmosphere baseline is called the **transition altitude**. Different airports have different transition altitudes, typically ranging from 3000 ft above runway altitude to 18,000 ft above MSL. To maintain safety, it is imperative that you remember to reset your altimeter baseline every time you pass through the transition altitude. All flight levels are defined above the transition altitude.

As with the nautical mile, ICAO has a non-binding recommendation [04] to discontinue the use of feet and transition to metres. In my opinion, this recommendation is impractical – the metric flight levels will have to be spaced out by 300 m, and pilots and air traffic controllers will become busy calculating whether 9600 m and 11,800 m are acceptable altitudes for cruise. If in a future age, aircraft become so large or so fast that 1500 feet of vertical separation becomes necessary, then that will be a good time to redefine the flight levels in multiples of 500 metres. Till then, feet are appropriate, and are what we use in this Article. ICAO's clubbing the foot with the nautical mile in its list of 'obsolescent' units will only ensure that the latter remains on the shelves long past its sell-by date. ■

Speed

Our choices of distance units lead naturally to those of speed. For horizontal speed, we use *km/hr* (which is also the ICAO 'recommended' unit). The conversion to SI is 1 m/s = 3·6 km/hr exactly. For vertical speed (i.e. climb or descent rate) we use *feet per minute (fpm)*. The SI conversion is 1 m/s = 196·85 fpm, so the approximate conversion factor of 200 incurs only 1·5 percent error. As for the total speed of the aircraft, in most situations the overwhelming contribution comes from the horizontal component, so we shall report that in km/hr as well. Typically, cruising speed is about 900 km/hr while takeoff speed is approximately one third of that; 3000 fpm corresponds to an aggressive climb, of the kind typically used immediately after takeoff. For Concorde, the typical horizontal and vertical speeds were 2150 km/hr and 5000 fpm or more but it was a different kind of plane altogether. The aviation industry standard for measuring speed is knots*, where one knot denotes one nautical mile per hour. 1 knot equals 1·852 km/hr exactly, so that 1 m/s equals 2 knots to 3 percent error.

* Despite sounding similar to "naut", the word "knot" is etymologically unrelated – it comes from the knots made at regular intervals on a floating rope which was used centuries ago to measure the speed of boats.

As with altitude, speed measurement also has a few subtleties. We have already defined the airspeed (§05; to repeat, it is the magnitude of the aircraft's velocity vector with respect to the surrounding air). Let us now call it the **true airspeed** for a reason to become clear shortly. The magnitude of the aircraft's velocity with respect to the ground is called **ground speed**. The two are unequal if there is a wind. Now, the airspeed indicator in the cockpit measures speed in terms of pressure on a tube, so the reading also depends on the density of the air through which the plane is flying. This reading is called the **indicated airspeed**. Indicated airspeed is defined to equal true airspeed when the air density corresponds to MSL in the standard atmosphere; at high altitudes, where air density is less, indicated airspeed is less than the true airspeed. Correcting the indicated airspeed for known errors in installation of the speedometer, we get the **calibrated airspeed**; on modern jetliners, this calibration step is generally unnecessary. In addition to density, if we also account for the compressibility of the air, then we get something called **equivalent airspeed**. The speed of the aircraft expressed as a percentage of the speed of sound is called **Mach number**. Unless otherwise stated, Mach 1 corresponds to 1060 km/hr. This is a lot of speeds. In this Article, we'll need only true air and ground speed, for more general situations, the indicated airspeed is also very important. We'll see why this is so in §28. ■

Force

SI wins this one – *Newton* is the only unit we shall use. As with masses, the values involved are in the thousands or more, so the kilo form will be the most convenient. As I have already mentioned while discussing mass, we shall give a wide berth to kgf (and we won't even consider poundweight or lbf). The weight of the aircraft in kN is ten times its mass in tons to 2 percent error, so the conversion here is easy. More difficult to handle is engine thrust, which has a regrettably common tendency of appearing in lbf. Indeed, those of us, myself included, who have at all paid attention to engine thrust values are almost certain to have absorbed them in these units. As late as 2013, the British company Rolls Royce, manufacturing engines for the European company Airbus under an exclusive contract, named the products Trent XWB 84 and XWB 97, the numbers referring to their takeoff thrust measured in thousands of lbf. Even approximate conversion from lbf to kN is not easy – 4 kN corresponds to 900 lbf. How then to wean or kick an lbf habit ?

The most practical solution, and the one I myself have adopted, is perhaps to proceed similarly to the kg masses – memorize the kN thrusts of a few standard engines and then think of other engines in terms of this scale. To facilitate this, I am giving below the TOGA (maximum permissible) thrusts of some representative engines. In the first column, I have first given the engine name as most people are familiar with, and then within brackets stated the sub-class, phylum etc which actually possesses the thrust I've listed (different variants of the same engine have different thrust ratings, usually within a narrow range). Data are taken from the type certificates issued by the European Aviation Safety Agency [05].

Engine	Aircraft	TOGA thrust (kN)
CFM56 (-7B24)	Boeing 737-800 (2x)	108
IAE V2500 (V2533-A5)	Airbus A321 (2x)	141
Olympus 593	Concorde (4x)	142 dry, 169 wet
Rolls Royce RB211 (-524HX)	Boeing 747-400 (4x)	265
Engine Alliance GP7000 (7270)	Airbus A380 (4x)	332
Rolls Royce Trent XWB 84	Airbus A350-900 (2x)	375
General Electric GE90 (-115B)	Boeing 777-300ER (2x)	514

Table 02 : *Kilonewton thrusts of some common aircraft engines. For Olympus 593, "dry" means full throttle without afterburner while "wet" means full afterburner.*

As you can see by comparison with Table 1, the biggest aircraft are powered by four medium-sized engines; slightly smaller aircraft often get two of the biggest engines.

We now get a chance to take on our first quiz question, Q06. From Tables 01 and 02, we find the following thrust-to-weight ratios.

Aircraft	A321	Concorde	B777	B747	A380
TTW ratio	30·4	37·3	29·8	25·7	23·6

Table 03 : *Thrust-to-weight (TTW) ratios of some airliners.*

Clearly, 25 percent is the correct answer to Q06. Right now, we answered the quiz question in a general knowledge kind of way; later we shall have ample opportunity to examine the consequences of the 25-30 percent thrust-to-weight ratio. It is no surprise that Concorde has the highest value among all the aircraft considered. That apart, the twinjets tend to have a higher value than the quadjets. This is because all transport aircraft are designed to be able to fly with one engine failed. One failure on a quadjet reduces thrust by 25 percent while one failure on a twinjet reduces thrust by 50 percent, so twinjets have to have more powerful engines.

Even though Concorde emerged the winner in Table 03, you might still be wondering that its thrust-to-weight ratio is rather low. After all, it is more than 2·5 times faster than A321; how can it be only 25 percent more powerful ? This is because the TOGA rating is with the aircraft static. As the speed increases, the thrust of all engines decreases – power is thrust times speed and the engine's power output has to be bounded. With Concorde's engine, this decrease is much more gradual than with A321's engine. Hence, even though Concorde exceeds A321 by only 25 percent at zero speed, it exceeds by maybe 100 percent* at 800 km/hr. This enables Concorde to smash through the sound barrier while A321 maxes out well before it. The really high thrust-to-weight ratios – 100 percent or greater – are seen in fighter jets which are designed to pull fancy manoeuvres requiring huge thrust. Concorde was not called upon to perform such feats, and was designed accordingly.

* I don't know the exact number by which Concorde exceeds A321 in terms of thrust-to-weight ratio at 800 km/hr. Suffice it to say that the number is very great.

Thrust is shown to the pilot neither as an absolute kilonewton value nor as a percentage of the TOGA value. Rather, cockpit instruments show thrust in terms of either percentage N1 or engine pressure ratio (EPR). N1 refers to the rotational speed of the low pressure rotor, and percent is defined relative to a manufacturer-defined baseline. 100 percent N1 may or may not correspond to TOGA power – for example [05], on GE90-115B the TOGA rating is 110 percent N1 (100 percent being 2355 rpm) while on Trent 900 the TOGA rating is 97 percent N1 (100 percent being 2900 rpm). The increase of thrust with N1 is definitely faster than linear; so far I have not found a good graph or equation connecting the two. Reference [06] contains a picture which is physically plausible but whose provenance I haven't been able to establish. Since thrust decreases with speed, the relation between N1 and thrust also depends on the speed of the aircraft. EPR is the ratio of the pressures forward and aft of the engine – it is a number between 1 and approximately 2, with thrust being directly proportional to EPR–1. In this Article however, we will not refer to N1 or EPR but use percentage thrusts, with percentage being relative to the TOGA value. ■

Angle

For all angles, we use the *degree*, symbol °. The SI conversion is 1 radian equals 57·30°. Degree is near-universal aviation convention, and typical pitch and attack angles can be as small as a couple of degrees, which are quite difficult to express in radians. As for the sign, we treat a rotation as positive if it is counterclockwise as viewed from the positive side of the axis of rotation. This disagrees with the aviation convention of measuring angles clockwise positive. Accommodating that convention shall mean a redefinition of cosines and sines, rotation matrices and heaven knows what else – in short, an obscene amount of labour and an extremely high probability of calculational mistakes. To avoid ambiguity as a result of our sign convention, we'll use suitable terminology, which I shall introduce in the appropriate Sections. ■

Other physical quantities will either not appear in this Article or play at best a peripheral role during model derivation and manoeuvre analysis; for all those we shall use SI.

§08 **Types of pilot, roles of the two pilots.** A small amount of general knowledge regarding pilots goes here for want of a more appropriate location. When a student pilot learns to fly, the first licence which he acquires is the private pilot licence or PPL. This enables him to take an aircraft into air, so long as he doesn't earn money from this activity. The types of aircraft which he can fly with a PPL are also specified in the licence or its supplementary documentation – usually they are propeller planes with one internal combustion engine. The next step up from a PPL is a commercial pilot's licence or CPL. This enables the holder to fly air taxis, charter aircraft, business jets and the like, but not airline flights. The default aircraft which a CPL holder is certified to fly is again a flying car; for more sophisticated aircraft, he needs to have the appropriate type rating, obtained after training and examination. Finally, the most advanced qualification is the air transport pilot licence or ATPL. Holders of this licence are inevitably trained on jets and are certified to fly for passenger airlines.

In the last paragraph you may have noted my use of the pronoun "he" to denote the pilot. This is for practical convenience. The pilot will appear repeatedly throughout this Article and every time if I have to say s/he and him/her then it will appear cumbersome. It is a fact that the bulk of air transport pilots are men – India has the world's highest ratio of female pilots at a measly 15 percent [07]. Majority wins the gender pronoun contest here, with apologies to female pilots.

Today's airliners are all operated by two pilots (ultra-long-haul flights have four, but only two are active at any time). The higher ranked one is the captain, left hand or no. 1 pilot, who always sits on the left in the cockpit. The lower ranked one is the first officer, right hand or no. 2 pilot, who always sits on the right in the cockpit. Both are ATPL holders, and on any given flight, *either one may be doing the actual flying i.e. manipulating the controls*. That pilot is referred to as the pilot flying. The other pilot monitors the progress of the flight and handles radio communications; he is called the pilot monitoring. Airliners are designed, and pilots certified, such that any one pilot may fly the whole aircraft on his own in case the need arises. The presence of two persons reduces the workload of each and quadratically reduces the probability of human error. Although the captain is the higher-ranked pilot, an ideal cockpit should see the two pilots operating as a team rather than as master and servant. All flight-related decisions should be the result of discussion and consensus, and not the junior's meek or grudging acceptance of his senior's corner-cutting. As we have already seen in Fig. 06, both pilots have equal access to the stick, rudder pedals and other controls; each has the authority to grab them and override the other one should the latter be compromising the safety of the flight. To achieve the proper intra-cockpit relationship, the designations left-hand and right-hand (or no. 1 and no. 2) pilot are perhaps more suitable than captain and first officer, which are anyway carryovers from naval operations. **Crew resource management** refers to the area of personnel training which deals with the relation between the two pilots.

§09 **Environmental impact of aviation.** This material is unpleasant but necessary and I'll keep it as brief as possible. There is no denying that aircraft have a significant contribution to environmental pollution on account of the huge carbon dioxide and other greenhouse gas emissions from their powerful engines. As per the International Energy Agency [08], one passenger flying one kilometre results in emission of about

150 g of CO_2. Values for other transport modes are 10 g for an efficient train, about 50 g for a bus and anywhere between 60 g and 300 g for a personal car. While this last statistic doesn't say good things about planes, it certainly says something about cars. At least today, alternative or renewable energy sources for powering aircraft do not appear realistic. Hence, flying is a pleasure which is best enjoyed in moderation.

A second adverse impact of aviation on environment is the phenomenon of bird hits, where aircraft ram into birds near airports and in other low-altitude regions. These impacts, while sometimes damaging for the aircraft itself, are invariably fatal for the birds. Various measures such as constructing effigies, spraying gases, making suitable noises etc are adopted at airports themselves but currently there are little or no measures in the airspace along the arrival and departure paths. With the improvement of drone technology, it may be possible to use drones to report sightings of birds along human aviation corridoors and take appropriate action such as chasing the birds away, recommending a deviated flight path or itself taking the hit in cases where that extreme measure helps.

Mitigating these adverse aspects of aviation is one direction in which research is currently progressing and more is necessary in future. That however is a good topic for a different Article. This Article is about the positive side of aviation, about the amazing science and technology which has made it possible for us to fly. Our focus here will be to understand this technology better and hence use it better.

B. INTRODUCTION TO NAVIGATION

There are two protocol by which pilots ensure that their aircraft fly to their destinations instead of getting lost in the air. They are called VFR or visual flight rules and IFR or instrument flight rules. **ATC or air traffic control** is the agency which guides and regulates the progress of almost all flights including every single transport flight – we shall need this definition in what follows.

§10 **VFR or visual flight rules – course maintenance.** VFR refers to the mode of flying where the pilot uses his eyesight to ensure that the plane is going where he wants it to go. Eyesight also serves to achieve separation from other nearby aircraft. To achieve VFR flight, the visibility must be above certain well-defined minima. Typically, line of sight must extend for at least 5 km, and the aircraft must maintain a minimum distance of 500 to 2000 ft away from clouds (local regulations prescribe the exact numbers). As immediately follows, flying VFR through a cloud is unconditionally prohibited. Weather conditions permitting VFR are called **VMC or visual meteorological conditions**. VFR is allowed at night, provided that there are lighted landmarks on the ground all along the flight path. VFR is most commonly used for **general aviation (GA)**, which refers to civil aviation for non-commercial purposes. Typically, general aviation includes sport and recreational aviation, and is performed in a propeller plane powered by a car engine. Depending on the flight path, a VFR flight may or may not require prior clearance from and en route communication with ATC.

Navigation in VFR is a pretty simple affair. Before starting the flight, you have to have a precise idea of the distance and direction from your source to your destination (or, for a longer flight, the distance and direction between each of a set of successive landmarks which you decide to overfly). Direction is of course an angle, for whose measurement we need a suitable baseline. The universal convention is to choose this baseline as *local magnetic North* – angles are measured clockwise positive from this reference direction. Magnetic North is different from true North – the angle *from* true North *to* magnetic North, measured clockwise positive, is called the magnetic variation or **magnetic declination**. Magnetic declination everywhere on the Earth's surface is widely available in the form of tables; you must use these to convert direction from true to magnetic. Given the measurement convention, two angles are actually relevant for VFR navigation. The first is the **track**, which is defined as the angle made with respect to magnetic North by the horizontal projection of the instantaneous tangent to the flight path (i.e. the aircraft's velocity vector) as observed from the ground frame. The second is the **heading** which is defined as the angle made with respect to magnetic North by the horizontal projection of the straight line running from the tail of the

aircraft to its nose. In simpler but less precise language, track is the map direction in which the plane is flying while heading is the map direction which the plane is facing.

Track and heading are equal when there is no crosswind, i.e. no horizontal wind perpendicular to the heading. If there is a crosswind however, then the two are no longer equal. This is because the velocity of the aircraft relative to the ground is the vector sum of the velocity of the aircraft relative to the wind and the velocity of the wind relative to the ground. The first one is directed along the heading; should the second have a perpendicular component, then the ground velocity vector will also acquire this component, and its direction, the track, will no longer equal the heading. All cockpits display the heading using a magnetic compass or equivalent instrument; a typical GA aircraft does not display track. However, an easy calculation using the parallelogram of velocities can enable the pilot to determine the track given the true airspeed and heading, and the wind speed and direction. These latter must be known from the source, destination or en route airports; GA aircraft typically do not feature a wind speed indicator on board. Note that wind direction is always given as which way the wind is *coming from* – thus wind 270° means that it is blowing from the West. Pilots usually have calculators which perform the track calculation for them. Navigation using distance and direction alone is called dead reckoning – it is the most basic navigational procedure which pilots learn during their initial training. In this procedure, errors compound with time, so it is essential that the flight path be periodically corrected with visual reference to known landmarks. VFR can also use navigational techniques other than dead reckoning – since VFR is not what is used in the bulk of aviation, these are no longer of interest here.

§11 **VFR – departures and arrivals.** To ensure safe operation, VFR aircraft often have to follow a particular process when departing from or arriving at an airport. This is especially true for GA airports which may or may not be monitored by ATC. These airports have a **traffic circuit** or traffic pattern*, consisting of a large rectangle whose one side is the runway. The circuit is typically located at an altitude of 1000 ft above the airport. An example traffic circuit is shown in Fig. 01 below. This image is taken from Ref. [01].

* Brit vs Yank again. British English favours "circuit", American "pattern". In this case, "circuit" is more descriptive of the concept.

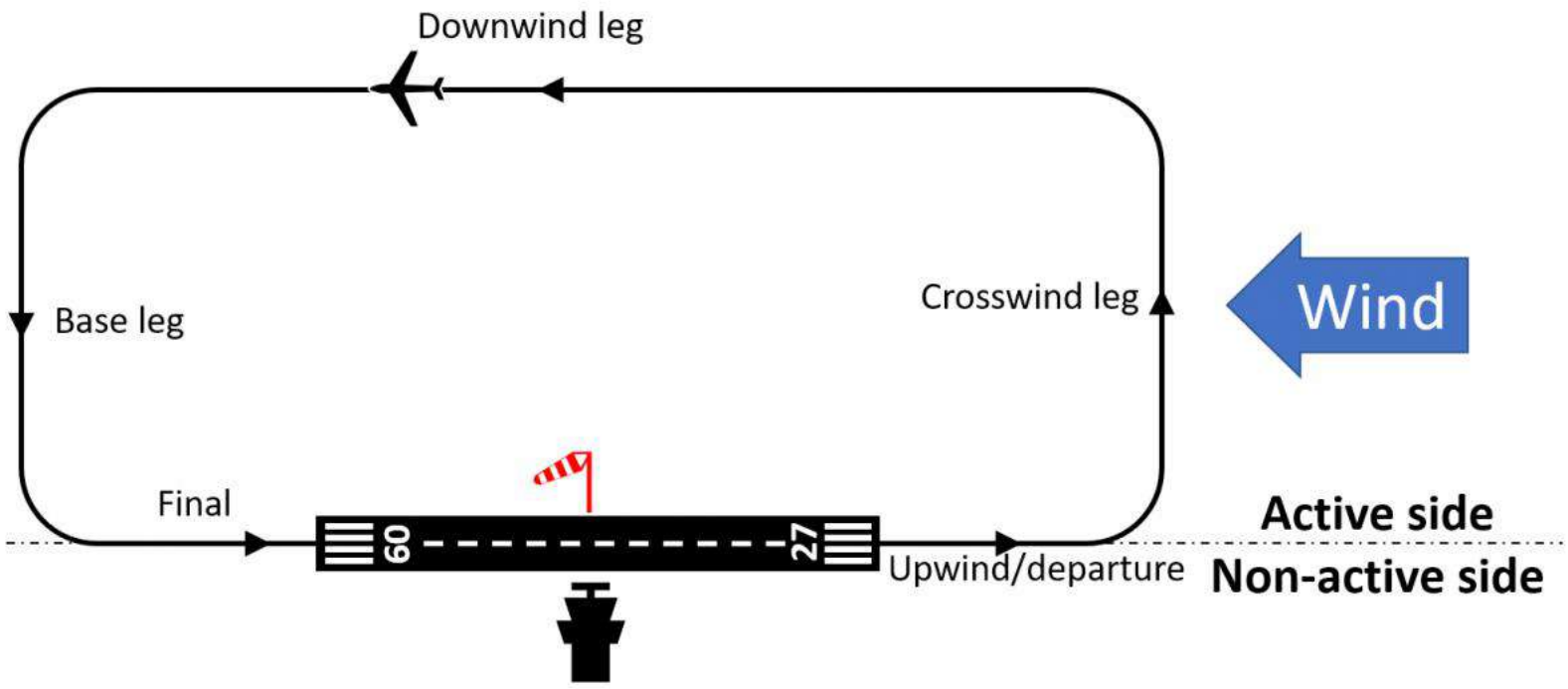


Figure 01 : *Typical traffic circuit around a runway. The original figure [01] carries appropriate permissions for this usage. The runway is oriented East-West. Takeoffs and landings occur due East if the wind has an Easterly component and due West if the wind has a Westerly component. For this reason, the legs of the circuit are labelled relative to the wind. If there is no wind or dead North-South wind, then any one runway direction is chosen for operations; this choice is determined by regulation. In this case too the names for the legs of the circuit remain unchanged. The orange and white thing is a windsock, a device which indicates the strength and direction of the wind.*

Arriving aircraft join the circuit at the downwind leg, then turn 90° onto the base leg and then 90° more onto the final leg. Once on this leg, they start descending, visually aiming for a particular point on the runway where they intend to land. At many airports, the runways are quite short and the desired point is the base of the runway. The number of the runway is written at this point, so a landing which uses the full

length of runway is sometimes called "landing on the numbers". A **straight-in approach** is one which bypasses the traffic circuit and intercepts the final leg directly. This requires ATC authorization but saves time compared to flying in the circuit. Straight-in approach is routine procedure when a larger-than-GA aircraft is making a VFR approach of a busier-than-GA airport; we shall cover this case under IFR departures and arrivals.

§12 **IFR or instrument flight rules – course maintenance.** IFR – in other words, using radar – is how real planes fly. The word "instrument" here refers not just to the airspeed indicator, altimeter etc but to a different set of navigational instruments present in the cockpit. These instruments enable aircraft to fly at night, in cloud, in low visibility conditions and at speeds where maintaining visual separation becomes a joke. Every single air transport flight in the world is equipped with IFR instruments and operates on IFR; exceptions to IFR operation are a handful in number and come with pages of documentation. The transition from VFR to IFR is considered difficult by some student pilots; nevertheless, mastering the technique opens up a huge range of possibilities which are out of bounds for VFR operations alone. IFR also increases safety since these flights are always monitored by ATC, automatically ensuring separation, and since they also don't need emergency avoidance of sudden adverse weather events. Weather which requires IFR flight is called **IMC or instrument meteorological conditions**.

At the heart of IFR navigation are two radar devices called **VOR or very high frequency omnidirectional range** and **DME or distance measuring equipment**. These are mounted on the ground, at intervals of dozens to hundreds of kilometres along the routes which aircraft are intended to use. All major airports have a combined VOR/DME on site; some are built at other strategic locations also to facilitate navigation. VOR and DME both transmit radio waves in a cylindrical region having radius several hundred kilometres on the Earth's surface and height well exceeding that of the highest flight level. These waves are picked up by the instruments on aircraft within the detection range. Picking up the VOR waves, the flight instruments calculate and display to the pilot the angle made with respect to mag North by the (horizontal projection of the) line joining the VOR to the aircraft's current position. Of course, VOR must operate over distance scales where magnetic declination is constant and Earth's curvature negligible. Picking up the DME waves, the flight instruments calculate and display the distance between the DME and the aircraft. To be accurate, DME measures the straight-line distance between the DME (on ground) and the plane (in air) and not the horizontal distance; the altitude is either ignored or corrected for, depending on the fanciness of the equipment on board the aircraft. When VOR and DME are collocated, which they usually are, the plane picks up the signal to know its exact coordinates on the map relative to the location of the VOR/DME. When there are neighbouring VOR/DMEs, they each transmit radio waves at different frequencies so that the pilot can tune in to one or more of them by selecting the appropriate frequency/ frequencies. These frequencies are also called channels.

We know that the shortest distance between any two points on Earth's surface is the great circle joining them*. When the points are close together, like for many domestic flights in India, the great circle reduces to a straight line on the map. If it were permitted, a flight would have preferred to travel along a great circle (or straight line) between its origin and its destination, to minimize time and fuel. IFR however does not permit such a route. What it does permit is to travel along certain fixed and designated corridors in the sky which are called **ATS routes** (ATS means air traffic service). This is just as in road or railway navigation – to travel from Delhi to Kanpur, you would have wanted to take a train or a car along the straight line route joining them but the railway happens to run via Aligarh and Hathras, significantly South of straight line while the road (National Highway 19) happens to run parallel or even farther South. Unlike in road or rail where 'Up' and 'Down' lanes are separated laterally, the opposite directions of ATS routes are in general separated vertically – we have already seen the concept of RVSM in §07, and planes maintain the appropriate flight levels while traversing a given route in the appropriate direction. This raises the question, how do we define ATS route ? It is not that there are highways or railway tracks in the sky.

* This mathematical statement is in fact the single most difficult to prove assertion in this entire Article. It requires differential geometry, while the maths that we'll need and use don't even come close.

What we do is, we define ATS route in terms of VORs. At its simplest, the straight line joining two adjacent VORs becomes an ATS route. To stay on the route, the aircraft must maintain the prescribed angle from the VOR at either end. By triangulating using both the VORs or one VOR and a DME, the flight instruments can automatically calculate the deviation from the route, and tell the pilot which way to go to stay on route. In Fig. 02 below, we show a section of ATS routes in the airspace above northern India.

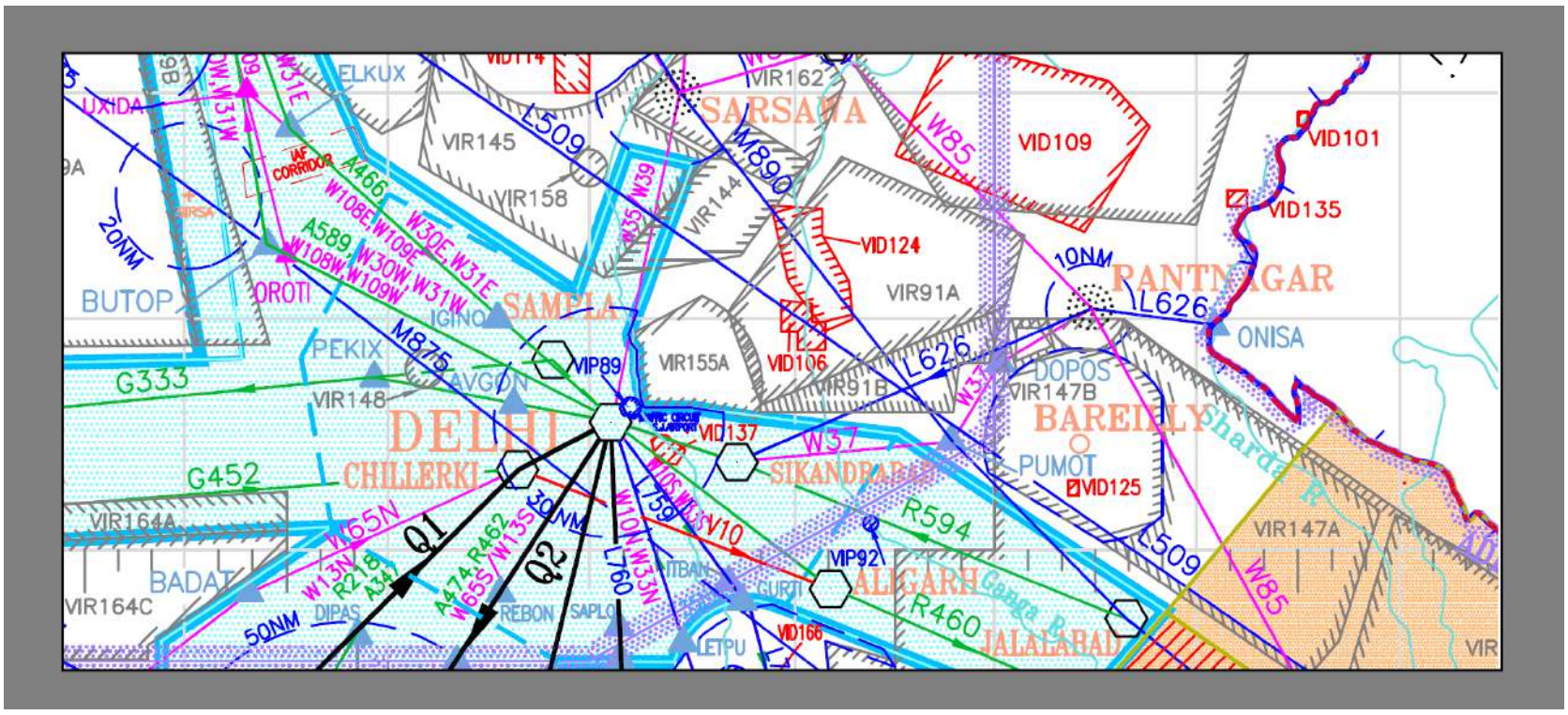


Figure 02 : *ATS routes in the airspace above North India.*

The hexagons here denote VOR/DME stations – we can see a clump of them around the city of Delhi. These are named after the cities or villages in which they are located – Delhi is at the airport itself (the main passenger airport, ICAO code VIDP, see §15) while Sampla and Chhilerki are nearby villages, shot to international fame by housing these equipments. Sikandrabad, Aligarh (same as the one in the last paragraph) and Jalalabad are cities in Uttar Pradesh, which also house VOR/DME devices. The green lines on the map denote international ATS routes. East of Delhi, we can see R460 running from Delhi to Aligarh VOR/DME and then continuing eastwards (towards Lucknow VOR/DME, not shown), while R594 runs from Delhi to Sikandrabad and thence to Jalalabad. Note that an ATS route can change direction at every VOR. West of Delhi, the situation is more interesting. A466 and A589, both favourites of international traffic to and from USA and Canada, do not run westwards to other VOR/DMEs but change directions at blue triangles named ELKUX and BUTOP. What are these ?

Before answering this question, I must introduce a further terminology. A **radial** for a particular VOR is defined as a straight line on the map which has one end at that VOR. Radials are indexed by the angle which this line, treating the VOR as origin, makes with magnetic North – angles are measured clockwise positive. Thus, R460 between Delhi and Aligarh corresponds to Delhi radial 126 (the degree is understood and generally not written). Note that in the 3-dimensional space near the VOR, a radial is actually a *plane** since it is valid at every altitude. When moving away from a VOR along a radial, the aircraft's track is the same as the radial, but when moving towards a VOR along a radial, the track is the radial plus or minus 180°. Opposite tracks, i.e. values separated by 180°, are called reciprocal. The aircraft's heading is also close to the assigned radial when moving away from the VOR (outbound) and close to the reciprocal of the radial when moving towards the VOR (inbound).

* A geometric plane, not an airplane.

Now coming to the blue triangles in Fig. 02, these are **waypoints**. A waypoint can be defined in any of two ways : (*a*) a point on a given radial at a given distance from a particular VOR/DME, or (*b*) a point at the intersection of two given radials from two VORs (the DME is not required for this definition). Thus, waypoint IGINO on the map corresponds to distance 74 km on radial 312 from Delhi (all radials and distances are taken from Ref. [02] rather than from official diagrams, to which I don't have access; the numbers may be slightly inaccurate). Waypoint ELKUX on the other hand, where A466 has a kink, is

defined as the intersection of 312 radial Delhi and 159 radial Amritsar VOR/DME (North-West of Fig. 02 map boundary). A pilot located at the northern boundary of Fig. 02 and flying into Delhi along A466 tracks radial 159 Amritsar by tuning the first set of navigation instruments to the Amritsar channel. Simultaneously, he tunes the second set of navigation instruments to Delhi channel and monitors the aircraft's radial with respect to that VOR. When that radial approaches close to 312, i.e. he is approaching ELKUX, he lets go of Amritsar and performs a left turn to intercept that radial from Delhi, this way staying on A466. Note that the plane's track is now 132°. Near busy airports, airways are often made unidirectional – thus, near Delhi, A589 is an 'Up' route, used by flights leaving it while A466 is a 'Down' route, used by flights arriving into it. Northwest of waypoint ASARI near Moga, Punjab, A466 is bidirectional and can be used by all traffic.

Apart from the ones shown, there are hundreds of other waypoints in the airspace depicted on the map. Many of them are close to Delhi and serve to guide departing and arriving traffic. Waypoints are programmed into the flight computer ahead of the flight, and the autopilot itself performs the task of tuning and tracking the appropriate VOR/DMEs and turning the aircraft so that it stays on its planned flight path. Most waypoints have five-letter all-capital names like IGINO and BUTOP which are in general not real words in English or any other language but can nevertheless be pronounced as words. Sometimes, the names are real words. For example a waypoint at the India-Pakistan border has the name TIGER while a waypoint near Guna, Madhya Pradesh has the name PUKES. Two more word-waypoints, this time drawing on Hindi words, are AKELA (alone) near Ringas, Rajasthan and DOSTO (friends) near Chalthan, Gujarat. Waypoints must be unique within a local region and preferably within a country; globally however, there are duplicate names. It beats me why waypoints which are close to a city or village cannot be named after the corresponding place, since those names are also familiar to people outside of aviation and easily convey where the waypoint is. But this is the convention and we have no choice but to follow it.

An IFR **flight plan**, filed much before the flight itself and approved by ATCs of all concerned regions, consists of a sequence of waypoints which the flight intends to cover en route. Usually, the filed plan starts from a waypoint some distance away from the origin and ends at a waypoint some distance away from the destination. The start and end points are chosen to match the flight path, thus, Air India 101 from Delhi to New York usually files BUTOP as the first waypoint, while Air India 102 on the return leg has IGINO as the last. The transitions between the boundary waypoints and the source and destination airports are handled by the instrument arrival and departure procedures, which we cover in the next Section. The flight plan in addition contains the altitude which the aircraft desires to maintain along the route – ATC might well assign it a couple of thousand feet higher or lower.

Yet another essential component of IFR flight is **transponder**. This is a radio device which enables ATC to identify the flight on its screen. Each aircraft within a particular ATC territory is asked to set its transponder to a particular number, called squawk. This number enables ATC to track the aircraft easily. There are three special squawks which are used by aircraft in emergency situations. One is 7500, which is when the aircraft has been hijacked. The second is 7600, when there is a complete failure of radio communications. The third is 7700, when the aircraft has declared emergency due to technical malfunction or other reason. Transponder is also the basis for the **TCAS* or traffic collision avoidance system** present on modern aircraft. This automatically tracks the airspace near a particular aircraft and determines whether there is threat of a collision. If yes, it also tells the concerned pilots what to do to avoid collision, typically issuing the neighbouring aircraft opposing instructions like climb while turning left and descend while turning right. Collision avoidance instructions received from TCAS are final and binding, taking precedence over all ATC commands. Evidently, the transponder must remain on at all times during an IFR flight, and it is the pilot's responsibility to ensure this. Flying with a switched off or defunct transponder amounts to gross negligence and is – and deserves to be – punished with suspension or revocation of the pilot's licence. Transponder off was one of two contributory factors behind the accident on 29 September 2006 involving collision between Gol Transportes Aereos Flight 1907 and an American business jet in Brazilian airspace. The business jet was the one which was negligent; the transport flight was the one which crashed. If your

* Pronounced rhyming with "kickass".

transponder malfunctions en route, it is upto you to immediately communicate the problem and work out a solution together with ATC which maximizes safety for everyone.

§13 **IFR – departures and arrivals.** So far we have seen the structure assigned to the sky at altitude; now we look at how to transition between these radar pathways and physical runways. We start from the convention used to number runways. In most cases the number of a runway is one tenth of the track of an aircraft taking off or landing along it, rounded to the nearest integer. Thus, Runway 27 at Mumbai Airport is oriented at 271·5° from mag North. Note that the *same* strip of asphalt operating in the reverse direction is designated Runway 09. Departure and arrival procedures for Runway 27 are completely different from those for Runway 09, so for these purposes, the asphalt strip 27–09 at Mumbai counts as two runways. Note also that the runway direction convention is different from wind direction convention – Runway 27 means that the plane is going towards 270° i.e. West while wind 270° means wind is coming from West. When an airport has two parallel runways (two separate asphalt strips), they are usually labelled with R and L for left and right; thus John F Kennedy International Airport in New York City (ICAO code KJFK) has two parallel runways 31L–13R and 31R–13L (it also has two more runways 04L–22R and 04R–22L). Occasionally however, parallel runways can get numbers shifted by one, for example Delhi's erstwhile 29–11 (primary runway) and 28–10 (secondary runway). This airport also has a 27–09 (tertiary runway) which is not parallel to these two. Moreover, a new runway parallel to the existing big two is currently undergoing construction, so that erstwhile 29–11 has become 29L–11R and the newcomer is slated to get the tag 29R–11L. This is a non-standard numbering scheme – three parallel runways at the same airport are typically numbered L, C and R for left, centre and right, thus Singapore Airport has 02L–20R, 02C–20C and 02R–20L. Airports with four or more parallel runways must use two different sets of numbers, such as three 17–35s and two 18–36s at Dallas Fort Worth, USA. I think we've had enough of runway numbering; the main point is that the number gives a good idea of the direction in which the runway lies.

The departure procedure for major airports is called **SID or Standard Instrument Departure**. This consists of a prescription of what the pilot must do between takeoff from a particular runway and attaining the first waypoint on the filed flight plan. It consists of waypoints which he must follow, altitudes which he must attain at these waypoints, the VOR/DMEs which he must tune into and other stuff. SIDs may also have speed targets and/or restrictions which the pilot should attain or obey. A blanket restriction applying to nearly all instrument departures is a limit of 250 knots (465 km/hr) indicated airspeed under 10,000 ft*. Exceptions are granted only if the aircraft is operating near MTOW and needs a higher speed to achieve flap retraction following takeoff – the pilot must get the exception pre-approved by ATC. Every runway has its own set of SIDs connecting to different neighbouring waypoints. We'll see an example in the next Section, where we do a case study of an airport's arrival and departure procedures. Another important component of IFR departure and arrival procedures is **radar vectors**, which are directions assigned by ATC in real time. These usually take the form "maintain heading X°" or "turn left and maintain heading Y° until intercept Z radial inbound from W VOR" or equivalent.

* Since indicated airspeed is less than true airspeed at altitude, the restriction amounts to a true airspeed of 540 km/hr at F100, the upper limit of its validity. For the calculation, see (3B–23) in §28.

The arrival to a major airport can itself be divided into two phases – initial approach and final approach. Initial approach is governed by a set of published procedures called **STAR or Standard Terminal Arrival Route**. Like SID, this consists of a prescription of pilot actions from the last waypoint on the filed flight plan to the point where final approach is begun, called the final approach fix. The speed restriction of 465 km/hr indicated under 10,000 ft generally applies; STARs may or may not contain other customized speed restrictions. STAR is often complemented with radar vectors from ATC. Again, we'll see an example in the case study of the next Section.

The **final approach** is the journey from the final approach fix, typically 2000-3000 ft above ground and 12-18 km behind the airport, to the runway. While SID and STAR all rely on VOR/DME, final approach uses a different radio instrument called **ILS or instrument landing system**. To understand the function of ILS, we start from the **runway threshold**. This is a point on the runway which acts as a reference for arriving aircraft. It is marked using a row of white stripes, with the stripes being parallel to each other

and to the runway (see Fig. 03, coming shortly). Many runways have the threshold right where they start, but some have the threshold located some distance into the runway, in which case it is called displaced threshold. For example, Runway 29L of VIDP has the threshold 1460 m away from the base (it can afford to since the total runway length is 4430 m). What ILS does is, it creates a reference flight path inclined at 3° below the horizontal, having the same track as the runway and passing through a point 50 ft* above the lateral centre of the threshold. This reference path is called **glideslope**. When the cockpit instruments tune into the ILS waves, they display to the pilot both the horizontal and vertical deviation from the glideslope. Note that this is a significant difference between VOR/DME and ILS – while VOR/DME generates reference planes (radials) in the three-dimensional space, ILS generates a reference *line*. Usually, the pilot transitions from initial to final approach first horizontally and then vertically. In other words, to accomplish the transition, he first performs a turn, prescribed by published procedures or guided by radar vectors, onto the vertical plane in which the glideslope lies. Once in this plane, he brings the aircraft onto the glideslope itself. This interception is usually done from below, i.e. after entering the vertical plane, the aircraft usually maintains constant altitude for a while before attaining the slope. Interception from above is non-standard approach practice but may happen due to technical malfunction, pilot error, exceptional congestion or expedited arrival requirement.

* 3° and 50 ft are the most common values. Minor variations are often present, written in the approach procedures for the airport in question.

The category of the ILS determines how close to the runway it can take the pilot before its accuracy decreases due to physical proximity and its guidance becomes unreliable. CAT-1, the minimum, is designed to guide the aircraft upto a point 200 ft above the runway and about 1 km behind the threshold; higher categories achieve lower altitudes and closer distances. At this point, the pilot makes a transition to visual flight. First he must take visual stock of the runway; if it is not properly visible or it is occupied by traffic*, then he has to perform a **go-around or missed approach**. In this procedure, TOGA power and suitable elevator inputs are applied to abort the descent and start climbing and accelerating. The height above ground at which ILS transitions to visual is called the **decision height** and the corresponding altitude the decision altitude (we have seen the difference between "height" and "altitude" in §07). **RVR or Runway visual range** is defined as the maximum distance from which the runway is clearly visible – the category of ILS determines the minimum RVR required for a successful landing.

* Traffic may be another aircraft, a maintenance car, a refuelling tanker, anything. Not supposed to happen in a perfect world but everyone makes mistakes occasionally.

If the landing is continued past the decision height, the pilot flies visually upto the touchdown. The switch from instrument to visual does not cause a change in the aircraft's trajectory – it continues along the glideslope, flying over the threshold at 50 ft and coming to earth about 300 m ahead of it. To enable visual conformity to glideslope, runways are provided with a special marking called aiming point marking about 400 m forward of the threshold. If the plane is on the glideslope, the aiming point remains at the same position on the pilot's windshield. Note a significant difference between VFR and IFR landings – while the former often targets the numbers (or the threshold), the latter aims for a point 300-plus metres ahead of the numbers. For each runway, the touchdown zone is defined as a region on both sides of the aiming point, within which it is acceptable for an aircraft to land. This zone is indicated with special markings. Landing outside the touchdown zone may have adverse effects on safety; if a pilot sees he's headed for such a landing, he should abort it. In the below Figure, we see the markings for threshold, centreline, aim point and touchdown zone on a schematic runway.

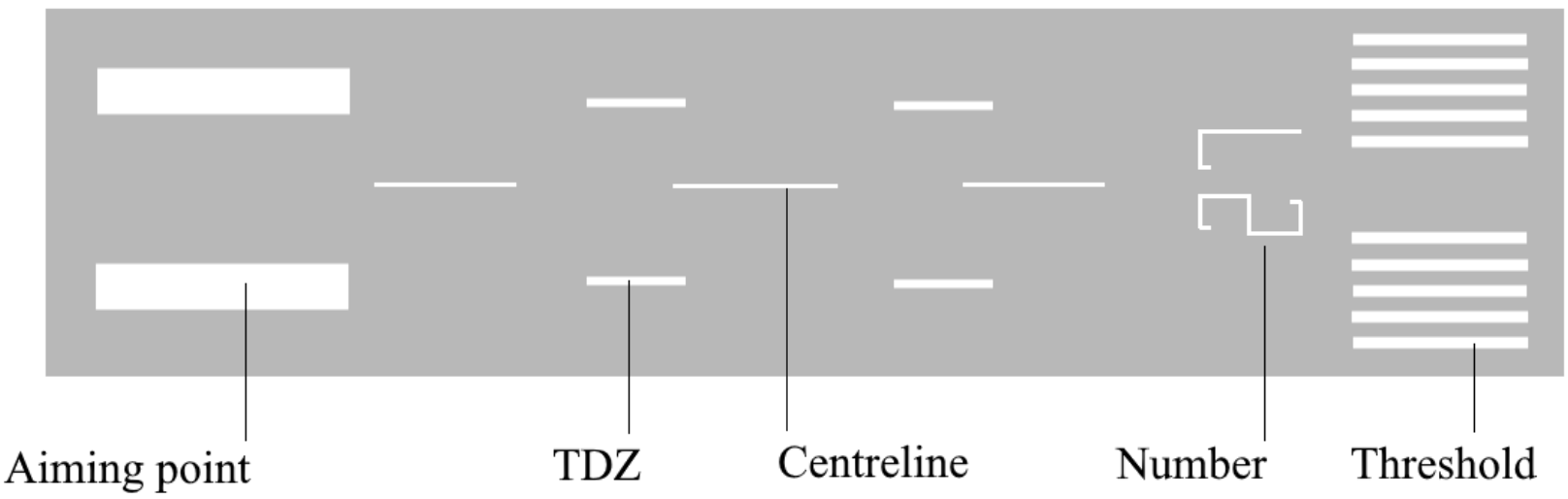


Figure 03 : *Schematic representation of some of the markings on a runway. The size and position of the individual markings are not drawn to any scale.*

The size, description and position of all the markings are determined by ICAO recommendations and universal across the globe. For night flight, every marking has its unique equivalent in lighting. Since we aren't doing Piloting 101 here, I will skip further details of markings and lightings.

In some situations, for example when radar vectors are not available, the instrument approach features a **procedure turn** between the STAR and final approach segments. This is when the tail end of the STAR features overflying the runway in the reverse of the intended landing direction. This segment is necessary to acquire the proper horizontal position with respect to the ILS. Passing the final approach fix, the pilot continues on the 'wrong way' for a given time (usually two minutes) and then performs a sweeping turn which sees him back at the same location but now heading the 'right way'. Again passing the final approach fix, he now intercepts glideslope and descends towards the airport. An IFR approach which bypasses procedure turn is called **straight-in approach**. Note that this word thus has different meanings in VFR and IFR contexts; in both cases however it represents a clean, expedited approach schema featuring a minimum of fuss.

Sometimes, the final approach to a major airport features VFR despite having the latest ILS systems. One famous example is Runway 19 of Ronald Reagan National Airport (ICAO code KDCA) in Washington DC, USA. Here, a full ILS approach is ruled out because the glideslope from this runway, perforce a straight line, would have passed right above the National Mall (a complex consisting of Washington Monument, Capitol and other federal buildings) which is prohibited airspace. For this reason, aircraft arriving at Runway 19 of KDCA are required to use VOR/DME and/or radar vectors to reach waypoint FERGI above the Potomac River* at an altitude of 3000 ft, and thereafter descend continuously while visually flying along the river. The river having numerous meanders in this stretch, this is easier said than done. When the planes seem about to pass the airport altogether, they make a sharp starboard turn to shift from river to runway track and land immediately after.

* If you are familiar with Washington DC geography, FERGI is located very close to the bridge on the Capital Beltway over the Potomac.

To facilitate VFR approaches, airports are equipped with special lights called **PAPI or precision approach path indicator** (also called VGSI or visual glideslope indicator) which provide visual estimation of glideslope to the pilot. PAPI is like a torch whose beam is split into two components along a plane, as shown below.

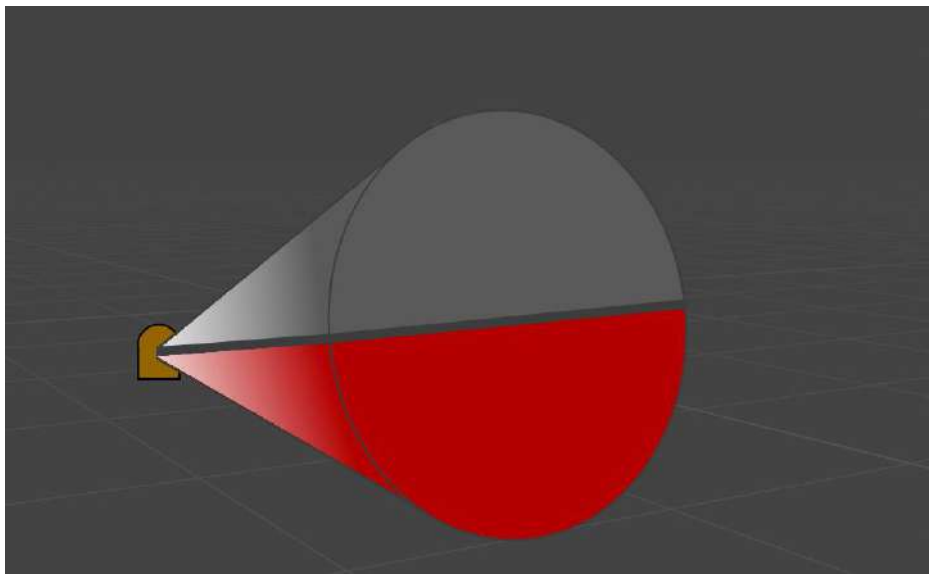


Figure 04 : *Schematic representation of a PAPI beam viewed from in front and to left. The grid lines suggest the ground; the plane demarcating the white from the red half-beam has the inclination of the glideslope.*

The upper half-beam is white and the lower one is red. The torch is mounted such that the splitting plane makes an angle of 3° (or whatever is the inclination of the glideslope) to the horizontal. In a multi-light PAPI array (the standard configuration), different lights have different angles so that, on the glideslope, the pilot sees an equal mixture of white and red. Since red is used for the lower half-beam, more red than white means that the aircraft is below glideslope while more white means aircraft is above glideslope. If you understand how PAPI works, you should not have to rely on silly mnemonics like "white and white, you are as high as a kite" to convert the light colours to your position.

As with any VFR flight, these approaches require VMC – if those conditions are not present, you need a different runway, and if that's not available, a different airport. Flying VFR into IMC and then into another aircraft or the ground is a soft way of crashing a plane, but in general aviation as well as charter flights it is regrettably common. In many cases, the decision to fly despite impermissible weather follows from an attitude of bravado or from fear of the consequences of playing by the book and cancelling. This type of accident is best avoided by acquiring IFR training. As you can see, VOR/DME and ILS is not such a big deal to learn, and mastering it can really be a life-saver.

§14 **STAR and SID example – John F Kennedy International Airport.** As a concrete example of the material we've been seeing so far, let's take a look at the arrival and departure procedures into KJFK Airport. In Fig. 04 below, we see one among maybe a dozen STARs for this airport. This one is called ROBER TWO. The name derives from that of one of the waypoints on this STAR while the number refers to the version number. If and when this STAR is updated, the new version will be called ROBER THREE. The numbers ensure that ATC and pilots are on the same page – if ATC tells pilot to do ROBER 3 and pilot has this sheet with him, then he must request for the list of waypoints instead of blindly doing ROBER 2 and perhaps setting off TCASes all round. A flight approaching from the North-East, like Air India 101, might well use ROBER 2.

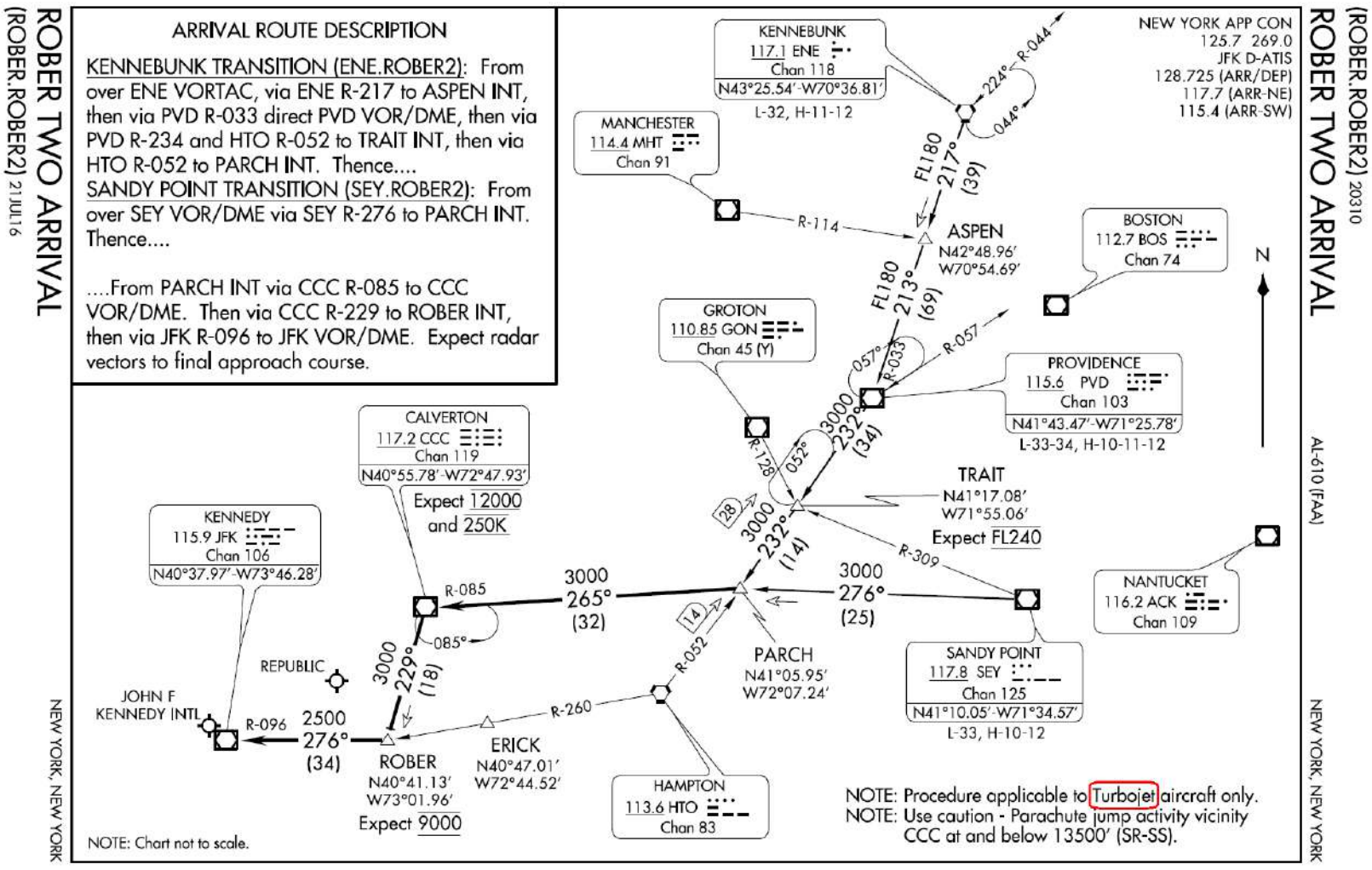


Figure 05 : *ROBER TWO STAR for John F Kennedy International Airport, New York City. The word "Turbojet" in the bottom right corner (my highlighting) is a mistake – it should read "jet", as contrasted with "propeller". The last time a true turbojet aircraft landed at KJFK was in 2003, when Concorde used to cater to this airport.*

It begins at the VOR Kennebunk, from which the pilot tracks the radial 217. Right under Kennebunk are given the frequency of its waves (117·1 MHz) and the channel number to which the pilot must tune (118) to catch these waves. 39 NM i.e. 72 km after crossing Kennebunk, the flight will arrive at the waypoint ASPEN, defined as the intersection of Kennebunk radial 217 with Manchester* 114. So, en route to ASPEN, the pilot of Air India 101 will have his first VOR receiver tuned to Kennebunk and the second to Manchester. After ASPEN, the STAR features a journey to Providence VOR/DME by tracking its radial 33 inbound – while the large font degree angle 213 may refer to either Kennebunk or Providence, the smaller R-033 next to the flight path clarifies that the latter is the case. Upon intercepting Manchester's 114 radial, Air India 101 will turn 4° to the left, let go of Kennebunk, tune into Providence and start tracking its 33 radial. Passing Providence, it will turn right 19° and track its 232 radial outbound upto the waypoint TRAIT, defined by triangulation with Groton as well as Sandy Point VOR/DME. TRAIT is labelled as "expect FL 240" meaning that ATC is likely to assign F240 to Air India 101 while it passes TRAIT; an expectation is obviously not a guarantee. In this way, the approach proceeds all the way to ROBER, where the pilot should expect F090.

* Manchester here refers to a city in New Hampshire, USA named after its more famous British counterpart.

Note that the STAR begins way behind the airport – a procedure for New York includes Boston. The loops over Kennebunk, Providence, TRAIT etc indicate **holding points**. If aircraft are prevented from approaching KJFK due to bad weather, congestion or other factors, then ATC may assign them to hold at these points. In such a case, the holding pilot must follow a 'racetrack' course consisting of two legs at the indicated tracks (for instance 85° and 265° if holding at Calverton) joined by 180° turns. The sense (clockwise or counter-clockwise) in which the racetrack must be covered is also given in the chart, by the arrows (it's counter-clockwise at Calverton). After ROBER, the STAR just shows a 63 km trip to KJFK along direction 276°, but reality is not so simple. If nothing else, 276° does not correspond to any runway at KJFK. What happens is that the STAR is practically over at ROBER; after that we need to consult the final approach charts.

Here is one of them – the one for Runway 31R. Generally, 31R–13L and 04R–22L at KJFK are used for landings while the longer 31L–13R and 04L–22R are used for takeoffs. Note that the magnetic declination at KJFK is –13·5°, so that the runways have tracks of 30°, 120°, 210° and 300° with respect to true local North.

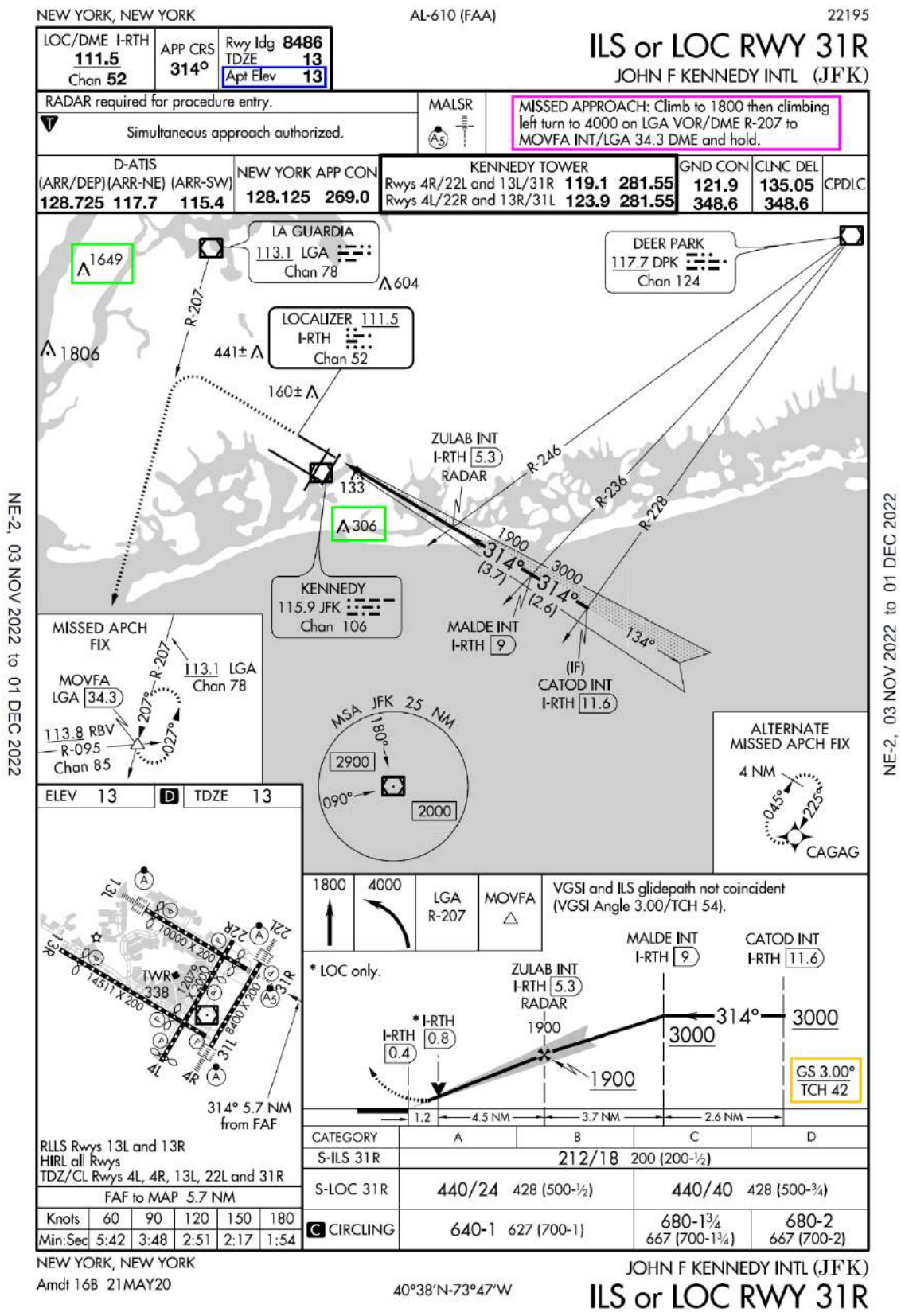


Figure 06 : *Final approach diagram for Runway 31R at John F Kennedy International Airport, New York City.*

This diagram has a lot of info, but we'll only look at the most salient features. First is that a final approach trajectory is always shown both in top view and in profile view. Next, this particular approach is shown beginning at CATOD, which is 22 km behind the threshold; since the STAR ended 63 km away from the airport, the intermediate step must be flown using radar vectors and speed and altitude guidance assigned by ATC. From the top view, we can see that the approach track is 314°, same as the runway track; it is identified by the ILS (localizer I-RTH) whose channel number is given. The ILS also contains a DME which identifies the waypoints CATOD, MALDE and ZULAB at 11·6, 9·0 and 5·3 NM respectively; in case this DME is inoperative, the waypoints are also identifiable by triangulation via Deer Park VOR/DME. The profile view shows the approach to feature level flight at 3000 ft from CATOD to MALDE, followed by a descent to 1900 ft at ZULAB. All numbers are altitude and not height – the airport elevation is given at the top as 13 ft (I have boxed in blue). The lightning bolt sign as well as X sign at

ZULAB in the profile view identify this as the final approach fix, the point where the pilot intercepts the slope. The slope profile is given (yellow box in bottom right) – GS 3·00° TCH 42, implying that the glideslope inclination is exactly 3° and it passes over the threshold at a height of 42 ft (TCH : threshold clearance height). Note that the descent from MALDE to ZULAB is slightly shallower than glideslope – perhaps it is determined by terrain or other. We can see that the slope is intercepted first horizontally and then vertically, and the latter from below. A caret followed by a number (I have marked a couple of these by green boxes) indicates a terrain obstruction – a hill, a building or a tree – having that altitude. The diagram also gives the procedure for a missed approach (magenta box) – since a go-around might well be a stressful situation inside the cockpit, it helps to know in advance what to do after aborting a landing, instead of getting directions from ATC in real time.

After arriving at KJFK, the aircraft has to park at its assigned location. For this, we need the diagram of the airport itself.

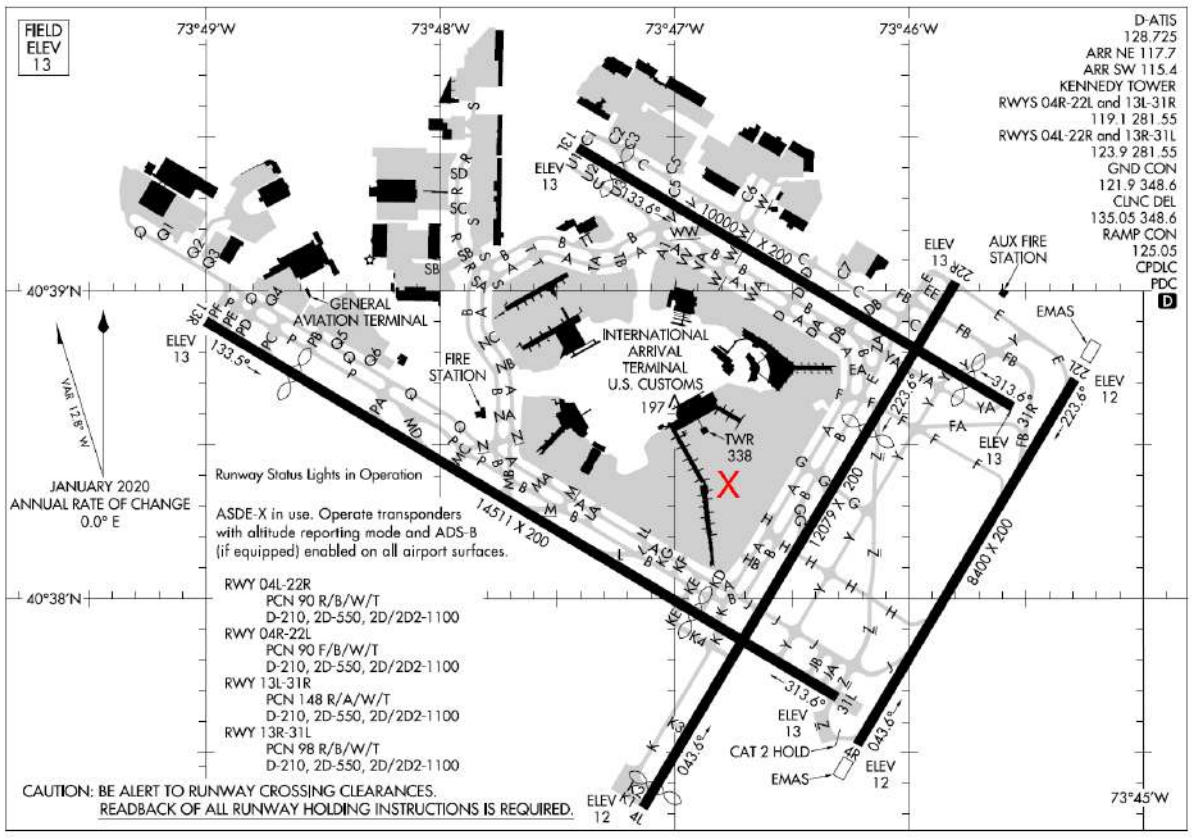


Figure 07 : *Airport diagram showing apron and runways at John F Kennedy International Airport, New York City.*

We can see the four runways – their lengths in metres are 4423 m for 31L–13R, 3682 m for 04L–22R, 3048 m for 31R–13R and 2560 m for 04R–22L. KJFK also has a complex array of taxiways. These are identified by one letter, two letters or a letter followed by a number. Usually, Air India 101 parks somewhere around the location I have marked with a red X. The place where an aircraft parks for de-boarding and boarding passengers is called a stand (the "gate" is technically the structure through which the passengers enter and exit the terminal). After a 31R landing, the aircraft should expect to exit the runway via taxiway WW or V, turn onto taxiway A and follow it all the way to its assigned stand. Of course, ATC will specify the exact route to be taken. After remaining at KJFK for a few hours, the same aircraft returns home to Delhi as Air India 102. If the departure runway is assigned as 31L, then the taxi route is pretty short. Simply follow taxiway H across the runway 04L–22R (if 31L–13R is being used, 04L–22R is always inactive), then turn right onto taxiway Z and right onto 31L for a full-length departure. On the other hand, a 13R departure means a lot of taxiing – come out from the stand onto taxiway A, then via N onto P and finally turn onto the runway via any of PD through PF. The last option gives the full length, while the other two give marginally smaller lengths. Full or nearly full runway is good to have in this case because Air India 102 is a very heavy aircraft – a Boeing 777-300 ER filled to the brim with fuel. A lighter aircraft being cleared for 13R departure from the same stand might backtrack only upto PA and turn onto the runway from there. Such a takeoff is called intersection departure.

After departure, we need the SID chart, below.

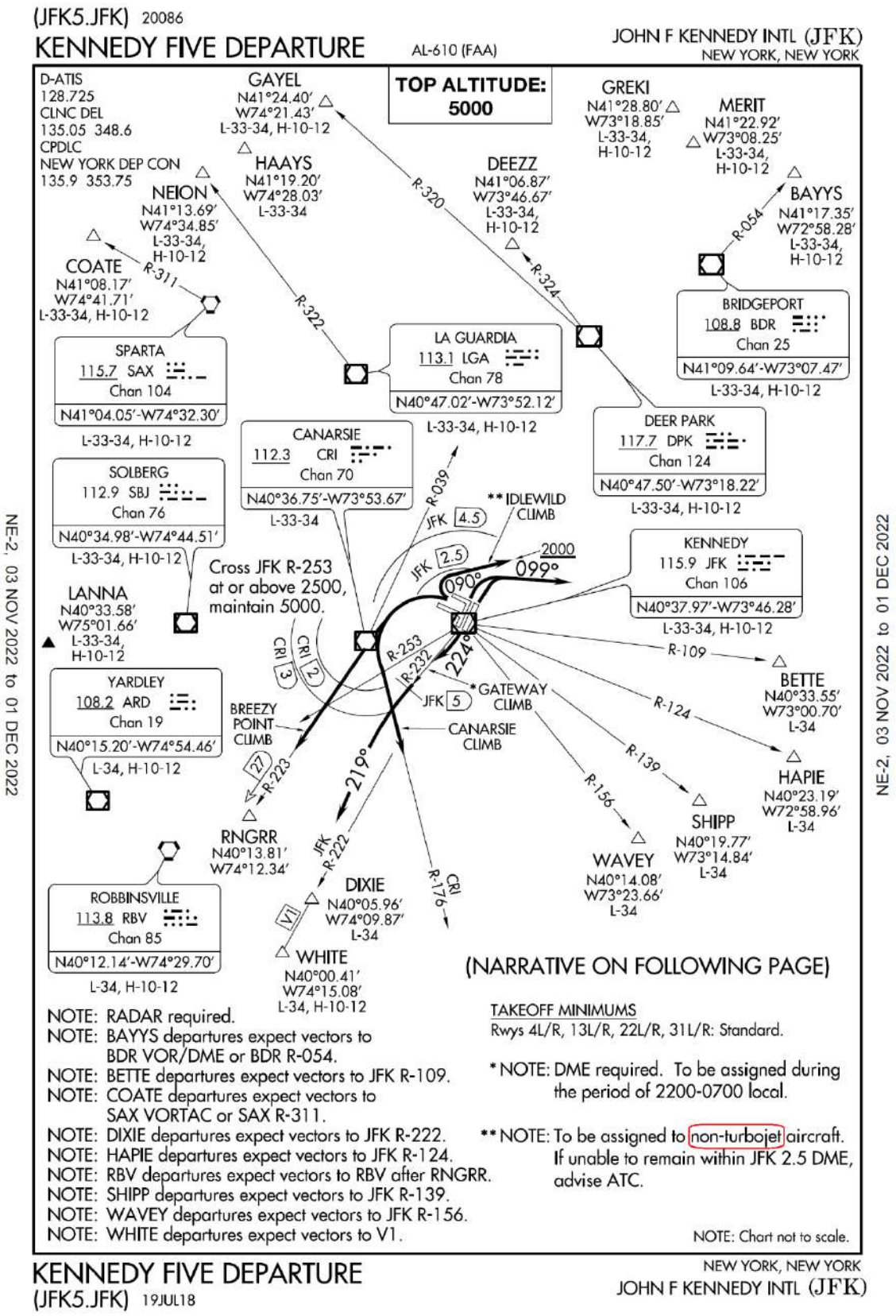


Figure 08 : *SIDs for John F Kennedy International Airport, New York City. Again the word "non-turbojet" (my highlighting) refers to propeller planes and not to all aircraft except Concorde's ghost.*

Despite KJFK being a large airport, its SIDs quite simple, so that the procedures for all runways fit into the same chart. For 31L, the written instruction (given on a separate page of the chart) is as follows. "Breezy Point climb : Climbing left turn direct CRI [Canarsie] VOR/DME. Make turn east of CRI R-039 (remain within JFK 4·5 DME), then via CRI R-223 to RNGRR/CRI 27 DME. Cross CRI 3 DME or JFK R-253 at or above 2500, thence ….. Canarsie climb : Climbing left turn direct CRI VOR/DME. Make turn east of CRI R-039 (remain within JFK 4·5 DME), then via CRI R-176. Cross CRI 2 DME or JFK R-253 at or above 2500, thence ….." After going upto "thence ….." for all the other runways, the procedure continues "via radar vectors to assigned route or fix, maintain 5000. Expect clearance to filed altitude/ flight level ten minutes after departure". This is pretty simple – ATC will tell the pilot whether to use Breezy Point or Canarsie climb and the pilot will follow that procedure. Only the instruction to turn staying East of Canarsie 39 radial benefits from elaboration. During the takeoff run, the aircraft's radial from Canarsie is about 60 and decreasing. The turn should be timed such that this decrease does not take the radial below 39 – the radial should hit a minimum before that and start increasing as the plane approaches and passes Canarsie and then flies away from it. Note that Canarsie is a higher-performance climb than Breezy Point

– the minimum altitude of 2500 ft is attained at a shorter distance from the runway, and during a steeper turn. A straight departure from 31L takes the aircraft virtually bang over Manhattan and then towards airspace belonging to the nearby Newark Airport; the sharp turn both prevents a potential airspace conflict and ensures that lowly irritants such as aircraft noise do not waft up (or rather down) into the plush lives of the denizens of downtown New York City.

All of §12-14 was classical IFR. Nowadays there's another instruments navigation protocol called **RNAV or area navigation**, which uses GPS instead of radio. Here, waypoints are defined in terms of their GPS coordinates, and the onboard computer tells the pilot which way he needs to go to proceed from one waypoint to the next. The principles are the same as in IFR and the implementation is easier. Trajectories such as curved final approaches, which are impossible with classical IFR, are possible with RNAV. Unlike the transition from VFR to IFR, the one from classical IFR to RNAV is a breeze, so we need not spend further time and space on this topic.

C. RUDIMENTS OF COMMUNICATION

Communication with ATC is a vital part of aircraft operations. In this communication, it is essential that both sides hear each other properly and understand what they have heard. To achieve this, communication takes place not in everyday English but using a set of code words and grammatical structures designed to eliminate ambiguity. We see very basic aspects of this in the two upcoming Sections.

§15

Spelling alphabet, airport and airline codes. Two international organizations are in charge of worldwide civil aviation. One is ICAO and the second is IATA or International Air Transport Association. In an approximate way, the difference between the two is that ICAO is responsible for the operational aspects of flying such as adherence to safety procedures etc while IATA is responsible for the commercial aspects of flying such as ticketing. Our Article is much more in line with the scope of ICAO than IATA.

As per ICAO guidelines, English is the only language in which aviation communications may be carried out. This is so that all communications are intelligible to all persons hearing it, which is ATC and all pilots in the nearby airspace. That way, if Pilot A hears ATC issuing an instruction to Pilot B which will put B on a collision course with A, A can immediately understand and object to the flawed instruction. Also, the proper communication phraseology and definitions have been formulated only for English. There are few exceptions to the mandatory use of English irrespective of nationality. Basically, aviation without English is possible (without violating guidelines) only if you are flying VFR in a non-English-speaking country and your flight plan either does not require communication with ATC or requires communication with only small-scale, regional facilities catering only to regional pilots. A flight with no English cannot include a major or halfway-major airport as an endpoint or a waypoint. It is much easier to learn aviation English (as it is called) than to hunt for the conditions which will permit one to legitimately fly without it. And just to be clear, international airports where ATC routinely uses non-English languages are flying in the face of ICAO guidelines and getting away with it.

Many communications involve speaking a letter or sequence of letters. Now, many English letters such as "bee", "cee" and "dee" all sound the same and can easily be confused for one another. Hence, ICAO has constructed a spelling alphabet where each letter is represented by a codeword which begins with that letter. In oral communication, the codeword should be pronounced in place of the letter. I give the spelling alphabet below.

Letter	Word	Letter	Word	Letter	Word	Letter	Word
A	Alfa	H	Hotel	N	November	T	Tango
B	Bravo	I	India	O	Oscar	U	Uniform
C	Charlie	J	Juliett	P	Papa	V	Victor
D	Delta	K	Kilo	Q	Quebec	W	Whiskey
E	Echo	L	Lima	R	Romeo	X	Xray
F	Foxtrot	M	Mike	S	Sierra	Y	Yankee
G	Golf					Z	Zulu

Table 01 : *The ICAO spelling alphabet, showing the words which should be enunciated as substitutes for each English letter.*

Similarly for numbers, the digits zero through eight are pronounced as in normal English while nine is pronounced "niner" to avoid confusion with "five". Two- and three-digit numbers are communicated by reading out the digits one after the other. "Hundred" and "thousand" are both acceptable words. The decimal point is read as "decimal".

In almost all cases, the codewords and number styles should be used in oral communications*. Thus, Taxiway H at John F Kennedy Airport is referred to as Taxiway Hotel, and Taxiway Z as Taxiway Zulu. The code KJFK itself is read out Kilo Juliett Foxtrot Kilo. The ATS routes in Fig. 02 are Alfa four six six and Alfa five eight niner. The altitude 5500 ft is read five five hundred while 17,000 ft is read one seven thousand. Feet are understood and usually left implicit. One exception to the use of the code words is in runway designations – L, C and R are read out left, centre and right. A second exception is for ultra-familiar acronyms such as VOR and ILS – in this case one says "vee-oh-are" and "eye-ell-ess" instead of "Victor Oscar Romeo" or "India Lima Sierra".

* Even outside aviation, I have found the ICAO code words to have their use, for instance in spelling one's name over the telephone. Since these words are standardized and are chosen to be distinct in pronunciation from each other, they work much better than "A as in Apple, B as in Bat" etc.

ICAO and IATA both assign codes to all airports so as to save the trouble of writing the full name every time. The catch here is that the two agencies assign different codes. IATA codes have three letters and are what appear on passenger tickets and boarding passes. They are the ones which hoi polloi uses. ICAO codes have four letters and appear in STAR charts, airport diagrams and the like. These are used by pilots, ATC controllers and others 'in the business'. (After reading this Article, you can impress your friends with ICAO codes.) In USA, the ICAO code is derived by adding the letter K before the IATA code. Thus, John F Kennedy International Airport has the IATA code JFK and the ICAO code KJFK*. In other countries, the IATA code is derived from the name of the airport while the ICAO code is assigned systematically, based on its country and continent. Thus, Delhi International Airport has the IATA code DEL and the ICAO code VIDP (which we've already seen) while London Heathrow Airport has LHR and EGLL. Cities which have undergone name changes after initial assignment of codes often have codes corresponding to the old names; thus Mumbai has BOM and VABB, both derived from its earlier name Bombay (an unfortunate name which sounds like the bomb bay of a military aircraft).

* Since this Article deals with the ICAO aspects of flying, I am using ICAO codes throughout. Also, the STAR and SID chart for KJFK don't include the leading K – this is an American quirk and not an internationally standard practice.

As with airports, IATA and ICAO have separate codes to denote airlines. IATA codes are what appear on tickets, such as AI for Air India, 9W for Jet Airways (both the erstwhile form and the under construction new incarnation), AA for American Airlines etc. ICAO codes appear on ATC screens and in pilots' logbooks. For the three airlines mentioned above, the codes are AIC, JAI and AAL respectively. In addition, all airlines have **callsigns**, which is what are used to verbally identify their flights during communication with ATC. These callsigns are not the ICAO code spelt out as per Table 01 but a name identical or related to that of the airline. Thus, Air India has the callsign "Air India", Jet Airways has "Jet Airways" and American Airlines has "American". Air France has "Air France" but pronounced as it would be in English. Some callsigns are exceptional, such as "Speedbird" for British Airways and

"Springbok" for South African Airways*. For ATC communications, flights are identified by the airline callsign followed by the flight number, thus "Air India one zero two" or "Speedbird two niner three". "Air Force One" is technically the callsign of any aircraft carrying the President of the United States, and not the name of the specially outfitted Boeing 747 which usually does the hallowed duty. Should for whatever reason the President get on board AAL 1275 from Washington DC to Los Angeles, then that flight will use the callsign "Air Force One" instead of "American 1275".

* Which incidentally was founded by a Briton.

Aircraft themselves have five- or six-character registration codes, of which the characters may be letters or numbers. The first one or two characters denote the country. Important countries have suggestive single-letter codes, thus USA has N*, Canada has C, UK has G (Great Britain), France has F, Germany D (Deutschland) etc. Some countries have two letter codes of which one suggests the country, like HA for Hungary, PH for The Netherlands (H : Holland) and AP for Pakistan. Some countries have random codes like S2 for Bangladesh, TF for Iceland and 9V for Singapore. And then there is India, which has VT for Viceroy's Territory. This was the pre-Independence allocation, and no move was made after 1947 to change it to something more representative or at least something neutral. By the time the clamour for a new code arose, which was already in this millennium, relevant codes such as IN, BH or even HI (-ndustan) had already been taken. Demands for a change are underway even as I write this; it remains to be seen whether these demands bear any fruit.

* The logic for this seems to run thus : in an earlier age, before the country codes were systematized, American aircraft were registered by a number rather than a string of letters. When forced to adopt an initial letter, USA chose "N" for "number" – in other words, N12259 is simply aircraft number 12259, which it was even before the systematization. Thus, the N is effectively no code at all, a code which only the most influential country can adopt. This nomenclature is akin to how a fan of MOZART's music may in a conversation refer to his String Quintet in G minor simply as "516" with everything else being implicit – any other composer's 516th opus will carry the name of the author, the cataloguer, the genre etc.

§16 **Good communication practices.** An aircraft establishes communication with a particular ATC by selecting a particular frequency on the communication radio. The process is the same as the frequency selection for IFR navigation, and the relevant frequencies are published in charts. All aircraft communicating with a particular ATC control tower, as well as the tower itself, use the same frequency. All communication can be heard by all parties, and only one person can communicate at any given time. Hence it is important to keep communications short and to the point, and to clearly identify the aircraft with whom communication is taking place. This identification is achieved using the callsign. Thus, ATC giving an instruction to AIC 102 will start off "Air India one zero two" and then proceed with the rest of the message. In its acknowledgement of the message, AIC 102 will conclude with the phrase "Air India one zero two". On the other hand, when AIC 102 is making a spontaneous communication to ATC, it will start with its callsign and then relay the message.

To ensure clarity, certain words and phrases which may appear strange are routinely used. For instance, "affirmative" and "negative" are used for "yes" and "no". "Roger" and "copied" are used to mean "I have got that" or its equivalent; it is good practice to demonstrate your understanding by reading back the message in its entirety or in a compacted form. "Roger" and "affirmative" are different – to see this, consider the following example dialogue (excluding callsigns and other technicalities) between ATC and an aircraft cruising at F350.

ATC : Can your aircraft do F370 ?
Pilot : Affirmative.
ATC : Climb to F370 after crossing waypoint ABCDE.
Pilot : Roger, F370 after ABCDE.

"Say again" substitutes for repeat. This Article is not a phrasebook so I won't cover a thousand different phrases and their implications. Instead, we'll just see a handful of the most important ones.

The word "Mayday" repeated thrice denotes an inflight emergency. A pilot in this unfortunate situation will first transmit Mayday, then state the callsign of the aircraft and finally the nature of the

problem. A Mayday* call means that ATC will do its utmost to help the stricken aircraft and emergency services such as firefighters, ambulance etc will rush to follow up after a possible accident. The word "emergency" has the same standing as Mayday – your plane is in serious trouble and needs every bit of help it can get. ATC worldwide are trained to recognize the gravity of these words, and not necessarily their synonyms. So if you are in an emergency, don't use words like "priority" or "urgent". A word along similar lines but for a less troublesome situation is "Pan", repeated multiple times. You make a Pan call when your aircraft has a technical malfunction or other situation which may be troublesome but as of yet doesn't threaten an accident. For instance, suppose you lose one of two engines during cruise. Then you will want to descend and land quickly, but it's not an emergency since twinjets are designed to fly with one engine out. So you will call Pan. Upon hearing a Pan, emergency responders are alerted but they don't go haring off to a potential crash site. It's important to note that Pan is not something which may or may not result in an accident – it's something which, ceteris paribus, won't result in an accident. If there *may* be a crash, then it's *Mayday*, since the emergency staff *will* have to be on scene. Then if the flight lands safely, that will be good for everyone.

* This phraseology has given rise to the name "Mayday" for a television series focussing on aviation accidents. This series is popular with aviation enthusiasts. In our Article, we add yet another dimension to accident analysis – model-based understanding and simulation.

Two other important words when dealing with ATC are "unable" and "request". These are important when you wish to refuse or negotiate ATC instructions. While most instructions are meant to be obeyed without question, there are reasonable exceptions. For instance, ATC sometimes gives instructions which are outside your or your aircraft's performance envelope or which may compromise the safety of the flight in some way. Examples are assigning a vector to a VFR flight which requires passing through a cloud, asking for a climb gradient or time-to-altitude beyond your aircraft's capability or asking for an approach speed which is too close to your stall speed. In these cases, you have to reply "unable" and then state the reason why so. ATC is obligated to give you an alternative instruction which is compliant with your and your aircraft's performance. Of course, unable is all the more important if ATC gives you an instruction which is totally wrong (rare but happens). For instance, in the crash of Gol Transportes Aereos 1907 on 29 September 2006 (see §12), the other contributory factor apart from the error by the business jet pilot was ATC assigning F370 on the same ATS Route to both the business jet and the passenger airliner. If assigned such an instruction, say unable immediately and point out the conflict.

Negotiations arise when ATC gives you an instruction which you can obey but would prefer not to. For example, Airbus A340-300 and A380 are somewhat underpowered aircraft which struggle to maintain a climb gradient when loaded close to MTOW. So for Korean Air Flight 82, a loaded A380 from KJFK to Seoul, South Korea, it might happen that Breezy Point departure is achievable at the regular climb thrust while Canarsie departure will require extended application of TOGA thrust. If ATC assigns it Canarsie, it might respond "Request Breezy Point departure due to heavy aircraft and lower climb performance". Depending on the traffic conditions etc, the request may be granted or denied. But, if your request is reasonable, there's no harm in asking.

Inessential communications between pilots and ATC, i.e. informal chit-chats, are restricted but not prohibited. The reason for the restriction is obvious; the restriction is not upgraded to a ban because ICAO recognizes that pilots and controllers are both human, and, during periods when traffic is relaxed, a bit of conversation rather than a stiff radio silence can make the job pleasanter for both parties. Better work environment can lead to better performance and hence safer flying. Pilots are not allowed to indulge in inessential communication – with ATC, with passengers, with cabin crew and even among each other – whenever the aircraft is below F100. This is called **sterile cockpit** rule. The rule is designed to maximize the probability of a safe approach and landing by eliminating one source of distraction.

While chit-chats are only restricted, what is unconditionally prohibited is bad behaviour. Courtesy is a cornerstone of the pilot-ATC communication policy. There is no scope for rudeness on either side. Occasionally, pilots make requests or ATC issues instructions which are less than brainy. In such a case, the request or instruction has to be politely denied. Ad hominem remarks, sarcasm or yelling on the radio

are completely unacceptable. Adult words too are very strongly discouraged. If one side is behaving rudely in an interaction, the other side must still maintain composure and courtesy – once in a blue moon even the most professional pilot or controller may have a bad day. If lack of civility is a recurrent problem with a particular pilot or controller, the issue may be reported to the appropriate higher authorities for suitable action.

The phraseology of communications, which sometimes appears artificial or contrived to a non-aviation specialist, makes for entertaining jokes regarding these communications. Here are a few of the better ones (not my inventions).

Pilot is approaching airport for straight-in landing to Runway 01.

Tower : Say altitude.

Pilot : Altitude.

Tower : Say airspeed.

Pilot : Airspeed.

Tower : Say cancel approach clearance, turn right heading two seven zero, maintain six thousand.

Pilot : My altitude is four five hundred and airspeed one seven zero knots.

A Lufthansa and a British Airways aircraft are taxiing at Frankfurt International Airport.

Lufthansa pilot : [something in German].

Tower : Say again last message, in English.

Lufthansa pilot : I am a German, flying for the German airline at a German airport. My aircraft, an Airbus, is partly German as well. Why should I speak English ?

British Airways pilot : Because you lost the bloody war.

A Piper Cub, a Cessna Caravan, a Fokker Friendship and a Boeing 747 takeoff from an airport one behind the other.

Tower to 747 : You have a Piper at your two o'clock, three miles out, confirm in sight.

747 pilot : Affirmative, Piper two o'clock.

Tower : You also have a Cessna at your niner o'clock, two miles out, confirm.

Pilot : Affirmative, Cessna niner o'clock.

Tower : And you have a, um, Friendship straight ahead, one thousand below, confirm in sight.

Pilot : Affirmative. Of course I can see that little Fokker.

---- o ----

3

THE AIRCRAFT DYNAMIC MODEL

Having completed the preparations, we can now begin the technical core of this Article. In this Chapter, we derive the equations of motion of the aircraft in the pitch, yaw and banking planes.

A. AXES AND ANGLES, LIFT AND DRAG

§17 **Axis and angle conventions – full treatment.** This and the next Section both describe the axis and angle conventions which we shall use. In this Section, I adopt a rigorous approach, defining the yaw, pitch and bank of the aircraft and the azimuth and elevation of its flight path in terms of Euler angles and Davenport chained rotations. Even though our focus is on two-dimensional motions, a three-dimensional description is essential to achieve consistency of axes and angles in the pitch, yaw and banking planes. If you are familiar with three-dimensional rigid body rotations, then this is the Section for you. If not, then please skip to §18. Note that parts of this Section will reappear verbatim in that Section.

By definition, all axis triplets will be dextral and orthogonal, and all rotations counter-clockwise positive. We shall treat the ground frame as a true inertial frame in an Euclidean (i.e. flat) space. This assumption incurs negligible error while analysing a short-duration manoeuvre such as takeoff or a turn. Let the axes x,y,z be fixed in the ground frame with x and y in the horizontal plane and z vertically upwards. The direction of x in the plane is insignificant and will be determined by convenience. Let x',y',z' denote a basis parallel to x,y,z with the origin at the centre of mass (CM) of the aircraft. Let the axes q,d,o be fixed to the aircraft body with q pointing directly to starboard, d running from tail to nose and o being the mutual perpendicular, as shown below.

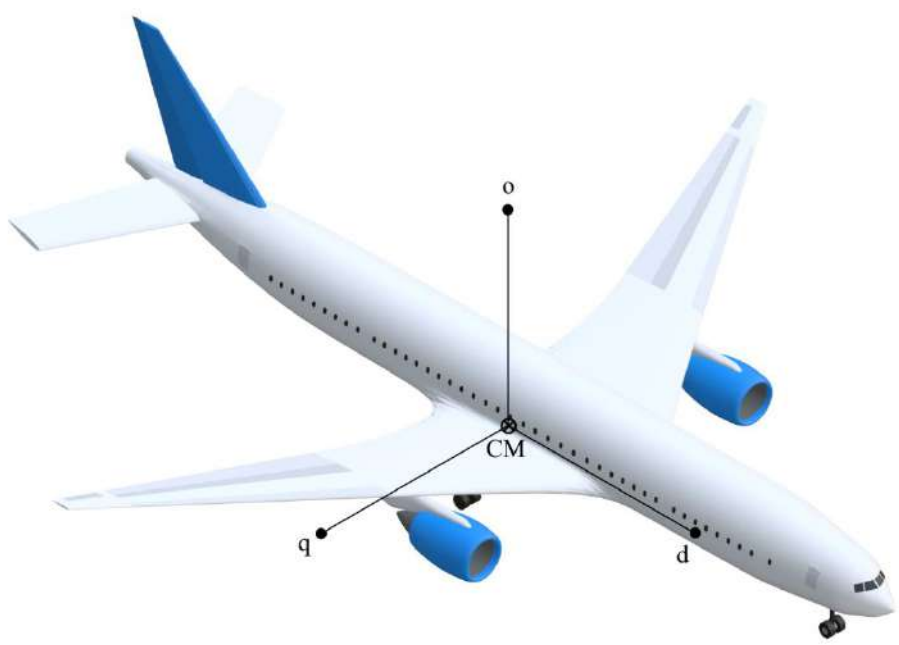


Figure 01 : *Isometric view of Our Plane (note the stabilator, which makes it Our Plane and not Our Plane Prime) showing the* q,d,o *axis triplet. The position of CM is consistent with the numerical values I will introduce later.*

The axis names here stand for "quadrature", "direct" and "orthogonal"; I have named the triplet as q,d,o rather than d,q,o since it makes most sense for the direct axis to be the fuselage centreline and the quadrature axis to run along the wings instead of the other way around.

One way of describing the orientation of the aircraft basis with respect to the ground basis is by using Euler angles i.e. Davenport chained rotation formalism [01,02]. I now specify the convention we will use for such a description. Define q,d,o to be coincident with x',y',z' when all three rotation angles are zero. For

the purposes of specifying orientation, the translation of the origin is irrelevant and I will drop the primes on x,y,z in the subsequent discussion. When the Euler angles are not zero, we go from x,y,z to q,d,o as follows. Starting from x,y,z, the first rotation is the **yaw** through angle φ about the z-axis. This gives the basis n,t,v where v is the same as z. The axis names here are meant to suggest "normal", "tangent" and "vertical", which describe their functions during a level turn. Note however that t is NOT the tangent to a climbing or descending turn, so the names, unlike those for q,d,o, are suggestive only. The second rotation is the **pitch** through angle θ about the n-axis. This gives the basis a,b,c where a is the same as n. The last rotation is the **bank** through angle ψ about the b-axis. This gives us the basis q,d,o with d same as b. Our convention is thus a 3-1-2 Euler angle convention. To prevent overcounting configurations, yaw and bank have a 360° range while pitch has a 180° range. We see the individual transformations below.

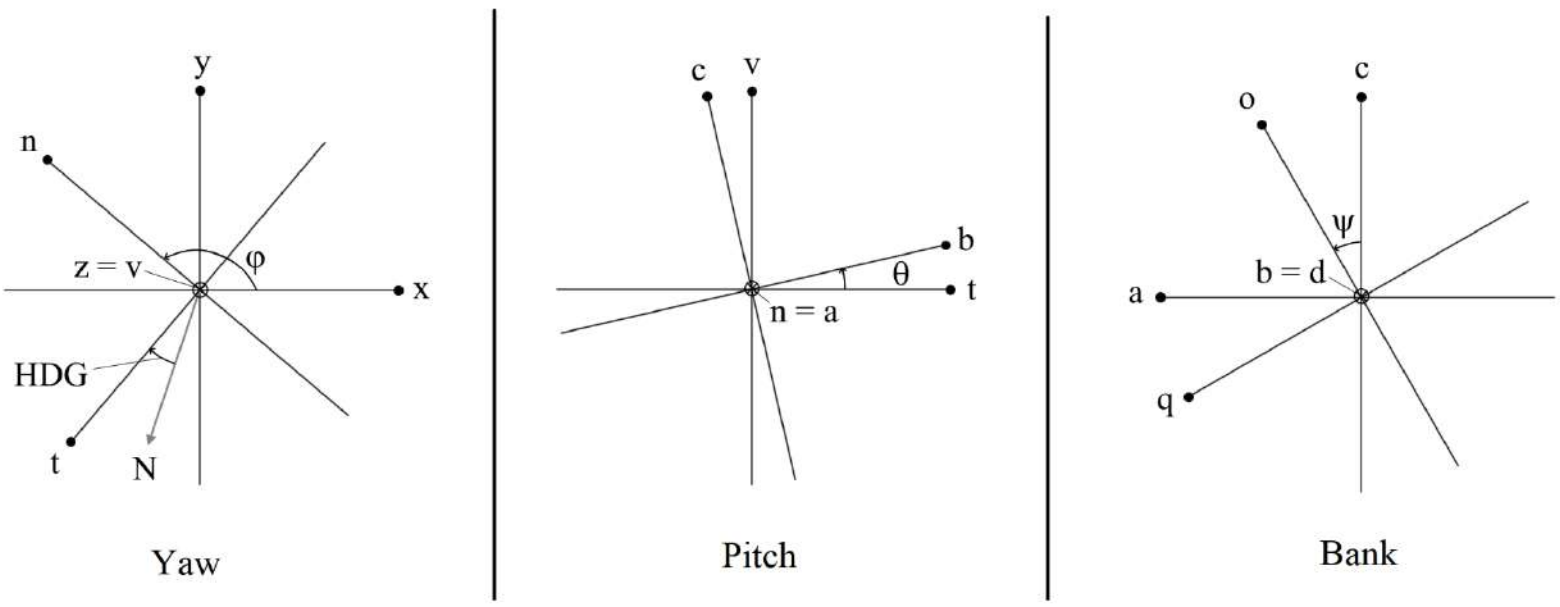


Figure 02 : *The three fundamental rotations, viewed individually.* ***N*** *in the panel for yaw denotes local magnetic North and HDG denotes heading. The composite transformation from* x,y,z *to* q,d,o *consists of these transformations implemented in series. A more graphic representation of yaw, pitch and bank, though taken only one at a time, is Fig. 05 in the next Section. You might want to refer to that even if you otherwise stick to the rigorous presentation of this Section.*

In this Article, only one angle will be nonzero at any given time. The yaw φ is the same angle as the heading, just measured in a different way. φ is counter-clockwise positive measured from an arbitrarily chosen baseline x while heading is clockwise positive measured from local magnetic North. I will use "yaw" whenever I want to refer to the mathematical measurement convention and "heading" whenever I want to refer to the aviation convention – this should avoid ambiguity between the two measurement systems. Bank is also called **roll**; my preference is for "bank" since "roll" can also suggest the rolling of the wheels which is actually a pitching motion; nevertheless I will not go so far as to say "barrel bank" or "Dutch bank".

Note that the convention here is different from the one used in many flight dynamics books, for example, most of Refs. [1A–01-1A–20]. In these works, the first body axis is our d and the second one is our q. This forces the third body axis to be the negative of our o. Since for zero rotation, the three body axes are identical to the three ground axes, the third ground axis in this convention must be the negative of ours i.e. z must point vertically downwards. For most of us, this runs heavily contrary to our pre-existing intuition and experience, so I have elected to keep z as vertically up. In our convention, positive yaw means that the aircraft is facing left (port) of the reference, positive pitch means that the nose is above horizontal and positive bank is clockwise when viewed from the perspective of the pilot or a passenger. Such a bank makes the starboard wing dip below the port wing; since it causes the aircraft to turn to starboard*, it is also called a starboard bank. In the Literature convention, positive yaw means that the aircraft is facing right (starboard), while the positive directions of the other rotations are the same. Hence, the primary tradeoff of having z point upwards is that positive ψ gives rise to negative φ; I think we can live

* An everyday observation, not just with aircraft but also with birds of prey, whose dynamics are mimicked by aircraft to a great extent. To see it mathematically, jump ahead to §31.

with this. A potential secondary tradeoff is that the direct axis is the second rather than the first axis of the triplet, though this is minor.

Throughout, we shall use subscripts to indicate components, thus F_x for the x-component of force **F** and V_o for the o-component of velocity **V**. We shall use hat to denote unit vectors thus $\hat{\mathbf{y}}$ and $\hat{\mathbf{V}}$ for unit vectors along y and **V**. While componental equations of motion are the immediate output of NEWTON's Second Law, in this particular case an especially transparent and insightful representation of the dynamics can be obtained by transforming to the *space vector* representation. For this representation, we work in terms of the magnitude of the velocity vector (i.e. the speed) and its direction relative to the ground. This direction is the same as that of the instantaneous tangent to the flight path. In the general case, it has two components – **azimuth** and **elevation**, which we can define in terms of Euler angles as well as projections. For Euler angles, starting from the basis x,y,z if we rotate about the z-axis through azimuth ξ and then about the new x-axis through elevation η, then the resulting new y-axis will be parallel to **V**. In other words, **V** will be along the second axis of the triplet obtained by implementing the first two steps of the 3-1-2 Euler angle rotation from the x,y,z basis, through angles ξ and η. For projections, let **P** be the projection of **V** onto the horizontal plane. Then, the angle from the y-axis to **P** is the azimuth ξ while the angle from **P** to **V** is the elevation η. We see this schematically in the below Figure.

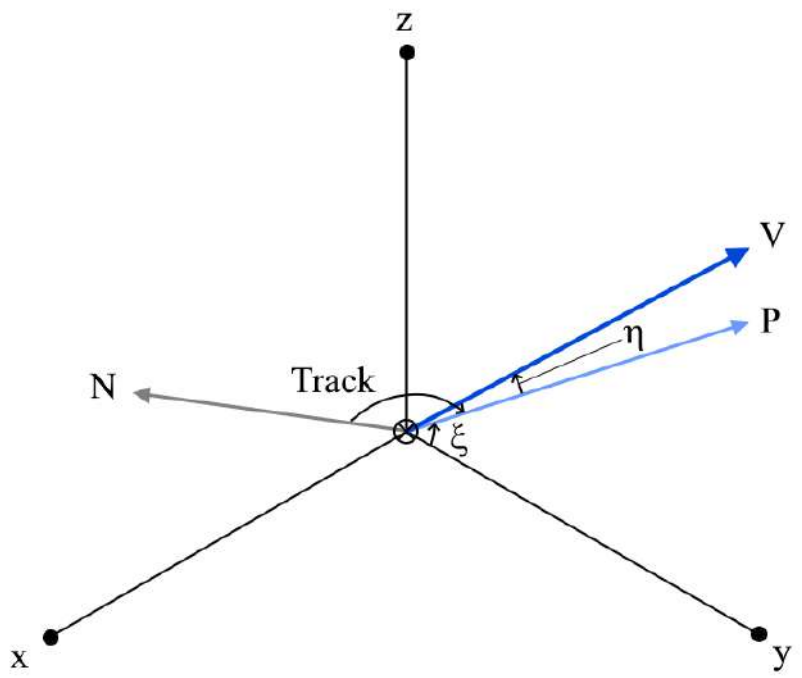


Figure 03 : *Azimuth* ξ *and elevation* η. ***V** is the airplane's velocity vector, **P** its projection onto the horizontal (*x-y*) plane and **N** is local magnetic North.*

As with the yaw and heading, the azimuth is the same as the track, just measured as per a different convention (different baseline, reversed sign). Again, to avoid ambiguity, I will use "azimuth" when referring to the angle as per mathematical convention and "track" when referring to it as per aviation convention. One thing is worthy of note : in general, the velocity vector does NOT lie along the aircraft fuselage. $\hat{\mathbf{V}}$ and $\hat{\mathbf{d}}$ will be parallel if and only if $\varphi = \xi$ and $\theta = \eta$. While the first of these relations is desirable and indeed holds true 99 or more percent of the time, the second one is completely unrealistic (except over time intervals of measure zero), as we shall see when we analyse the motions in the pitch plane.

Before concluding this Section, let me note that the axis names a,b,c and q,d,o as well as the word "space vector model" are borrowed from power electronics [03]. I have gone with these choices since they are physically transparent in the current context also.

§18 **Axis and angle conventions – simplified treatment.** If you have read and fully understood §17, then this material is not for you, except maybe Fig. 05. Otherwise, this entire Article after all deals with two-dimensional rotations, and it is pedagogically senseless to make the whole contingent on three-dimensional rotations for a nearly trivial reason – that of definition. Hence, in this Section we define the yaw, pitch and bank of the aircraft and the azimuth and elevation of its flight path in terms of two-dimensional rotations alone. Mathematically, this is somewhat sloppy as these piecewise definitions don't tell us anything about

what happens if two or more of the angles are simultaneously non-zero. But since we don't need this case in this Article, we can excuse the sloppiness and focus on the intuitive character of the treatment. Parts of the upcoming text are verbatim repeats of extracts from the previous Section.

By definition, all axis triplets will be dextral and orthogonal, and all rotations counter-clockwise positive. We shall treat the ground frame as a true inertial frame in an Euclidean space. This assumption incurs negligible error while analysing a short-duration manoeuvre such as takeoff or a turn. Let the axes x,y,z be fixed in the ground frame with x and y in the horizontal plane and z vertically upwards. The direction of x in the plane is insignificant and will be determined by convenience. Let x',y',z' denote a basis parallel to x,y,z with the origin at the centre of mass (CM) of the aircraft. Let the axes q,d,o be fixed to the aircraft body with q pointing directly to starboard, d running from tail to nose and o being the mutual perpendicular, as shown below.

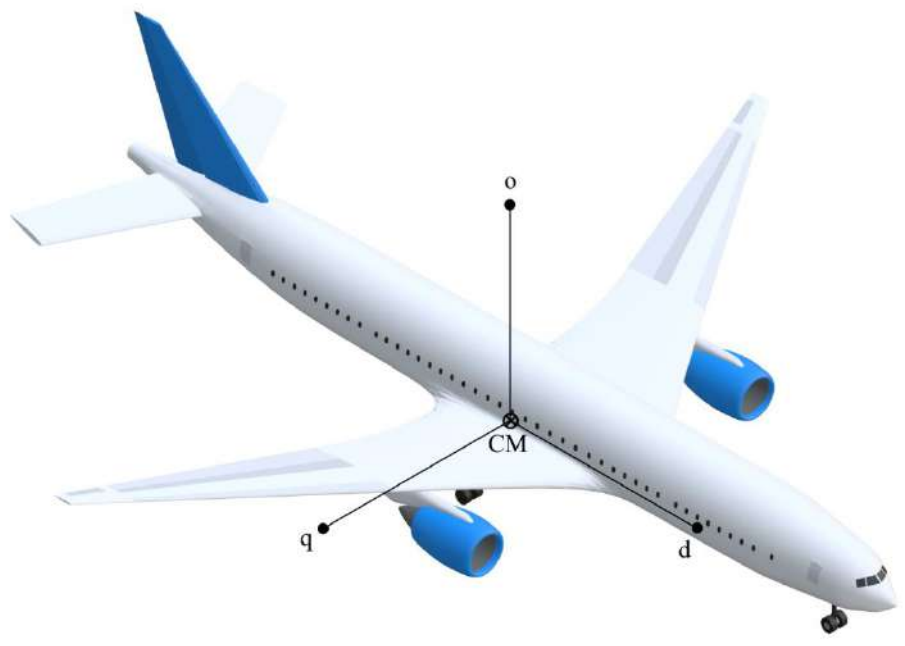


Figure 04 : *Isometric view of Our Plane (note the stabilator, which makes it Our Plane and not Our Plane Prime) showing the* q,d,o *axis triplet. The position of CM is consistent with the numerical values I will introduce later.*

The axis names here stand for "quadrature", "direct" and "orthogonal"; I have named the triplet as q,d,o rather than d,q,o since it makes most sense for the direct axis to be the fuselage centreline and the quadrature axis to run along the wings instead of the other way around.

We define q,d,o to be coincident with x',y',z' when all three rotation angles are zero. For the purposes of specifying orientation, the translation of the origin is irrelevant and I will drop the primes on x,y,z in the subsequent discussion. The **pitch** θ is a rotation about the x-axis. The q-axis remains the same as the x-axis while the d- and o-axes make angles of θ with the y- and z-axes. Positive pitch means that the aircraft's nose is above the horizontal. The **yaw** φ is a rotation about the z-axis. The o-axis remains the same as the z-axis while the q- and d-axes make angles of φ with the x- and y-axes. φ is the same angle as the heading, just measured in a different way. φ is counter-clockwise positive measured from an arbitrarily chosen baseline x while heading is clockwise positive measured from local magnetic North. I will use "yaw" whenever I want to refer to the mathematical measurement convention and "heading" whenever I want to refer to the aviation convention – this should avoid ambiguity between the two measurement systems. Positive yaw means that the aircraft is facing left (port) of the reference. Finally, the **bank** ψ is a rotation about the y-axis. The d-axis remains the same as the y-axis while the q- and o-axes make angles of ψ with the x- and z-axes. Positive bank means that the starboard wing dips below the port wing, i.e. it is a clockwise bank when viewed from the perspective of the pilot or a passenger. Since such a bank causes the aircraft to turn to starboard*, it is also called a starboard bank. Bank is also called **roll**; my preference is for "bank" since "roll" can also suggest the rolling of the wheels which is actually a pitching motion; nevertheless I will not go so far as to say "barrel bank" or "Dutch bank". We can see all three rotations below.

* An everyday observation, not just with aircraft but also with birds of prey, whose dynamics are mimicked by aircraft to a great extent. To see it mathematically, jump ahead to §31.

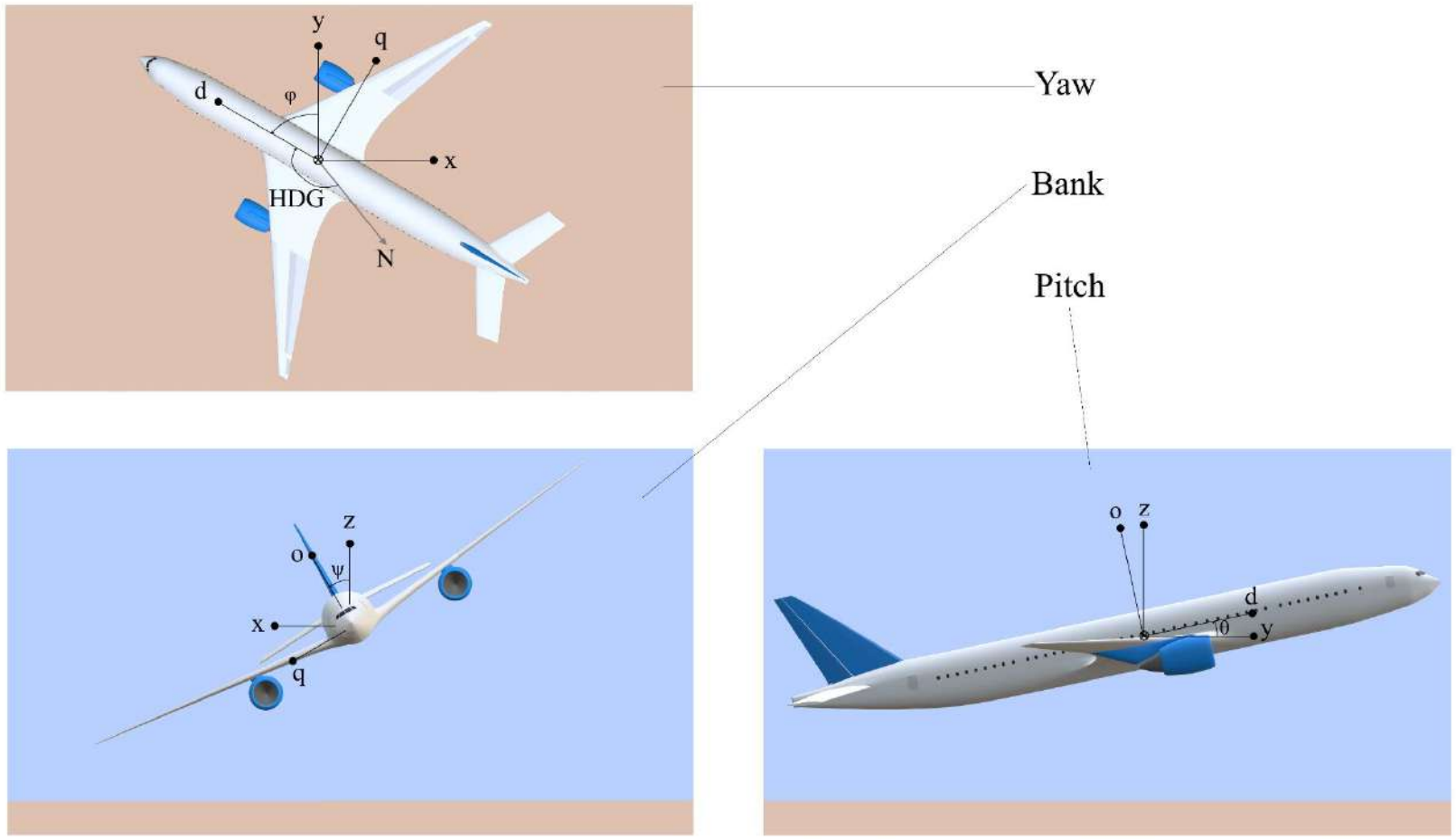


Figure 05 : *Orthographic views of the three fundamental rotations. We position the views in the conventional placement, noting that yaw is seen in top view, bank in front view and pitch in right profile view. The line between blue and brown represents the horizon with sky above and ground below.* ***N*** *denotes local magnetic North and HDG denotes heading. In the front view, I have not shown the origin and the parts of the axes near this point as I didn't want to defile Our Plane by drawing circles and lines across its face. The pitch, yaw and bank angles are all positive; their values are 12º, 60º and 30º, the first and third being very typical for actual aircraft (the second can of course be arbitrary).*

Throughout, we shall use subscripts to indicate components, thus F_x for the x-component of force $\mathbf{F}$ and V_o for the o-component of velocity $\mathbf{V}$. We shall use hat to denote unit vectors, thus $\hat{\mathbf{y}}$ for a unit vector along y and $\hat{\mathbf{V}}$ for a unit vector along $\mathbf{V}$. While componental equations of motion are the immediate output of NEWTON's Second Law, in this particular case an especially transparent and insightful representation of the dynamics can be obtained by transforming to the *space vector* representation. For this representation, we work in terms of the magnitude of the velocity vector (i.e. the speed) and its direction relative to the ground. This direction is the same as that of the instantaneous tangent to the flight path. It is characterized by two angles, the **elevation** η and the **azimuth** ξ. Elevation is defined in the pitch plane (y-z or d-o plane). It is the angle made by the flight path relative to the y-axis. Azimuth is defined in the yaw plane (x-y or q-d plane). It is the angle made by the flight path relative to the y-axis. We show these two angles below.

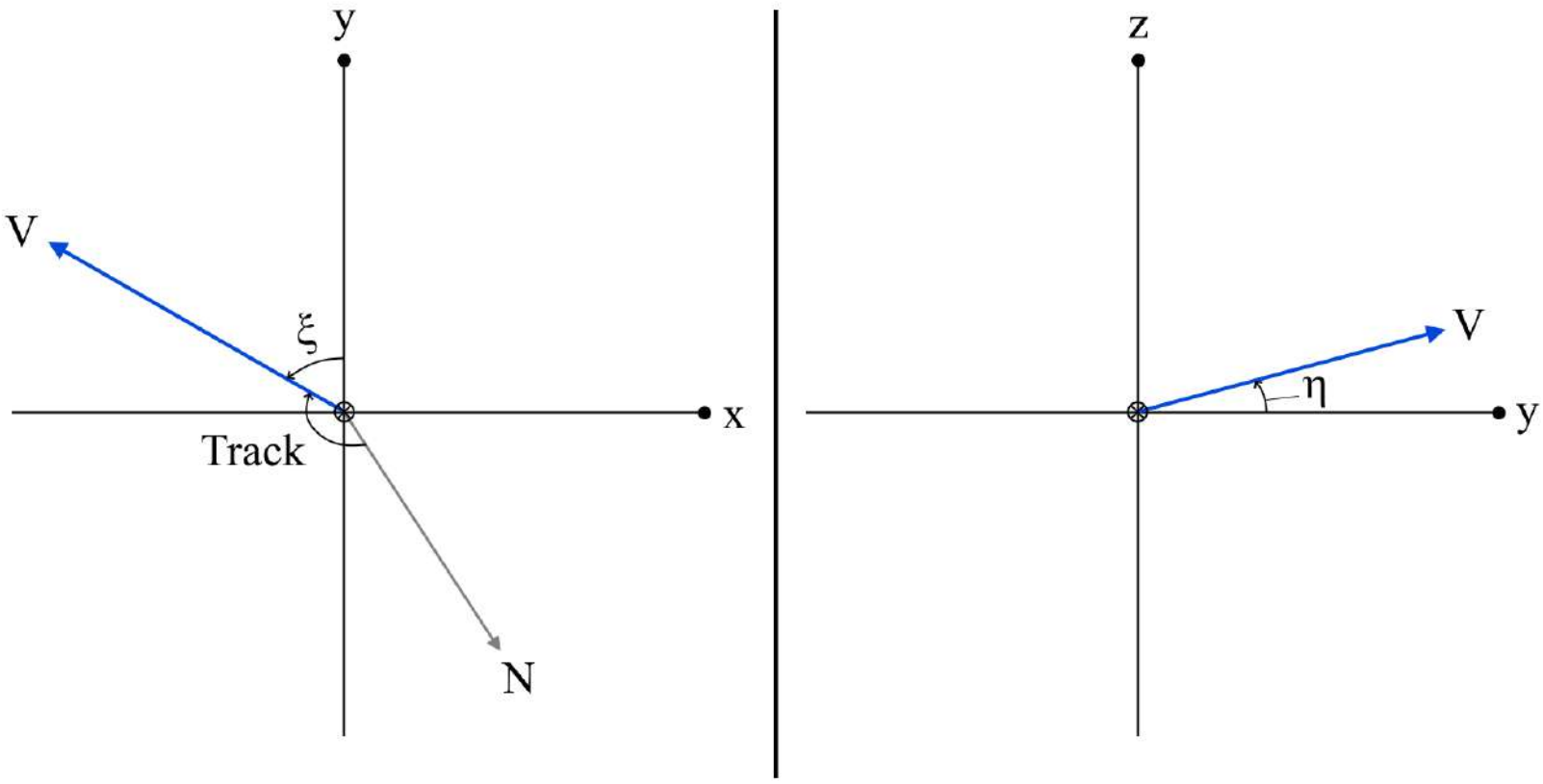


Figure 06 : *The aircraft's velocity* **V** *in the* x-y *and* y-z *planes, showing the track, azimuth* ξ *and elevation* η. ***N*** *denotes local magnetic North.*

As with the yaw and heading, the azimuth is the same as the track, just measured as per a different convention (different baseline, reversed sign). Again, to avoid ambiguity, I will use "azimuth" when referring to the angle as per mathematical convention and "track" when referring to it as per aviation convention. One thing is worthy of note : in general, the velocity vector does NOT lie along the aircraft fuselage. $\hat{\mathbf{V}}$ and $\hat{\mathbf{d}}$ will be parallel if and only if $\varphi = \xi$ and $\theta = \eta$. While the first of these relations is desirable and indeed holds true 99 or more percent of the time, the second one is completely unrealistic (except over time intervals of measure zero), as we shall see when we analyse the motions in the pitch plane.

Before concluding this Section, let me note that the axis names a,b,c and q,d,o as well as the word "space vector model" are borrowed from power electronics [03]. I have gone with these choices since they are physically transparent in the current context also.

§19 **Different theories of lift.** Lift is fundamental to aviation – it is what differentiates an aircraft from an automobile. Air flowing past an airfoil generates lift. Since the equations of fluid mechanics are invariant under Galilean transformation, a stationary airfoil mounted in an airflow with far field velocity (velocity far away from the airfoil) **U** is entirely equivalent to the airfoil moving through stationary air with velocity **V** = –**U**. The former representation is conventional for calculating aerodynamic forces; the latter is what actually happens with the aircraft*. Lift is defined as an aerodynamic force acting on the body which is orthogonal to **U**. The established scientific Literature has three explanations of what gives rise to lift on an airfoil (a very recent new explanation is coming after these three). We look at these below.

* When there is no wind. When there is a wind, Galilean invariance assures us that only the relative velocity has any significance.

BERNOULLI's principle

This explanation states that the air flowing over the top surface of the airfoil is faster than that flowing under the bottom. Since $P + (1/2)\rho v^2 = \text{const.}$ (P pressure, ρ density, **v** fluid velocity), P is greater on the bottom surface and the resultant force is upward. A few issues with this explanation are :

- Why does the air flow faster on the top surface than the bottom ?
- $P + (1/2)\rho v^2 = \text{const.}$ holds everywhere only for an irrotational flow. The flow around an airfoil is rotational. In this case the relation holds only along individual streamlines. The top and bottom of the airfoil do NOT lie on the same streamline.
- The lift is determined by the pressure right at the airfoil surface and not even a millimetre away. Air is a viscous fluid and the flow velocity exactly at the surface is exactly zero, both on top and

bottom. Hence, if BERNOULLI's principle were counter-factually to be applicable to this situation, the pressure would have been constant everywhere and the resultant force zero.

Even if we were to suspend our disbelief of the above inconsistencies, the BERNOULLI's principle argument cannot give us a quantitative expression for the lift. Hence, it is not worthy of further consideration. ■

NEWTON's peashooter argument

A much more plausible explanation of lift originates with Sir ISAAC NEWTON. He treated the airfoil as a flat plate, the air as a collection of little particles (I think he called them corpuscles) and reasoned as follows. Suppose we mount the airfoil in vacuum and use a pea-shooter to shoot peas at it with velocity **U**. The peas collide elastically with the airfoil and the collisions impart (or at least try to impart, since the airfoil is held stationary) a momentum along the normal to the airfoil. Think of the fluid as an infinitude of infinitesimal peas impacting the airfoil continuously, and the resulting transfer of momentum manifests as the lift force.

This explanation is far more plausible than the previous one. Firstly, it correctly gives the dependence of lift on U^2 (one U from the momentum transferred by each pea, the second from the number of peas hitting the airfoil per unit time). Secondly, it gives the direction of lift to be along the normal to the airfoil (the previous explanation is mum about the direction and mum about that fact as well). This means that, in addition to lift, the airfoil also experiences a drag, which is in agreement with reality. Thirdly, the increase of lift with increasing angle of attack (see the next Section) is also plausible. From a logical perspective, a gas does consist of molecules moving about randomly along their mean free paths and modeling them as peas appears satisfactory.

There are some problems with the peashooter explanation however :

- It cannot explain the velocity profile of the air above the airfoil and the suction arising on the top surface.
- It cannot explain the phenomenon of stall.
- It predicts a flat plate wing to be as effective as an airfoil with the special cross-section that wings actually have, which is clearly not the case.
- If the airfoil is cambered, the lift obtained from this approach might be totally garbage.

For these reasons, we hesitate to unconditionally accept the peashooter argument as well. ■

Kutta-Zhukovsky explanation

This models the airflow as inviscid and irrotational. The boundary condition at a rigid body immersed in such a flow is that the velocity component *normal to the surface* be exactly zero. It can easily be shown that such a flow occurring past an airfoil generates no lift. What the Kutta-Zhukovsky argument does next is to insert a 'line vortex' i.e. infinitesimal source of infinite circulation* somewhere inside the airfoil (where, that can be calculated). If the back of the airfoil is an infinitely sharp corner, then it turns out that the flow velocity at this corner must either be infinity or zero. Since the latter is the only plausible case, we impose on the flow this condition, called Kutta condition. This leads to a value for the strength of the line vortex in terms of the shape of the airfoil; thereafter a routine (even if lengthy) calculation leads to the value of lift. The dependence of the result on U and angle of attack are correct and the numerical value of lift shows good agreement with experiment for many airfoils. The direction of lift comes out to be normal to **U**, instead of normal to the airfoil. Consequently, the airfoil is drag-free.

* A line vortex for a flow field is equivalent to a line of charge or a current wire for an electromagnetic field, except that sources of electromagnetic fields are extrinsic to the fields themselves.

On the face of it, this explanation is close to ideal. Yet, it has some conceptual shortcomings. The most important is that air is not an inviscid fluid. A viscous fluid (howsoever small the viscosity) imposes the boundary condition at the surface of an immersed rigid body that *all* components of the velocity at the

surface be zero. Inviscid flow past an airfoil has no lift unless the line vortex is artificially added. When viscosity is present, one possible explanation of what happens is that the flow velocity at the airfoil surface becomes exactly zero, the velocity in a very small region near the surface (the boundary layer) gets determined by the viscosity and acquires a circulation, and the velocity beyond that region resembles an inviscid, irrotational flow. How does this complex flow of a viscous fluid relate to the line vortex of an inviscid fluid ? A second limitation of the argument is that a real airfoil can never have an infinitely sharp corner at the back – it can be very sharp but that's all. The moment this happens, the Kutta condition falls through. From a practical viewpoint, the absence of drag is a weakness; the drag on an airfoil rides piggy-back with the lift and is actually quite significant.

Different authors have accepted the Kutta-Zhukovsky explanation to different degrees. LANDAU and LIFSHITZ [04] as well as KUNDU and COHEN [05] treat it as perfectly sound. CLAES JOHNSON [06] on the other hand calls it a "non-physical fiction". A balanced perspective comes from GEORGE BATCHELOR [07]; quoting verbatim : "It is a remarkable fact that in practice a circulation is generated round an airfoil ….. and that when the airfoil is in motion, it is established with just this special value [the one satisfying Kutta condition]. This fortunate circumstance, that the effect of viscosity acting in the boundary layer initially is to cause the establishment of precisely the value of circulation that enables viscosity to be ignored (since no separation of the boundary layer occurs) in the subsequent steady motion, is usually given the name ZHUKOVSKY's hypothesis." BATCHELOR was one of the leading figures of fluid dynamics, and his attributing the Kutta-Zhukovsky explanation to a "fortunate circumstance" does not do it much credit. ■

The preceding discussion explains the position taken by The Scientific American [08] as late as 2020 that more than a century after the first human flight, its mechanism is poorly understood. Just last year, a new theory of lift has been proposed [09]. This states that viscosity is not necessary for lift. Rather, an inviscid and irrotational flow with line vortex is sufficient to generate, explain and calculate lift, with the strength of the vortex being given not by the Kutta condition but by the constraint that the spatial integral of acceleration be minimized. This constraint expands the applicability of the theory to airfoils without artificially sharp corners. The new theory of lift has no drag, and no demonstration has been made as of yet as to how the results may be altered by the addition of viscosity. On this last point, a rebuttal has been posted [10] long after I had written the first version of this paragraph, forcing me to amend this material to include this latest development.

Suffice it to say that, as of today, we lack a comprehensive and universally accepted explanation of lift. In this Article, what we will do is use the momentum theory. This will be an adaptation of the Newtonian theory which introduces a couple of constants to overcome its primary limitations.

§20 **Momentum theory of lift, drag.** The moment I make a selection of any explicit theory of aerodynamic forces, some of you will react with scepticism. This scepticism will take the form that lift and drag cannot be captured by any simple theory, that their expressions i.e. C_L, C_D and C_m can come only from wind tunnel experiments or computational fluid dynamics simulations, and that any aircraft model predicated on heuristic theories like the ones in the last Section is bound to be inaccurate or unrealistic. What is important to note is that *simplified theories are enough to give the forces; their inadequacy lies in describing the airflow around (and especially behind) the aircraft*. If we were studying formation flight and wanted to calculate the aerodynamic influence of the leading aircraft on the trailing aircraft, then a lift and drag theory like Newtonian or Kutta-Zhukovsky theory would not work. Ditto if we were analysing wake turbulence – the spatiotemporal velocity fluctuations in the air behind an aircraft, which is actually the limiting factor in determining the longitudinal separation between two successive departures from the same runway. However, for analysing the dynamics of a single aircraft, the profile of the surrounding flow field is completely unnecessary as long as we have the forces on the aircraft. Models based on data tables may be extremely high-fidelity but, as we have already seen, they cannot be used to generate insight into aircraft motions. As regards the fidelity of our model based on momentum theory, I will present the totality of Chapters 4 and 5 as evidence that this model is accurate. There will be dozens, probably hundreds, of major and minor points where our model will agree with, and hence account for, real observations made on real

aircraft. Concurrently, we will not see even one significant discrepancy between model predictions and reality. While making a selection of an explicit theory vis-a-vis an experimental or numerical data table, we effectively have a choice between mathematically analysing takeoffs, landings and the like, and not doing so; in this Article we have made the former decision.

A simple airfoil is a thin, prismatic body with a specially designed cross-section as shown below.

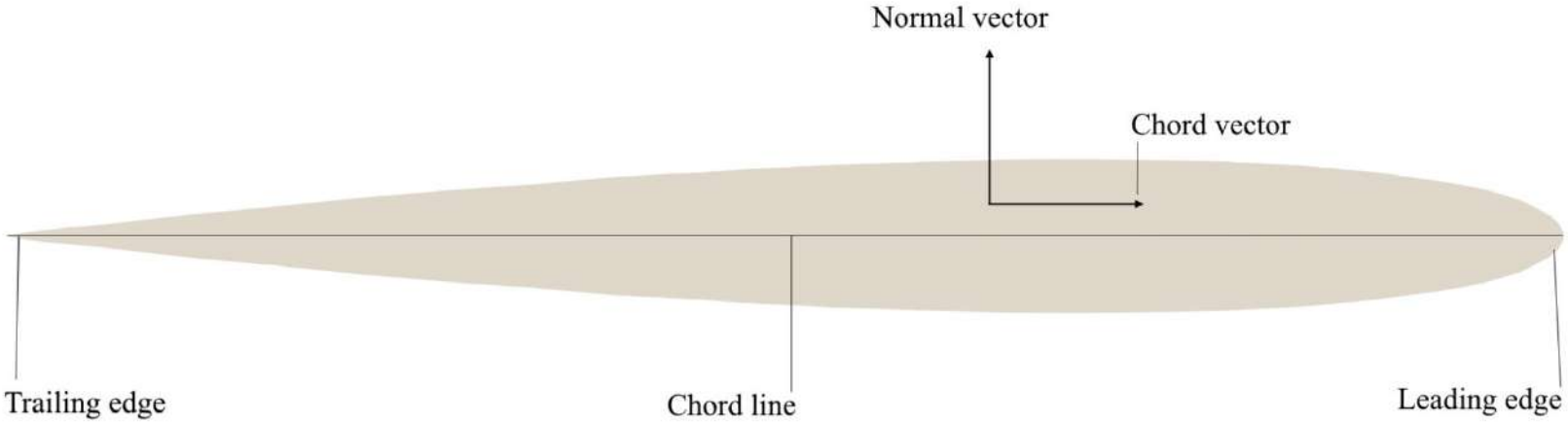


Figure 07 : *An airfoil. The span vector comes out of the plane of the page. This shape is called NACA 0012, and is what we have been using for the cross-sections of all aerodynamic surfaces of Our Plane.*

The front of the airfoil is called the leading edge and the back the trailing edge. We can easily identify three orthogonal directions – the span, the chord and the normal, as shown above. The chord line is a straight line joining the two edges and the chord vector is parallel to this line, running from back to front. The span is perpendicular to the chord, coming out of the plane of the airfoil while the normal is perpendicular to both of these. We can see that the three form a dextral triplet which we call e_1,e_2,e_3 (for an aircraft with wings making a 90° angle to the fuselage, they more or less correspond to q,d,o). When an airfoil is mounted in an airflow (i.e. the airfoil is stationary with respect to the ground and the air is moving), the e_1-component of the flow plays no role in generating lift, so we assume that the flow occurs in the e_2-e_3 plane only. Without loss of generality, we fix the airfoil's e_1 to be along ground's x and the flow **U** to be along $-y$; we rotate the airfoil about the e_1-axis to achieve different flow geometries.

Let the axes e_2 and e_3 make angle α with y and z as shown below. The angle α is called the **angle of attack** and is of paramount importance in aviation.

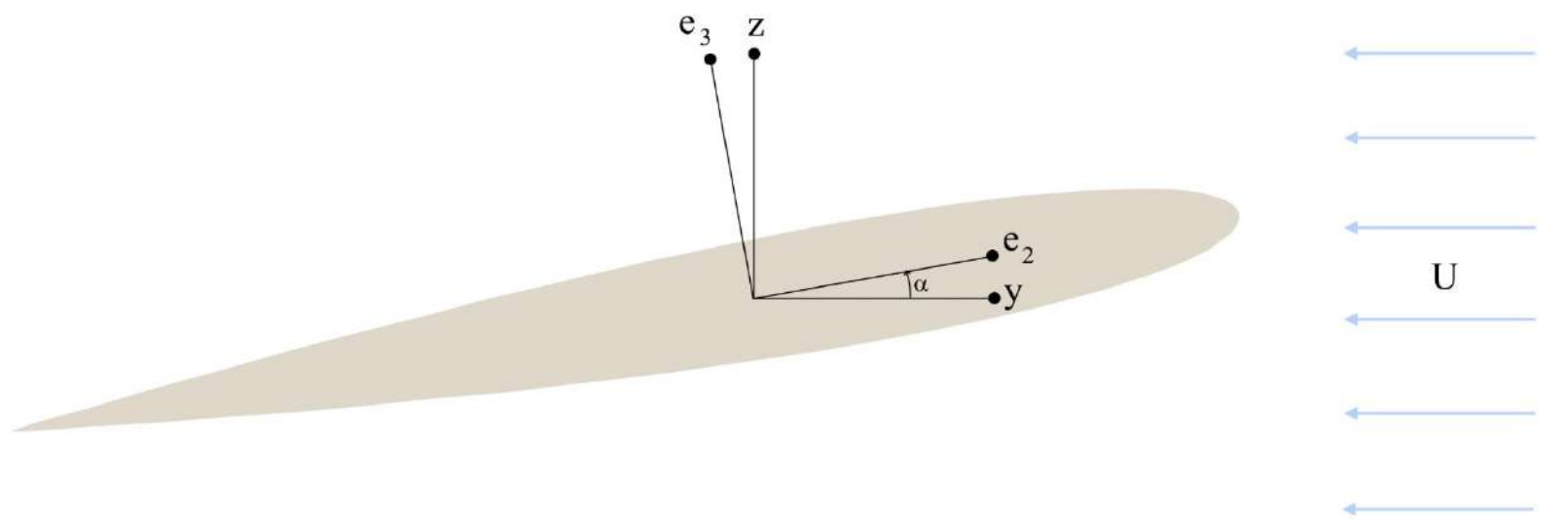


Figure 08 : *The airfoil showing the definition of angle of attack α. **U** represents the airflow in a reference frame where the airfoil is stationary.*

A more formal definition of angle of attack*, valid in three spatial dimensions, is as follows. Consider a reference frame in which the air is stationary. In this reference frame, the angle of attack is the angle *from* the e_2-e_3 projection of the airfoil's

* Angle of attack is also called angle of incidence, especially in UK. In an international subject like aviation, we can freely mix and match elements from different varieties of English, picking the most appropriate or nice-sounding word in each instance.

velocity vector *to* the airfoil's chord line. The symbol α for angle of attack is universal, be it in the science, engineering or piloting Literature.

Now let's see what happens if we replace the airfoil by a flat plate and apply NEWTON's peashooter argument. Incidentally, the conception of a wing as a flat plate, i.e. as a *plane*, gave rise to the name "airplane" for the device under consideration in this Article. Let the airflow have speed U, and the plate have length L and width (e_1-direction) w. We assume that each packet of air (pea) of mass Δm collides elastically with the plate. The collision imparts momentum to the plate along the normal; this momentum is the mass of the air packet times twice the component of its velocity normal to the plate, which is $2\Delta mU \sin\alpha$. The number of air packets impacting the foil per unit time is proportional to U. It is tempting to count this number as $LwU\sin\alpha$ times the number σ of air packets per unit volume, as shown below.

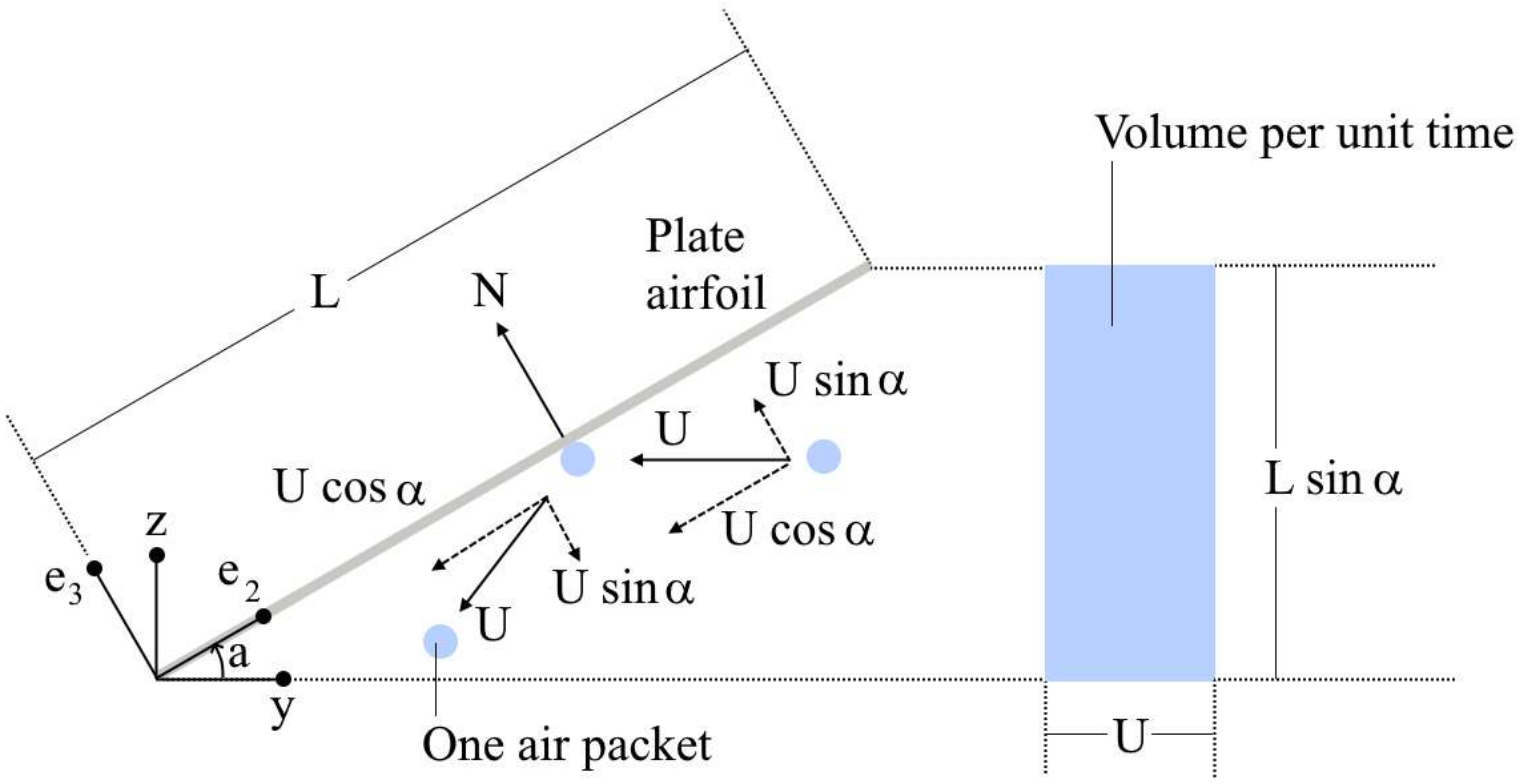


Figure 09 : *Schematic representation of air packets hitting a flat plate airfoil. The sky blue dots show one packet approaching the airfoil, striking it and then reflecting away from it. The blue area is a plausible expression for how much air hits the plate per unit time – to get the volume, we must multiply the area by the width* w *perpendicular to the plane of the page.*

If we do this, then the total momentum transferred per unit time, i.e. the force on the airfoil, works out to $2\sigma\Delta mLwU^2\sin^2\alpha$. We can multiply the packet density σ by its mass Δm to get ρ, the density of the air. The resulting expression shows good agreement with experiment in many aspects but not in all. In particular, the dependences on ρ, L, w and U are correct but that on α is incorrect – the correct angular dependence should have been $\sin\alpha$, as obtained from the Kutta-Zhukovsky theory. A possible source of the error is that the calculation neglects collisions between air packets moving towards the plate and packets leaving the plate. These collisions can deflect packets towards or away from the plate or cause them to strike it with a higher or lower velocity. Anyway, we take the correct factor of $\sin\alpha$ from the experiments and write

$$\mathbf{F} \propto \left(\rho LwU^2 \sin\alpha\right)\hat{\mathbf{e}}_3 \quad . \tag{01}$$

I am leaving things as proportional so that I don't have to keep adjusting the constant of proportionality; after identifying and isolating the dependences of interest, I'll bunch all the rest into a K. It has also taken a while for our first equation to appear; now that the flow has started however, we'll keep it up.

By definition, the component of **F** normal to the airflow (i.e. the z-component) is called **lift** and the component parallel to the flow (i.e. the y-component) is called **drag**. Thus, the lift and drag on the plate airfoil are

$$F_L \propto \rho LwU^2 \sin\alpha\cos\alpha \quad , \tag{02a}$$

$$F_D \propto \rho LwU^2 \sin^2\alpha \quad . \tag{02b}$$

Experiments on real airfoils show good agreement with the above, with some caveats. In Fig. 10, taken from Ref. [11], we see the lift on an airfoil as a function of α. This shows an overall $\sin 2\alpha$ ($= 2 \sin\alpha \cos\alpha$) profile as in (02a) with prominent kinks at 15° and 170°. We shall address these kinks in the next Section; before that I must mention two other disparities between experiments and (02).

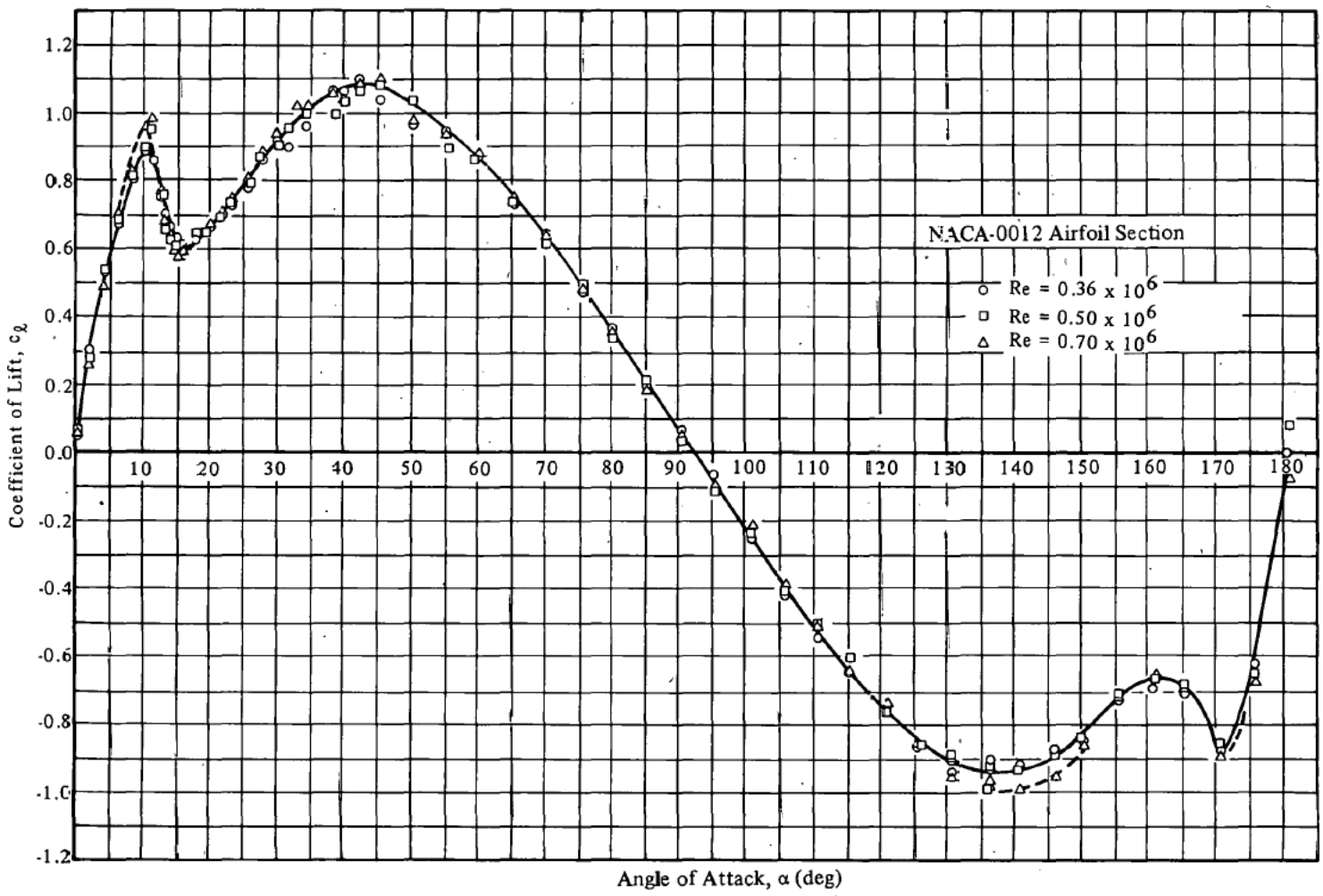


Figure 10 : *The lift coefficient (the part of* F_L *dependent on* α*) as a function of* α *for the NACA 0012 airfoil.*

Firstly, equation (02) gives the ratio of F_L to F_D, called **L/D or lift-to-drag ratio**, as $\cot\alpha$. In other words, L/D depends only on the angle of attack and nothing else. With real airfoils however, it is possible to adjust this ratio by designing the shape of the airfoil. Secondly, real airfoils can have **camber*** built into them. This means that they have a non-zero angle of attack 'frozen in' to their design and can generate lift even when α is zero. Such airfoils generate zero lift only when α is negative. Camber is implemented by adding curvature to the airfoil – below we see an airfoil with camber.

* The word "camber" means a completely different thing when applied to road vehicle engineering. Whereas in a plane a cambered wing has a prefabricated non-zero pitch, in a car a cambered wheel has a prefabricated non-zero bank. Such a bank in an aircraft wing is on the other hand called "dihedral". Adopting the term "dihedral" in automotive engineering will eliminate this needless confusion. In railway engineering, the word "camber" sometimes denotes a height difference between the two rails of one track, although the substitutes "cant" and "superelevation" are more common (and more appropriate).

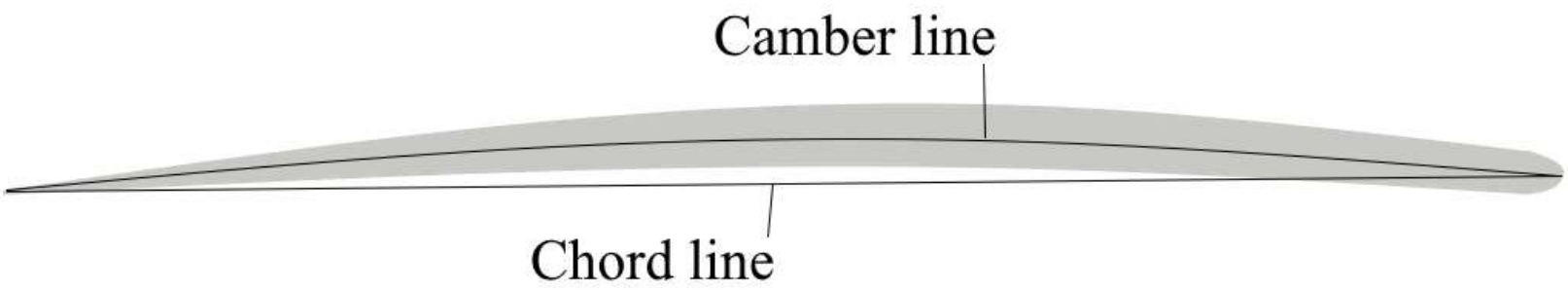


Figure 11 : *A cambered airfoil. The camber line is the line equidistant between the top and bottom of the airfoil while the chord line is the straight line from back to front. The two coincide if the camber is zero i.e. the airfoil is symmetric.*

Recall from Fig. 2A–03 that when flaps and slats are extended, the aircraft's wing acquires an inverted U shape. This curviness adds camber to the wing. However, (02) cannot account for the presence of camber.

To circumvent these limitations, we introduce two parameters γ and ε. We say that the aerodynamic force on a real airfoil mounted in the airflow with angle of attack α is equivalent to that on a Newtonian plate mounted with angle of attack $\alpha' = \varepsilon(\alpha+\gamma)$. Here ε is a scale factor which is positive and of order unity, and γ is the camber. Let e'_2 and e'_3 denote axes rotated though α' relative to y and z, as below.

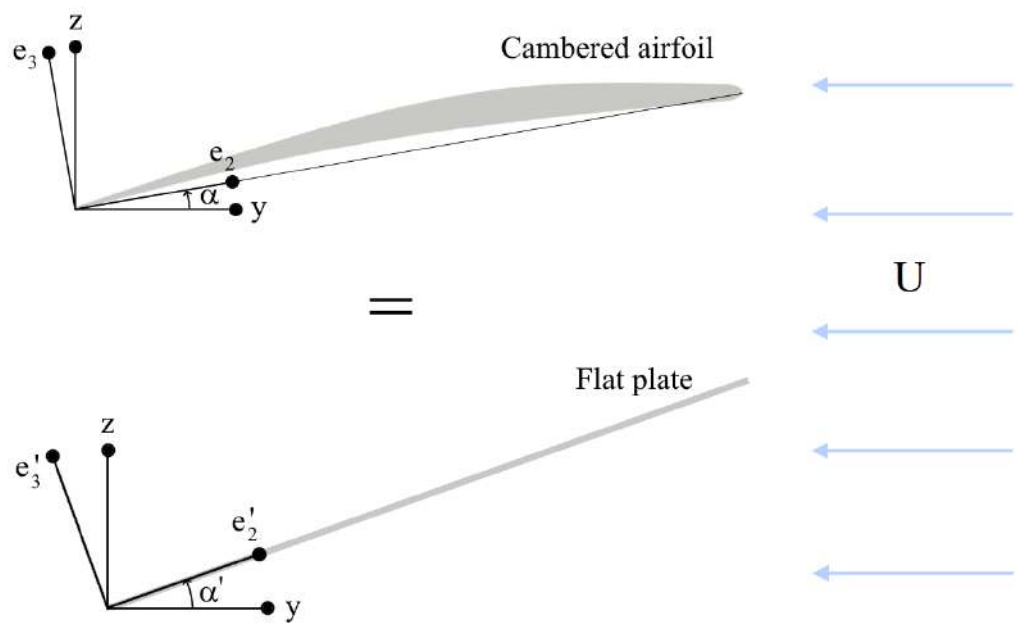


Figure 12 : *Equivalence between the actual airfoil making an angle of attack α and a flat plate making angle of attack α′. We can also see the primed and unprimed axis systems.*

Then, as per our model, the aerodynamic force on an airfoil with angle of attack α is

$$\mathbf{F} \propto \left(\rho L w U^2 \sin\alpha'\right)\hat{\mathbf{e}}'_3 \quad \text{, where} \tag{03a}$$

$$\alpha' = \varepsilon\left(\alpha+\gamma\right) \quad . \tag{03b}$$

This has the components

$$F_L \propto \rho L w U^2 \sin\alpha'\cos\alpha' \quad , \tag{04a}$$

$$F_D \propto \rho L w U^2 \sin^2\alpha' \quad . \tag{04b}$$

If γ is positive, then F_L is nonzero even when $\alpha = 0$. When the true angle of attack is α, L/D is $\cot\alpha'$ or $\cot\left(\varepsilon(\alpha+\gamma)\right)$. For an airfoil without camber, this reduces to $\cot\varepsilon\alpha$. The value of ε can be chosen to match the experimental results.

Real airfoils generate optimal lift only when the angles α and γ are small. Since ε is of order unity, α' is small as well. When this is true, we can insert an extra $\cos\alpha'$ term into (03), thus

$$\mathbf{F} \propto \rho L w U^2 \sin\alpha'\cos\alpha'\hat{\mathbf{e}}'_3 \quad . \tag{05}$$

The advantage of this insertion is that $U\cos\alpha'$ is the negative of the component of **U** along the e'_2-direction while $U\sin\alpha'$ is the component of **U** along the e'_3-direction. Then, we can write (05) as

$$\mathbf{F} \propto -\rho L w U_{e'2} U_{e'3}\hat{\mathbf{e}}'_3 \quad , \tag{06}$$

which is a polynomial in components of **U**. This is great news since (*a*) polynomials are the most tractable mathematical functions and are easy to differentiate for calculating Jacobians etc, and (*b*) polynomials in components remain so under rotation of axes, a manoeuvre which we shall require more times than we can count*. Finally, we can give a clear definition to the proportionality relations in the past six equations. For modeling the aircraft, we shall need the aerodynamic force on wings of fixed size and shape, and, for small-duration manoeuvres, we can also assume the density of air to be constant. Hence, we can sweep everything in (06) into a proportionality constant K, determined experimentally for each wing, which we call the lift constant. In terms of this constant, we can write the force as

$$\mathbf{F} = -K U_{e'2} U_{e'3}\hat{\mathbf{e}}'_3 \quad . \tag{07}$$

* These considerations will become doubly important when we attack the three-dimensional version of this problem, and the equations involved will be hellish in their complexity.

This is the expression for aerodynamic force which we shall use in this Article.

The distribution of **F** over the surface of the airfoil determines the torque exerted on it. The torque is equivalent to the entire force acting through one point called the **centre of pressure (CP)**. Here we won't need to calculate its location explicitly; rather we shall treat its location as a given. Note that CP is different from the aerodynamic centre (AC) – the latter is a point about which the torque of the lift is independent of the angle of attack. We won't have much use for AC in this Article, but it comes up a lot in some works on flight dynamics, and this is what it means. Right now, please also take note of a semantic imprecision which I shall permit myself in the rest of this Article. Although (07) features both a lift and a drag, it's the former component which is dominant and which is of interest. Hence, I will freely refer to the **F** of (07) as the "lift" in future discussion, whenever this terminology doesn't create confusion.

In this Article, we shall make a simplification to (07). Since we shall be performing the stability analysis and demonstrating the simulation manoeuvres for a model aircraft rather than an actual one, let us take $\gamma = 0$ and $\varepsilon = 1$ so that $\alpha = \alpha'$ and $\hat{\mathbf{e}}_{2,3} = \hat{\mathbf{e}}'_{2,3}$. This assumption makes the geometry easier to visualize while not throwing away any physical phenomena. When using the model to account for the motions of a particular aircraft, we can always re-introduce ε and γ to achieve the best fit. As an aside, it is interesting to note that GEORGE BRYAN [1O–01] had also used the formula $U^2 \sin\alpha$ for lift in an example showing the explicit calculation of the stability derivatives.

In addition to lift on an airfoil, we shall also need a formula for the drag acting on a bluff body (non-aerodynamic object), which is what the fuselage happens to be. Newtonian theory is the only one which has drag. When a bluff body is mounted in an airstream of velocity **U**, this theory gives the drag as

$$\mathbf{F}_D = CU^2 \hat{\mathbf{U}} \quad , \tag{08}$$

where C, like K in (07), is a constant which factors in the density of air, the dimensions of the body and other quantities unrelated to the flow geometry. There is no minus sign in (08) since the drag acts in the same direction as the airflow – when the body is moving through the stationary fluid, the direction becomes the opposite of the body's motion. At higher flow speeds (those relevant for aircraft), the formula (08) agrees well with experiments, and is what we shall use here. Like the force (07), the drag too has a CP whose location we shall treat as a given.

§21

Aerodynamic stall. The lift formula (07) is valid for small angles of attack. Figure 10 shows a sharp drop in lift at $\alpha = 15^o$ which makes invalid any formula which is continuous at that angle. What happens at and beyond 15^o is called aerodynamic stall. This is when the airflow around the foil abruptly changes character from laminar to turbulent, resulting in a precipitous drop in lift and an equally sudden and steep increase in drag. Stalling is a universal phenomenon across all airfoils. It is always triggered by exceedance of angle of attack beyond a critical value, and not by the speed of the airflow. Let's call the critical α as α_S. Its value is typically about 15^o, as for the airfoil of Fig. 10; the particulars of the design can adjust by it a few degrees on each side. Cambered airfoils stall at lower angles of attack than symmetric ones – if an airfoil has intrinsic camber γ, then its α_S will be $15^o - \gamma$, give or take. There is no theoretical framework – not even one with limitations – for calculating lift and drag on an airfoil at $\alpha > \alpha_S$. Indeed, the forces become time-dependent even if the far field flow is steady, and the time-averaged values can only be determined from experiments.

In this Article, we shall use a completely ad hoc formula for calculating the aerodynamic forces on a wing in stall. Whenever $|\alpha| > \alpha_S$, in place of (07) we shall use

$$\mathbf{F} = \min\left(\left| KU_{e2}U_{e3} \right|, \frac{\text{peak nonstall lift}}{3} \right) \hat{\mathbf{e}}_3 \quad . \tag{09}$$

This states that the aerodynamic force is directed along e_3 and has the magnitude given by either (07) or one-third of the force as per (07) evaluated at $\alpha = \alpha_S$, whichever is lower. The only realistic feature of stall which (09) captures is the drastic reduction in force across $\alpha = \alpha_S$. In addition, a stalled airfoil acts a lot like a bluff body with huge drag. We shall model this as

$$\mathbf{F}_D^S = C_1 \sin\alpha U^2 \hat{\mathbf{U}} \quad , \tag{10}$$

where the superscript S indicates stall and the $\sin\alpha$ takes into account that more and more wing area is exposed to the airflow as α increases beyond the stall angle.

The groundwork for constructing the aircraft's dynamic model is now complete. The next step is to actually put the pieces together to formulate the model itself.

B. PITCH PLANE EQUATIONS OF MOTION

In this Subdivision, we consider the motions in the pitch plane i.e. the *y*-*z* or *d*-*o* plane. This is the most important of the three planes since it is where the lift is actually generated. Our analysis here will also pave the way for the calculations in the other planes. Unless explicitly mentioned otherwise, we shall assume that the air is still (i.e. there is no wind) and that the aircraft is not in a stall.

§22 **Geometry, variables and parameters.** In Fig. 01 we can see Our Plane in the *y*-*z* plane. The point B is the CM or Barycentre of the aircraft, C the CP of the wings and E the tail or Empennage. Technically, E should be the CP of the tail but since the tail is small compared to the plane, it doesn't matter. We assume that C and E are both located on the direct axis. **V** is the velocity of B; by our assumption of still air, **V** can be with respect to both air and ground. η is the angle of elevation i.e. $\eta = \arctan(V_z/V_y)$ and θ is the pitch, so that $\alpha = \theta - \eta$ becomes the angle of attack. Let m be the aircraft mass, d_1 the length BC and d_2 the length BE. Let h be the distance from the d-axis to the centreline of the engines – in most jetliners, the engines hang below the fuselage centreline. While defining distance variables, one has a choice between two sign conventions : (*a*) positive if the displacement is parallel to the positive axis, or (*b*) positive in the direction which is conventional for an aircraft. Thus, d_1, d_2 and h will be negative as per the first convention and positive as per the second. While deriving the equations of motion, I shall go with the first convention since that is more general, and will be easier to use in a systematic treatment of the three-dimensional problem. However, since most of us, myself included, are intrinsically more comfortable with positive quantities, I shall then define $\bar{d_1}$ to be $-d_1$, $\bar{d_2}$ to be $-d_2$ and $\bar{h}$ to be $-h$, and actually write the equations in terms of these.

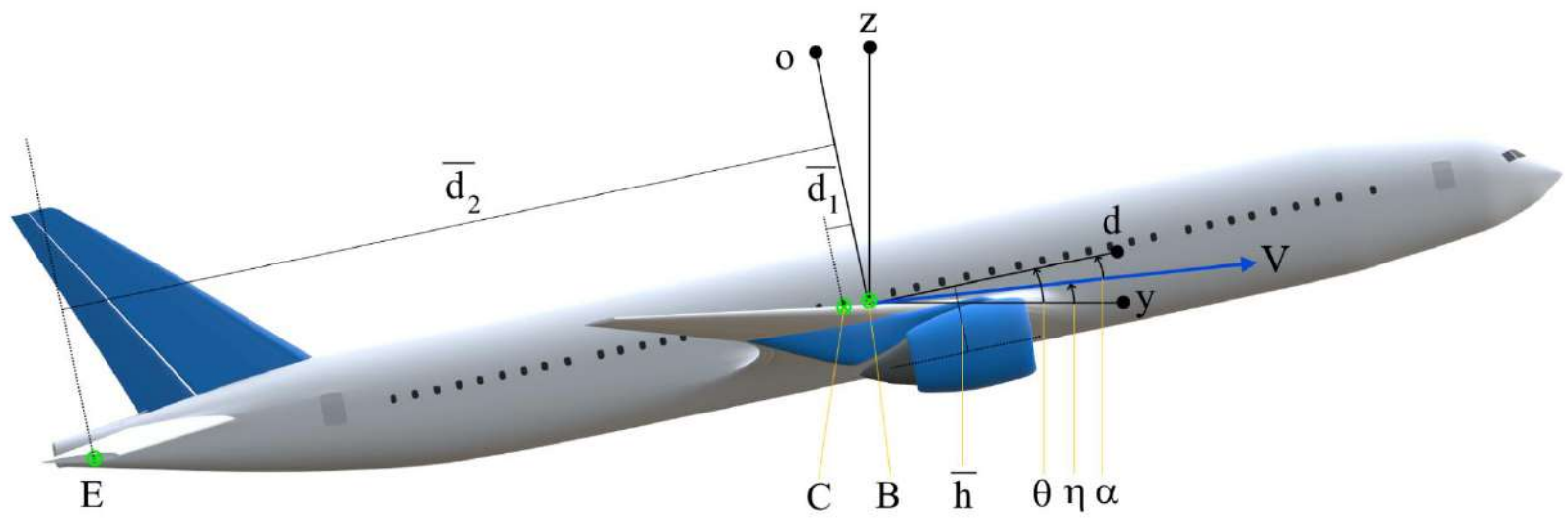


Figure 01 : *Our Plane showing the various points and dimensions. Pitch is 12º and angle of elevation 6º, which are realistic. The ratio of approximately 25 between $\bar{d}_1$ and $\bar{d}_2$ is realistic as well. While I could have introduced exaggerations for the sake of increasing clarity of the diagram, I have opted for realism because pictures are often retained in the mind better than text, and you should not be remembering a distorted picture of your jetliner.*

Let K_C be the lift constant of the wings and k_E be that of the horizontal tail; let C be the drag constant of the fuselage.

§23 **The horizontal tail or elevator (stabilator).** Just as the explicit formulae (3A–07,08) for lift and drag enable to us to bypass the tabulated functions C_L and C_D, an explicit model of the elevator will result in the short-circuiting of the unknown C_m. We have seen in §05 that the tail has a horizontal stabilizer and an elevator, that the two can be merged into a stabilator, and that this is what Our Plane has. Why this assumption

doesn't compromise generality, that we'll see a little later. Since "stabilator" is an unfamiliar word however, I shall refer to it simply as "elevator" in what follows.

We can see a schematic representation of an elevator in Fig. 02. Like the wing, it is an airfoil; unlike the wing, it is pivoted to the fuselage instead of being rigidly attached. It is also connected to the stick in the cockpit. When the pilot manipulates the stick, a torque acts about the pivot. In planes without fly-by-wire, the connection between stick and elevator is mechanical; a hydraulic mechanism creates a torque directly proportional to the force with which the pilot pulls or pushes the stick. Boeing 747-400 is probably the latest aircraft of this type; the amplification generated by the hydraulics is of the order of millions. In fly-by-wire aircraft, the torque on the elevator is electronically controlled, and is made a suitable function of the force or deflection applied on the stick.

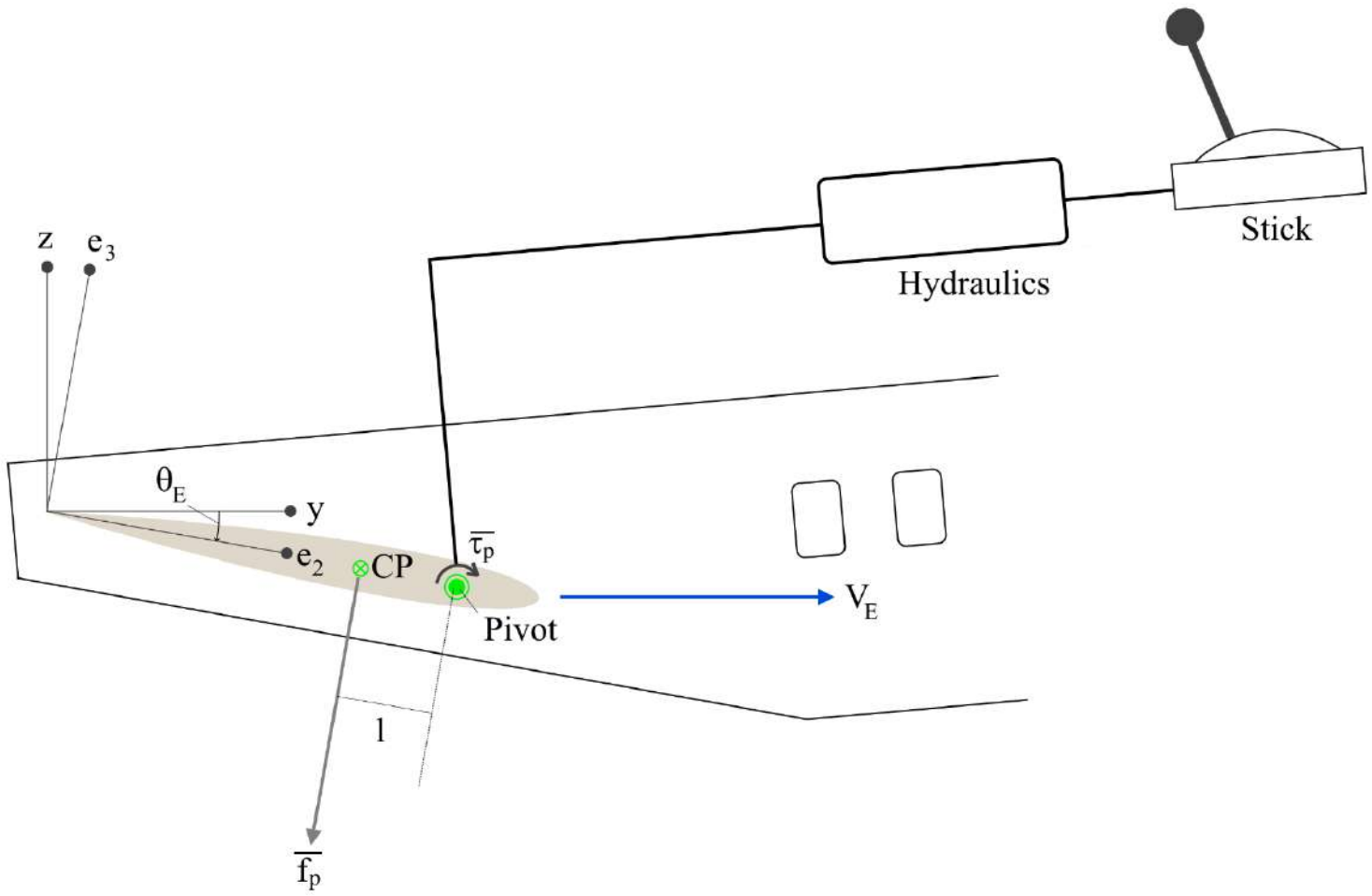


Figure 02 : *Schematic representation of the elevator pivoted to the fuselage. We can see the aft section of the fuselage, minus the vertical tail. In this Figure we assume that the elevator's velocity* $\mathbf{V}_E$ *is horizontal, for easier understanding. The angle of attack of the elevator is negative, so the lift is negative also.*

Let τ_p (to be technically accurate, $\tau_p \hat{\mathbf{e}}_1$ where e_1, e_2, e_3 is the elevator airfoil basis) be the torque applied on the elevator by the pilot (the subscript p stands for pitch). If we (very realistically) treat the elevator as massless, then the elevator must always be in a state of torque equilibrium. The only external torque acting on the elevator comes from the lift, as shown in Fig. 02. Let's call this lift f_p. By the formula (3A–07) and our assumptions of $\varepsilon = 1$ and $\gamma = 0$, f_p acts through the CP along the e_3-direction; evidently, $\tau_p = lf_p$ with l being the distance from the CP to the pivot. The pivot must always be forward of the CP; why this is so, we can understand only in §33. If τ_p is positive, f_p is positive as well. Henceforward, we shall treat f_p rather than τ_p as the fundamental pilot-inputted quantity.

Given f_p, our next task is to determine the elevator deflection. Let θ_E be the angle it makes with the horizontal i.e. the y-axis, let $\mathbf{V}_E$ be its velocity vector with respect to the ground and let the angle of elevation of $\mathbf{V}_E$ (i.e. angle between $\mathbf{V}_E$ and y-axis) be η' (we have taken η' to be zero in Fig. 02). The angle of attack of the elevator then is $\alpha_E = \theta_E - \eta'$; expressing (3A–07) in terms of magnitude and angle rather than components we have

$$f_p = \frac{k_E}{2} V_E^2 \sin 2\alpha_E \quad \text{, or} \tag{01a}$$

$$\alpha_E = \frac{1}{2}\arcsin\frac{2f_p}{k_E V_E^2} \Rightarrow \theta_E = \eta' + \frac{1}{2}\arcsin\frac{2f_p}{k_E V_E^2} \quad . \tag{01b}$$

Note that if the stick force is zero, then the elevator lies *parallel to the flight path and not to the fuselage*. More generally, the elevator deflection, i.e. the angle $\theta_E - \theta$ between elevator and fuselage, is not directly related to f_p.

Equation (01b) specifies a maximum (absolute) value for f_p at a given V_E – that for which α_E equals the stall value α_S. If a higher f_p is commanded, the lift will be unable to balance the applied torque τ_p at any angle, sending the elevator into free spin. Practically, its motion will be mechanically restrained; in a fly-by-wire aircraft, such a command will never be given to begin with. Hence, an actual stalled tail is an unrealistic scenario. While running the simulator at low flight speeds, we will however need to make sure that the commanded f_p generates an α_E within the nonstall regime. At high speeds, f_p will not be constrained by stall but by the maximum force which the elevator can withstand without being shorn off the fuselage.

To obtain the direction of stick input (push or pull) in terms of the sign on f_p, we look at Fig. 01. We can see that the aircraft nose will pitch up if the tail exerts a negative lift i.e. f_p is negative. Since pitch up corresponds to pulling the stick, we see that pull causes a negative f_p while push causes a positive f_p. Figure 01 further shows that during steady flight, since the wings generate a positive lift acting at C, torque equilibrium about B can be achieved only if the elevator generates negative lift at E. Indeed, this is what happens in most aircraft, which causes us to define the positive $\bar{f}_p$ as $-f_p$. Equilibrium would have required positive elevator lift if the CM had been aft of the CP of the wings; this configuration however has adverse implications on stability, which we shall see in §33 (again, and this is not a coincidence – the issue of elevator pivoting is related to stability). Hence, almost all planes have the CM, the CP and the tail arranged in that order, which we call B-C-E for short. A few fighter and aerobatics planes are designed with CP forward of CM; we call this configuration C-B-E.

In a B-C-E aircraft with a stabilator, the constant pull-back required for maintaining steady flight is tiring for the pilot (of course it doesn't matter if the autopilot is flying). In an aircraft with separate stabilizer and elevator, this is where the trim mechanism enters the picture. The stick connects to the elevator, and steady level flight using that alone would again require a constant pull force. Instead of that however, what the pilot does is, he uses the trim wheel to set the stabilizer to a constant deflection, chosen such that the entire tail force comes from the stabilizer alone. Then, an elevator force of zero i.e. hands off the stick is sufficient to maintain the angular equilibrium. Only when the pilot wishes to change the pitch does he pull or push on the stick. Flight in different conditions, such as different speeds and altitudes, requires different trim settings for stick-free equilibrium. In GA aircraft, trim is implemented in a different manner. The stabilizer is fixed at a constant deflection and trim is adjusted by 'freezing' the elevator at a constant nonzero angle. Further details of this mechanism are outside our scope. But when actually flying, it is very important that you know how the trim works on your aircraft, how the autopilot auto-adjusts trim and how you can take control of the mechanism if you so desire.

Now we can see why our assumption of stabilator in Our Plane does not compromise the generality of the model. The net effect of changing the stabilizer and elevator deflections is the selection of an arbitrary (within limits) force at the tail. The stabilator is automatically capable of this since $\bar{f}_p$ is a variable. We can always choose $\bar{f}_p$ of Our Plane to equal the sum of the two forces in a conventional plane. Just to clarify, this does not mean that Our Plane and a conventional dual-tail plane have identical dynamics and handling characteristics. What it means is that the equation of motion of the dual-tail can be derived from that of Our Plane by using a suitable substitute equation for (01). In this Article, we won't do the quantitative analysis of a dual-tail aircraft but will qualitatively highlight the principal differences between single- and dual-tailed planes in the appropriate contexts.

The two accidents featuring Boeing 737-MAX – Lion Air Flight 610 on 29 October 2018 and Ethiopian Airlines Flight 302 (ETH 302) on 10 March 2019 – were caused by erroneous activation of an

automatic controller of the horizontal stabilizer. To make the handling characteristics of 737-MAX similar to those of previous 737 variants, Boeing had inserted a software called Maneuvering (sic) Characteristics Augmentation System (MCAS) which automatically adjusted the horizontal stabilizer deflections. To achieve a quicker and cheaper certification of the airplane, Boeing (colluding with FAA or Federal Aviation Administration of the US) had withheld the existence of MCAS from all stakeholders, including airlines, air crews and aviation safety agencies of other countries. In both the accident flights, a defective angle of attack sensor caused MCAS to detect an impending stall when there was no such threat, and automatically sent the horizontal stabilizers to maximum nose-down trim. The pilots being unaware of the existence of MCAS had no idea of what was happening – they simply found the nose pitching down even though they were applying maximum pull force on the stick. Following the two accidents, the aircraft remained grounded for many months. Recertification of airworthiness was achieved after hundreds of modifications, chief among which were redesign of MCAS to (*a*) rely on data from multiple angle of attack sensors and not just one, (*b*) not activate repeatedly within a short time-frame, and (*c*) not apply any force greater than the maximum which the pilot can override manually. In addition, all pilots of 737-MAX underwent the simulator training which should have been provided prior to the initial type certification.

It is sometimes wondered why, if the problem with the 737-MAX was indeed one of design, did both the accidents occur with less prestigious airlines. This was because the MCAS-induced crashing had to be triggered by a malfunctioning port side angle of attack sensor – while that sensor functioned properly, this mode of crashing would not get activated. Then, it so happened that the less prestigious airlines were the first two to experience this malfunction in flight – the subsequent grounding prevented other airlines, prestigious or not, from following in their footsteps. Airliners are typically designed to suffer as many simultaneous malfunctions as possible without suffering an accident, and a fault on one angle of attack sensor is a situation which can easily be managed by an ATPL pilot flying manually. That it led to deadly accidents in this case was a consequence of erroneous design.

The 737-MAX crashes are the first aviation accidents and incidents which we examine in this Article (if we exclude the crash of Gol Transportes Aereos Flight 1907 considered in §12,16 which did not have any underlying dynamic phenomenon involved)*. The difference between an accident and an incident – at least the one which we shall use – is that an accident features at least one serious injury or fatality while incident involves only minor injuries or better. Analysis and hence prevention of these is one of the most practical and relevant aspects of flight dynamics, and it is one of the highlights of our model-based approach that it can extract the dynamical lessons from multiple adverse events throughout recent aviation history. ICAO has the following policy regarding accident investigations – "The sole objective of the investigation of an aircraft accident or incident shall be the prevention of accidents and incidents. It is not the purpose of this activity to apportion blame or liability." – which we wholeheartedly support and adhere to throughout this Article.

* It is very common to refer to an aviation accident by the flight number alone and nothing else, as in "ETH 302 was the last nail in the coffin for the 737-MAX, at least for a long while". Semantically, this is incorrect as ETH 302, or any other flight number, refers to a particular *route*, which has been operated thousands of times prior to and possibly after the accident (many times, airlines change the number of a route which crashes). At least when referring to an accident for the first time, it is better to say "ETH 302 of 10 March 2019 was ….." or, if (as is likely) you don't remember the date, then "The crash of ETH 302 was …..". In subsequent references in context, the flight number usually suffices.

§24 **Forces and torques.** In the Figure below, we can see the forces acting on the aircraft.

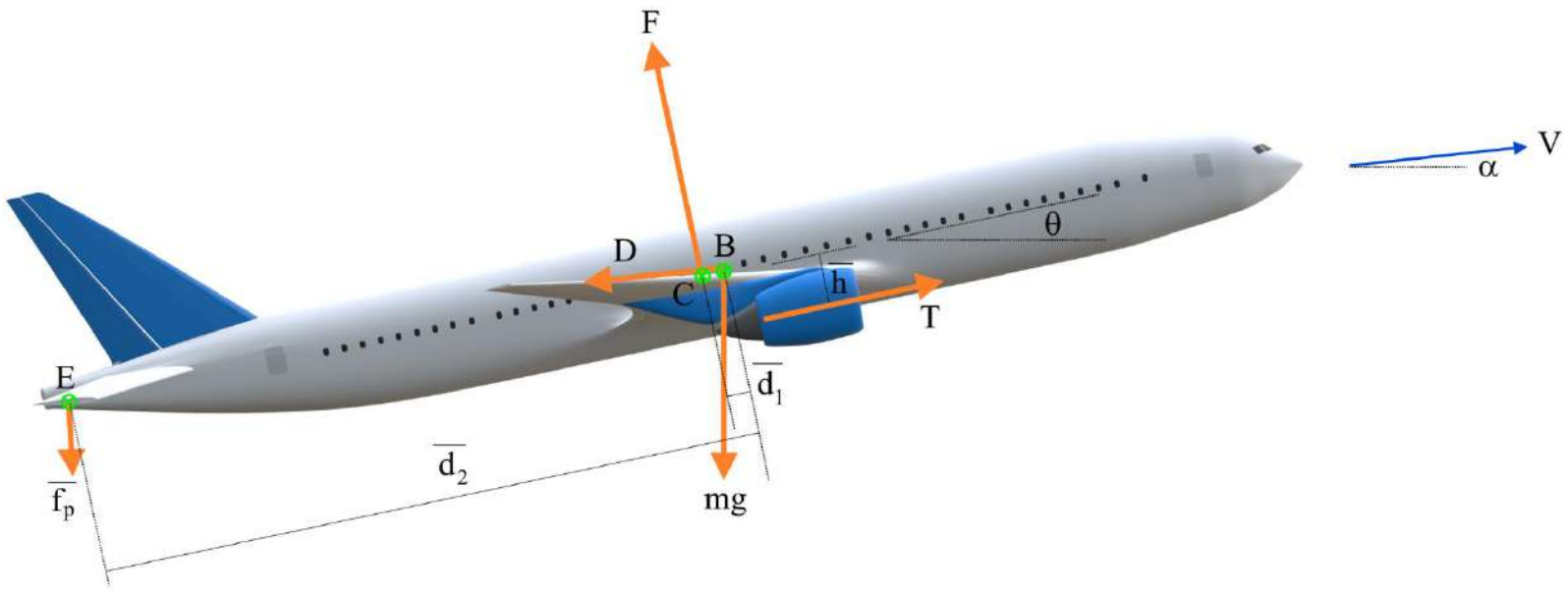


Figure 03 : *Forces acting on Our Plane.* F *is the lift,* mg *the weight,* T *the thrust and* D *the drag. Other symbols carry over from Fig. 01 and accompanying text. Pitch and elevation are 12º and 6º as in Fig. 01; the elevator deflection is –3º from the flight path and –9º from the fuselage. The directions of all forces as well as the velocity are accurate but their magnitudes are not drawn to scale.*

We assume that the wings are mounted parallel to the fuselage so that their chord coincides with the direct axis. Hence, we need three sets of bases – y,z attached to ground, d,o attached to the fuselage and shared by the wings, and e_2,e_3 attached to the tail. The angle θ takes us from y to d, giving the rotation matrices

$$\begin{bmatrix} \mathcal{V}_d \\ \mathcal{V}_o \end{bmatrix} = \begin{bmatrix} \cos\theta & \sin\theta \\ -\sin\theta & \cos\theta \end{bmatrix} \begin{bmatrix} \mathcal{V}_y \\ \mathcal{V}_z \end{bmatrix} \quad , \quad \begin{bmatrix} \mathcal{V}_y \\ \mathcal{V}_z \end{bmatrix} = \begin{bmatrix} \cos\theta & -\sin\theta \\ \sin\theta & \cos\theta \end{bmatrix} \begin{bmatrix} \mathcal{V}_d \\ \mathcal{V}_o \end{bmatrix} \quad , \tag{02}$$

where $\mathcal{V}$ denotes an arbitrary vector. A rotation matrix is by definition orthogonal, so its inverse is the same as its transpose. Since vectors transform the same way as coordinates, we can also write, with more than a little linear algebraic licence,

$$\begin{bmatrix} \hat{\mathbf{d}} \\ \hat{\mathbf{o}} \end{bmatrix} = \begin{bmatrix} \cos\theta & \sin\theta \\ -\sin\theta & \cos\theta \end{bmatrix} \begin{bmatrix} \hat{\mathbf{y}} \\ \hat{\mathbf{z}} \end{bmatrix} \quad , \quad \begin{bmatrix} \hat{\mathbf{y}} \\ \hat{\mathbf{z}} \end{bmatrix} = \begin{bmatrix} \cos\theta & -\sin\theta \\ \sin\theta & \cos\theta \end{bmatrix} \begin{bmatrix} \hat{\mathbf{d}} \\ \hat{\mathbf{o}} \end{bmatrix} \quad . \tag{03}$$

This is sloppy linear algebra because unit vectors are themselves two-component entities which cannot be put inside box brackets like they were scalars. However, equations of this form are very popular in mechanics and their meaning is transparent. As long as we are aware of their insecure mathematical foundations, there is no harm in using them. The angle θ_E takes us from y to e_2; we have

$$\begin{bmatrix} \mathcal{V}_2 \\ \mathcal{V}_3 \end{bmatrix} = \begin{bmatrix} \cos\theta_E & \sin\theta_E \\ -\sin\theta_E & \cos\theta_E \end{bmatrix} \begin{bmatrix} \mathcal{V}_y \\ \mathcal{V}_z \end{bmatrix} \quad , \tag{04a}$$

$$\begin{bmatrix} \mathcal{V}_d \\ \mathcal{V}_o \end{bmatrix} = \begin{bmatrix} \cos(\theta-\theta_E) & \sin(\theta-\theta_E) \\ -\sin(\theta-\theta_E) & \cos(\theta-\theta_E) \end{bmatrix} \begin{bmatrix} \mathcal{V}_2 \\ \mathcal{V}_3 \end{bmatrix} \quad , \tag{04b}$$

and you can invert these transformations yourself.

Let us now list the various forces acting on the plane, and the contribution of each to the torque about B. Since the plane has no fixed point, CM is the only point about which the relation $d\mathbf{L}/dt = \boldsymbol{\tau}$ holds true and we may perform a moment balance.

Wings

Using (3A–07), the lift is

$$\mathbf{F} = -K_C V_{Cd} V_{Co} \hat{\mathbf{o}} \quad , \tag{05}$$

where $\mathbf{V}_C$ denotes the velocity of point C. This has two contributions, one from the translation of the plane and the other from the rotation of the plane about B. That is,

$$\mathbf{V}_C = \mathbf{V} + \omega \hat{\mathbf{q}} \times d_1 \hat{\mathbf{d}} \quad , \tag{06}$$

where $\mathbf{V}$ is the velocity of B and $\omega = \dot{\theta}$ is the plane's angular velocity (here and henceforth, an overhead dot denotes d/dt). In a typical scenario, the first term outweighs the second by orders of magnitude, so we drop the latter and write

$$\mathbf{F} = -K_C V_d V_o \hat{\mathbf{o}} \quad . \tag{07}$$

Note that K_C takes into account both wings. The torque which the lift generates about the CM is

$$\boldsymbol{\tau} = d_1 \hat{\mathbf{d}} \times F_L \hat{\mathbf{o}} = d_1 F_L \hat{\mathbf{q}} \quad . \tag{08}$$

Since d_1 is negative, the torque is negative if the lift is positive, as is evident from Fig. 03. ■

Tail

The force is

$$\mathbf{F} = f_p \hat{\mathbf{e}}_3 \quad . \tag{09}$$

In (01), $\mathbf{V}_E$ has the form $\mathbf{V}_E = \mathbf{V} + \omega \hat{\mathbf{q}} \times d_2 \hat{\mathbf{d}}$; neglecting the second term we can write

$$\theta_E = \eta + \frac{1}{2} \arcsin \frac{2 f_p}{k_E V^2} \quad . \tag{10}$$

Note that η' of (01b) has become η since we have assumed $\mathbf{V}_E = \mathbf{V}$. The torque is

$$\boldsymbol{\tau} = d_2 \hat{\mathbf{d}} \times f_p \hat{\mathbf{e}}_3 \quad , \tag{11}$$

which, using (04b), gives

$$\boldsymbol{\tau} = f_p d_2 \cos\left(\theta - \theta_E\right) \hat{\mathbf{q}} \quad . \tag{12}$$

When f_p is negative, its torque is positive, consistent with Fig. 03. ■

Thrust

The force is $T\hat{\mathbf{d}}$ and its torque is $\boldsymbol{\tau} = -Th\hat{\mathbf{q}}$. Since h is negative, this torque is positive if T is positive, as is clear from Fig. 03. ■

Gravity

The force is $-mg\hat{\mathbf{z}}$ and the torque is zero since gravity acts through the CM. ■

Drag

The force is $-CV^2\hat{\mathbf{V}}$ as per (3A–08). We assume that the fuselage drag acts through the CM, so that its torque can be taken as zero. There is however a drag torque which will be generated when the aircraft rotates in pitch. On account of the high forward speed, the transverse motion arising from rotation will impart momentum to a large mass of air and thus be resisted by a substantial force. The moment of this force can be calculated from an analysis of the motions of the fuselage and the wings. Since drag torque is a less important phenomenon however, we refrain from this calculation and use a heuristic $\boldsymbol{\tau} = -\Gamma\omega\hat{\mathbf{q}}$, with Γ to be determined from measurements of actual aircraft. ■

Having obtained all the forces and torques, we must substitute them into Sir ISAAC's laws of motion, which read

$$m\frac{\mathrm{d}\mathbf{V}}{\mathrm{d}t} = \mathbf{F} \quad , \tag{13a}$$

$$I\frac{\mathrm{d}\omega}{\mathrm{d}t} = \tau \quad . \tag{13b}$$

In the second equation above, I is the moment of inertia of the plane about the q-axis and we have got rid of the vector nature of ω and τ since they are all about the q-axis. While this is simple in principle, the algebra involved becomes quite cumbersome, so I have used the computer algebra software called

WXMaxima to evaluate the RHSes. The Maxima input is in terms of d_1, f_p etc but while reporting the results I will express them in terms of the positivized $\bar{d}_1$, $\bar{f}_p$ and the like.

With this, we are ready to present the model equations. Over the next three Sections, I will give three representations of these equations with hardly any comment; only after the third one will I include a discussion of their relative merits.

§25

The xyz model. To obtain this form of the equations of motion, we write NEWTON's law in the *y*-*z* plane, in terms of V_y and V_z. Maxima gives the following set of equations. First, the tail angle θ_E satisfies

$$\frac{k_E}{2}\left[\left(-V_y^2+V_z^2\right)\sin 2\theta_E + 2V_yV_z\cos 2\theta_E\right] = \bar{f}_p \quad , \tag{14}$$

and then the bulk equations are

$$\frac{\mathrm{d}y}{\mathrm{d}t} = V_y \quad , \tag{15a}$$

$$\frac{\mathrm{d}z}{\mathrm{d}t} = V_z \quad , \tag{15b}$$

$$\frac{\mathrm{d}V_y}{\mathrm{d}t} = \frac{1}{m}\left\{\begin{array}{l}\frac{K_C}{4}\left[\left(V_y^2-V_z^2\right)\left(\cos 3\theta-\cos\theta\right)+2V_yV_z\left(\sin 3\theta-\sin\theta\right)\right]- \\ \bar{f}_p\sin\theta_E + T\cos\theta - CV_y\left(V_y^2+V_z^2\right)^{1/2}\end{array}\right\} \quad , \tag{15c}$$

$$\frac{\mathrm{d}V_z}{\mathrm{d}t} = \frac{1}{m}\left\{\begin{array}{l}\frac{K_C}{4}\left[\left(V_y^2-V_z^2\right)\left(\sin 3\theta+\sin\theta\right)-2V_yV_z\left(\cos 3\theta+\cos\theta\right)\right]+ \\ \bar{f}_p\cos\theta_E + T\sin\theta - mg - CV_z\left(V_y^2+V_z^2\right)^{1/2}\end{array}\right\} \quad , \tag{15d}$$

$$\frac{\mathrm{d}\theta}{\mathrm{d}t} = \omega \quad , \tag{15e}$$

$$\frac{\mathrm{d}\omega}{\mathrm{d}t} = \frac{1}{I}\left\{-\Gamma\omega + \frac{K_C\bar{d}_1}{2}\left[\left(-V_y^2+V_z^2\right)\sin 2\theta + 2V_yV_z\cos 2\theta\right] + \bar{f}_p\bar{d}_2\cos\left(\theta-\theta_E\right) + T\bar{h}\right\} \quad . \tag{15f}$$

You can see why Maxima is necessary for the derivation. The first two equations (15a,b) are uncoupled from the rest of the system since the coordinates *y* and *z* are cyclic. The rest of the system, (15c-f), constitutes a fourth order nonlinear system for the variables in question. Note that V_y is the forward speed of the aircraft and V_z the climb rate. The wing and tail lift forces are indeed quadratic polynomials in the velocities, as our formula (3A–07) guarantees.

§26

The qdo model. For this, we make Maxima write the equations of motion in the *d*-*o* plane, using those components of velocity. Maxima says

$$\frac{k_E}{2}\left[\left(V_d^2-V_o^2\right)\sin 2(\theta-\theta_E) + 2V_dV_o\cos 2(\theta-\theta_E)\right] = \bar{f}_p \quad , \tag{16}$$

and then

$$\frac{\mathrm{d}y}{\mathrm{d}t} = V_d\cos\theta - V_o\sin\theta \quad , \tag{17a}$$

$$\frac{\mathrm{d}z}{\mathrm{d}t} = V_d\sin\theta + V_o\cos\theta \quad , \tag{17b}$$

$$\frac{\mathrm{d}V_d}{\mathrm{d}t} = \frac{1}{m}\left\{-\bar{f}_p\sin\left(\theta-\theta_E\right) + T - mg\sin\theta - CV_d\left(V_d^2+V_0^2\right)^{1/2}\right\} \quad , \tag{17c}$$

$$\frac{\mathrm{d}V_o}{\mathrm{d}t} = \frac{1}{m}\left\{-K_CV_dV_o - \bar{f}_p\cos\left(\theta-\theta_E\right) - mg\cos\theta - CV_o\left(V_q^2+V_o^2\right)^{1/2}\right\} \quad , \tag{17d}$$

$$\frac{\mathrm{d}\theta}{\mathrm{d}t} = \omega \quad , \tag{17e}$$

$$\frac{\mathrm{d}\omega}{\mathrm{d}t} = \frac{1}{I}\left\{-\Gamma\omega + K\bar{d}_1V_dV_o + \bar{f}_p\bar{d}_2\cos\left(\theta-\theta_E\right) + T\bar{h}\right\} \quad . \tag{17f}$$

As in the xyz model, the position coordinates are cyclic and the core system is fourth order nonlinear.

§27 **The space vector model.** For this representation, our variables are V and η. We have

$$V_y = V\cos\eta, \qquad V_z = V\sin\eta \quad , \tag{18}$$

wherefrom

$$V = \left(V_x^2 + V_y^2\right)^{1/2} \Rightarrow \frac{\mathrm{d}V}{\mathrm{d}t} = \frac{1}{V}\left(V_y\frac{\mathrm{d}V_y}{\mathrm{d}t} + V_z\frac{\mathrm{d}V_z}{\mathrm{d}t}\right) \quad , \tag{19}$$

and

$$\eta = \arctan\frac{V_z}{V_y} \Rightarrow \frac{\mathrm{d}\eta}{\mathrm{d}t} = \frac{1}{V^2}\left(V_y\frac{\mathrm{d}V_z}{\mathrm{d}t} - V_z\frac{\mathrm{d}V_y}{\mathrm{d}t}\right) \quad . \tag{20}$$

This is of course a transformation from Cartesian to cylindrical polar coordinates.

Getting Maxima to use (18-20) on (14-15), we find the preliminary

$$\frac{k_E V^2}{2}\sin 2\left(\eta-\theta_E\right) = \bar{f}_p \quad , \tag{21}$$

and then the all-important

$$\frac{\mathrm{d}y}{\mathrm{d}t} = V\cos\eta \quad , \tag{22a}$$

$$\frac{\mathrm{d}z}{\mathrm{d}t} = V\sin\eta \quad , \tag{22b}$$

$$\frac{\mathrm{d}V}{\mathrm{d}t} = \frac{1}{m}\left\{\frac{K_C V^2}{4}\left[\cos 3\left(\theta-\eta\right)-\cos\left(\theta-\eta\right)\right] + \bar{f}_p\sin\left(\theta_E-\eta\right) + T\cos\left(\theta-\eta\right) - mg\sin\eta - CV^2\right\} \quad , \tag{22c}$$

$$\frac{\mathrm{d}\eta}{\mathrm{d}t} = \frac{1}{m}\left\{\frac{K_C V}{4}\left[\sin 3\left(\theta-\eta\right)+\sin\left(\theta-\eta\right)\right] - \frac{\bar{f}_p\cos\left(\theta_E-\eta\right)}{V} + \frac{T\sin\left(\theta-\eta\right)}{V} - \frac{mg\cos\eta}{V}\right\} \quad , \tag{22d}$$

$$\frac{\mathrm{d}\theta}{\mathrm{d}t} = \omega \quad , \tag{22e}$$

$$\frac{\mathrm{d}\omega}{\mathrm{d}t} = \frac{1}{I}\left\{-\Gamma\omega - \frac{K_C\bar{d}_1 V^2}{2}\sin 2\left(\theta-\eta\right) + \bar{f}_p\bar{d}_2\cos\left(\theta-\theta_E\right) + T\bar{h}\right\} \quad , \tag{22f}$$

which is the key equation of this Article. Once again, it is fourth order nonlinear with two cyclic coordinates.

§28 **Interpretation of the space vector model.** Here we discuss some features of the space vector model which are apparent on inspection (those which are not apparent thus, and which are legion in number, will be the subject of the next Chapter). The first thing is that the model is fully explicit i.e. there are no hidden dependencies in any terms. T and $\bar{f}_p$ are inputs received from the cockpit – the selection of thrust and elevator force may be made by the pilot or the autopilot, depending on who is flying the plane. For brevity, and since the focus of our Article is to improve piloting technique rather than autopilot design, I shall refer to either as "pilot" in future. These inputs will in general be functions of time, and also of position, speed etc since we expect the pilot to react to the current trajectory of the aircraft and apply the controls to achieve the desired trajectory. Next, we see from Fig. 01 that $\theta-\eta$ is α, the angle of attack of the wings. The explicit appearance of α in the model is a good thing since (*a*) it is fundamental to the generation of lift, and (*b*) it directly determines whether the aircraft will stall. Note that α does not appear directly in any of the other models.

Now let's look at (22) term by term. Before this we note that, in normal operation of transport aircraft, the elevation η is very small. The steepest climb, immediately following takeoff, features an angle of 10° or less while the approach to the landing is typically inclined at –3°. α is small as well [typically less than 15° so that the aircraft doesn't stall, which is both undesirable and outside the scope of (22)]. Although (22) is

not a small-angle model, thinking of the angles as small helps in its qualitative interpretation. The first two equations in the set are just geometrical definitions, the remaining ones are each worth a separate discussion.

(22c)

This gives the rate of change of speed. Since there is no wind, airspeed and ground speed are equivalent. The first term on the RHS here is $\cos 3\alpha - \cos \alpha$; for $\alpha = 0$ it is zero and for positive α it is negative, its size increasing with α. For negative α, it behaves identically to positive α since cos is a symmetric function. Hence, this term is a drag term. It is quadratic in velocity. Note however that it is the lift constant K_C rather than the drag constant C which is the coefficient here; this is because this drag rides piggyback on the lift as per the modified Newtonian theory (3A–07). The next term is the tail force term; since tail force is usually much smaller than wing force, it is ignorable at this level. Then comes the thrust – for small α, $\cos \alpha$ is close to unity so the bulk of the thrust goes towards generating acceleration. Next is $-mg \sin \eta$; gravity tends to slow the plane down during a climb or speed it up during descent, just as it acts on a block sliding up or down an inclined plane. The last term is the 'conventional' quadratic drag which again retards velocity. In summary, acceleration is determined by a competition between thrust and drag, with gravity adding or subtracting from the mix, a very intuitive scenario. ■

(22d)

Change in η at constant V (more generally, a fast change in η with a slower change in V) means a change in the rate of climb or descent. The first term on the RHS here is the big positive term – the lift, which is zero for $\alpha = 0$ and increases with increasing α. As before, we neglect the second term which is the tail force. The third term shows that the $\sin \alpha$ component of thrust also helps to increase η; since this is the minor component, the effect is largely ignorable. Last comes the big negative term, which is the weight. In the absence of lift, weight would rapidly cause η to head towards -90^o, and this is reflected in this term. In summary, this equation describes climb or descent as a competition between lift and weight, which is again very intuitive. Slightly less intuitive, at least for beginners to aviation, is the following. To maintain constant η, the lift must balance the weight i.e. α must be strictly positive. Then, θ must be greater than η, implying that the plane does NOT point in the direction in which it is flying (see §17,18). This is a basic fact of aviation but it is unexpected for those without prior experience, since we are so used to road vehicles facing the direction in which they go. ■

(22f)

For obvious reasons, we do not devote a paragraph to (22e). The first term in the RHS of (22f) is the damping of rotational motion. If the damping is high enough, then the equation becomes 'overdamped', i.e. a constant torque translates to a constant angular velocity instead of a constant angular acceleration. Practically, such a relation holds true to a good extent. We will have more to say on the overdamped approximation in §41. The second term on the RHS is the lift, which exerts a negative torque with a moment arm of $\bar{d_1}$. Then comes the elevator force, which exerts positive torque with moment arm of $\bar{d_2}$. Finally is the thrust, whose moment is also positive since the engines are below the fuselage centreline in this case. In general, the torque of thrust is smaller than those of the wings and the tail. In summary, the torque balance features an opposition between the wings and the tail, with the thrust playing an auxiliary role. ■

One thing to note here is that the terms K_C, k_E and C are all proportional to the density of air, and the density varies with altitude. We have factored this out and treated the terms as constants because we shall focus on manoeuvres which feature only small changes in altitude. Equation (22) is not suitable for describing manoeuvres such as extended climbs and descents – for that, we'll need to explicitly account for the density, which is a function of z. All the ρ-dependent terms however feature the multiplicative term V^2. Thus, flight through air at density ρ_1 with speed V_1 will be dynamically extremely similar to flight through air of density ρ_2 at speed V_2, if $\rho_1 V_1^2 = \rho_2 V_2^2$. This is precisely the effect which the indicated airspeed captures. The indicated airspeed V^i is defined in terms of the true airspeed V^t as

$$V^i = \left(\frac{\rho}{\rho_0}\right)^{1/2} V^t \quad , \tag{23}$$

where ρ_0 is the density of air in the standard atmosphere at mean sea level and ρ is the density of air where the plane is actually flying. By definition, $V^i = V^t$ at sea level; at high altitude, V^i gives a better picture of the dynamics than does V^t. Hence the importance of the indicated airspeed.

We have already seen in §23 that maintaining level flight requires a steady pull back on the stick. So does flight at any constant η, be it a climb or a descent, since that too is an equilibrium between lift and weight, as per (22c). It does not require a mathematical model to predict that to make the plane accelerate, the pilot must increase thrust while to make it decelerate, he must decrease thrust. What is more interesting is, how can he change the climb or descent rate. Let us say the aircraft is flying level, when the pilot wants to initiate a climb without changing the speed. That means, he has to increase $\mathrm{d}\eta/\mathrm{d}t$ at constant V. The increase must come from the first term in (22d), and that will be achieved by increasing θ. Hence the pilot must raise the nose or pitch up the aircraft to make it climb. Equations (22e,f) now tell us how to raise the nose – the greater the total torque, the faster the nose will go up. To increase torque, the pilot must increase the positive term in (22f) i.e. increase $\bar{f}_p$. In other words, he should pull back on the stick to make the plane climb. In the overdamped limit, a constant $\bar{f}_p$ will lead to an approximately constant rate of increase in pitch and a continuous and rapid increase in climb rate – when the desired rate is reached, the pilot should again let go of the stick. Simultaneously, he should also advance the thrust levers to ensure that the plane does not lose speed during the climb. Conversely, the pilot can initiate a descent by pushing the stick forward until the desired rate is reached and then again letting go of it, while parallelly retarding the thrust levers.

Transient pulls and pushes on the stick to initiate climbs and descents is probably the first thing one learns in flying school. It is reassuring that this elementary flying strategy can be derived so easily from our model. A misconception among novices who have some familiarity with cockpit instruments (or their electronic equivalents) is that the stick must be pulled continuously during a climb and pushed continuously during a descent. As you can see, that is not the case. If we had wanted to figure out this flying basic from the xyz equations (15), then that too would have been quite easy. A typical configuration features $V_y >> V_z$; for a climb, the pilot will need to maximize $\mathrm{d}V_z/\mathrm{d}t$, the largest term there is $K_C V_y^2 (\sin 3\theta + \sin\theta)/4$, and so he will need to increase θ. The torque equation (15f) is similar to (22f) and the rest of the logic follows. From the qdo model however, figuring this out is not too easy. It is not clear that to initiate a climb, should one increase V_d or V_o. As it happens, neither. Since α is small [though α does not appear explicitly in (17)], $V_d >> V_o$; in (17b), V_d is attached to $\sin\theta$ and hence an increase in θ is necessary for a climb. This reasoning is tortuous. Hence, the qdo equations are more difficult to interpret than the xyz and space vector equations. Nevertheless, qdo has the simplest mathematical structure and might well be the preferred model to use on a simulator if we want to maximize its computational performance. This is the advantage of having many representations of the same dynamics – use whichever one is convenient for whichever situation.

§29 **Model in some special situations.** Here we first see a highly simplified form of the space vector model (22) and then construct the aircraft model in the cases where the wing stalls and where there is a wind.

Oversimplified model

For this, we quantitatively implement some of the small angle assumptions which we had made in the qualitative treatment of (22). We use sin (small) = small and cos (small) = 1 on $\theta - \eta$ as well as $\theta_E - \eta$ though not on η itself. This means that angles of attack are small though the trajectory of the aircraft can be steep – I haven't made η small as well because that will militate against the primary future use of the oversimplified model. Further, since the elevator lift is in general much smaller than the wing lift, we neglect $\bar{f}_p$ from the force balances (22c) and (22d), though not from the torque balance (22f) since the torques of wing and tail lift are of equal or comparable size. Doing these, we get

$$k_E V^2 (\eta - \theta_E) = \bar{f}_p \quad , \tag{24}$$

and

$$\frac{\mathrm{d}V}{\mathrm{d}t}=\frac{1}{m}\left\{T-mg\sin\eta-CV^2\right\}\quad , \tag{25c}$$

$$\frac{\mathrm{d}\eta}{\mathrm{d}t}=\frac{1}{m}\left\{K_C V\left(\theta-\eta\right)+\frac{T\left(\theta-\eta\right)}{V}-\frac{mg\cos\eta}{V}\right\}\quad , \tag{25d}$$

$$\frac{\mathrm{d}\omega}{\mathrm{d}t}=\frac{1}{I}\left\{-\Gamma\omega-K_C\bar{d}_1V^2\left(\theta-\eta\right)+\bar{f}_p\bar{d}_2+T\bar{h}\right\}\quad . \tag{25f}$$

Here I have displayed only the subset of the equations which is non-trivial; nevertheless I have kept the numbering c,d,f for these so as to achieve consistency with (22). In aircraft seats, it is routine to skip letters so that smaller aircraft achieve conformity with larger ones; thus an ATR 72 with 2+2 seats in each row usually numbers them A,C and D,F in analogy with an Airbus A320 which has A,B,C and then D,E,F while an Airbus A330 with 2+4+2 per row often goes A,C then D,E,F,G then H,K in analogy with a ten-abreast Boeing 777 which goes A,B,C then D,E,F,G then H,J,K.

The advantage of the form (25) is that the equilibria or fixed points are easy to solve for, as we shall see in §34,36. Equation (25) is also useful for pen-and-paper calculations, for example in no-electronics exams. The drawback however is that the errors made in going from (22) to (25) are not always small. For one, there are some double and triple angle terms in (22); though the angle of attack itself is quite small, twice or thrice that is less so. Also, the error in treating cos terms as unity is numerically greater than that in treating sine terms as the angles themselves. Indeed, as we shall see in §36, the equilibria of (25) are considerably different from the numerically calculated equilibria of (22). Hence, (25) is of limited overall utility and will play only a small role in the discussion which follows. ■

Stall model

Here, the lift **F** is given by (3A–09) and the extra drag by (3A–10). While we can take the fuselage drag to pass through the CM, the wing drag will not do so in general. Indeed, in one of the manoeuvres we shall analyse, the wing drag in stall actually plays a significant role. Hence, we have to take its effect into account in an explicit way. Let D be the point through which the drag effectively acts (there is no reason for stall drag to act through the nonstall CP of lift), with d_3 being the distance BD. Since drag acts along the velocity line, let $\hat{\mathbf{b}}_2$ and $\hat{\mathbf{b}}_3$ denote two axes directed along **V** and 90° counterclockwise to it. We have (sloppy linear algebra)

$$\begin{bmatrix}\hat{\mathbf{b}}_2\\ \hat{\mathbf{b}}_3\end{bmatrix}=\begin{bmatrix}\cos\left(\theta-\eta\right) & -\sin\left(\theta-\eta\right)\\ \sin\left(\theta-\eta\right) & \cos\left(\theta-\eta\right)\end{bmatrix}\begin{bmatrix}\hat{\mathbf{d}}\\ \hat{\mathbf{o}}\end{bmatrix}\quad , \tag{26}$$

so that the drag force (3A–10) generates the torque

$$\begin{aligned}\boldsymbol{\tau}&=d_3\hat{\mathbf{d}}\times F_D^S\hat{\mathbf{b}}_2\\ &=\left(-F_D^S d_3\sin\alpha\right)\hat{\mathbf{q}}\quad .\\ &=\left(C_1V^2d_3\sin^2\alpha\right)\hat{\mathbf{q}}\end{aligned} \tag{27}$$

If d_3 is positive i.e. the centre of drag is forward of the CM, then this is positive, as Fig. 03 suggests it will be (in that Figure, imagine the drag acting at the nose).

We are now ready to write the equations of motion. The tail angle (21) remains as is since the tail always forms a nonstall angle with the travel direction. The core of (22) becomes

$$\frac{\mathrm{d}V}{\mathrm{d}t}=\frac{1}{m}\left\{F\sin\left(\theta-\eta\right)+\bar{f}_p\sin\left(\theta_E-\eta\right)+T\cos\left(\theta-\eta\right)-mg\sin\eta-CV^2-C_1V^2\sin^2\left(\theta-\eta\right)\right\}\quad , \tag{28c}$$

$$\frac{\mathrm{d}\eta}{\mathrm{d}t}=\frac{1}{m}\left\{\frac{F\cos\left(\theta-\eta\right)}{V}-\frac{\bar{f}_p\cos\left(\theta_E-\eta\right)}{V}+\frac{T\sin\left(\theta-\eta\right)}{V}-\frac{mg\cos\eta}{V}\right\}\quad , \tag{28d}$$

$$\frac{\mathrm{d}\omega}{\mathrm{d}t}=\frac{1}{I}\left\{-\Gamma\omega-F\bar{d}_1+\bar{f}_p\bar{d}_2\cos\left(\theta-\theta_E\right)+T\bar{h}+C_1d_3V^2\sin^2\left(\theta-\eta\right)\right\}\quad , \tag{28f}$$

where F is given by (3A–09). We can see that if F here is replaced by (3A–07) and C_1 set equal to zero, then we recover (22). ■

Model in the presence of wind

So far, we have assumed that the air is still; now we consider the case where there is a wind blowing with velocity **U** with respect to the ground. In most cases, **U** will be directed along y alone, though vertical air currents are also observed especially near hills. In general, **U** will be a function of y and z. Because of these dependences, we shall consider the xyz model. In the presence of wind, the LHS of the equations of motion (15) will remain as is. This LHS is that of NEWTON's law in the inertial frame, and it can't be affected by wind. On the RHS however, wind is going to affect all the aerodynamic forces i.e. lift and drag. These are determined by the velocity of the aircraft relative to the wind. Hence, whenever we have a term involving **V** in (15), we shall now have to replace it with **V**–**U**. Doing so, we find

$$\frac{\mathrm{d}V_y}{\mathrm{d}t}=\frac{1}{m}\begin{Bmatrix}\dfrac{K_C}{4}\Big[\Big((V_y-U_y)^2-(V_z-U_z)^2\Big)(\cos 3\theta-\cos\theta)+2\big(V_y-U_y\big)\big(V_z-U_z\big)(\sin 3\theta-\sin\theta)\Big]-\\ \bar{f}_p\sin\theta_E+T\cos\theta-C\big(V_y-U_y\big)\Big((V_y-U_y)^2+(V_z-U_z)^2\Big)^{1/2}\end{Bmatrix}, \quad (29c)$$

$$\frac{\mathrm{d}V_z}{\mathrm{d}t}=\frac{1}{m}\begin{Bmatrix}\dfrac{K_C}{4}\Big[\Big((V_y-U_y)^2-\big(V_z-U_z\big)^2\Big)(\sin 3\theta+\sin\theta)-2\big(V_y-U_y\big)\big(V_z-U_z\big)(\cos 3\theta+\cos\theta)\Big]+\\ \bar{f}_p\cos\theta_E+T\sin\theta-mg-C\big(V_z-U_z\big)\Big((V_y-U_y)^2+(V_z-U_z)^2\Big)^{1/2}\end{Bmatrix}, \quad (29d)$$

$$\frac{\mathrm{d}\omega}{\mathrm{d}t}=\frac{1}{I}\begin{Bmatrix}-\Gamma_p\omega+\dfrac{K_C\bar{d}_1}{2}\Big[\Big(-(V_y-U_y)^2+(V_z-U_z)^2\Big)\sin 2\theta+2\big(V_y-U_y\big)\big(V_z-U_z\big)\cos 2\theta\Big]+\\ \bar{f}_p\bar{d}_2\cos\big(\theta-\theta_E\big)+T\bar{h}\end{Bmatrix}. \quad (29f)$$

Since **U** is a function of y and z, this time those two coordinates are no longer cyclic.

Recall that the airspeed is the magnitude of the relative velocity **V**–**U** while the ground speed is the magnitude of **V** itself. If we had defined the vectorized airspeed or airvelocity **W** = **V**–**U**, then the RHS of (29) would have looked more transparent. However, (29) is what must enter a simulator as is, since d**W**/dt does not have a simple form. In this Article, we shall not explicitly simulate a situation with wind, but shall restrict ourselves to qualitative discussions of wind after simulating without wind. Nevertheless, if one desires to add wind to the equations, (29) shows how it can be done.

If we try to express (29) in space vector form, then we run into a problem with the elevation η. Suppose an aircraft has the velocity $100\hat{\mathbf{y}}+10\hat{\mathbf{z}}$ in the ground frame, and the wind has the velocity $-20\hat{\mathbf{y}}$ in this frame. Then, from the ground frame, the elevation will be $\eta=\arctan(1/10)$. In the frame moving with the wind however, the elevation will be $\eta'=\arctan(1/12)$. Now, the LHS of (22) arises from a coordinate transformation on NEWTON's law, which deals with inertial i.e. ground frame velocities. Hence, this will continue to feature η when the wind is added. On the other hand, the RHS involves aerodynamic forces, which depend on the angle of attack relative to the oncoming airflow. This is $\theta-\eta'$. So the RHS will feature η' when the wind is added. Hence, just as the presence of rotor magnets destroys the symmetry between d and q in a synchronous motor [3A–03], the presence of wind breaks the parity between the ground and air angles of elevation in the aircraft; the upshot is that the space vector model is not attempted in either case. ■

C. YAW AND BANKING PLANE EQUATIONS OF MOTION

Having come thus far, yet another Subdivision with a title similar to the previous one might tempt you to quit altogether. This time however, our task will be short. The heavy lifting has already been done in the previous few Sections; now we shall just apply what we have learnt there to derive these equations in short order.

§30 **Yaw plane equations of motion.** Below we see the forces on Our Plane in the yaw plane. For the space vector representation we shall use the azimuth angle ξ which is measured from the y-axis as shown. The d-axis positions of B, C and E remain as they were; the extra dimension we need is w, the q-axis distance from B to the line of action of the engine thrusts. Let T_1 be the thrust of engine no. 1 and T_2 that of engine no. 2; in general they will be equal but they can be different if (*a*) the pilot so commands, or (*b*) there is an engine malfunction.

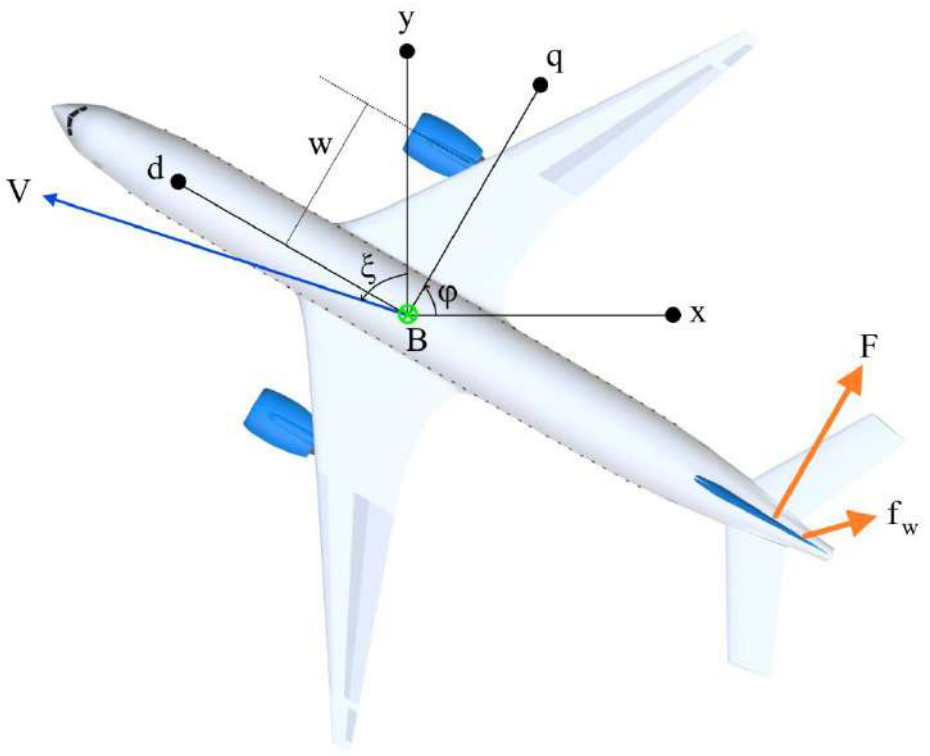


Figure 01 : *Our Plane in the yaw plane.*

As we have seen in §05, the vertical tail consists of two components – a stabilizer and a rudder. This time we don't merge them into a 'stabirudder' but treat them separately. This is because the stabilizer – more generally, a lifting airfoil located aft of the CM – is really essential for stability. In the pitch plane, the wing already achieves stability and the tail is primary for control. In the yaw plane, the stabilizer and the rudder perform the respective functions. We assume that the forces of both elements act at the point E.

Let φ be the yaw angle of the aircraft and φ_E the yaw angle of the rudder (the stabilizer is rigidly attached so it makes angle φ also). Let k_S and k_R denote the lift constants of the stabilizer and rudder respectively, and let f_w (subscript w for "yaw" since y is already taken up by an axis) denote the force commanded by the pilot to be applied on the rudder. This command is generated by pressing the rudder pedals. f_w acts along the e_1-axis where e_1,e_2,e_3 is the airfoil basis attached to the rudder. Similarly, the lift of the stabilizer acts along the d-axis. Following the steps leading to (3B–21,22), we find

$$-\frac{k_R V^2}{2}\sin 2\big(\varphi_E-\xi\big)=f_w \quad , \tag{01}$$

as the equation for φ_E. The space vector model then works out to be

$$\frac{\mathrm{d}x}{\mathrm{d}t}=-V\sin\xi \quad , \tag{02a}$$

$$\frac{\mathrm{d}y}{\mathrm{d}t}=V\cos\xi \quad , \tag{02b}$$

$$\frac{\mathrm{d}V}{\mathrm{d}t}=\frac{1}{m}\left\{\frac{k_S V^2}{4}\Big[\cos 3\big(\varphi-\xi\big)-\cos\big(\varphi-\xi\big)\Big]+f_w\sin\big(\varphi_E-\xi\big)+\big(T_1+T_2\big)\cos\big(\varphi-\xi\big)-C_w V^2\right\} \quad , \tag{02c}$$

$$\frac{\mathrm{d}\xi}{\mathrm{d}t}=\frac{1}{m}\left\{\frac{k_S V}{4}\Big[\sin 3\big(\varphi-\xi\big)+\sin\big(\varphi-\xi\big)\Big]-\frac{f_w\cos\big(\varphi_E-\xi\big)}{V}+\frac{\big(T_1+T_2\big)\sin\big(\varphi-\xi\big)}{V}\right\} \quad , \tag{02d}$$

$$\frac{\mathrm{d}\varphi}{\mathrm{d}t}=\omega_w \quad , \tag{02e}$$

$$\frac{\mathrm{d}\omega_w}{\mathrm{d}t}=\frac{1}{I_w}\left\{-\Gamma_w\omega_w-\frac{k_S\bar{d}_2V^2}{2}\sin 2(\varphi-\xi)+f_w\bar{d}_2\cos(\varphi-\varphi_E)+(T_2-T_1)w\right\}\quad . \tag{02f}$$

Here, C, I and Γ have acquired subscripts of w since their values may be different from those in the pitch plane. Note also the differences between (02a,b) and (3B–22a,b) arising because of the difference in definition between η and ξ.

A case of practical use is when an external force f_{ex} acts along the q-axis. Let this force act at the CM so that it is torque-free. In this case, repeating the Maxima routine gives the modifications needed to the above equations. The changes occur only in the third and fourth equations, which now become

$$\frac{\mathrm{d}V}{\mathrm{d}t}=\frac{1}{m}\left\{\begin{array}{l}\dfrac{k_SV^2}{4}\left[\cos 3(\varphi-\xi)-\cos(\varphi-\xi)\right]+f_w\sin(\varphi_E-\xi)+(T_1+T_2)\cos(\varphi-\xi)+\\ f_{ex}\sin(\varphi-\xi)-C_wV^2\end{array}\right\}\quad , \tag{03c}$$

$$\frac{\mathrm{d}\xi}{\mathrm{d}t}=\frac{1}{m}\left\{\begin{array}{l}\dfrac{k_SV}{4}\left[\sin 3(\varphi-\xi)+\sin(\varphi-\xi)\right]-\dfrac{f_w\cos(\varphi_E-\xi)}{V}+\dfrac{(T_1+T_2)\sin(\varphi-\xi)}{V}-\\ \dfrac{f_{ex}\cos(\varphi-\xi)}{V}\end{array}\right\}\quad . \tag{03d}$$

During a turn, f_{ex} provides the centripetal acceleration, hence (03) is the relevant equation for modeling a turn.

§31 **Banking plane equations of motion.** Here is Our Plane in the banking plane. ψ is the angle of bank, and F_{L1} and F_{L2} the lifts of the two wings. We need the quadrature axis distance q_1 from the CM to the CP of each wing (the direct axis component of this vector is d_1). The horizontal tail exerts its usual force $\bar{f}_p$ and the vertical tail perforce exerts no force since that would require a relative yaw but a yaw plus a bank would not remain two-dimensional.

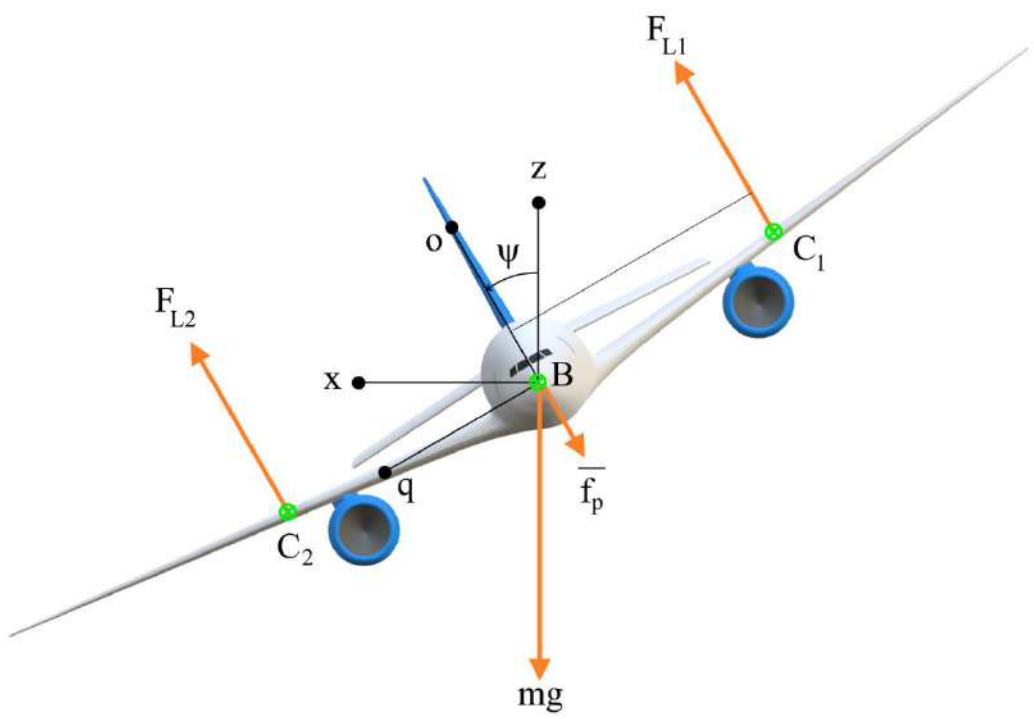


Figure 02 : *Our Plane in the banking plane. C_1 and C_2 are the CP's of the two wings. Everything else is self-explanatory. Bank angle is 30°.*

In this plane, there are no airfoils and the xyz model is apparent on inspection,

$$\frac{\mathrm{d}x}{\mathrm{d}t}=V_x\quad , \tag{04a}$$

$$\frac{\mathrm{d}z}{\mathrm{d}t}=V_z\quad , \tag{04b}$$

$$\frac{\mathrm{d}V_x}{\mathrm{d}t}=\frac{1}{m}\left(F_{L1}+F_{L2}-\bar{f}_p\right)\sin\psi\quad , \tag{04c}$$

$$\frac{\mathrm{d}V_z}{\mathrm{d}t} = \frac{1}{m}\left\{\left(F_{L1} + F_{L2} - \bar{f}_p\right)\cos\psi - mg\right\} \quad , \tag{04d}$$

$$\frac{\mathrm{d}\psi}{\mathrm{d}t} = \omega_r \quad , \tag{04e}$$

$$\frac{\mathrm{d}\omega_r}{\mathrm{d}t} = \frac{1}{I_r}\left\{-\Gamma_r\omega_r + \left(F_{L1} - F_{L2}\right)q_1\right\} \quad . \tag{04f}$$

Here, the subscript r denotes roll, since b for bank is already taken up by an axis name in the general three-dimensional case. We can see that if ψ is positive, then $\dot{V}_x$ is positive – the lift acquires a positive x-component which provides the centripetal acceleration for a turn to the right. To change the angle of bank, the pilot can make F_{L1} and F_{L2} unequal by deploying the ailerons. Extending ailerons downward on wing no. 1 (port) and upward on wing no. 2 (starboard) will make $F_{L1} > F_{L2}$ and generate a positive ω_r. Since the major component of velocity is perpendicular to the banking plane, the primary component of drag will also be in the same direction; the secondary components will be significantly smaller than the lifts. Hence, I have neglected these terms in the above.

D. CHAPTER CONCLUSION

§32 **Limitations of yaw and banking plane models, concluding remarks to Chapter 3.** Among the three planes, the pitch plane dynamics (3B–21,22) has the richest structure and is of greatest interest. This is not a surprise, since gravity and lift both act in this plane, and it is the interaction of these two forces which lies at the heart of aviation. The yaw plane dynamics (3C–01,02) is derivative in form, since this plane also features two airfoils – stabilizer and rudder, equivalent of wing and elevator – but does not have gravity. Finally, the banking plane dynamics (3C–04) is trivial on account of the absence of aerodynamic surfaces in this direction.

Physically, the pitch plane equations have full standalone significance while the other two equations sets don't. For the yaw equations, note that for a level turn, the aircraft needs a nonzero α and hence nonzero θ to keep itself aloft. Two nonzero Euler angles are however outside the scope of our two-dimensional treatment, so the yaw plane dynamics is forced to treat θ as zero and work with an approximate configuration of the aircraft. The part of the drag which rides piggyback on the lift must also be thrown in by hand into C_w. As for the banking plane equations, we not only have the problem of approximating a lift-generating non-zero θ by a zero value but also cannot account for the fact that, when a real aircraft changes its direction of motion, it simultaneously changes its yaw angle so as to face the way it is flying. Factoring in any of these would immediately run into the problem of two or more nonzero angles, so we must assume that these problems are somehow taken care of. Hence, the majority of our subsequent analysis will deal with the pitch plane equations (3B–22).

When we consider the three-dimensional aircraft model, there will no longer be three separate models (3B–22), (3C–02) and (3C–04) but a single model with 12 (!) equations which will reduce to these three subsets in the appropriate limits. That master equation will not have different components of different physical significance, but will be suitable for analysing everything from takeoff to spiral dives in one go. Nevertheless, to quote KLEINBERG and TADROS [01], the three-dimensional model "is for another time and another [Article]; and, as for us, we are done".

---- o ----

4

STABILITY AND CHARACTERISTIC CURVES

Given any nonlinear dynamical system, a natural first step is to find its fixed points and determine their stabilities (as in dynamical systems theory, we use the terms "fixed point", "equilibrium" and "steady state" interchangeably). For the aircraft, this exercise has a double benefit. Firstly, the stability conditions give insight into the design considerations which maximize stability or manoeuvrability. Secondly, plots of the fixed points, which we shall call the characteristic curves, give insight into the performance of the aircraft and act as the natural starting point from which to plan manoeuvres such as takeoff and landing. Performance characteristics are very common and very useful in the analysis of electrical machines; for aircraft they are not half so common but I hope they may prove just as useful. For this Chapter, we consider only the pitch plane equations since they are self-contained and non-trivial.

§33 **Static stability, difference between one- and two-piece tails, CM position limits.** In this Section, we consider a subset of (3B–21,22) to gain insight into the stability of the aircraft. Let the aircraft be mounted on a stand, like a mantelpiece display item, and let this stand be moved in the y-direction with speed V. We assume that the stand connects to the plane at its CM and that the plane is pivoted to it, so that it is free to pitch up and down (imagine Fig. 3B–03 with a stand at B). This reduced model thus captures the dynamics of θ while eliminating V and η. The equation of motion in this case is (3B–22e,f) with $\eta = 0$, which is

$$\frac{\mathrm{d}^2\theta}{\mathrm{d}t^2} + \frac{\Gamma}{I}\frac{\mathrm{d}\theta}{\mathrm{d}t} = \frac{1}{I}\left\{ -\frac{K_C \bar{d}_1 V^2}{2}\sin 2\theta + \bar{f}_p \bar{d}_2 \cos\left(\theta - \theta_E\right) + T\bar{h} \right\} \quad . \tag{01}$$

Here, just as in the full system (3B–22), T and $\bar{f}_p$ are externally determined quantities while θ_E is determined in terms of $\bar{f}_p$ by (3B–21). Consider the special case where T and $\bar{f}_p$ are constant. Since η is constant (equal to zero), θ_E is constant as well from (3B–21). A fixed point $\theta = \theta^*$ will be achieved only if the curly bracket on the RHS of (01) is zero, i.e.

$$-\frac{K_C \bar{d}_1 V^2}{2}\sin 2\theta^* + \bar{f}_p \bar{d}_2 \cos\left(\theta^* - \theta_E\right) + T\bar{h} = 0 \quad . \tag{02}$$

While it is possible to analyse (02) to death using (3B–21), I shall settle here for a more qualitative treatment, since we are anyway analysing a reduced system. For the B-C-E aircraft (§23), $\bar{f}_p$ is positive and θ_E is negative. Its value will be in the range of 0 to −15° or so, to avoid stalling of the elevator. If θ^* is small and positive, consistent with operation in a nonstall lift-generating region, then the first term of (02) is negative while the second and third are positive. At $\theta^* = 0$, the first term is zero. As θ^* increases, it grows in size on the negative side while the second (positive) term shrinks in size; the third term is evidently independent of θ^*. It does not require a stretch of imagination to see that unless the coefficients are chosen badly, the three terms will balance each other and hence a root will exist at some positive θ^*. In the case that the angles in (02) are mathematically small and the torque of thrust is negligible, the equilibrium pitch acquires a very simple expression,

$$\theta^* = \frac{\bar{f}_p \bar{d}_2}{K_C \bar{d}_1 V^2} \quad . \tag{03}$$

The balance between the torques of wing lift and tail lift is evident here. Now, if the stand is to be redundant i.e. exert no force, then the wing lift must equal the weight (assuming the tail lift to be negligible in comparison). So, $K_C V^2 \theta^* = mg$ or $\theta^* = mg/K_C V^2$ and, from (03), equilibrium can be achieved at only one

particular value of $\bar{f}_p$, namely $\bar{f}_p = mg\bar{d}_1/\bar{d}_2$. Even without the simplifying assumptions in (03), the concept of angular equilibrium at one particular $\bar{f}_p$ remains valid, as we shall see over the next three Sections.

What will happen if the plane is perturbed from the fixed point (02) ? Let the perturbed angle be $\theta^*+\Delta\theta$; plugging this into the expression for torque on the RHS of (01) and Taylor expanding to first order in $\Delta\theta$ yields

$$\tau = \tau(\theta^*) + \left[-K\bar{d}_1 V^2 \cos 2\theta^* - \bar{f}_p \bar{d}_2 \sin\left(\theta^* - \theta_E\right) \right] \Delta\theta \quad . \tag{04}$$

For a typical nonstall θ^*, both terms here are negative (the second since θ^* is positive and θ_E is negative), implying that the torque is restoring and brings the plane back to its equilibrium. The interpretation of this result is as follows. At the equilibrium pitch, the wings generate positive lift and negative torque, while the tail generates negative lift and positive torque. Now let the plane pitch up slightly from the equilibrium. Then, the angle of attack increases so the wings generate more lift which adds to the negative torque. The tail's torque is positive; since $\bar{f}_p$ and θ_E are constant, the pitch up causes the direction of the tail's lift to become more parallel to the d-axis, so that its torque becomes less. Both these effects tend to restore the pitch to its equilibrium value.

In most cases, stability of the equilibrium is highly desirable – we most certainly do NOT want an Airbus or Boeing shooting skywards (or worse still, groundwards) at the smallest deviation from equilibrium. Sometimes however, for example in aircraft designed to thrill (and unfortunately also those designed to kill), this stability might become boring. In these situations, we might really want the plane to enter a sharp climb or a vertical dive at a moment's notice. Then, what the aircraft designers do is they intentionally make the plane unstable in pitch. In (04) we can see that if $\bar{f}_p$ is zero, then a negative $\bar{d}_1$ will amplify a disturbance instead of reducing it. Negative $\bar{d}_1$ means the configuration C-B-E instead of B-C-E. Qualitatively, in a C-B-E aircraft, the wings generate positive lift and positive torque while the tail generates positive lift and negative torque. Pitching up from equilibrium causes the wings to generate more positive torque; the change in tail torque gets determined by whether θ_E (now positive) is less than or greater than θ^*. In the former case the tail torque becomes less negative while in the latter it becomes more negative. If the contribution of the wings dominates that of the tail, or if the two contributions have the same sign, then a pitch up will give rise to a net positive torque which further amplifies the motion, rendering the aircraft unstable in pitch. Indeed, aircraft which are designed for high manoeuvrability are of this type with the intrinsic instability being curbed by continuous inputs from the onboard computers. Aircraft which are stable and unstable in pitch are often described as having "positive" and "relaxed" stability respectively. After our first success with the Quiz back in §07, another question now cracks – Q02. The overall instruction "assume performance and handling characteristics of a modern passenger airliner" is directly relevant to this question, and identifies the correct answer as Choice A.

At this point, we can understand why the elevator needs to be pivoted forward of CP (a fact we saw back in §23). Although for modeling purposes we treated the elevator as a massless object in a perpetual equilibrium, it is in reality a mechanical object which needs to attain the equilibrium and remain there in the presence of perturbations. In other words, the equilibrium has to be stable. Now, with a pivot and a CP, the structure of the elevator is identical to that of the aircraft on the stand with $\bar{f}_p = 0$. Hence, if the pivot is forward of CP, the equilibrium will be stable while if the pivot is aft of the CP, it will be unstable. Note also that the AC (aerodynamic centre – see §20), although located forward of CP, is not a suitable location for the pivot. That is a point about which the lift is independent of α – as α varies, the position of the CP changes in just such a manner as to keep the position of AC unchanged. So if the pivot is located at AC, a given torque τ_p applied by the pilot can result in any and all values of elevator deflection and $\bar{f}_p$. Only if the pivot is forward of the AC will a higher τ_p result in a higher $\bar{f}_p$ and the stick will work properly.

Now let's look at the case where the stand-mounted plane's tail consists of two pieces, a quasi-fixed horizontal stabilizer and a movable elevator, instead of one movable stabilator. While we shall not get into the quantitative details of the two-piece configuration, some qualitative insights into the difference between the one- and two-piece tails will be a useful thing to possess. For this discussion, we make the small angle approximation so that the lift forces of both wing and tail can be treated as vertical and the sines can be

linearized. Further, we ignore the torque of the thrust, just as we did in (03). Let's say the stabilizer makes a constant deflection δ with the fuselage and the elevator floats freely i.e. exerts no force. Since δ is negative, we can write it as $-\bar{\delta}$, so that $\theta_E = \theta - \bar{\delta}$ ("E" now denotes "empennage" not "elevator"). The wing lift is $K_C V^2 \theta$ and the tail lift from (3B–21) is $k_E V^2 \theta_E$, which is $k_E V^2 \left(\theta - \bar{\delta}\right)$. A torque equilibrium at $\theta = \theta^*$ is possible if and only if

$$-K_C V^2 \theta^* \bar{d}_1 - k_E V^2 \left(\theta^* - \bar{\delta}\right) \bar{d}_2 = 0 \quad , \tag{05}$$

which implies

$$\theta^* = \frac{k_E \bar{d}_2 \bar{\delta}}{K_C \bar{d}_1 + k_E \bar{d}_2} \quad . \tag{06}$$

If the stand is to be made redundant, then $K_C V^2 \theta^* = mg$ (neglecting the tail force as small); (05) then yields

$$-mg\bar{d}_1 - \frac{k_E}{K_C} mg\bar{d}_2 + k_E V^2 \bar{d}_2 \bar{\delta} = 0 \quad . \tag{07}$$

This is an equation for V; it has the solution

$$V = \sqrt{\frac{mg\left(\bar{d}_1 + \frac{k_E}{K_C}\bar{d}_2\right)}{k_E \bar{d}_2 \bar{\delta}}} \quad . \tag{08}$$

The implication of this is that, given the stabilizer deflection, an equilibrium can be achieved only at one particular value of speed. Since $\bar{\delta}$ is adjusted using the trim wheel, the speed (08) corresponding to a given trim setting is called the **trimmed airspeed**. Since the LHS of (07) is the torque on the aircraft, we can also see that a speed lower than the trimmed speed causes the aircraft to pitch down while a speed higher than the trimmed speed causes it to pitch up. This is a big difference from what happens with (03); once again, the phenomenon continues to hold even if the calculation-simplifying assumptions are done away with. In the next Chapter, we shall (again qualitatively) see the implications of these differences during actual operation of the aircraft. As with the stabilator aircraft, the layout B-C-E ensures that the aircraft with the two-piece tail is stable, while the C-B-E layout makes the aircraft unstable.

The limits of CM position of an aircraft also follow from this discussion. For a B-C-E aircraft, the aft limit comes from the fact that we do not want it to turn into C-B-E, hence the CM must be forward of the CP of the wings. For the forward limit, let the wing lift be mg; as the CM is moved forward and its moment arm $\bar{d}_1$ is increased, a higher and higher $\bar{f}_p$ will be required to balance the wing torque in equilibrium and overcome it during transients. The forward limit will be arrived at when the required $\bar{f}_p$ for stability and control becomes equal to the maximum force which the tail can withstand without structural damage. Note also that the required $\bar{f}_p$ for stability and control increases with the aircraft weight, so the most conservative forward limit will be obtained for MTOW.

To conclude this Section, let me emphasize that this analysis was for only a subsystem of the full equations – real planes aren't mounted on stands. While stability of the mantelpiece display is essential for that of the flying machine, it is by no means sufficient. To find the stability of the real McCoy, we must analyse (3B–22) in its full generality, which is the task we turn to now.

§34

Modes of motion and their stabilities. For the full-scale stability analysis of (3B–22), we must first exclude from consideration the equations for position (3B–22a,b). It is patently absurd to expect that the aircraft will be stable to changes in position. Rather, stability should be to changes in velocity as well as pitch, so only the subsystem (3B–22c-f) will be relevant for the analysis. As in the last Section, we treat T and $\bar{f}_p$ as constants, which we call T^* and f^* (a bar, a star and a subscript on one letter are probably overkill); let the fixed point values of speed, elevation and pitch be V^*, η^* and θ^*. f^* leads to the fixed point tail angle θ_E^* in terms of V^* and η^* via (3B–21). At fixed points, ω^* must be zero; V^*, η^* and θ^* must satisfy

$$\frac{K_C V^{*2}}{4}\left[\cos 3\left(\theta^*-\eta^*\right)-\cos\left(\theta^*-\eta^*\right)\right]+f^*\sin\left(\theta_E-\eta^*\right)+ T^*\cos\left(\theta^*-\eta^*\right)-mg\sin\eta^*-CV^{*2}=0 \quad , \tag{09a}$$

$$\frac{K_C V^*}{4}\left[\sin 3\left(\theta^*-\eta^*\right)+\sin\left(\theta^*-\eta^*\right)\right]-\frac{f^*\cos\left(\theta_E-\eta^*\right)}{V}+ \frac{T^*\sin\left(\theta^*-\eta^*\right)}{V}-\frac{mg\cos\eta^*}{V}=0 \quad , \tag{09b}$$

$$-\frac{K_C\bar{d}_1 V^{*2}}{2}\sin 2\left(\theta^*-\eta^*\right)+f^*\bar{d}_2\cos\left(\theta^*-\theta_E\right)+T^*\bar{h}=0 \quad . \tag{09c}$$

This is a coupled set of transcendental equations which we shall solve using Newton-Rhaphson method on a computer. Note that equilibrium is also referred to as "trimmed condition", and a flight operating at an equilibrium is said to be "in trim". Conversely, a flight which is not at an equilibrium is called "out of trim". In many other science and engineering disciplines, the words "steady state" and "transient" are also used to denote the same concepts.

For the oversimplified model (3B–24-25), an analytical solution for the fixed points exists if we further assume that η^* is small. The equilibrium equations in this case are

$$T^*-mg\eta^*-CV^{*2}=0 \quad , \tag{10a}$$

$$K_C V^*\left(\theta^*-\eta^*\right)+\frac{T^*\left(\theta^*-\eta^*\right)}{V^*}-\frac{mg}{V^*}=0 \quad , \tag{10b}$$

$$-K_C\bar{d}_1 V^{*2}\left(\theta^*-\eta^*\right)+f^*\bar{d}_2+T^*\bar{h}=0 \quad , \tag{10c}$$

with $\theta_E{}^*$ being given by

$$\theta_E{}^*=\eta^*-\frac{f^*}{k_E V^{*2}} \quad . \tag{11}$$

Equation (10c) gives $\theta^*–\eta^*$ in terms of V^* and constants; if we substitute this into (10b) and multiply by V^{*3} throughout, then we get a standalone (trivial quadratic) equation for V^*. Solving it and using the obtained value together with (11) in (10a) gives η^*. What we find is

$$V^*=\sqrt{\frac{-T^*\left(f^*\bar{d}_2+T^*\bar{h}\right)}{K_C\left(f^*\bar{d}_2+T^*\bar{h}-mg\bar{d}_1\right)}} \quad , \tag{12a}$$

$$\eta^*=\frac{T-CV^{*2}}{mg} \quad , \tag{12b}$$

$$\theta^*=\eta^*+\frac{f^*\bar{d}_2+T^*\bar{h}}{K\bar{d}_1 V^{*2}} \quad . \tag{12c}$$

We can see that V^* (and hence a fixed point) exists only for well-chosen values of f^*; this is realistic since arbitrary f^* might not correspond to a torque equilibrium at any speed.

I must confess that I find (12) to be of limited utility; while it could have acted as a starting guess for Newton-Rhaphson on (09), I have opted to find this guess using another method, which will more naturally find a place in §36. Hence, (12) is primarily for those who appreciate analytical expressions, including approximate ones, over numerical work. Even with the oversimplified model (3B–25) however, the hand-calculation for stability leads pretty quickly leads to an obstacle. Hence, we abandon this line of inquiry and instead bring the computer into play for the stability analysis, going back to the full system equation (3B–22).

With the computer on board, now is a good time to attribute some numbers to Our Plane, which we've been seeing so far only in pictures. The relevant parameter values are given in Table 01 below.

Parameter	SI Unit value	Other unit value
m (MTOW)	1,00,000	100 tons
g	9·8	
K_C	1500	
k_E	150	
T (TOGA)	3,00,000	300 kN
$\bar{d_1}$	1	3·3 ft
$\bar{d_2}$	25	82 ft
$\bar{h}$	0·5	
C	3	
I	$64m$	
Γ	$3I$	

Table 01 : *Parameter values for Our Plane. These are what we shall use now for stability analysis and later for flight simulations.*

Before anything else, let me clarify that these values are realistic but don't actually correspond to the parameters for any one particular airliner. Now let's see the reasoning behind some of the choices. The first thing to note is that all parameters are chosen to represent flight at altitudes close to 0 feet (fully dense air). From Tables 2A–01-03, we can see that the dimensions, weight and thrust of Our Plane are closest to the Airbus A321, in-between the Boeing 737 and the wide-bodies. $K_C = 1500$ stems from our desire to have the minimum total drag at a physically plausible speed – see §36. It is reasonable that the lift constant of the tail be $1/10$ of that of the wings, since the tail has about $1/10$ the area of the wings. The value of C comes from the typical cruise thrust – again we elaborate in §36. $I = 64m$ is arbitrary; given the dimensions of the aircraft, a radius of gyration of 8 m seemed plausible. Finally, the value of Γ leads to rapid damping of angular motions, as is observed in practice, and also agrees with real observations, as I shall describe later in this Section. Making it proportional to I ensures the same rate of decay of motions at all weights, a minor convenience during the simulations.

For this model plane, we solve (09) using Newton-Rhaphson to find the fixed points. Then, for stability, we have to plug the fixed points into the Jacobian of (3B–22c-f). My assumption is that you know how to do a linearized stability analysis; if you don't, see for example Ref. [1O–45]. To calculate this Jacobian, we must first wade into the mess of the substitutions arising from (3B–21), a step I avoided in the last Section. Letting $\bar{\alpha_E}$ denote $\eta - \theta_E$, we note that this is a first quadrant angle (the bar on α_E is because the tail angle of attack is $\theta_E - \eta$). Equations (3B–22) feature the cos and sin of $\bar{\alpha_E}$ (note that $\theta - \theta_E$ in the sixth equation can be written as $\theta - \eta + \bar{\alpha_E}$), while (3B–21) gives us the sin of $2\bar{\alpha_E}$. From this, we readily have

$$\cos 2\bar{\alpha}_E = \sqrt{1 - \frac{4\bar{f}_p}{k_E^2 V^4}} \quad , \tag{13}$$

and then the half-angle formulae, memorization favourites for competitive examination candidates, lead to

$$\cos \bar{\alpha}_E = \left(\frac{1}{2} \left[1 + \sqrt{1 - \frac{4\bar{f}_p^2}{k_E^2 V^4}} \right] \right)^{1/2} \quad , \tag{14a}$$

$$\sin \bar{\alpha}_E = \left(\frac{1}{2} \left[1 - \sqrt{1 - \frac{4\bar{f}_p^2}{k_E^2 V^4}} \right] \right)^{1/2} \quad . \tag{14b}$$

The first quadrant nature of $\bar{\alpha_E}$ determines the signs at this step. We can see that both of these are functions of V (and fortunately no other variable). Hence, the derivatives of both with respect to V will be needed in the Jacobian. These derivatives are

$$C' = \frac{\mathrm{d}}{\mathrm{d}V}\cos\bar{\alpha}_E = \frac{2}{\cos\bar{\alpha}_E}\left(1-\frac{4\bar{f}_p}{k_E^2V^4}\right)^{-1/2}\frac{\bar{f}_p^2}{k_E^2V^5} \quad , \tag{15a}$$

$$S' = \frac{\mathrm{d}}{\mathrm{d}V}\sin\bar{\alpha}_E = \frac{-2}{\sin\bar{\alpha}_E}\left(1-\frac{4\bar{f}_p}{k_E^2V^4}\right)^{-1/2}\frac{\bar{f}_p^2}{k_E^2V^5} \quad . \tag{15b}$$

The fancy $\mathcal{C}$ and the prime should not cause confusion with the C of drag, while $\mathcal{S}$ is not a letter we have used before, fancy or otherwise.

In terms of these, the Jacobian is, taking variables in the order V,η,θ,ω,

$$\mathbf{J} = \begin{bmatrix} \mathbf{M}_1 & \mathbf{M}_2 \\ \mathbf{M}_3 & \mathbf{M}_4 \end{bmatrix} \quad \text{, where}$$

$$\mathbf{M}_1 = \begin{bmatrix} \frac{1}{m}\left\{\frac{K_CV}{2}\left(\cos3\alpha-\cos\alpha\right)-\bar{f}_pS'-2CV\right\} & \frac{1}{m}\left\{\frac{K_CV^2}{4}\left(3\sin3\alpha-\sin\alpha\right)+T\sin\alpha-mg\cos\eta\right\} \\ \frac{1}{m}\left\{\frac{K_C}{4}\left(\sin3\alpha+\sin\alpha\right)-\bar{f}_p\left(\frac{VC'-\cos\bar{\alpha}_E}{V^2}\right)-\frac{T\sin\alpha}{V^2}+\frac{mg\cos\eta}{V^2}\right\} & \frac{1}{m}\left\{-\frac{K_CV}{4}\left(3\cos3\alpha+\cos\alpha\right)-\frac{T\cos\alpha}{V}+\frac{mg\sin\eta}{V}\right\} \end{bmatrix} ,$$

$$\mathbf{M}_2 = \begin{bmatrix} \frac{1}{m}\left\{\frac{K_CV^2}{4}\left(-3\sin3\alpha+\sin\alpha\right)-T\sin\alpha\right\} & 0 \\ \frac{1}{m}\left\{\frac{K_CV}{4}\left(3\cos3\alpha+\cos\alpha\right)+\frac{T\cos\alpha}{V}\right\} & 0 \end{bmatrix} ,$$

$$\mathbf{M}_3 = \begin{bmatrix} 0 & 0 \\ \frac{1}{I}\left\{-K\bar{d}_1V\sin2\alpha+\bar{f}_p\bar{d}_2\left(C'\cos\alpha-S'\sin\alpha\right)\right\} & \frac{1}{I}\left\{K_C\bar{d}_1V^2\cos2\alpha+\bar{f}_p\bar{d}_2\left(\cos\bar{\alpha}_E\sin\alpha+\sin\bar{\alpha}_E\cos\alpha\right)\right\} \end{bmatrix} ,$$

$$\mathbf{M}_4 = \begin{bmatrix} 0 & 1 \\ \frac{1}{I}\left\{-K\bar{d}_1V^2\cos2\alpha-\bar{f}_p\bar{d}_2\left(\cos\bar{\alpha}_E\sin\alpha-\sin\bar{\alpha}_E\cos\alpha\right)\right\} & -\frac{\Gamma}{I} \end{bmatrix} . \tag{16}$$

Perhaps it's only fitting that something so complex as an aircraft should have at least one equation which looks like this. Now try imagining its three-dimensional 9×9 equivalent ….. For the stability analysis, the Jacobian must be evaluated at the fixed point. The entries of the Jacobian are the **stability derivatives** of the classical flight dynamics theory proposed by GEORGE BRYAN [1O–01].

Now, we consider Our Plane and plot the eigenvalues of (16) evaluated at the equilibria corresponding to level flight ($\eta^* = 0$) at a range of speeds from 250 to 700 km/hr. The eigenvalues happen to work out to two complex conjugate pairs in different regions of the complex plane, so we show them as two Figures below. Here's the first pair – blue denotes one eigenvalue and green the other. The labels on the plot show the flight speed.

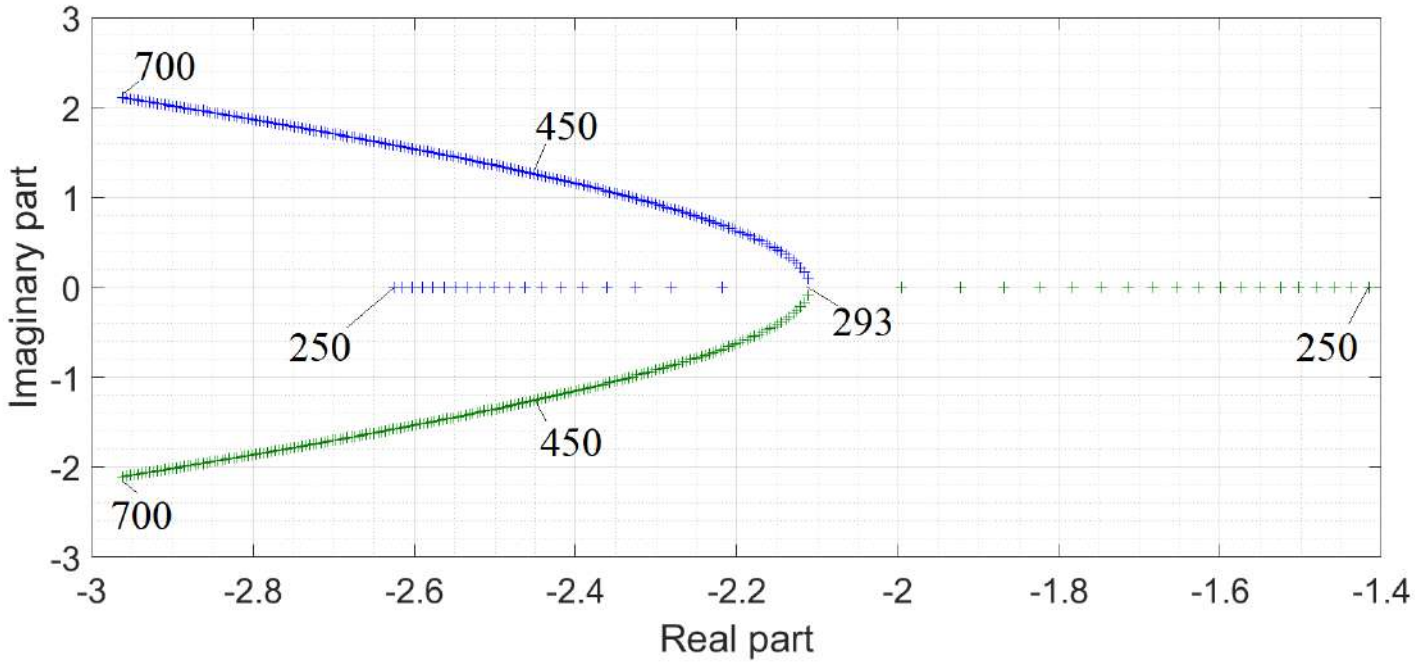


Figure 01 : *One pair of eigenvalues of (16) as the speed is varied in 200 steps from 250 to 700 km/hr. The speed (km/hr) is labelled on the plot at significant or representative points.*

At 250 km/hr this eigenvalue pair manifests as two negative real eigenvalues, which approach each other as the flight speed increases. At 293 km/hr, they merge and then head off into the complex plane. The real part becomes more negative and the frequency increases as the speed increases. In the lower speed range, this eigenvalue pair is qualitatively similar to an overdamped harmonic oscillator where the damping decreases with increasing speed; 293 km/hr is the speed at which the damping transitions from supercritical to subcritical. Beyond this point though, the damping again increases with increasing speed. In the oscillatory region, the motion has a frequency of about 1 rad/s, corresponding to a period of a few seconds. It is also damped out within a second or so. This mode is called the **short period** mode.

Here's the second eigenvalue pair.

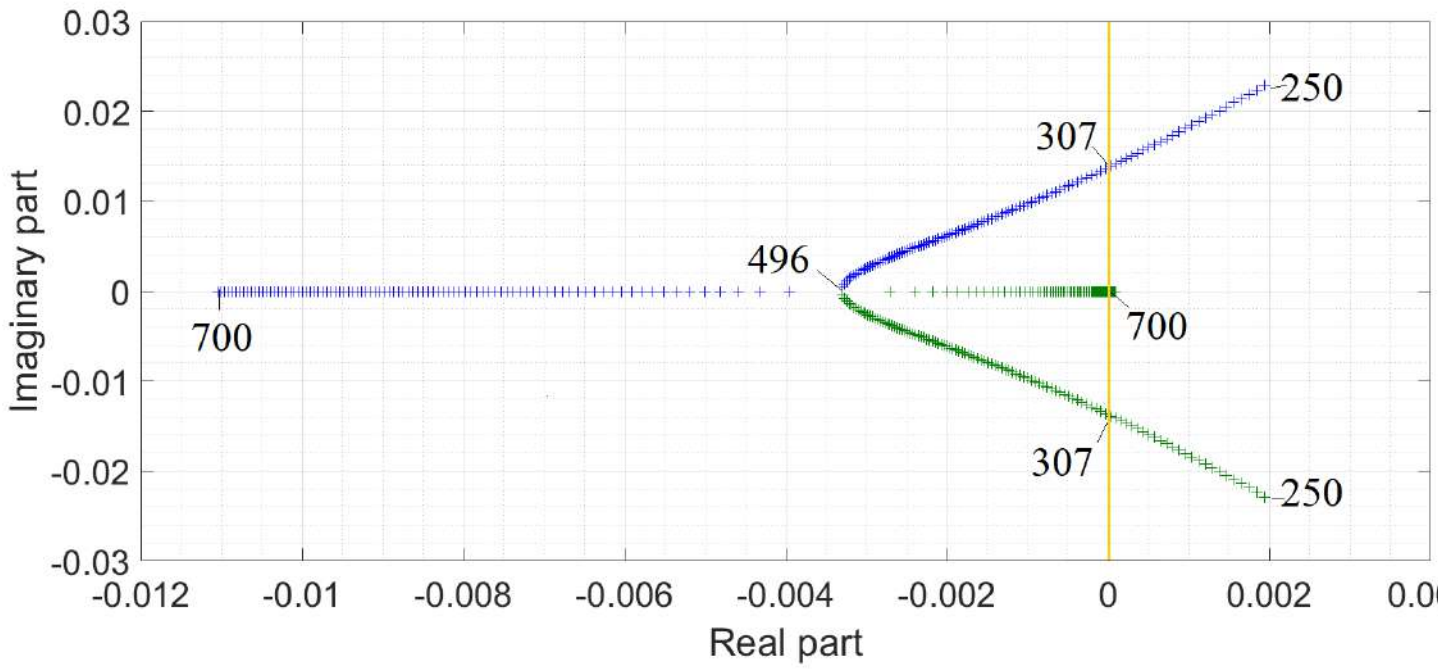


Figure 02 : *The second pair of eigenvalues of (16) as the speed is varied in 200 steps from 250 to 700 km/hr. The speed (km/hr) is labelled on the plot at significant or representative points.*

This time it's Fig. 01 in reverse – a complex pair at lower speeds transitions to a real pair at higher speeds. Three features are of interest : (*a*) at low speeds, the real part is *positive*, implying negative damping and unstable motions, (*b*) even after entering the positive damping regime (at 307 km/hr), the damping is extremely low, and (*c*) in the oscillatory regime, the frequency, at about 1/100 of the short period mode, is very low as well. Considering that (3B–22) features heavy damping on both translational and rotational motions, it is a huge surprise that it should have a normal mode with nearly zero or even negative damping. Real aircraft do have such a mode however – oscillation with a period of minutes which may be stable or unstable. It is called the **phugoid** mode.

Note that 700 km/hr is an unrealistically high speed for travel at low altitude – by the time the plane reaches that kind of speed, it is at least 10,000 feet above ground, and the air is much less dense. Indeed, speeds above 500 km/hr at ground altitude are quite rare. On the other hand, a typical takeoff speed is about 300 km/hr, so, for an aircraft at MTOW, that is an approximate minimum practical speed of operation. We can see that, in this speed range, both the short period and phugoid* modes are oscillatory, as is observed in reality. Of course, the actual numbers in the plots are of limited significance since the parameter values represent a fictitious aircraft rather than an actual one. For example, after fixing all the other parameters, I hand-picked the value of Γ (perhaps the parameter which is most difficult to estimate physically) to make the modes come out like this – making Γ too high caused the short period mode to have all real eigenvalues while making it too low resulted in an unstable phugoid mode everywhere. The numerical values of the eigenvalues will also change depending on the implementation of the horizontal tail. Here, we evaluated everything for constant $\bar{f}_p$, treating it as a fundamental parameter. If on the other hand we have a two-piece tail, then our fundamental parameter will be the deflection $\bar{\delta}$. In this case, the fixed points and their stability eigenvalues will be suitably modified.

* The word "phugoid" was coined by FREDERICK LANCHESTER to mean "flight-like"; unfortunately, as he himself later admitted [01], the root "phug-" or "fug-" means "flight" in the sense of "escape" rather than aviation. It is the source of the words "centrifuge", "fugitive" as well as "fugue" in music. JOSEPH HAYDN was aware of the last one : in the finale of the string quartet Op. 20 No. 2, a knotty four-voice fugue, he inscribed the comment "sic fugit amicus amicum" – "thus, friends fly from each other".

A very lightly, or even negatively, damped mode (phugoid) in an aircraft might appear unrealistic or false – surely a fully functional* plane is very strongly stable in the sky ? Indeed it is. What is strongly stable however is the combination of plane and pilot, whereas what we analysed is the plane on its own (we treated the pilot inputs T and $\bar{f}_p$ to be constants). A lightly damped mode, or even an unstable mode with a sufficiently high growth time constant and sufficiently long period, is not a worry because the pilot will kill it manually as soon as he observes it taking shape. If there's a decrease in speed, he'll increase thrust; if there's a tendency to gain altitude, he'll pitch down the nose. What would have been worrisome is a growing mode with time constant of the order of a pilot's reaction time (for instance, if the real part of the short period eigenvalues had been positive rather than negative) or an oscillatory mode with period of order equal to the reaction time (for instance, if the phugoidal frequency had been 10-100 times higher). Fortunately however, the physics of lift and drag is such as to ensure that fully functional aircraft do not have such modes (I keep saying "fully functional" because with a compromised aircraft, for example one missing its elevator, anything can happen).

* By "fully functional", I mean that all components which affect the dynamics and control of the aircraft are working normally. It does not necessarily imply that the reading light on seat 37K turns on when the switch is pressed.

To my mind, a detailed analysis of the short period and phugoid modes does not cast too much light on the motions of a well-designed aircraft (that analysis *is* very important during the aircraft design phase). This is because flight with no control inputs is an unrealistic condition, and the details of these modes don't really help us understand how the plane will respond to the throttle and the stick. For this reason, we will not spend further time on this topic now, but instead take a quick look at these modes after introducing the flight simulator in the next Chapter. Apart from short period and phugoid, real planes have three other modes called roll subsidence, Dutch roll and spiral mode. The first one refers to the spontaneous decay of rolling or banking motions. We can see this immediately from the banking plane equation (3C–04f). The other two modes represent couplings between yaw and bank, so they are quintessentially three-dimensional and we kick them off to future work.

§35 **Pilot-induced oscillation.** This is an instability, quite different from phugoid or short period, which some airplanes may experience under certain conditions. This happens when the plane may be intrinsically stable or marginally unstable but the pilot's input causes it to oscillate with growing amplitude or steady large amplitude. Pilot-induced oscillations occur as a result of delay in the feedback loop consisting of the flight instruments, the pilot and the controls. To consider a simple example, suppose that the climb rate indicator in a particular aircraft actually shows the climb rate of two seconds previously, and that the pilot, unaware

of this delay, wishes to transition from a 1000 fpm to a 1500 fpm climb. Assume that all other steps are instantaneous. To initiate the transition, the pilot pulls the stick back, prepared to ease off when 1500 fpm is reached. But, because of the delay, when the climb rate is actually 1500 fpm the indicator will be showing say 1400 fpm. The pilot will keep pulling until he sees 1500, at which point the rate has actually become 1600. Two seconds later, seeing the 1600, the pilot will push the stick as corrective measure. If he keeps the pressure on until the indicator approaches 1500, the plane will now shoot through 1400 before he eases off, and then the cycle will begin all over again. Of course, this is an oversimplified picture but you get the logic. Delay can also occur from the pilot's reaction time and, if thrust control is involved, from the time it takes the engines to transition from one to another commanded power level.

Pilot-induced oscillation can occur in a variety of contexts, for instance in trying to damp out the phugoid, trying to achieve a prescribed climb or descent rate, trying to stabilize the aircraft on the glideslope and so on. Because of this, I shall not present its mathematical theory in a particular context but in a more general way. Suppose x is a dynamical variable which you are trying to control to a steady value of zero. Suppose further that in the absence of control, x obeys the differential equation

$$\ddot{x} + a\dot{x} + bx = 0 \quad . \tag{17}$$

While not all systems obey this equation, it is certainly a very common equation which results from linearization of a mechanical system. The variables in the phugoid mode for example obey (17) with b positive and a small positive if the mode is stable and a small negative if the mode is unstable. In the control scheme, you add a spring term and a damping term so that the equation with control is

$$\ddot{x} + (a + C)\dot{x} + (b + k)x = 0 \quad , \tag{18}$$

where k and $\mathcal{C}$ are positive. Again, these are not universal but very plausible forms of a control strategy. For example, a pilot who increases elevator force if the plane descends from target altitude is effectively applying a k term while one who increases elevator force if the climb rate drops below target is effectively applying a $\mathcal{C}$ term. If $a + \mathcal{C} > 0$ and $b + k > 0$ hold true, then all solutions of (18) decay to zero in time and the control objective is achieved. Hence, for successful control, we need to satisfy these two criteria.

With delay in the loop, what happens is that in the control terms, $x(t)$ becomes replaced by $x(t-\tau)$. In words, the control force now depends not on what the value of x is now but on what it was τ seconds ago (τ, the standard notation for a delay, has previously done duty as a torque but there shouldn't be any confusion since the contexts are completely separate). With this modification, (18) acquires the form

$$\ddot{x} + a\dot{x} + bx + C\dot{x}(t-\tau) + kx(t-\tau) = 0 \quad . \tag{19}$$

This is called a delay differential equation (DDE). The theory of DDE is an advanced topic in nonlinear dynamics [02,03]. Here however, we shall need only the tip of this iceberg; for this part, I will use two facts from delay theory with no attempt at proof and derive the rest from the ground up. The question we ask is as follows. Let's say the parameters are chosen such that the solutions of (19) are stable if $\tau = 0$. Given a, b, k and $\mathcal{C}$, for what minimum value of τ does (19) undergo a change in stability i.e. acquire temporally growing solutions ?

Since (19) is linear and constant-coefficient, we try a solution of the form $x = e^{\lambda t}$ (the first DDE fact : we can do this). Plugging yields the characteristic equation which we can solve for λ; if any of the roots has a positive real part then (19) will have growing solutions. We know that when $\tau = 0$, the characteristic equation has two roots with strictly negative real parts. Now the second DDE fact : when an infinitesimal τ is added, infinitely many more roots emerge, in general complex, but they all have their real parts close to $-\infty$. As τ increases, the roots move rightwards across the complex plane. Given this behaviour of the roots, we will first encounter growing solutions when either (*a*) a single real root moves across the imaginary axis, or (*b*) a pair of complex roots move across this axis. At the instant of stability transition, the root will have the value zero in the first case and the value $\pm j\Omega$ in the second case, where Ω is some real number. To find the transition, we will have to analyse these cases separately.

Case $\lambda = 0$

In this case, $\lambda = 0$ is a root, so $x = \text{const.}$ is a solution of (19). Letting this constant be x_0 and plugging into (19), we find

$$(b+k)x_0 = 0 \quad . \tag{20}$$

Since x_0 is not zero, this implies that $b+k$ must be zero. This condition doesn't even feature τ and it doesn't hold true unless k and b are chosen in a very special manner. We can assume that this special choice is not made, and neglect this case from further consideration. ■

Case $\lambda = j\Omega$

In this case, we substitute $x = e^{j\Omega t}$ into (19), where Ω is unknown. This yields

$$-\Omega^2 + j\Omega a + b + j\Omega C e^{-j\Omega\tau} + k e^{-j\Omega\tau} = 0 \quad . \tag{21}$$

Equating the real and imaginary parts, we have

$$\begin{aligned} -\Omega^2 + b + \Omega C \sin\Omega\tau + k\cos\Omega\tau &= 0 \\ \Omega a + \Omega C \cos\Omega\tau - k\sin\Omega\tau &= 0 \end{aligned} \quad . \tag{22}$$

Here a,b,k,C are known while τ and Ω are unknown, so we have a consistent system. To solve it with minimum hassle, we rearrange some terms and write it in a matrix-vector form, thus :

$$\begin{bmatrix} \cos\Omega\tau & \sin\Omega\tau \\ -\sin\Omega\tau & \cos\Omega\tau \end{bmatrix} \begin{bmatrix} k \\ \Omega C \end{bmatrix} = \begin{bmatrix} \Omega^2 - b \\ -\Omega a \end{bmatrix} \quad . \tag{23}$$

Now on the LHS we can recognize the rotation matrix implying that the vector $[k;\ \Omega C]$ is the vector $[\Omega^2 - b;\ -\Omega a]$ rotated through the angle $\Omega\tau$. Forthwith we have two conditions : (*a*) the two vectors must be having the same length, and (*b*) the cosine of the rotation angle must be the dot product of the vectors divided by the product of their lengths. These conditions lead to algebraic expressions for Ω and τ, as we shall now see.

The first condition (equal length) implies

$$\sqrt{k^2 + \Omega^2 C^2} = \sqrt{\left(\Omega^2 - b\right)^2 + \Omega^2 a^2} \quad . \tag{24}$$

Squaring both sides, we find a quadratic equation for Ω^2 which has the solution

$$\Omega^2 = \frac{-a^2 + 2b + c^2 \pm \sqrt{\left(-a^2 + 2b + c^2\right)^2 - 4\left(b^2 - k^2\right)}}{2} \quad . \tag{25}$$

This gives us two possible values Ω_1^2 and Ω_2^2 corresponding to the upper and lower signs before the radical. On the other hand, the plus-minus signs on Ω_1 and Ω_2 obtained after extracting the roots is irrelevant since $+\Omega$ and $-\Omega$ for a frequency mean the same thing. Hence, we can ignore the negative and work with positive Ω_1 and Ω_2 only. Note that any or both of Ω_1 and Ω_2 as per (25) may be (non-trivially) complex, which contradicts the starting form of the solution assumed for arriving at (25); if one Ω is complex, then we throw that away while if both are complex then it means that the chosen values of a,b,k,C have no stability transition for any τ.

The second condition on (23), i.e. the one featuring the cos of the angle, is

$$\cos\Omega\tau = \frac{\left[k;\quad \Omega C\right] \cdot \left[\Omega^2 - b;\quad -\Omega a\right]}{\text{len}\left(\left[k;\quad \Omega C\right]\right)\text{len}\left(\left[\Omega^2 - b;\quad -\Omega a\right]\right)} \quad , \tag{26}$$

(len denotes length) which leads to

$$\tau = \frac{1}{\Omega}\arccos\frac{k\left(\Omega^2 - b\right) - \Omega^2 aC}{\sqrt{\left(k^2 + \Omega^2 C^2\right)}\sqrt{\left(\left(\Omega^2 - b\right)^2 + \Omega^2 a^2\right)}} \quad . \tag{27}$$

Since we already have Ω from (25), we can substitute that into the above and complete the solution of (22). If Ω has two real values, then we shall have to plug both of them into (27) and find the corresponding τ (if one exists). If there are two τ's corresponding to the two Ω's then the smaller one will yield the true value of the stability transition. Just as with (25), if (27) has no positive real solution for τ then it means that the particular choice of $a,b,k,\mathcal{C}$ has no stability transition for any τ. ■

We have just one problem which is that the form (25,27) of the transition criterion conveys precious little insight. Explicitly substituting (25) into (27) will give us an equation the size of a Boeing 777; then what ? So, we now use Matlab to plot these solutions and gain insight into the system (19). Let us fix the values $a = 0$ and $b = 1$ so that the uncontrolled system is a harmonic oscillator of frequency 1. Then, we vary k from 0 to 50 and C from 0 to 15 (in 200 steps in both cases) and at each point plot the value of τ which causes the stability transition. We show this as a colour map, with higher value corresponding to a brighter colour.

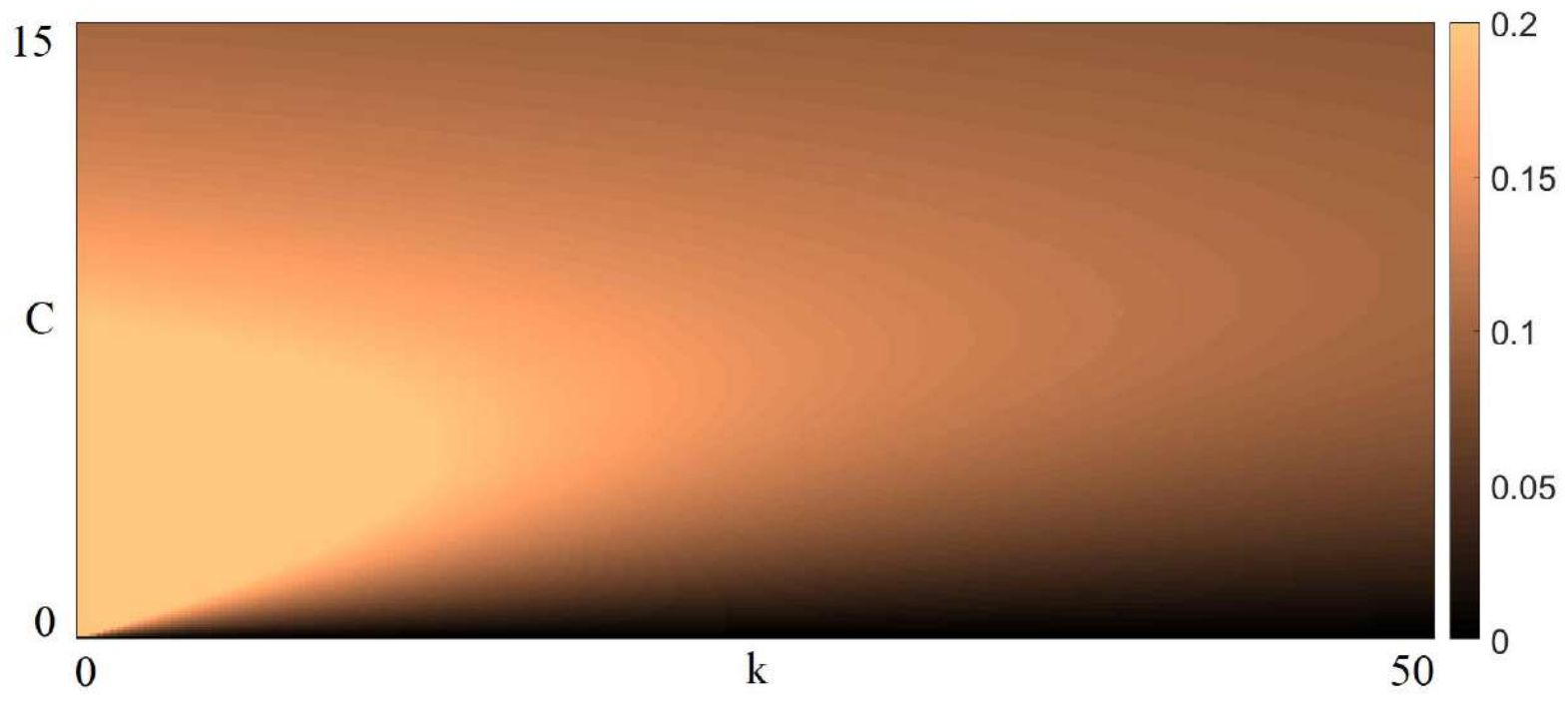


Figure 03 : *The value of* τ *at which the system transitions from stable to unstable, as a function of* k *and* C*. A brighter colour denotes a higher* τ*, as shown in the legend alongside. To increase legibility, values of* τ *greater than 0·2 have been rendered at the same brightness as* $\tau = 0{\cdot}2$*.*

In this plot, I have saturated the brightness at the value $\tau = 0{\cdot}2$ so as to make the bulk of the plot clear. There are still higher values in the bottom left corner. Now to interpret the results.

In the practical situation, a and b will be given (properties of the aircraft), τ will also be a given (properties of the flight instruments or pilot's reaction time) and the variables will be k and $\mathcal{C}$ (the aggressiveness of the control inputs). In Fig. 03, a higher τ corresponds to a more controllable aircraft-cum-pilot as it implies that the chosen k and $\mathcal{C}$ can accommodate a larger delay in the loop without adverse effect. Hence, the brighter the plot, the brighter the situation. The big surprise here is that the brightest region is the bottom left – small k and small $\mathcal{C}$. This is counter-intuitive since in the absence of the delay, large k and $\mathcal{C}$ (specifically, k as big as possible and $\mathcal{C} = 2\sqrt{k}$) correspond to faster damping of solutions and hence better control. Here however, that is not the case. At $\mathcal{C} = 0$, any k gives a critical delay of zero, which agrees with well-known results about delayed harmonic oscillators [02,03]. At fixed nonzero $\mathcal{C}$, increasing k actually makes the plane harder to control. Note however that the uncontrolled system (17) has a spring term a to begin with – if that had been absent or had had the wrong sign, then some k would have been required to achieve a good outcome. But too much of a delayed spring is counter-productive. For a fixed k on the other hand, the situation at first improves with increasing $\mathcal{C}$ and then again deteriorates somewhat.

Hence, too much of delayed damping is also not beneficial. Since k and C are proportional to the size of the pilot's control inputs, the best results correspond to small or moderate inputs and not large ones.

In summary, pilot-induced oscillation can occur if the control inputs are too delayed or too large. Delays due to pilot reaction time can be mitigated with practice and skill while delays due to instrument error etc cannot be reduced (except by replacing the instrument). Passenger airliners are designed to minimize the tendency for pilot-induced oscillation in the course of normal flight. Nevertheless, a non-standard situation such as a hasty interception of glideslope might give rise to such oscillation. In all cases, whenever you see a tendency towards pilot-induced oscillation, the recovery strategy has to be to consciously apply smaller control inputs. For example, if you were applying $\bar{f}_p = 10$ kN in response to a 10 ft deviation from slope and the plane starts wibble-wobbling about the slope, try applying $\bar{f}_p = 2$ kN instead. This may sound paradoxical, but that's what the math tells us, as does practical experience [04]. If the flight phase is such that a relaxation of control input may also be unsafe, then you have to immediately transition to an easier phase. Again by way of example, if you are oscillating about the glideslope, then relaxing the controls might also make the aircraft under- or overshoot the runway threshold. In that case, abort the approach and transition to level flight or a steady climb; redo the approach after intercepting the slope more carefully.

We can now answer Q20 of the Quiz. The question mentioned difficulty controlling a phugoid, and oscillations despite plausible control inputs. This suggests an unstable or marginally stable phugoid mode and pilot-induced oscillation in attempting to control it. The correct response will be to ease up on the controls and accelerate to a higher speed, which is Choice A. The weaker control inputs will mitigate the pilot-induced oscillation while the higher speed will increase the stability of the phugoid. Let us also see why the other answer choices are incorrect. Choice B, extending spoilers and undercarriage, will add damping no doubt, but a rogue phugoid is present despite the heavy damping coming from C and Γ. Adding more damping will have little or no effect on the relevant eigenvalues while the reduced speed arising from the spoilers will push them to the right. This is the opposite of what we want. Choice C, increasing the aggressiveness of control input will also amplify the pilot-induced oscillations so that will be another incorrect strategy. Finally, Choice D, entering a bank, is a non-sequitur – phugoid is a problem in the pitch plane, why should it be corrected by adding bank. Since a turn makes the overall task of flying more complicated, a bank can only cause harm in the present situation.

§36

Characteristic curves and their interpretation, normal and reversed command. Since the fixed points are stable, the aircraft will tend to gravitate towards them if left undisturbed. This means that, when thrust and elevator force are held constant, the aircraft will in the long run operate at the corresponding steady state speed, elevation and pitch. Hence, the steady state solutions are of considerable interest in the analysis of the aircraft's motions. They enable us to answer questions such as what will the aircraft do (on the long term) if we set say 50 percent thrust and 20 kN elevator force, and what thrust and elevator force should we use (again on the long term) if we want to maintain say a 5° climb at 500 km/hr.

The set of all fixed points of the aircraft consists of quintuplets $(V^*,\eta^*,\theta^*,T^*f^*)$ which satisfy (09). If we choose T^* and f^*, then the remaining three elements of the quintuplet are determined uniquely. Hence, all the fixed points together form a 2-dimensional surface in the 5-dimensional space of V, η, θ, T and $\bar{f}_p$. Because this structure is not easy to visualize (except perhaps to a sufficiently pure mathematician), we shall plot suitable cross-sections of it, showing two or three variables at time in the same plot. We shall call these plots the **characteristic curves** or characteristics of the aircraft. These curves are much in demand in the analysis of induction motors [3A–03]. I have not seen them being applied to aircraft however, except in one very restricted case which I shall discuss below. Nevertheless, they shall prove to be of great utility in the manoeuvre planning of the next Chapter.

To obtain the characteristics, we start from (09), but now we view it differently. First, we rewrite (09) using $\alpha^* = \theta^* - \eta^*$, getting

$$\frac{K_C V^{*2}}{4}\left(\cos 3\alpha^* - \cos\alpha^*\right) + f^* \sin\left(\theta_E{}^* - \eta^*\right) + T^* \cos\alpha^* - mg\sin\eta^* - CV^{*2} = 0 \quad , \tag{28a}$$

$$\frac{K_C V^*}{4}\left(\sin 3\alpha^* + \sin\alpha^*\right) - \frac{f^* \cos\left(\theta_E{}^* - \eta^*\right)}{V} + \frac{T^* \sin\alpha^*}{V} - \frac{mg\cos\eta^*}{V} = 0 \quad , \tag{28b}$$

$$-\frac{K_C \bar{d}_1 V^{*2}}{2}\sin 2\alpha^* + f^* \bar{d}_2 \cos\left(\alpha^* + \eta^* - \theta_E\right) + T^* \bar{h} = 0 \quad . \tag{28c}$$

In §34, we fixed T^* and f^* and solved for V^*, η^* and θ^*. In other words, given a throttle setting and an elevator force, we asked for the steady state motion. Now, we reverse the question. We ask, given the desired steady state motion, find the required throttle setting and elevator force. In other words, we prescribe V^* and η^* and solve for T^*, f^* and α^* (and hence θ^*).

To solve (28) for T^*, f^* and α^*, we must use Newton-Rhaphson; first however we hand-calculate the fixed points of the oversimplified model (3B–25). Its equilibria satisfy

$$T^* - mg\sin\eta^* - CV^{*2} = 0 \quad , \tag{29a}$$

$$K_C V^* \alpha^* + \frac{T^* \alpha^*}{V^*} - \frac{mg\cos\eta^*}{V^*} = 0 \quad , \tag{29b}$$

$$-K\bar{d}_1 V^{*2}\alpha^* + f^* \bar{d}_2 + T^* \bar{h} = 0 \quad . \tag{29c}$$

This system is really easy to solve; the first equation gives T^*, plugging that into the second equation gives α^* and then the third gives f^*. What we find is

$$T^* = mg\sin\eta^* + CV^{*2} \quad , \tag{30a}$$

$$\alpha^* = \frac{mg\cos\eta^*}{\left(K_C + C\right)V^{*2} + mg\sin\eta^*} \quad , \tag{30b}$$

$$f^* = \frac{1}{\bar{d}_2}\left(-\bar{h}\left(mg\sin\eta^* + CV^{*2}\right) + \frac{K_C \bar{d}_1 V^{*2} mg\cos\eta^*}{\left(K_C + C\right)V^{*2} + mg\sin\eta^*}\right) \quad . \tag{30c}$$

Unlike (12), these expressions have a transparent physical interpretation. First off, we can see that the thrust must balance drag and overcome the component of gravity along the flight path during a climb. Next, the angle of attack increases as the plane's weight and decreases as the square of its velocity (note that for small η^*, the first term in the denominator of (30b) greatly exceeds the second) – dependences which follow from the nature of lift on an airfoil. Finally, $\bar{f}_p$ increases as m increases, which we already saw in §33. Apart from their physical meaning, the results (30) have a still greater significance. For Newton-Rhaphson to work, it needs a starting guess which is close to the actual solution; otherwise it can converge to a spurious (even complex) root. And what better starting guess to solve (28) than (30) ?

Having solved (28) for Our Plane, we now display the results in the upcoming Figure. This is the archetype of a characteristic which we shall be plotting repeatedly throughout this Article, so let me explain the plotting conventions in some detail. We consider flight at speeds* ranging from 250 to 700 km/hr and at three discrete angles of elevation : (*a*) $\eta^* = \arctan(-0{\cdot}05)$ corresponding to a descent along a 5 percent slope like glideslope, (*b*) $\eta^* = 0$, corresponding to level flight, and (*c*) $\eta^* = \arctan 0{\cdot}1$ corresponding to climb along a 10 percent slope – a reasonably intense altitude gain. We get V^* lined up on the x-axis and use left and right hand y-axes for T^* and f^* respectively. Solid lines attach to the left hand y-axis and dashed lines to the right, and thrust is always as a percentage of TOGA rating. We use colour to distinguish the three elevations – the convention will always be blue, green and red in order of increasing η^*. If you get confused about which colour is for which curve, remember that higher elevation requires higher thrust.

* Since the model parameters are for the aircraft close to the ground, and since there's no wind by definition, indicated airspeed equals true airspeed equals ground speed.

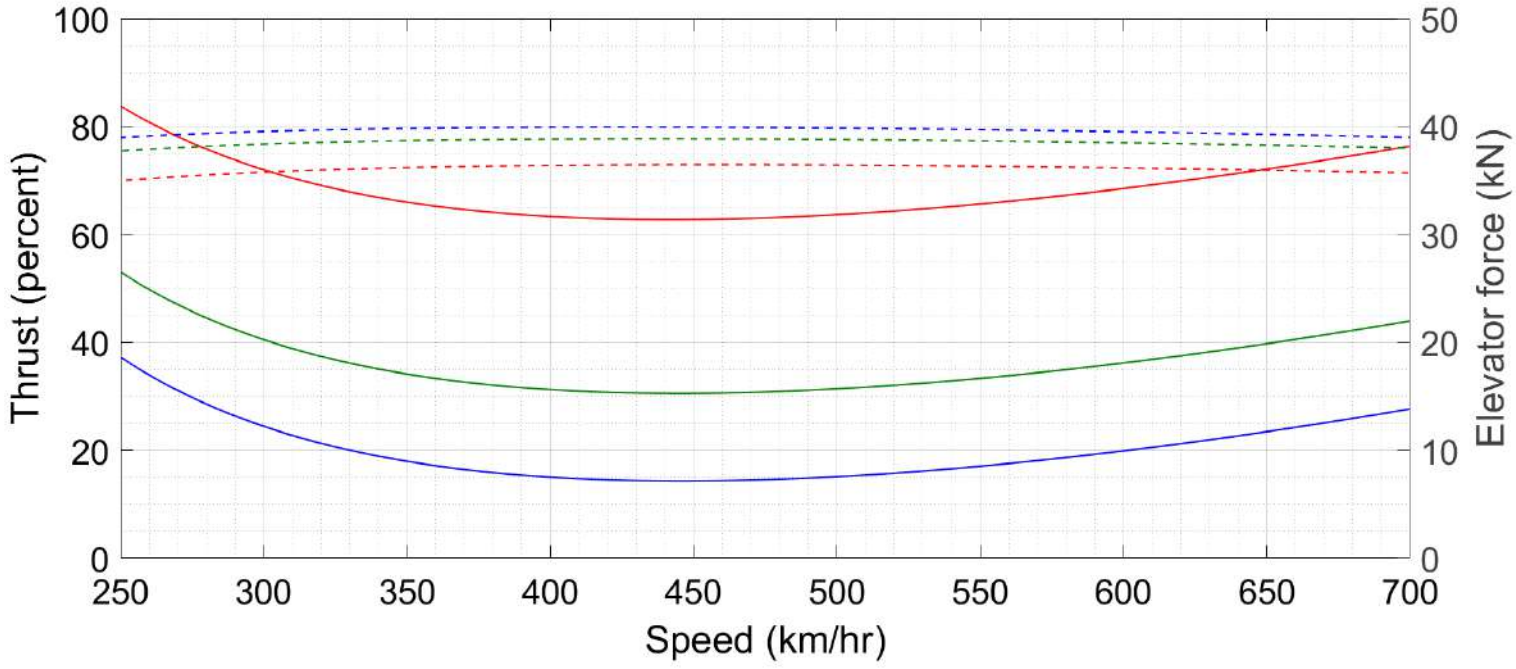


Figure 04 : *Characteristic curves for Our Plane. Solid lines attach to the left hand* y*-axis and dashed lines to the right hand* y*-axis. Blue, green and red denote climb gradients of –5 percent, 0 and 10 percent respectively.*

We can see that the thrust increases sharply as the elevation increases. This is intuitive since thrust balances the weight component along the gradient. The elevator force is approximately independent of both speed and elevation. This too makes sense since in all steady flight conditions, the wings' lift balances the bulk of the weight and hence is very close to mg; a constant lift exerts a constant torque, which must be balanced by another constant torque at the elevator and hence a constant $\bar{f}_p$. At this point, I can explain why I used (28) rather than (09) to numerically evaluate the fixed points in §34. This is because the same values of T^* and f^* can give more than one equilibrium solution – for example, one corresponding to a slow climb and the other to a faster descent. At the very least, fixed points separated widely in V^* and η^* can have the corresponding T^* and f^* very close together. While numerically solving (09), this degeneracy or almost-degeneracy of solutions was causing problems for the computer, which was finding fixed points erratically. On the other hand, the system (28) has a unique, well-defined solution for T^*, f^* and α^*, and the computer can find it easily. The unintuitive feature of the characteristics is that for each elevation, the thrust has a V-shaped (or parabola- or catenary-like shaped) profile rather than a monotonically increasing profile, as common sense [and (30a)] would have us expect. The curve of thrust vs speed is called the **drag curve** or **power curve** and is a well known curve in flight dynamics – this is the only instance where characteristics appear in prior Literature. Even so, there is one difference between Fig. 04 and the power curve as conventionally drawn, which I will discuss later in this Section.

Let us quickly note two points before analysing the V-shape of the characteristic. First is that, a typical cruising speed of 850-900 km/hr at altitude, where the air density is about 1/3 that at sea level, is equivalent to about 500 km/hr at sea level. In other words, the indicated airspeed during cruise is approximately 500 km/hr. At this speed, the thrust required is about 30 percent, which is what cruise thrusts typically are [05,06]. This consideration motivated my choice of C in Our Plane. The second point is that the accuracy of the approximate solution (30) is variable. Below we see a comparison between (30) and the exact solution for level flight at different speeds.

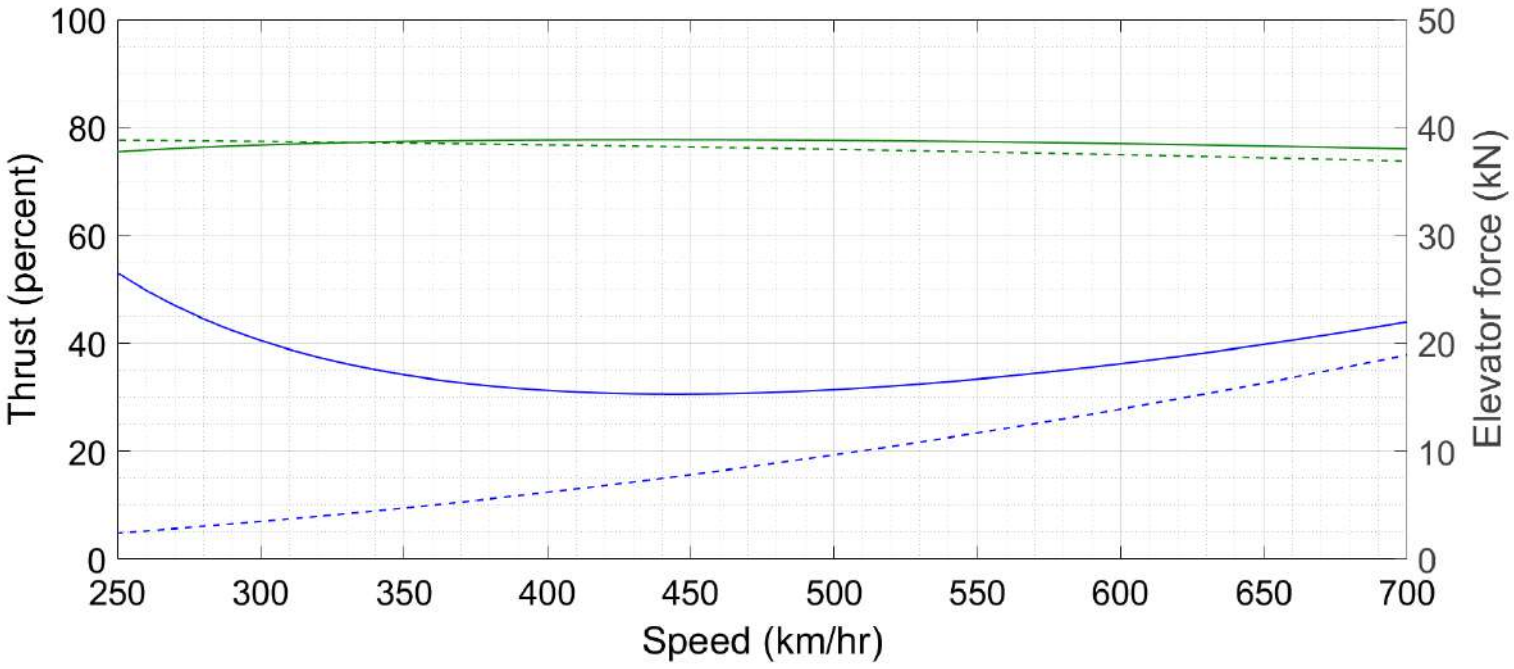


Figure 05 : *Exact and approximate characteristics for Our Plane. Thrust is in blue and elevator force in green – exact solutions are solid while approximate ones are dashed.*

The approximate $\bar{f}_p$ is very close to the actual one, but the thrusts differ a lot, especially at lower speeds. In particular, the approximate solution lacks the V-shape and hence lacks realism.

So, whence the V-shape ? For the speeds and elevations of Fig. 04 we now plot α^* as a function of V^*. We find that as V^* decreases, α^* increases. This is of course in line with intuition (same lift at lower speed requires higher angle of attack), and with (30b). α^* is also almost identical for all three elevation angles, since the wings' lift must be almost mg in each case.

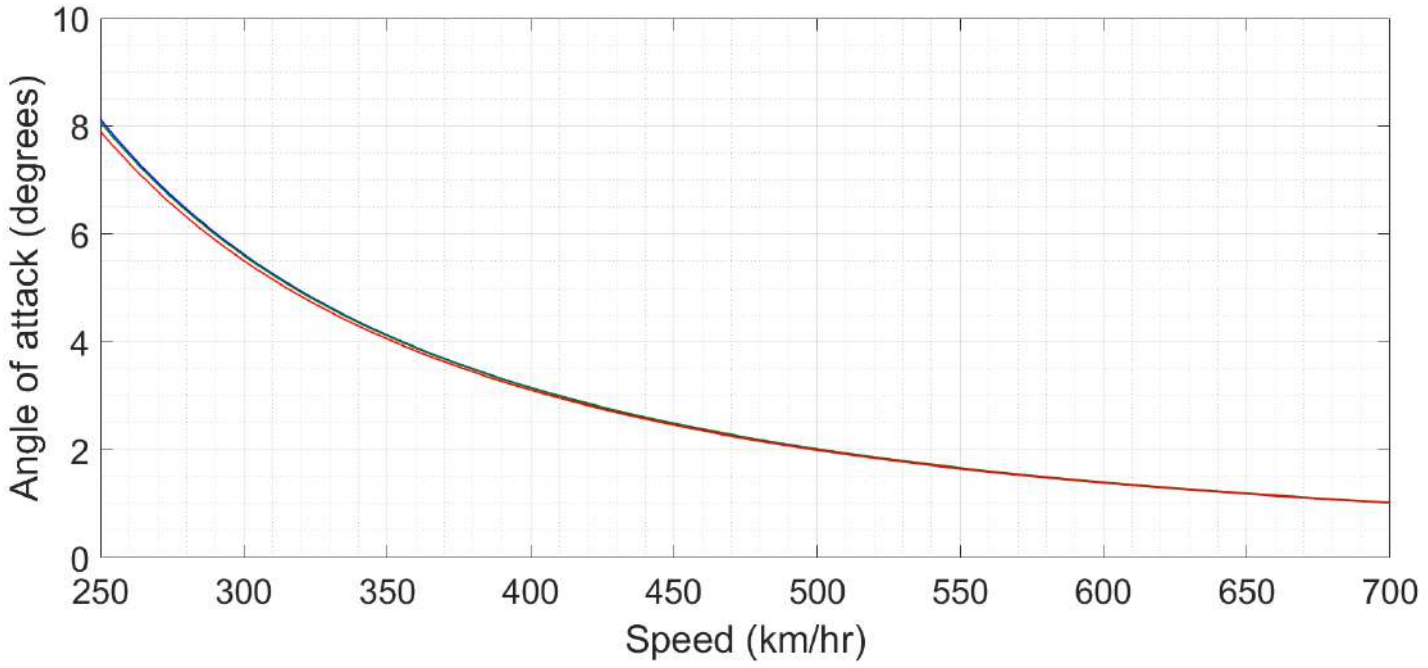


Figure 06 : *Characteristic curves for Our Plane.*

Now, we have seen in §28 that the term $K_C V^2(\cos 3\alpha^* - \cos\alpha^*)/4$ in (3B–22c) is a drag term. It is high when α^* is high, i.e. at low speeds, and it decreases with decreasing α^* and increasing speed. It arises from the component of **F** along **V** in Fig. 3B–03; the greater the value of α, the greater is this component. This drag is called the *induced drag*. On the other hand, the CV^2 drag term, also present in (3B–22c), increases monotonically with speed. This is called the *parasitic drag*. The resultant of the two drags gives rise to a V-shape; since the thrust must balance the total drag, it has a V-shape as well. As we have seen before, this drag rides piggyback on the lift in the modified Newtonian theory. On the other hand, it is zero in the Kutta-Zhukovsky theory*. This was one of the key factors motivating my choice of lift theory in §19-20. The parameter ε (unity for our aircraft) determines the size of the induced drag – the larger ε, the

* A modified form of Kutta-Zhukovsky theory, called lifting line theory, can account for the induced drag but only after assuming an airflow right through the wing i.e. from top to bottom of the wing. Even if the numerical answers from this theory aren't too bad, the physical basis appears a bit thin.

higher the drag. In the limiting case where ε is zero and K suitably infinite so that (3A–07) is finite, we get an airfoil with zero induced drag.

Now for the practical implications of the V-shaped characteristics. We can divide the aircraft operation into two speed regions – those to the right and the left of the minima in the thrust curves (note that the thrusts for different climb/descent rates have their minima at identical or nearly identical speeds). Operation in the right region is evidently more practical – who would want to use 40 percent thrust for level flight at 300 km/hr when the same thrust can get us level flight at 650 km/hr ? But there is more to it than just fuel economy. (Whenever you see fuel economy taking second place in importance, you can rest assured that safety is involved. Next to carrying passengers from A to B in one piece, the thing which airlines, and the aircraft manufacturers who supply them, worry most about is saving every penny.) To appreciate this, we redraw Fig. 04 with a slight modification. This time, we consider the thrust-speed characteristics for three different climb rates – 0, 200 and 500 fpm. Also, instead of the elevator force, we now plot the pitch $\theta^* = \eta^* + \alpha^*$ on the right hand y-axis.

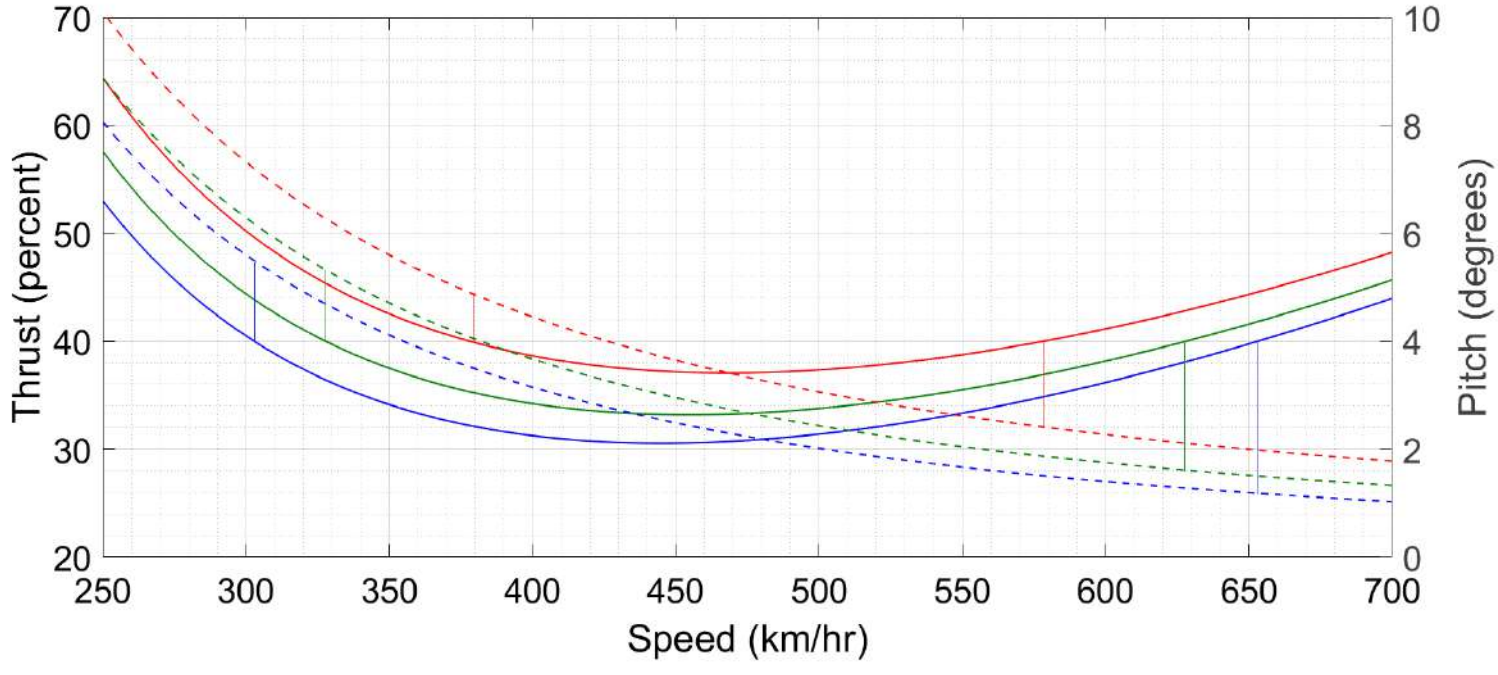


Figure 07 : *Characteristic curves for Our Plane. Solid lines attach to the left hand y-axis and dashed lines to the right hand y-axis. Blue, green and red denote climb rates of 0, 200 and 500 fpm respectively.*

Let us consider the fixed thrust level of 40 percent. For each of the three climb rates, this thrust level gives one equilibrium to the right and one to the left of the minima. For all six of these equilibria, let us also consider the value of θ^*. To facilitate graphical comparison, I have drawn a vertical line from the point (V^*, T^*) to the point (V^*, θ^*) in the appropriate colour – thus, the vertical blue line near 300 km/hr connects the equilibrium speed to the equilibrium pitch at 40 percent thrust, left of minima. Since actual numbers are more revealing than graphs, I now display these six equilibria in the below Table.

L					**R**			
Climb	0	200	500		**Climb**	0	200	500
Speed	303	327	378		**Speed**	654	628	579
Pitch	5·50	5·33	4·91		**Pitch**	1·17	1·61	2·40

Table 02 : *Climb rate (fpm), speed (km/hr) and pitch (degrees) for six equilibria corresponding to 40 percent thrust, with three equilibria to the left of the minima of thrust (denoted by L) and three to the right (denoted by R).*

Let us consider the right hand region first. As the climb rate increases, the speed decreases. This is in line with intuition of more thrust being required to sustain climb. Moreover, as climb rate increases, the pitch increases also, as every pilot learns on day 1 and as we saw in §28. Now let us consider the left hand region. Firstly, as the climb rate increases, the speed increases also. While this can still be rationalized on the basis of the V-shaped characteristic, the pitch is a total surprise. The pitch actually decreases as the climb rate increases ! In other words, to make the plane climb, the pilot should lower the nose instead of raising it, push the stick instead of pulling it ! Because of the unexpected behaviour of the aircraft in this regime, the region to the left of the thrust minima is called the **region of reversed command** or **the back side of the drag curve**. The region to the right of the minima is called the **region of normal command**.

As an aside, this is one instance where you can see the importance of doing things mathematically instead of relying on intuition alone. Intuition based on (3B–22) [or even on physical argument] can tell us to climb by raising the nose, but only a mathematical model and its fixed point analysis can tell us to climb by *lowering* the nose. Let me clarify that operation in the region of reversed command isn't dangerous per se. Concorde used to land in that region, as do many aircraft designed to thrill or to kill. However, operating here requires extra skill and attentiveness on the part of the pilot (Concorde pilots were British Airways and Air France's creme-de-la-creme). Should he become unmindful that he is operating on the back side of the drag curve and apply normal control inputs expecting normal results, then he might bring the aircraft to a dangerous configuration. We shall see one example of this in §52. Because of the requirement for increased pilot skill, and because passenger flights attempt to operate such that as many things as possible can go wrong before they crash, operation in this region is usually prohibited.

This raises the question, how to avoid this region. In Figs. 04 and 07, we can see that normal command begins only at a critical speed of around 450 km/hr or so – there is no option of staying on the ground until one is going that fast. To push the critical speed leftwards, we need to reduce the induced drag while preserving the lift. In §20 we have already calculated L/D for our airfoil to be $\cot\alpha$; since the drag in that Section is purely induced drag, we have

$$\frac{F_{D,I}}{F_L} = \tan\alpha \quad . \tag{31}$$

If we set $F_L = mg$ and treat α as small, then $\alpha = mg/K_C V^2$, and using this in (31) we get

$$F_{D,I} = \frac{m^2 g^2}{K_C V^2} \quad . \tag{32}$$

In other words, to reduce the induced drag for a given lift and given speed, we must increase K_C.

We do this by using the flaps. When flaps come out, they make the wing larger and also change the airflow to generate more lift at the same speed. Effectively, deploying flaps increases the value of K_C. Further, they increase the parasitic drag constant C, which further helps to shift the critical speed to the left. A third role which flaps play is that they increase the wing's camber, as we have seen in §05,20. This means that for a given actual value of α, the wing behaves as though it were at a higher α, enabling the aircraft to generate more lift without raising the nose as high (camber does not affect the command reversal speed). As I have already mentioned, in this Article we ignore the camber. On a typical aircraft, there are three to five discrete flap settings i.e. amounts by which the flaps can be extended in addition to the retracted setting. On Boeing aircraft, these settings are labelled by the degree angle which the flaps make, while on Airbus aircraft they are labelled by a number 1,2,3 etc. In all cases, a higher setting denotes a greater extension; retracted is also called "flaps up". Usually, the slower the flight, the higher the flap setting used. Thus, takeoffs typically occur at a moderate flap setting while landings are usually at the maximum setting.

The flap retraction profile following takeoff (velocities at which incremental retractions are undertaken), and similarly the flap extension profile during approach and landing, are often determined by the region of command rather than by physical feasibility of sustaining flight. For instance, in Fig. 07 (then tacitly and now explicitly drawn for the aircraft without flaps), the pitch for level flight at 350 km/hr is 4·5°. By definition, this is also the angle of attack, so the plane is nowhere close to stalling (α_S is typically around 15°). However, at this speed, retracted flaps will not be used. Rather, such a configuration will be used which keeps the aircraft in normal command without generating excessive parasitic drag. As the aircraft accelerates to the critical speed for the next lowest flap setting, that will be selected. For Our Plane, the ultimate retraction will be at 440 km/hr or so, when the flapless (called **clean**) aircraft has entered the normal command region. Note that real aircraft do indeed have their flap retractions around this speed – a fully loaded Airbus A320 goes clean at about 390 km/hr [07] while a fully loaded Boeing 777 goes clean at about 490 [08]. This consideration motivated my choice of $K_C = 1500$ in Table 01 (and of course, 1500 is a nice round number – it makes hardly any sense to say $K_C = 1230{\cdot}2$ when the whole aircraft is fictitious). Further, each flap setting has a maximum permissible speed of operation, exceeding which places undue aerodynamic loads on the flaps. This maximum speed decreases with higher and higher settings.

The big difference between the conventional power curve of the Literature and our characteristic curves is that the Literature curve makes no reference to the trim setting at different points on the curve. As we have seen in §33, with a two-piece tail and a given stabilizer deflection, a fixed point can be achieved only at one particular speed. If you change the thrust without changing the trim, then the steady state speed won't change at all. Instead, the steady state *angle of elevation* will change so that the thrust can balance the drag and the gravity component along the flight path. In other words, applying higher thrust will result in a higher climb rate but not a higher speed. To actually achieve level flight at different speeds, you need to change the trim in addition to the thrust. This is not represented in the power curve but is captured by our characteristics, since we are explicitly plotting all relevant variables and parameters. Our characteristics also show quantities such as pitch, which are outside the scope of conventional power curves, but are very useful for planning manoeuvres.

Now I must mention one very important cautionary point regarding the characteristics. This is that all these are depictions of steady state solutions and *give no information regarding the dynamics during transients*. In particular, the transient dynamics does NOT consist of a smooth translation along the appropriate characteristic curve. A simple example will clarify what I mean. Suppose we have a lightly damped vertical spring like a kitchen scales and we place a mass on it. The equilibrium displacement of the spring, measured from its natural length, will be $z^* = -mg/k$ (m : mass, g : gravity, k : spring constant). If we plot a graph of z^* vs m, then that will be the characteristic curve for the spring. Let's say that (10 kg, −10 cm) and (1 kg, −1 cm) are two points on this characteristic. This tells me that if I put a mass of 10 kg on the scales, its eventual displacement is −10 cm, while if I put a mass of 1 kg, its eventual displacement is −1 cm. However if I start with 10 kg at −10 cm and quickly but continuously remove mass until it becomes 1 kg, then the displacement will not be a smooth transition from −10 to −1 cm. Rather, the spring will oscillate in a manner which can be obtained only by solving its differential equation; only in the limit of long time will it come to the equilibrium point $z^* = -1$ cm.

When planning manoeuvres using the characteristics, this is something you must keep in mind. Because the fixed points of the aircraft are stable, it *does* hold true that if we plonk the plane down very close to a fixed point, then it will continue to hover round that point (the same is valid for our kitchen scale – put a mass of 1 kg and take it close to −1 cm with nearly zero velocity, and it will barely move). Again making an analogy with electrical machines, similar considerations apply to an induction motor – the torque-speed characteristics are given and the fixed points are stable, but transient operation poses its own design, analysis and control challenges.

Our discussion of regions of command, flap retraction speeds and manoeuvre planning has naturally brought us from hard calculation to the edge of actual flight operations. Let us not delay further in unveiling our simulator. We have had enough of mathematical theory – now it's time to fasten the seat belt, straighten the seat back, latch the tray table and open the window shades. And, on a simulator, we do NOT need to know the locations of the emergency exits.

---- o ----

5

FLIGHT SIMULATIONS

In this Chapter we put together everything that we have seen over the preceding pages. We use the aircraft equations of motion to construct a flight simulator and then analyse a series of manoeuvres ranging from takeoffs and landings to exotic acrobatics. In total, we shall see eight manoeuvres – six in the pitch plane and one each in yaw and bank. Four of these eight will require extensive analysis before, during and after the simulation. These are the pitch plane manoeuvres which are part and parcel of every flight, and must be executed proficiently to maximize safety. The other four manoeuvres – the specialized ones and the non-pitch plane ones – will be little treats which we can enjoy without having to work much for them. Each manoeuvre will get its own Subdivision.

A. THE ACADEMIC FLIGHT SIMULATOR

§37 **Description of the simulator.** Flight simulators come in different shapes and sizes. Firstly there are the professional-grade simulators used for pilot training. These feature a real cockpit and electronic screens recreating the external environment; the only difference is that the controls are connected to the instruments via a mathematical blackbox instead of an actual plane. Then there are the computer games where you press A to advance throttles and R to retard them, U to pitch the nose up and D to pitch it down and so on. Probably a good number of us have played with these at some point in our lives (I myself have for sure), not made much headway in understanding how the thing works, and then lost interest. Now, I propose the academic flight simulator for us to use in this Article. As the name suggests, it is a computer game with so many game-like features stripped off as to become a computer program. It is written in the language Matlab.

The purpose of this simulator is to actually explore the connection between model and manoeuvres. The model (3B–21,22) – we recall that the pitch plane is the most realistic one – features the externally varied T and $\bar{f}_p$ which are controlled by the pilot. In the simulator, we shall vary precisely these quantities and see how the aircraft responds to such variation. In our implementation, the user enters T and $\bar{f}_p$ in short simulation cycles while the program uses those values to integrate the equations of motion and calculate the flight variables during the cycle. The integration method is fourth order Runge Kutta with a time step of 0·0001 s.

A typical screenshot of the simulator will go a long way towards explaining how it works. In the below Figure, we can see a sample simulator screen during a landing.

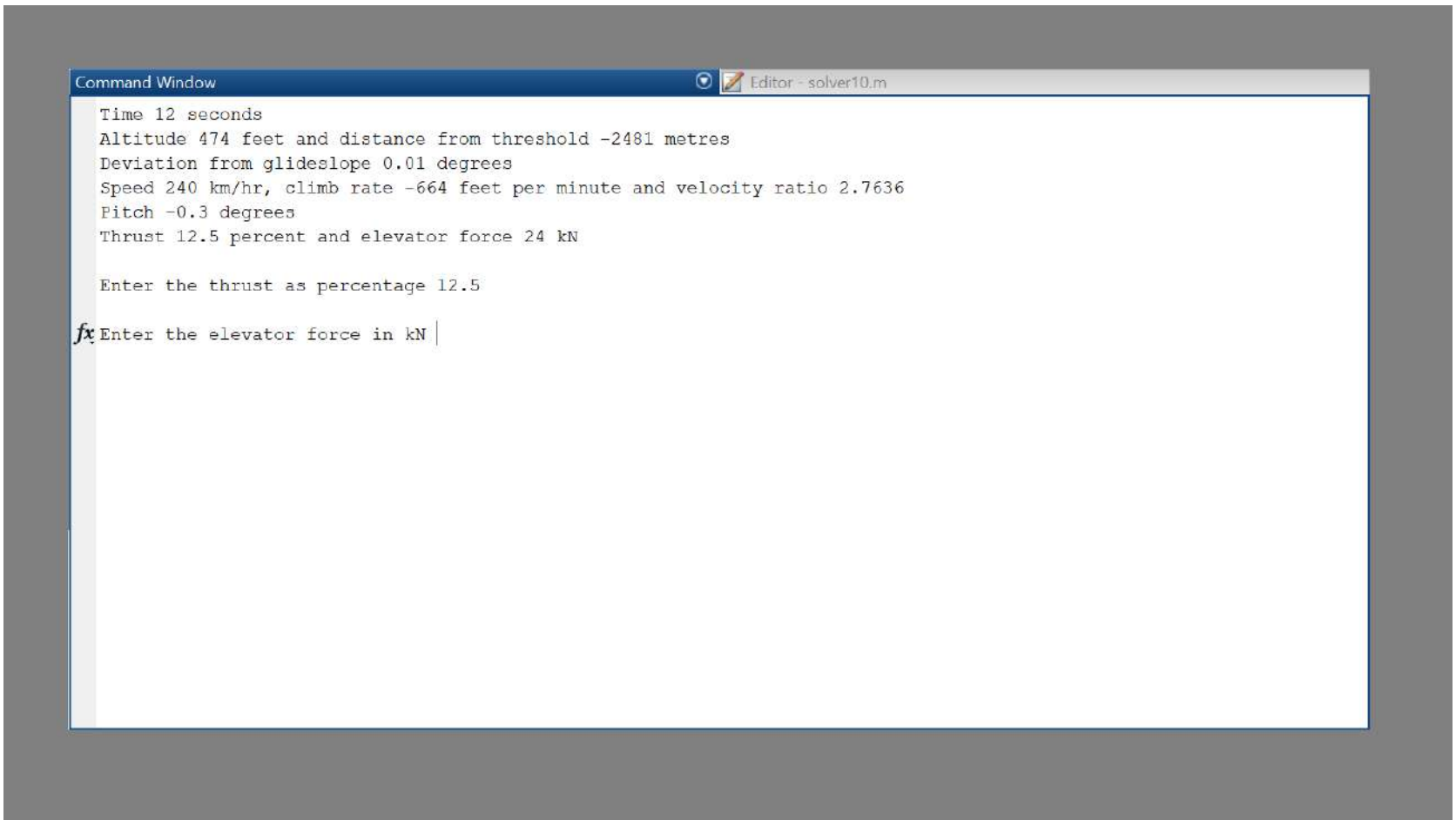


Figure 01 : *Screenshot of the academic flight simulator. Unfortunately, Matlab can't be configured to display the decimal point midline.*

We can see the 'flight instruments' displaying the relevant information – altitude, distance from the runway threshold (see §13), speed, climb rate etc. The parameters on display here are very typical of a modern passenger aircraft with a heavily electronic cockpit (velocity ratio is a new one, see §48). Note that the time refers to simulational time and not actual time – thus, the simulator has simulated 12 seconds of flight since it was started, even if the user has taken one hour to reach this point. The last line of the display information shows the values of T and $\bar{f}_p$ which the user had entered on the previous cycle. Then the simulator asks for the thrust and control force for the current cycle – in the example, the thrust has been entered as 12·5 percent while the control force has not been entered yet. Once the simulator receives the $\bar{f}_p$ input, it will use (3B–21,22) to move forward in time by one second, thus completing the current cycle. Then it will again generate the display screen and ask for T and $\bar{f}_p$. The cycle time is user-selected, so that, in situations where 1 s is too large, we can easily opt for a smaller time step. In this Article, we restrict ourselves to step sizes of 1/4 s or larger, consistent with an actual pilot's reaction time. A 1 s cycle of simulation takes approximately 0·03 seconds on a laptop computer, so the computation is one to two orders of magnitude faster than real time.

§38 **Characterization of the short period and phugoid modes.** Before releasing our simulator into the air, let's test it by plotting time traces of the short period and phugoid modes. These are with T and $\bar{f}_p$ held constant, so they show us how the simulator behaves in the absence of user input beyond the initial condition. This exercise also gives us a chance to look at some details of these modes, a topic which a typical flight dynamics course often covers in painstaking detail. With the parameters of Table 4O–01, let us focus on the equilibrium corresponding to a speed of 88 m/s (317 km/hr) at angle of elevation 0. Equation (4O–28) gives the thrust required as 1,13,530 N, the elevator force as 38,507 N and the equilibrium pitch as 0·087606 rad (we're doing calculations so all SI Units now). Linearization about this point gives the following eigenvalues and vectors :

$$\lambda_1 = -2.1614 + \text{j}0{\cdot}47249, \quad \lambda_3 = -0{\cdot}00030416 + \text{j}0{\cdot}012285 \quad , \tag{01a}$$

$$\mathbf{v}_1 = \begin{bmatrix} 0{\cdot}98363 \\ -0{\cdot}087548 - \text{j}0{\cdot}007505 \\ 0{\cdot}058969 - \text{j}0{\cdot}026874 \\ -0{\cdot}11476 + \text{j}0{\cdot}085947 \end{bmatrix}, \quad \mathbf{v}_3 = \begin{bmatrix} 1 \\ 0{\cdot}001576 - \text{j}0{\cdot}001285 \\ -0{\cdot}000417 - \text{j}0{\cdot}001270 \\ 0{\cdot}000016 - \text{j}0{\cdot}000005 \end{bmatrix} \quad , \tag{01b}$$

with λ_2 and λ_4 being the complex conjugates of λ_1 and λ_3, and the corresponding eigenvectors being conjugates also. We can see that λ_1, $\mathbf{v}_1$ correspond to short period mode while λ_3, $\mathbf{v}_3$ correspond to phugoid mode.

When a real-valued system of linear differential equations gives a pair of eigenvalues $\beta \pm \mathrm{j}\Omega$ and eigenvectors $\mathbf{u}_1 \pm \mathrm{j}\mathbf{u}_2$, then the corresponding real contributions to the general solution are

$$\mathbf{u} = \mathrm{e}^{\beta t}\left[\left(A\mathbf{u}_1 - B\mathbf{u}_2\right)\cos\Omega t - \left(B\mathbf{u}_1 + A\mathbf{u}_2\right)\sin\Omega t\right] \quad , \tag{02}$$

where A and B are arbitrary real constants. Now, from (01b) we can see that the real parts of both $\mathbf{v}_1$ and $\mathbf{v}_3$ (especially the latter) are like [1; 0; 0; 0]*. The imaginary parts on the other hand are more revealing, approximately equalling [0; 1; 4; –11] for $\mathbf{v}_1$ and [0; 1; 1; 0] for $\mathbf{v}_3$. Hence, to capture these modes, let us set off the system with initial conditions amounting to the equilibrium solution plus a perturbation proportional to the imaginary parts of the eigenvectors. This amounts to setting $A = 0$ and B non-zero in (02).

* Semicolons here separate successive entries of a column vector, just as they do in Matlab and other programming languages.

As the first test of the simulator, we plug in the initial conditions $V(0) = V^* = 88$, $\eta(0) = \eta^* = 0$, $\theta(0) = \theta^* = 0{\cdot}087606$ and $\omega(0) = \omega^* = 0$, and set T and $\bar{f}_p$ to be constant, equalling $T^* = 1{,}13{,}530$ N and $f^* = 38{,}507$ N respectively. Since these values correspond to a fixed point, V, η and θ should remain unchanged over time. When we run the simulation, their values change by less than one part in ten thousand over a 300 s duration (I am not showing this time trace). This check satisfactory, let's observe the short period behaviour by setting the initial conditions to be $V(0) = V^*$, $\eta(0) = \eta^* – 0{\cdot}01509$, $\theta(0) = \theta^* – 0{\cdot}053748$ and $\omega(0) = \omega^* + 0{\cdot}171894$. These perturbations are twice the numbers in the imaginary part of $\mathbf{v}_1$ in (01b). We also use $y(0) = 0$ and $z(0) = 300$. This is what happens over the next five seconds.

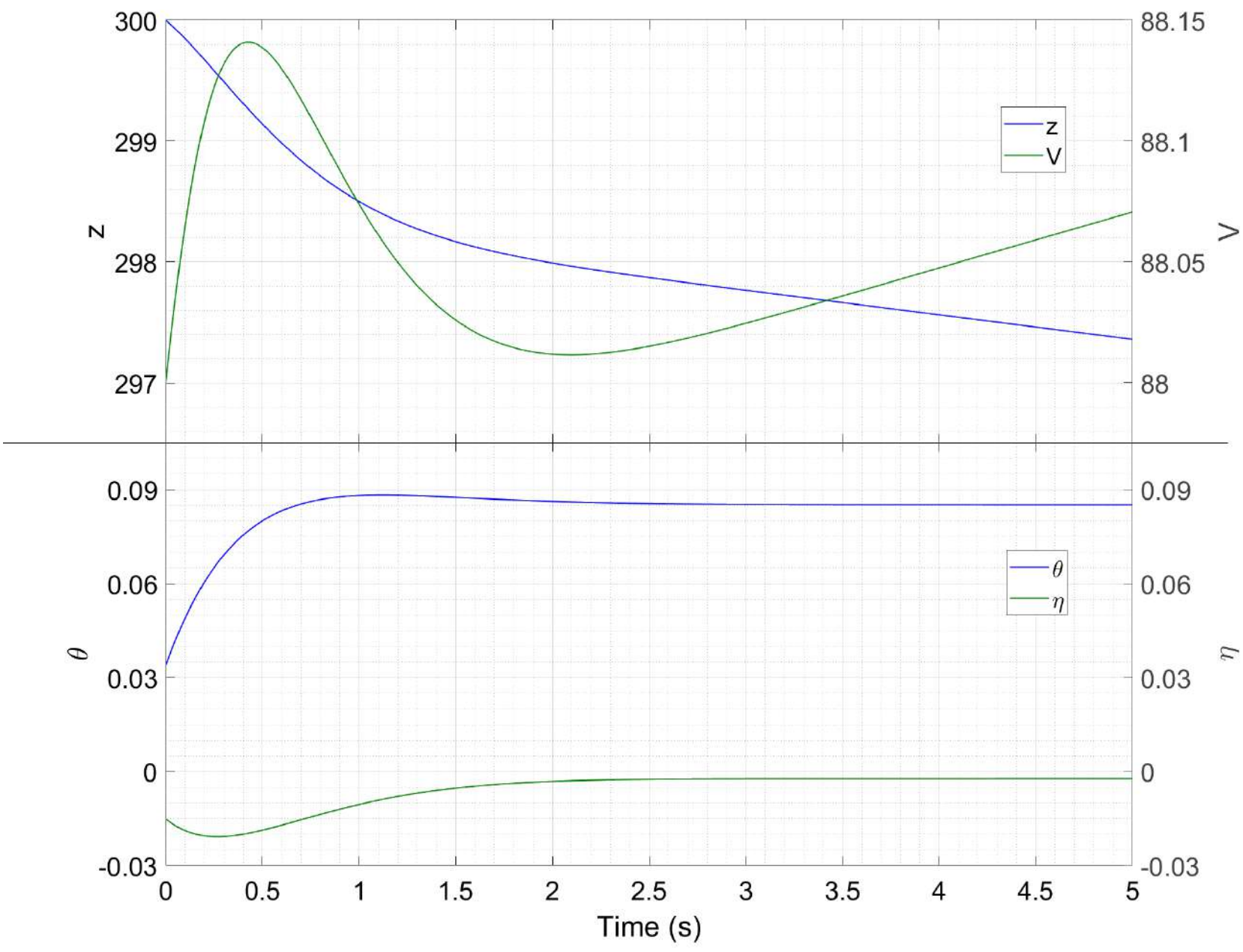


Figure 02 : *Time traces of the variables after an initial perturbation which excites the short period mode. All variables are in SI Units.*

Within a couple of seconds, the angles attain their equilibrium values. Hence, we can say that the short period mode consists primarily of the damping of pitching motions. This is plausible on account of the pitch stability we saw in §33 together with the high damping included in (3B–22f). The values attained after $t = 2$ s are slightly shifted from the original unperturbed ones, indicating that the aircraft has attained a neighbouring equilibrium instead of returning to the original one. This is not a cause for alarm because the aircraft has multiple fixed points featuring the same or almost the same value of f^*. Only a truly infinitesimal perturb-ation is guaranteed to take us back to exactly where we started.

To see phugoid in action, we now use the initial values $V(0) = V^*$, $\eta(0) = \eta^* + 0{\cdot}0038547$, $\theta(0) = \theta^* + 0{\cdot}0038091$ and $\omega(0) = \omega^*$. These perturbations are –3 times the numbers in the imaginary part of $\mathbf{v}_3$ in (01b). We also use $y(0) = 0$ and $z(0) = 300$.

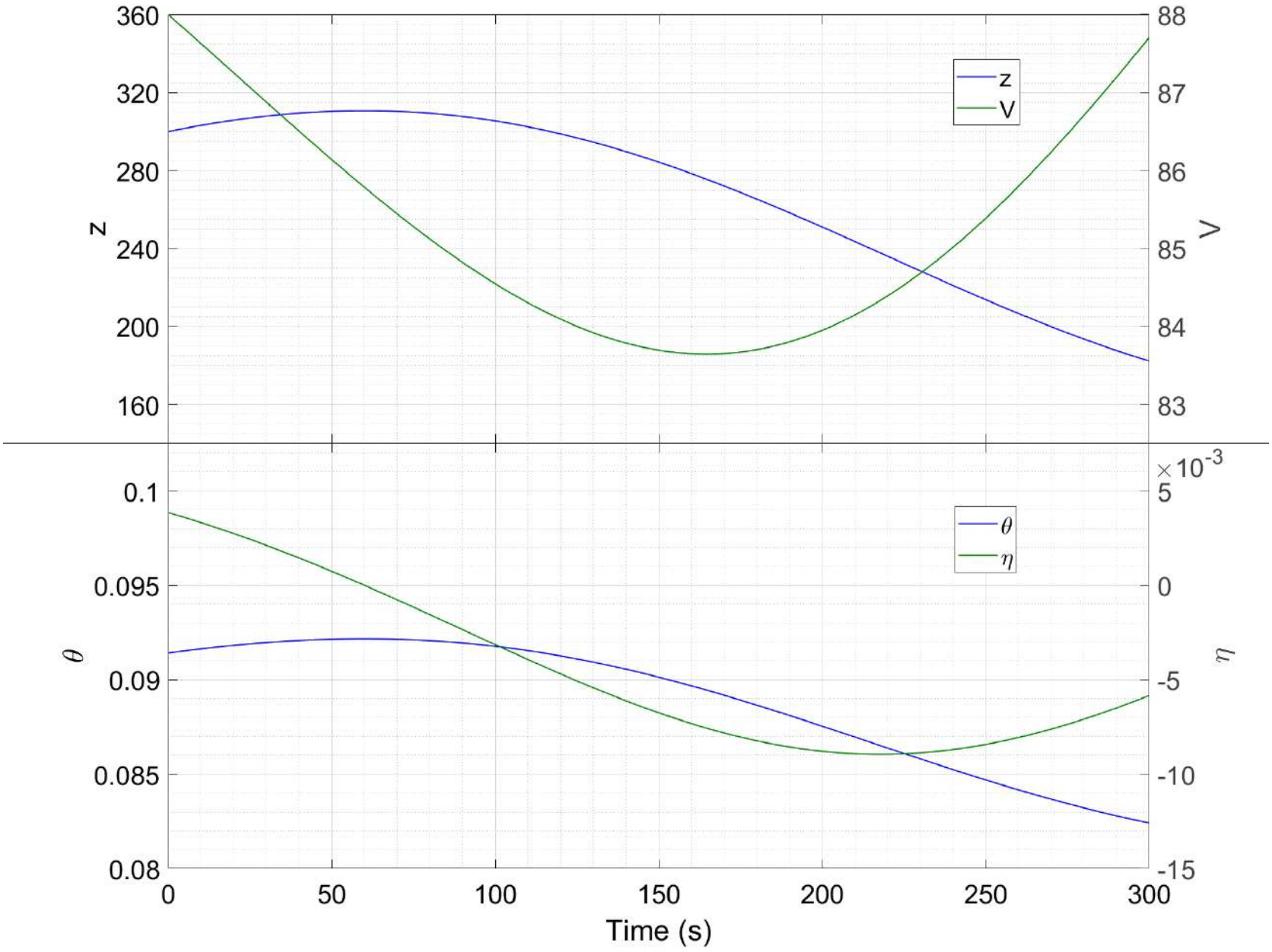


Figure 03 : *Time traces of the variables after an initial perturbation which excites the phugoid mode. All variables are in SI Units.*

This time, the angles (top panel) show an oscillatory behaviour, completing about half a period in the 300 s shown. This is consistent with the period of 511 s obtained from (01a). The speed and altitude (bottom panel) also show oscillatory behaviour, and the amplitude in the latter case is rather large. Starting at 300 m, the aircraft has descended below 200 m during the interval we can see, and is descending further. While this descent might appear scary, it is actually quite harmless. As we have already seen in §34, the long time-scale of the phugoid mode robs it of its fangs. As soon as the pilot sees the beginnings of a descent, he will raise the nose and increase power, and then the rest of the phugoid will not take place.

§39 **Structure of the following Subdivisions.** The above results have verified that the simulator produces the expected results when the pilot sits statuesque at the controls. Now we transition to the case where he is more active. In a very approximate way, we can visualize the pilot's command of the aircraft as follows. The thrust T controls the speed V [(3B–22c)], the elevator force $\bar{f}_p$ controls the pitch θ [(3B–22f)] and thence

the elevation η [(3B–22d)], the rudder force f_w controls the yaw φ [(3C–02f)], while the ailerons control the bank ψ [(3C–04f)] and thence the heading ξ [(3C–04c)]. While this picture is of course over-simplified and does not require a mathematical model to obtain, it will nevertheless serve as a good starting point in planning and executing the manoeuvres. Again, the bulk of our simulations will be in the pitch plane and will use (3B–21,22).

For each manoeuvre we shall take the following approach. First, I will state the objective of the manoeuvre. Then, we will use the model – qualitatively or quantitatively – to plan the required control inputs to the extent possible. After that I will show a simulation trace of the manoeuvre as performed by Our Plane. This trace will be a demonstration-grade execution, achieved with the aid of the initial planning and sufficient simulator practice (yes, that is necessary). After seeing the trace, we shall analyse it in detail. Finally, we will connect simulation to reality and contextualize the results in the backdrop of aviation accidents and incidents. We will also answer questions from the Quiz which are related to the particular manoeuvre at hand.

Before going on to the analyses, we have to look at two cautionary statements. First is that Our Plane is a fictitious aircraft (we've seen this before but it's important enough to warrant a repeat). Although its parameter values are plausible for a passenger airliner, they are arbitrary. These values are NOT taken from experimental results on any one particular aircraft. For this reason, the actual numerical values in our calculations and plots may not correspond to any given aircraft type or family, a fact which you should be aware of while reading and interpreting all plots. Rather, what is universal for all aircraft, model or real, is the *physics* underlying the numbers, and the *logic* of the calculations based on this physics. To take a concrete example, we shall find a takeoff-initiation speed (V_r, as we shall define it later) of about 295 km/hr for Our Plane by analysing the characteristics for the speed of best climb gradient and extrapolating backward using (3B–22e,f) to the pitching up point. Here, the figure of 295 km/hr is valid for Our Plane only – for a real aircraft it can be anywhere between 200 and 380 km/hr (Concorde had this one), depending on the aircraft design, its weight, its flap setting and other factors. What doesn't change is the procedure which leads to V_r i.e. finding the best climb speed from the characteristics and extrapolating backward from it. In everything that follows, please keep this in mind, and refrain from blindly applying numbers given here to your particular aircraft. To calculate the actual numbers for a given aircraft, we will need to use the dynamic model with the best fit parameter values for that aircraft. This however is work for a future study (see §68).

The second cautionary point is that simulator training can never substitute for actual flight training. The better the simulator, the more accurately it will capture the dynamics of a real aircraft, and the more familiar will you be with this dynamics when you actually step inside the cockpit. However, there's one aspect of real flight which even the best simulator on earth can't begin to cover. It cannot train you to overfly a set of landmarks such as power stations, rivers etc towards a destination airport. It cannot teach you to estimate your height above the ground by looking at structures and lights on it. While IFR is the mainstay of today's aviation, VFR skills are essential since even the most reliable instruments can occasionally malfunction or fail. That your plane has suddenly become unable to capture the VOR/DME waves is not an excuse for you to get lost in the sky – you have to decelerate and descend to VFR levels and take it to the nearest airport by eyesight alone. That your radio altimeter has frozen at a height of 100 ft is not an excuse to thud onto the runway at 750 fpm or float down a kilometre long – you have to know what the runway looks like when you are at the flaring height. Hence no simulator can ever replace a real aircraft. The best it can do is give dynamical insights which cannot be prised from the real thing and hence speed up the learning process and improve your skills.

And now, cabin crew, please go to your stations.

B. TAKEOFF

§40 **Description.** If one were to prepare a pie chart depicting the various phases of a typical long-haul flight by duration, one would need to zoom in five times before the takeoff would even become visible. And yet, in one of those phenomena which defy the laws of proportion, this the thousandth part of the flight burns the largest amounts of midnight oil on the part of the aircraft designers and manufacturers. Every single component from the engines to the elevators has to be built to withstand the extreme forces, torques, speeds and temperatures sustained during this one minute of a fifteen hour flight – a minute without which everything following it would not even exist.

Formulating the requirements of takeoff is easy – just get the plane in air. To model it, we shall also need to account for the dynamics of the aircraft when it is on the ground. Here, I have not gone into a detailed profiling of the undercarriage but opted for a simplistic model of the ground reactions which is physically plausible. The wheel struts of a real aircraft are like damped springs; here I have given them a natural length (height) of 3 m or 9·84 ft so that the plane CM is 3 m above ground if the plane is weightless. I have then added the normal reaction force

$$\mathbf{N}=\begin{cases}\left(-k\left(z-3\right)-C\dot{z}\right)\hat{\mathbf{z}} & \text{if } z\le 3\\ 0 & \text{otherwise}\end{cases}, \tag{01}$$

and the reaction torque

$$\boldsymbol{\tau}=\begin{cases}\left(kL(z-3)\theta-CL\omega\right)\hat{\mathbf{q}} & \text{if } z\le 3\\ 0 & \text{otherwise}\end{cases}. \tag{02}$$

The variables k and $\mathcal{C}$ are local to this paragraph, and have the values 10,00,000 and 50,000 SI Units respectively. This implies that the MTOW aircraft sits 2 m above the ground. The model (01,02) of normal reaction is grossly approximate, but then, we are not doing road vehicle dynamics here. So long as the reactions prevent a journey to the centre of the earth or a spontaneous pitch up to heaven, we will be happy. While we're on the topic of ground dynamics, let's also look at the **tail clearance**. This is the vertical gap between the tail and the ground. It is important since a pitch up, which initiates the takeoff, also brings the tail closer to the ground. If the clearance becomes zero, the tail hits the ground; this is called **tailstrike** and is highly undesirable. We define the tail clearance as

$$z_E=z-25\sin\theta \quad , \tag{03}$$

which follows from the geometry if we assume that the pitching up takes place about the CM and neglect fuselage thickness.

§41 **Planning – calculation of the V-speeds.** It's easy to say that takeoff means to get the plane in the air. Doing this with maximum safety and performance is however another matter, and requires careful planning. This begins from the characteristics. As we have already seen in §36, the clean aircraft is in reversed command upto 450 km/hr, so we need to deploy flaps. Here I have chosen the values $K_C=2250$ and $C=9$ to represent the flap configuration of takeoff – the numbers are plausible inasmuch as they feature more lift and more drag compared to the clean configuration, but are otherwise arbitrary. With these values, we now redraw the characteristics for three different climb rates – 0, 1000 and 2800 fpm.

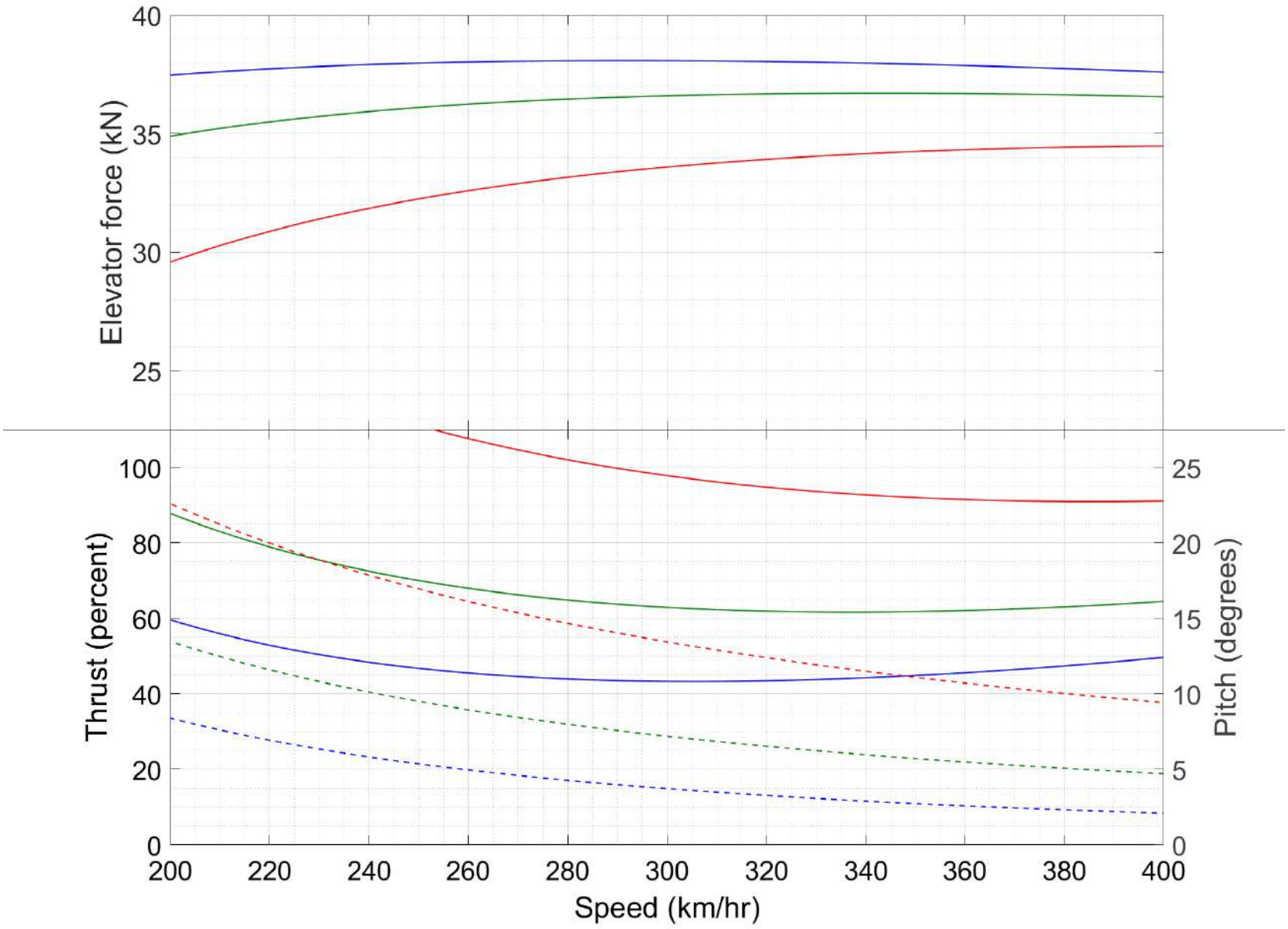


Figure 01 : *Characteristic curves for Our Plane in the takeoff flaps configuration. Solid lines attach to the left hand* y*-axis and dashed lines to the right hand* y*-axis. Blue, green and red correspond to climb rates of 0, 1000 and 2800 fpm respectively.*

The three curves here are not parallel because the same climb rate at different speeds gives different climb gradients. Hence, while the blue curve features $\eta = 0$ throughout, the green and red ones feature η's which decrease with increasing speed.

Takeoff is planned in terms of a succession of speeds which are denoted by $V_{(.....)}$ and hence together called the **V-speeds**. Much of the planning relates to the situation where one engine of a twinjet suddenly fails during the takeoff. Although this is a very rare occurrence, it is extremely serious because, unless priorly planned for, it can throw the pilots off balance during a critical flight phase and result in an accident. If an engine failure does occur during takeoff, the pilot has two choices – (*a*) *reject* the takeoff by retarding the other engine to idle or reverse, standing on the brakes and extending spoilers to full, or (*b*) *continue* the takeoff by setting the other engine to TOGA thrust (if not already there) and applying suitable control inputs. The V-speeds are the primary considerations influencing the pilot's decision to abort or proceed.

Typically, the lowest relevant V-speed is $\mathbf{V_{mcg}}$ (m : minimum, c : control, g : ground), the minimum speed at which the control surfaces can actually achieve control over the aircraft. For instance, we see from Fig. 01 that $\bar{f}_p = 38$ kN approx is required for level flight at any speed. If the elevator stall angle be 15°, then from (3B–21) and using $k_E = 150$ SI Units, we find a minimum speed of 60 km/hr at which the tail can exert such a force. The force required for pitch-up will be more than this, and will be attained at a still higher speed. V_{mcg} is actually defined not in terms of the elevator but the rudder – it is the speed at and above which the rudder alone can counteract the torque resulting from one engine failed and the other at TOGA power. If an engine failure occurs below V_{mcg}, there is no question of continuing the takeoff, and rejection is the only option. Similar to V_{mcg}, there is V_{mca} (a : air), the minimum speed at which the rudder alone can control the heading when the one-engined plane is airborne. V_{mca} is typically greater than V_{mcg}

since wheel friction assists in maintaining heading. It is not safe for an aircraft to be airborne until past V_{mca}.

The next V-speed we look at is $\mathbf{V_{mu}}$ or minimum unstick speed. If the aircraft accelerates along the runway at the maximum permitted pitch which does not cause a tailstrike, then V_{mu} is the speed at which it just separates from the ground*. To calculate V_{mu} for Our Plane, note that the undercarriage is a spring of height 3 m; immediately prior to lift-off, the weight on the spring will be zero and it will be at its unstretched length (assuming that transients in the wheel struts die out sufficiently rapidly). Then, using (03), we get zero tail clearance at a pitch of 6·89°. For level flight (blue curve), Fig. 01 features this pitch at about 220 km/hr. V_{mu} is an absolute minimum speed at which the aircraft can physically takeoff. Another physical minimum could have come from the stall speed V_s – the speed at which the angle of attack for level flight corresponds to the stalling angle for the wings. However, almost all aircraft are designed such that $V_{mu}>V_s$ [01], so that V_{mu} is the practical minimum takeoff speed – such a design is called geometric limitation. Note however that V_{mu} is by no means the speed at which you should actually plan to takeoff.

* The word "unstick", I believe, refers to the fact that the plane no longer 'sticks' to ground, and not to anything related to the control stick.

To calculate that speed we ask that, having become airborne, what is the speed at which we should intend to climb away from the airport. This initial climb, to a few hundred or one thousand feet, is usually undertaken at the takeoff thrust and made as steep as possible. In cases where a SID features a significant turn following departure, a sharp initial climb gradient eats up minimal distance along runway track in attaining the turning altitude, and thus allows a wider turn. High climb gradient also maximizes the altitude attained within the airport premises and hence minimizes the impact of noise on the surrounding communities (noise abatement). Now let's look at Fig. 01 for the speed which gives the best climb gradient at a given thrust. Recall from (3B–22c) that thrust is opposed primarily by three forces – induced drag, parasitic drag and component of gravity along the climb gradient. Since during level flight thrust balances drag alone, the blue curve of Fig. 01 tells us the sum of the two drags at different speeds. The less this sum, the more thrust we will have left over for achieving gradient. We can see that the blue curve has a minimum of 43·2 percent at 305 km/hr (the precision comes not from the graph itself but the underlying dataset). Hence, this will be the speed giving the best climb gradient. If we assume that takeoff thrust is 100 percent (i.e. 300 kN) and that all surplus thrust balances $mg\sin\eta$, then at this speed we get η of 10° for a gradient just above 17·5 percent* or 1 in 6.

* 17·5 percent in fact is an extremely steep slope – if you haven't already, try walking or biking for a few hundred metres along any slope of 10 or more percent, and you'll see what I mean.

So far, we've looked at best climb gradient in terms of performance. When one engine fails however, it acquires an even more important role in terms of safety. With a heavy, half-traction aircraft, maintaining any gradient at all is difficult, and the best-gradient speed ensures that the cripple hobbles out of the ground as fast as it can. If thrust is set to 50 percent, then the climb gradient at 305 km/hr works out to just above a measly 2 percent. At any other speed, it will be even lower since we'll be wasting unnecessary thrust to overcome drag. Hence, the speed for best climb gradient is extremely important, and is called $\mathbf{V_2}$. Note that the definition of V_2 can differ if the aircraft is lightly loaded and the single-engine performance is itself quite adequate. In such a case, V_2 is not the speed of maximum climb gradient but the minimum speed which enables a prescribed climb gradient.

For a normal takeoff (both engines functional), we would like to set the initial climb speed somewhat above V_2. This is because, if one engine fails during the climb itself, then there will automatically be a deceleration during the transition from the old mountain climb to the new molehill climb. After completing this transition (and the attendant deceleration), we want to be at or just above V_2 (there's normal command above V_2 and reversed command below it – hands up if you want reversed command in addition to a failed engine). How much retardation to incorporate here can be determined from simulation – a good rule of thumb is 5-10 knots or about 15 km/hr. Adding this margin to V_2, let's say our target initial climb speed is 320 km/hr. From Fig. 01 we can see that a climb rate of 2800 fpm at 320 km/hr requires about 95 percent thrust, so if we use full thrust, we shall have a bit left over for acceleration. This is good since we don't

want to lose speed at any time during climb – it can herald the beginnings of trouble. Note also that V_2 does not give the best climb rate (feet per minute) – the same 2800 fpm gives an acceleration reserve of 10 percent thrust at 370 km/hr. However, in most cases, it is the gradient and not the absolute rate which we want to maximize during the initial climb.

A plane speeding along the runway does not leave the ground on its own – the pilot has to pull the stick and raise the nose to generate lift and make the departure happen. Now we calculate the speed at which the nose raising should start. The pitching up motion is also called rotation, which is why the speed is called $\mathbf{V_r}$. We can see from Fig. 01 that the intended climb profile requires a pitch of about 12·5°; on the runway, pitch will be close to 0°. Let us aim to transition from the initial to the target pitch at a uniform rate. This rate should be chosen carefully – too slow will eat up runway unnecessarily while too fast can make the aircraft attain a high pitch attitude before it separates away from the ground, and result in a tailstrike. With zero lift, the MTOW aircraft sits 2 m above the ground, giving a maximum pitch of 4·6° for tailstrike – a rotation rate of 2°/s should be enough to prevent it while raising the aircraft cleanly out of the ground. This gives a total time of 6 s of pitching, at the end of which we should be at 320 km/hr. At this time, the acceleration of the aircraft will be nearly zero. At the start of rotation, the parasitic drag will be present while the induced drag will be zero due to no lift; at a speed of 300 km/hr we find an acceleration of about 8·5 km/(hr s). Assuming an average acceleration of 4 km/(hr s) during the six seconds of pitching gives us a V_r of 295 km/hr.

Given V_r, how much elevator force should we use to achieve the desired pitch rate ? This we can calculate approximately from (3B–22e,f) by using the overdamped approximation. For this, we combine (and slightly rearrange) the two into

$$\frac{\mathrm{d}^2\theta}{\mathrm{d}t^2}+\frac{\Gamma}{I}\frac{\mathrm{d}\theta}{\mathrm{d}t}=\frac{1}{I}\left\{-\frac{K_C\bar{d}_1V^2}{2}\sin 2(\theta-\eta)+\bar{f}_p\bar{d}_2\cos(\theta-\theta_E)+T\bar{h}\right\} \quad , \tag{04}$$

and then say that Γ is so large that the first term on the LHS can be neglected. Since the B-C-E aircraft is intrinsically stable in pitch*, this approximation is valid if Γ is large. Then, (04) reduces to

$$\Gamma\frac{\mathrm{d}\theta}{\mathrm{d}t}=-\frac{K_C\bar{d}_1V^2}{2}\sin 2(\theta-\eta)+\bar{f}_p\bar{d}_2\cos(\theta-\theta_E)+T\bar{h} \quad . \tag{05}$$

The RHS here is of course the torque applied on the aircraft. Now, we use the fact that $\bar{f}_p$ = 35 kN (approximately, see Fig. 01) corresponds to a torque equilibrium. Treating cos (θ–θ_E) as unity, if we apply $\bar{f}_p$ = 35+Δ kN, then the extra Δ contributes a positive torque 25Δ kNm and the steady state rotation rate generated by it is $\omega^* = 25{,}000\Delta/\Gamma$ rad/s. For the takeoff configuration, Γ = 1,92,00,000 SI Units; plugging in the values and converting the units shows that a pitch rate of 1°/s is achieved for Δ = 13·4 kN, so that 2°/s will be achieved for Δ=26·8 kN and $\bar{f}_p$ = 62 kN (approximately).

* Pitch stability is essential for the overdamped approximation to work for the following rather technical reason. In (04), if we treat θ as small and η as an externally determined quantity, then it becomes a damped driven harmonic oscillator equation for θ. The overdamped approximation gives us only the particular solution. Since the homogeneous solutions are decaying, the particular solution is dominant at all times greater than the decay time, and the approximation holds. If instead of a harmonic oscillator, we had a repeller, then also the particular solution obtained via the overdamped approximation would have been formally valid. In this case however, it would have been swamped by the exponentially growing homogeneous solutions and the replacement of the entire solution by the particular solution would have been nonsensical. Although (04) is nonlinear, the argument still holds.

There is only one significant V-speed left to reckon with, and that is $\mathbf{V_1}$, the decision speed. It is the speed on the runway below which an engine failure leads to the takeoff being rejected and above which the failure leads to the takeoff being continued on the remaining engine. Chronologically, V_1 comes between V_{mca} and V_r during the acceleration run. I won't give the details of the calculation for V_1 but will only show the reasoning involved. Let V_f be the speed at which the engine fails. Suppose V_f is 50 km/hr. Then it will obviously require far less runway to reject the takeoff and stop than to accelerate from 50 to 300-plus on one engine. Contrarily, suppose V_f is 285 km/hr. At this speed, rotation is a second away anyway, and it will surely take less runway to go ahead with it than to cancel thrust and attempt a stop. Logically, the

rejection distance increases with increase in V_f while the continuation distance decreases with increase in V_f. At some intermediate V_f, let's call it the crossover speed V_1', both options will require the same distance; this is called the **balanced field length**. The published takeoff distance for a particular aircraft type is the balanced field length corresponding to MTOW and TOGA thrust – it is substantially greater than the actual length of a typical takeoff run. For any departure, the available runway must exceed the balanced field length. Assuming that this holds true, *V_1 is the speed at which rejecting the takeoff will require the total available runway length*. If the available runway is less than the balanced field length, then V_1 does not exist – there is a range of speeds at which both rejection and continuation will require more than the available runway, and the takeoff should not be attempted at all. At the other extreme, in the limit of infinite runway, $V_1 = V_r$ since the takeoff can't be rejected after initiating rotation.

After completing the initial climb at 1000 ft, we will derate from TOGA to climb thrust, which I will take as 85 percent. We'll also ease the climb rate to 1000 fpm and focus on building speed. This is a standard procedure with most takeoffs – after attaining initial altitude, cut the power, cut climb rate to 1000 fpm and accelerate towards flap retraction velocity. This is also the phase for making the initial turn if the SID requires it. Once flaps are retracted, there is a second burst of climb to F100 (10,000 ft altitude), staying within the 465 km/hr limit (see §13) on indicated airspeed unless an exemption is authorized. This is followed by a second acceleration and a more gradual climb upto cruising altitude.

§42 **Execution.** The manoeuvre planned, we head over the simulator. The simulation equations are (3B–21,22) and the cycle time is 1 s throughout. The instrument readings displayed are altitude, speed, climb rate, pitch and tail clearance. The last one here is special to the simulator; the first four are elements of every cockpit and are what you need to focus on while executing a takeoff in practice. First is a profile view of the aircraft's trajectory during the manoeuvre, drawn to scale. At some representative points, I have also shown the plane itself, making the correct pitch at that point as determined from the simulations. To enhance clarity, the plane itself is over-large compared to the trajectory. Here, as in all subsequent simulations involving ground, I have assumed that the airport elevation is 0 ft so that altitude and height are the same.

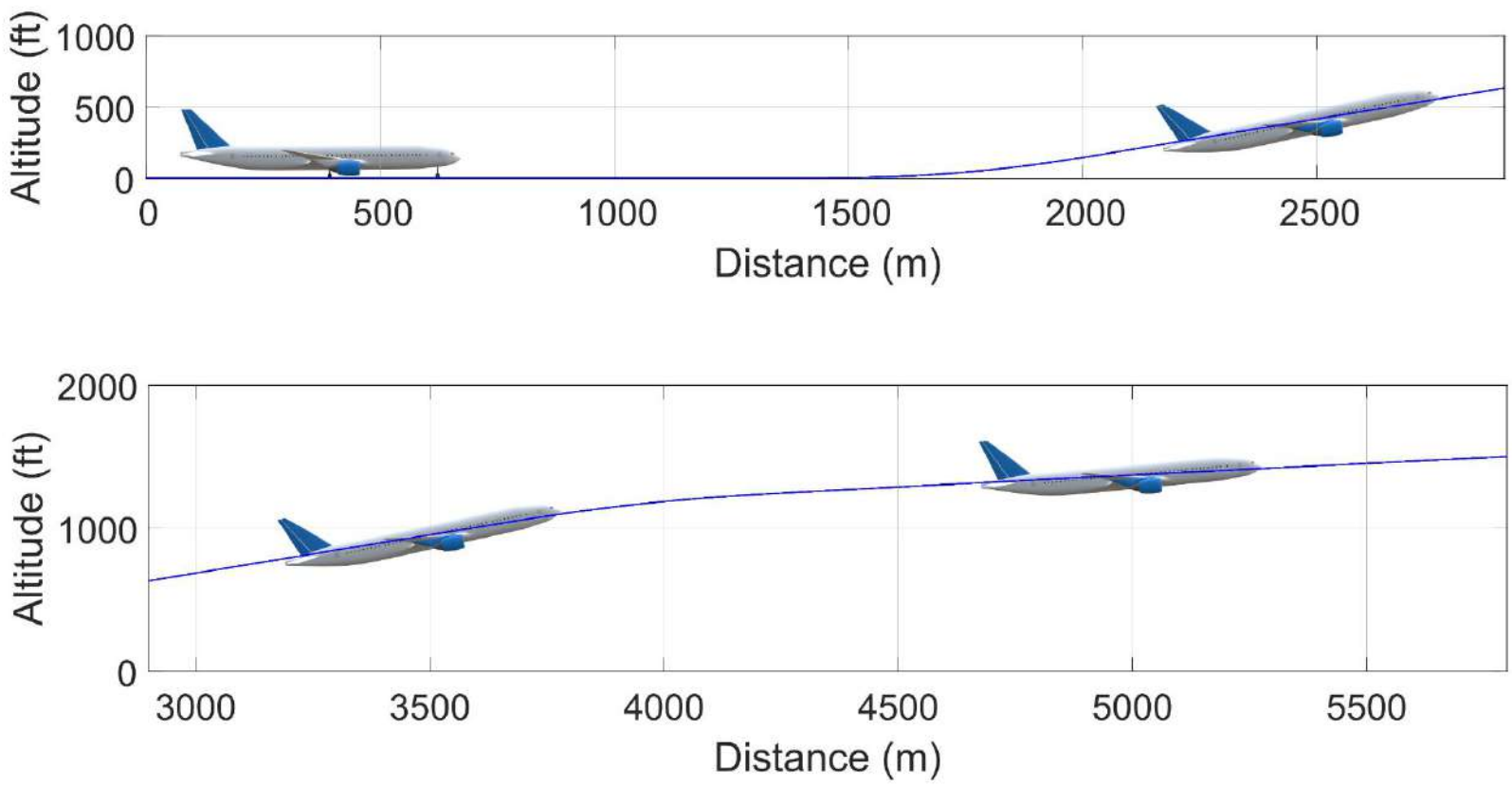


Figure 02 : *Profile of Our Plane during takeoff. The trajectory is to scale and the pitch is correct, so that the picture gives you as good an idea as possible of what things look like during an actual takeoff. The plane itself is over-large as it would otherwise look like a bee and diminish rather than enhance the total effect. The bottom panel continues on from the top. In this instance I have split the overall profile into two rows so as to prevent the ground run, steep climb and shallow climb from being compressed into a single 10:1 aspect ratio plot. Note the retraction of undercarriage between the first and second snapshots.*

We can see that the plane starts climbing at about 1·7 km distance, and the altitude of 1000 ft comes up at a distance of about 3600 m. Now, this distance is measured from the base of the runway. In a large airport, 3600 m from the base is still over the runway, so the aircraft is past 1000 ft when it crosses the airport perimeter. This is good for noise abatement.

Next comes the all-important time traces of the thrust, the elevator force and the various flight variables.

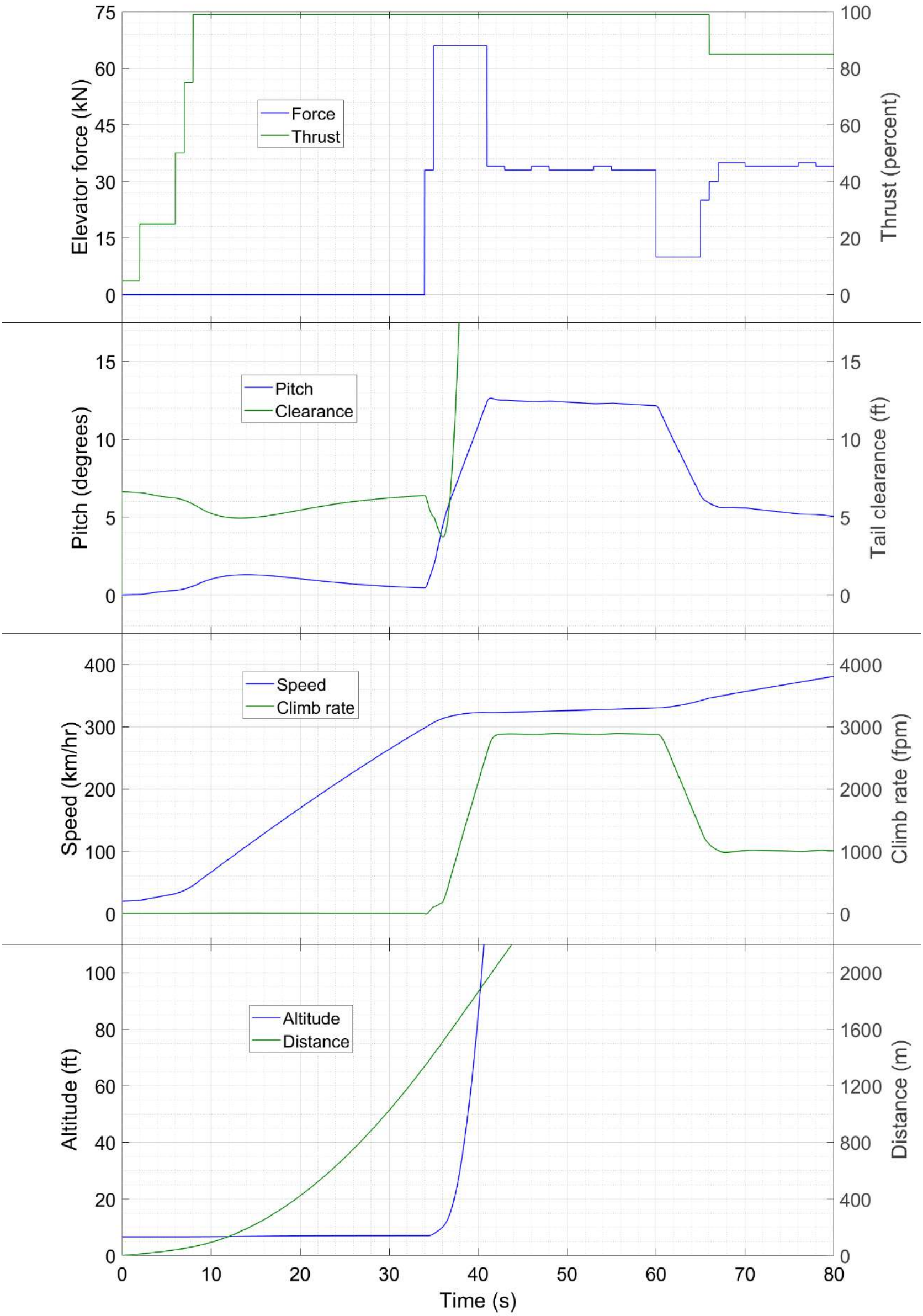


Figure 03 : *Time traces of different variables during the takeoff.*

In Fig. 03, we have started at 5 percent thrust (top panel), which we assume corresponds to ground idle, and 20 km/hr (third panel). This indicates a rolling takeoff, in which the pilot brings the plane onto the runway from the taxiway, aligns it with the runway centreline and proceeds with takeoff immediately. Rolling takeoff usually occurs when the clearance is received prior to runway entry. It is an essential skill to learn since at busy airports, a clearance for line up and takeoff means that you have to get out right now and not waste time on the runway. The next aircraft to use the runway might well be a lander, way down on the final approach – as we'll see in Subdivision 5D, delaying an approach by even one second is impossible. So if you drag your takeoff and hold up the runway, the lander will be forced to go-around and your clearance will likely be rescinded. The takeoff is not rolling when the departing aircraft is permitted to access the runway but not yet to actually fly. In this case, the aircraft enters the runway, aligns with centreline and halts, releasing brakes and taking off after getting the necessary clearance.

To begin the takeoff, we have used 25 percent thrust for 4 seconds before escalating to TOGA (99 percent). While this step is not necessary in a simulation, it is absolutely essential in reality. If you haven't already, pay attention to this the next time you fly as a passenger – at the beginning of the takeoff run, the hitherto mumbling jets will crescendo to a whine, hold the whine for a couple of seconds and only then explode into a roar* while you get pinned to the seat back. This is because all modern engines and their FADEC systems are designed to take the same amount of time to accelerate from 50 percent to [insert number greater than 50] percent N1, but the time taken to accelerate from [insert number smaller than 50] percent to 50 percent N1 can vary among engines. On a two-engine aircraft if the pilot selects TOGA thrust straight from ground idle (about 20 percent N1), then it can happen (and *has* happened) that one engine has reached full thrust while the other is still at close to zero thrust; the resulting thrust differential can steer the plane out of the runway. To prevent this, the pilot advances throttles to 50 percent N1, verifies that both engines have identical N1 and only then selects the takeoff power.

* Although, engines which cannot roar even at full power seem to be the fashion nowadays.

Here we have chosen takeoff power to be 99 percent thrust. This is appropriate since our model aircraft is at MTOW. In such cases, thrusts near or equal to TOGA are indeed used for departures. When the aircraft is lighter, for example on a short-range flight, a reduced or **derated** thrust is used for the takeoff since that is more beneficial for the engines. In many cases, takeoffs appear to be long (say 40-plus seconds of ground run on a narrow-body) only because the pilot has used a heavy derate and not because the aircraft is fully loaded and struggling to get off the ground. The derate is calculated beforehand by the onboard computers after factoring in the weight, the weather conditions, the available runway length etc. On an Airbus, the derated takeoff level is called flex thrust, and is selected by advancing the throttles to the flex/max* detent (notch), one step short of the TOGA detent. On a Boeing, derated thrust is selected by engaging the autothrottle after advancing both engines to 50 percent N1. In both cases, manually advancing the thrust levers enables a transition from derated to TOGA thrust at any time, should the need arise.

* The "max" in flex/max refers to the maximum continuous thrust which the engines can output, as against the TOGA thrust which can be used for upto five minutes.

As the plane accelerates on the ground, we can see (second panel) an increase and then a decrease of the pitch within a small range (about 1°). The increase happens because the thrust has a positive torque about the CM, and the assumed reaction torque (02) balances it at about 1° or so. The subsequent decrease is because the wings start generating lift as a result of this pitch up and wings tend to reduce pitch in a B-C-E plane. I am not sure as to how realistic or not this part of the dynamics is – as long as it doesn't cause spontaneous lift off, I don't really care. At 298 km/hr* I have initiated rotation (top panel) using $\bar{f}_p$ = 66 kN; to make it realistic, I have reached that level from zero in two seconds instead of one. After applying the peak $\bar{f}_p$, the plane takes about 6 s to pitch up from 2° to 12·5°, at which point I have dropped straight to the equilibrium $\bar{f}_p$ of 34 kN. The climb rate at this instant is 2880 fpm and the speed is 322 km/hr (third panel). Alternating $\bar{f}_p$ between 33 and 34 kN keeps the climb rate steady; the speed increases very slowly throughout the climb. All this is in good agreement with our calculations; the

* The closest to the planned value of 295 km/hr that we come in any simulation cycle.

force required to achieve unit pitch rate has turned out to be slightly higher, V_2–V_r and pitch at start of climb are exactly as calculated and the initial climb gradient of 16·2 percent with marginal acceleration reserve is also what we expected. The tail, 6 ft above the ground prior to rotation (second panel), dips to just below 4 ft as the plane pitches up on the runway before the rapid climb sends it skywards and the clearance becomes irrelevant. The undercarriage, not included in our simulation, is retracted as soon as the aircraft starts climbing, usually when it is still only a few feet above ground. When the aircraft separates from ground ($t = 37$ s), it has been less than 30 s since the start of TOGA thrust – even though it takes about 20 minutes to attain the cruising speed of 900 km/hr, the first third of it comes up in just half a minute on the ground itself. The full climb rate is established at $t = 42$ s, by which time the aircraft is more than 100 ft above ground. 1000 fpm on the other hand occurs at about 30 ft above ground (bottom panel). Formally as per ICAO definitions, an aircraft is considered airborne only after clearing the altitude of 35 ft and not as soon as the wheels leave ground – this definition allows for the aircraft to attain a reasonable climb gradient. We can see a horizontal distance of 1400 m at the start of rotation and 1700 m at altitude 30 ft – the action of leaving ground itself uses a surprisingly large amount of runway.

After reaching 1000 feet altitude, a reduction in elevator force sees a reduction in pitch and hence in climb rate. Approaching the desired 1000 fpm, I have derated to climb thrust of 85 percent and adjusted $\bar{f}_p$ to ensure that the climb rate is maintained. The average $\bar{f}_p$ during this time is about 34·5 kN, slightly less than the equilibrium values in Fig. 01. This is because constant climb rate at increasing speed is not a steady state flight condition – as we can see, the pitch is decreasing steadily during the acceleration, consistent with an elevator force below the steady state value. Flap retraction is something I haven't shown explicitly, but we have already seen one criterion for determining the retraction speeds in §36. Another criterion can be to make a transition whenever the thrust required for level flight (or 1000 fpm climb) at the current flap setting becomes equal to that at the next lower setting.

§43 **Further discussion, accidents and incidents.** Our simulations automatically tell us the most important items of the **takeoff checklist** – the one you run a couple of minutes prior to the takeoff. Firstly, the *flap setting* must be correct. Secondly, the *speeds* V_1, V_r and V_2 must be known to both pilots and their values must be plausible. Thirdly, assuming that the horizontal stabilizer and elevator are separate, the *stabilizer trim* must be correct. We most certainly don't want the aircraft to start pitching up on its own during the takeoff run; at the same time, the force exerted by the elevator alone (separate from the stabilizer) during rotation must not be excessive. Finally, the *thrust derate* calculated by the computer must be plausible also. During takeoff, the pilot monitoring makes callouts to help the pilot flying. The first is "takeoff thrust set" when the engines stabilize at the desired N1. The next is "100 knots" (for some airlines, 80 or 90 knots) when the plane attains this speed. This is approximately V_{mcg}. The third is "V_1" (pronounced "vee one" and not "Victor one") when this is attained. At this point, pilot flying makes a physical and mental transition from rejection to continuation mode. Physically, he shifts his hands from the throttles (ready to retard to idle) to the stick (ready to pull back), and mentally he becomes prepared for a takeoff senza one engine. Then is "rotate" for attainment of V_r, whereupon the pilot starts pulling the stick. After that is "positive rate of climb" which means what it looks like will mean. Right after is "wheels up", at which point, the pilot monitoring retracts the undercarriage (the pilot flying has his hands on the stick).

Qualitative arguments can give us some features of the V-speeds. Firstly, they all increase as the mass of the plane increases – since lift balances weight and is proportional to square of speed, we can say that $V_{(...)} \sim \sqrt{m}$. Figure 03 shows that the acceleration during the bulk of the run is quite close to uniform. If we treat it to be perfectly uniform, then the takeoff distance is $S = V^2/2a$ (V here will be approximately V_r). If thrust deration is used to achieve a constant acceleration irrespective of the weight of the plane, then $S \sim m$. If on the other hand, TOGA thrust is used for all weights, then $a \sim 1/m$ and $S \sim m^2$.

Further factors influencing the takeoff distance and speed are the atmospheric conditions. Recall that K_C depends on the density of air; if the airport is at a high altitude, K_C will be less and higher speed will be required to achieve the same lift. If the weather is hot, then also air density and K_C will be lower. For this reason, airports located in hot regions or at altitude tend to have longer runways than those in colder

regions near sea level. If an airport is both hot and high, then its runway/s might be especially long. For example, Denver, located at 5400 ft above MSL and having maximum temperatures in the mid-thirties ^{o}C, has the longest runway in USA (and the longest of any major airport in the world) at 4877 m. Heat also degrades the performance of the engines, resulting in increased takeoff distance and long runways in hotter countries such as the Middle East and India.

The simulations treat the case of no wind since (3B–22) is valid only in that condition [wind is modelled by (3B–29)]. If there is a wind, then the lift gets determined by the airspeed rather than ground speed. Hence, the aircraft lifts off from ground at a constant airspeed, which is about 310 km/hr in Fig. 03. Rotation must also be initiated at a given airspeed, 298 km/hr in our case. The takeoff distance on the other hand is determined by ground speed, how fast you are eating up runway. The less the ground speed, the shorter the run. Airspeed is greater than ground speed if there is a headwind while airspeed is less than ground speed if there is a tailwind. For this reason, *a headwind decreases the takeoff length while a tailwind increases it*. Transport aircraft try to takeoff into the headwind whenever possible. Similar considerations apply to landing – headwind gives a slower ground speed during approach and a smaller runway length. This is good since takeoffs and landings (at least at busy airports) are always parallel, to ensure a smooth traffic flow near the airport, and maximize safety. Note that the wind preferences for takeoff and landing are the reverse of those for cruise. For cruise, aircraft are optimized for a given airspeed; tailwinds add to the ground speed and finish the flight faster, so they are desirable. For ground ops however, we want the lowest possible ground speed, so headwinds are desirable.

There are two approximations in our simulation which I must mention. The first is that the retraction of undercarriage has not been demonstrated explicitly. Since the characteristics of Fig. 01 are for the aircraft with undercarriage retracted, and since those parameter values have been used throughout the ground run as well, there is a tacit assumption that this phase also takes place with undercarriage retracted. The second is that our simulation ignores **ground effect**. This refers to the reduction of induced drag on the wing when it operates close to the ground. Ground effect diminishes rapidly as the aircraft becomes airborne and goes to zero by the time it is at an altitude of 100 ft or so. Neither of these assumptions changes the simulation results in any way except for numerical detail.

It is also interesting to note that the response to stick input of an aircraft with a stabilator (like Our Plane) is perhaps more intuitive than that of one with a trimmable horizontal stabilizer. In §33 we have seen that the stabilator plane achieves equilibrium at a particular $\bar{f}_p$ while the dual-tail plane achieves equilibrium at a particular speed. In Fig. 03, maintaining constant or almost constant $\bar{f}_p$ during the acceleration to flap retraction gave us constant climb rate over a considerable range of speed. To achieve the accelerating climb in a conventional airliner, it would have required constant adjustment of the trim wheel as well. In the Subdivision 5D, while analysing the landing, we will get a fuller picture of the difference between our one-piece and a conventional two-piece tail. Just for the record, the phugoidal eigenvalues turn out to be a small positive and negative real pair for the initial climb, and very lightly damped long period oscillations for the second climb. We didn't worry about them during planning and execution, and lost nothing.

Now is a good time to answer a few of the Quiz questions. For Q19, the overdamped approximation tells us that the pitch rate is proportional to the elevator force applied over and above the trim. The simulation results also show this relation to hold true. Hence the correct answer is Choice B. Note that for this question, the assumption of aircraft like a passenger airliner is relevant, since it is B-C-E and has a lot of damping. If the aircraft were a C-B-E one, then the correct option would have been Choice D, increasing pitch rate while the elevator force is held constant. Q03 asks for the takeoff and landing runway given the wind. The wind is from South-East i.e. it is coming from approximately 135^{o} direction. By definition, Runway 13 has an approximately 130^{o} orientation while Runway 31 has an approximately 310^{o} orientation*. A wind from 135^{o} is a headwind for a Runway 13 and a tailwind for Runway 31. Since both takeoffs and landings are into headwind, the correct runway allocation will be 13L for arrivals and 13R for departures, which is

* For KJFK, we saw in §14 that the 13–31 runways have the orientations of 134^{o}/314^{o}. The exact numbers are not necessary to solve the question however.

Choice A. Q08 deals with takeoff from a dry vis-a-vis wet runway. If the runway is slippery, then the performance of a normal takeoff is almost unaffected since ground friction is a negligible force during acceleration. However, the performance of a rejected takeoff will be severely affected because the stopping distance is highly dependent on the wheel braking performance, and the rain will cause it to degrade. To maximize the available runway for the rejected takeoff, we would like to make the normal takeoff as short as possible, which will be achieved by selecting a higher thrust rating. Choice D is the only one which expresses this.

Q11 deals with a mistaken flap setting – the actual is lower than calculated. Lower flaps means higher speed to generate the same lift, so V_{mu}, V_r and V_2 will all go up (recall from Fig. 4O–04 that V_2 – the minima of drag – for our clean model aircraft is 440 km/hr). In fact, attaining the new V_2 might well require more than the available runway length, so V_2 as a reference has to be scrapped. Having botched the flap and realized the mistake late, the safest procedure will be to rotate slowly towards the tailstrike pitch when the end of the runway is close, and hope that V_{mu} has been crossed and the aircraft lifts off. The initial climb gradient for such a departure should be lower than planned. It is a safe assumption that the new climb will occur at much below the new V_2, and this can support only a shallower gradient. These two options are expressed by Choice C. Q17 features the pilot mistakenly using a shorter runway. The rotation speed V_r comes by backtracking from V_2, which depends on the aircraft characteristics alone and not on runway length. So it will remain constant. On the other hand, V_1 depends on the runway length – the longer the runway, the higher it will be. Hence, with a shorter runway V_1 will decrease while V_r remains same, which is Choice B. The explicit specification of $V_r < V_1$ for the full runway rules out the marginal case where the full-length as well as the intersection departure have so much runway that $V_1 = V_r$ for both, in which eventuality Choice D would have been the correct answer.

Now let's come to a few accidents and incidents involving takeoff. As a preliminary comment, let me mention that I have taken all accident and incident information, not just in this Subdivision but anywhere in the Article, from the following sources : news media for qualitative descriptions, Wikipedia [02], Skybrary [03] and Aviation Herald [04] for summary technical information, and the interim and/or final reports released by the relevant investigative agency for detailed technical information and analysis. In addition, Flightradar24 [05] provides high quality, publicly available (paid subscription required) data of speed, altitude etc time traces as obtained from ground for all flights including incident or accident flights; tracking normal flights on that website can be also be a fun pastime. I shall not be citing these sources explicitly every time I discuss a historical aviation occurrence.

Incidents due to pilot error during takeoff are usually the result of mismatch between the parameters entered into the flight computer and the reality. On 20 March 2009, Emirates Flight 407, an Airbus A340-500 departing Melbourne (Australia) headed for Dubai (UAE) made a tailstrike and impacted multiple ground structures during departure. The incident occurred because the pilots had incorrectly inputted the weight of the aircraft as 263 tons instead of the 363 which it actually was – *OOPS*. This resulted in gross underestimates of V_1, V_r and V_2 as well as a substantial deration of thrust. Not recognizing the calculated values as garbage, the pilots initiated rotation at the specified V_r and hit the tail on the runway. Thereafter advancing to TOGA thrust and accelerating, they made a second, successful attempt to leave the ground but this time they ran out of runway, became airborne from grass and hit some ILS antennae and approach lights on the way out. Luck alone ensured that the thing remained only an incident. On 15 September 2015, Qatar Airways Flight 778, a Boeing 777-300ER from Miami (USA) to Doha (Qatar), struck the lights beyond the end of the runway due to excessively low altitude following liftoff. The error occurred because the pilots opted for takeoff from an intersection instead of using the full runway length, as had been programmed into the computers (the phenomenon of Quiz Q17). Not only was the available runway (2610 m) less than the balanced field for the fully laden aircraft but the computer also implemented a thrust derate which failed to get the aircraft airborne and on climb gradient before the reduced runway ran out. A similar incident though without impaction of ground structures occurred with Jet Airways Flight 117 on 30 August 2016. The aircraft, a Boeing 777-300ER from London Heathrow (UK) to Mumbai (India), had been programmed for full-length departure from Runway 27L at Heathrow with available length 3658 m, but the pilots actually initiated takeoff from an intersection featuring 2589 m only. A heavy derate of thrust

was employed (92 percent N1 against a TOGA rating of 110 percent) leading to late attainment of climb gradient following airborne and unusually low altitude while crossing the airport perimeter. The best way of preventing incidents like this is for the pilot monitoring to have a good feel for what kind of thrust level is suitable for which departure (of course there's the option of not making the data entry error in the first place but that's the trivial solution). If the engine-selected takeoff N1 seems low, or the acceleration seems too slow, then instead of mechanically calling out "takeoff thrust set", you should yell for TOGA thrust or yourself advance the levers and maximize the safety of the departure even if it puts increased load on the engines.

Instances of engine failure right during takeoff are rare but not without precedent. On 07 June 2016, Biman Bangladesh Flight 49, a Boeing 777-300ER from Dhaka (Bangladesh) to Dammam (Saudi Arabia) experienced a failure of its no. 2 engine at 275 km/hr on the ground. This was just prior to V_1 and the pilots correctly brought the aircraft to a stop on the runway. A similar phenomenon, though at a lower speed, occurred on 27 May 2016 with Korean Air Flight 2708, a Boeing 777-300 (not ER) from Tokyo (Japan) to Seoul (South Korea). On the other hand, on 13 June 1996, Garuda Indonesia Flight 865, a McDonnell Douglas DC10 from Fukuoka (Japan) to Jakarta (Indonesia) erroneously attempted to reject takeoff after failure of the no. 3 engine (starboard – no. 2 is on the tail) between V_r and V_2, when the aircraft was at a high pitch and 9 ft clear of ground. Returning to the runway but speeding uncontrollably, the aircraft crashed through the perimeter wall of the airport and burst into flames, killing three passengers and injuring more than half of the remaining passengers and crew. Another post-continuation engine failure incident occurred as I write this. On 27 February 2023, SpiceJet (SEJ) Flight 83, a Boeing 737-800 from Kolkata (India) to Bangkok (Thailand), experienced a failure of the no. 1 engine somewhere between ground and 200 ft of altitude* – from 310 km/hr at liftoff, it decelerated to an equilibrium climb at 296 km/hr (presumably V_2) and 1000 fpm, declared Mayday, levelled off at 1900 ft and returned to Kolkata for an overweight landing at high speed (325 km/hr). The flight profile shows a clean response to the failure and a stable final approach (more in Subdivision 5D), indicating good airmanship by the pilots.

* The precise instant at which the failure occurred is not released to the public yet. This and all other comments regarding SEJ 083 incident are my own interpretations of Flightradar24 data.

It is important to note however that V_1 etc are defined specifically with respect to engine failure, and not just any technical fault – an angle of attack indicator failure might not require aborting the flight at all while a cabin/cargo hold fire or a loss of control surfaces might make rejection the safest option at any speed, even if the plane overshoots the runway. Such a choice had to be made by the crew of Ameristar Charters Flight 9363 on 08 March 2017. The McDonnell Douglas MD-83, scheduled to fly from Ypsilanti (USA) to Washington DC (USA), experienced a jam of its elevator which the pilots found out when trying to rotate on the runway. Despite maximum force on the stick, the nose did not rise. The takeoff was then rejected forthwith, at 55 km/hr above V_1; although the aircraft could not stop within the runway, it came to rest at the periphery of the airport. There was only one minor injury.

A full simulation of a takeoff with engine failure after V_2 will be as interesting as it will be instructive. For that however, we shall have to wait for the 3-dimensional sequel to this Article since staying on course with the asymmetric thrust will require simultaneous management of pitch, yaw and bank. Meanwhile, takeoff is optional but landing is compulsory, so let's shift our focus to that phase of the flight. Before taking it on though, let's eat a bonbon. The upcoming manoeuvre is not only quick to analyse, but it also features pitching up and nothing else.

C. IMMELMANN TURN

§44 **Immelmann turn.** This is a spectacular manoeuvre performed by aircraft at airshows*. This manoeuvre is shown in the below Figure – it consists of a 180° vertical loop from straight flight at the original heading to inverted flight on the reciprocal

* Also in combat. It was invented by the German World War I era fighter pilot MAX IMMELMANN in this regrettable context.

heading, followed by a 180º bank to nullify the inversion. The objective of the manoeuvre is to achieve a rapid climb and reversal of direction. Here we shall analyse only the half-loop part of the manoeuvre as that takes place in the pitch plane alone.

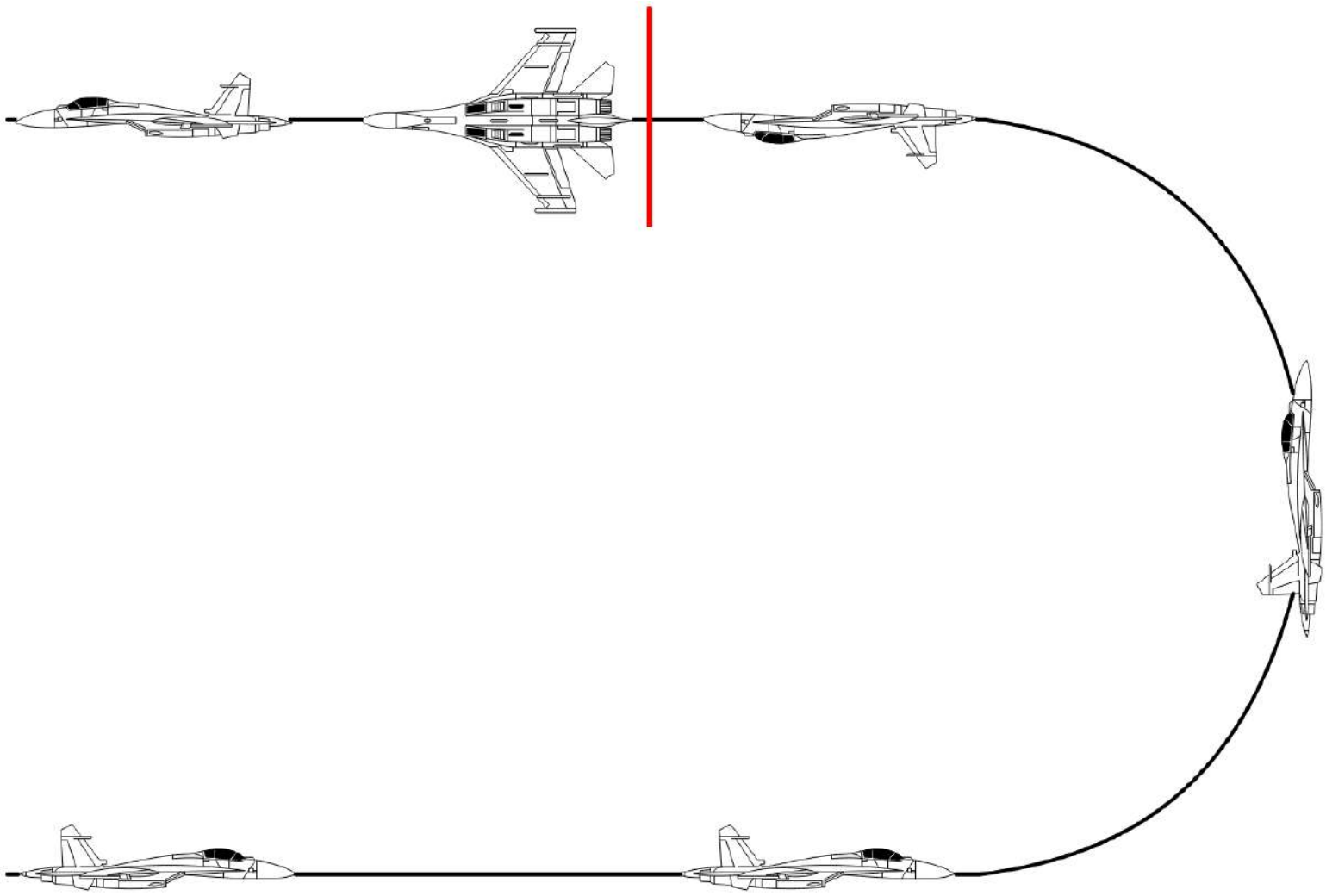


Figure 01 : *Schematic of an aircraft performing an Immelmann turn. The image [01] carries the appropriate permissions for this usage. The red line is where we will cut the manoeuvre off, to remain within the constraints of our model.*

I am a big fan of the Immelmann turn because (*a*) it shows the versatility of our model, and (*b*) unlike takeoff and landing, it is trivial to execute on a computer.

To pull an Immelmann turn, we need to command maximum $\bar{f}_p$ so as to pitch up as fast as possible. For our model plane, let this maximum be 100 kN. Throughout the manoeuvre, the angle of attack remains small, so the elevator points approximately along the direction of travel and a positive $\bar{f}_p$ gives counterclockwise pitch rate. When the plane is inverted, the lift required to balance gravity must be negative (relative to the plane's q,d,o axes) and so the angle of attack must be negative also. Here I will transition from positive to negative angle of attack when the plane is close to inverted. Let the plane mass be 80 tons, initial altitude be 1000 ft and initial speed 600 km/hr. A climb against gravity will require as much thrust as possible to minimize the loss of speed, so I will keep the throttles set to 99 percent throughout.

And that's all there is to the manoeuvre. Here's Our Plane doing it instead of Wikipedia's plane.

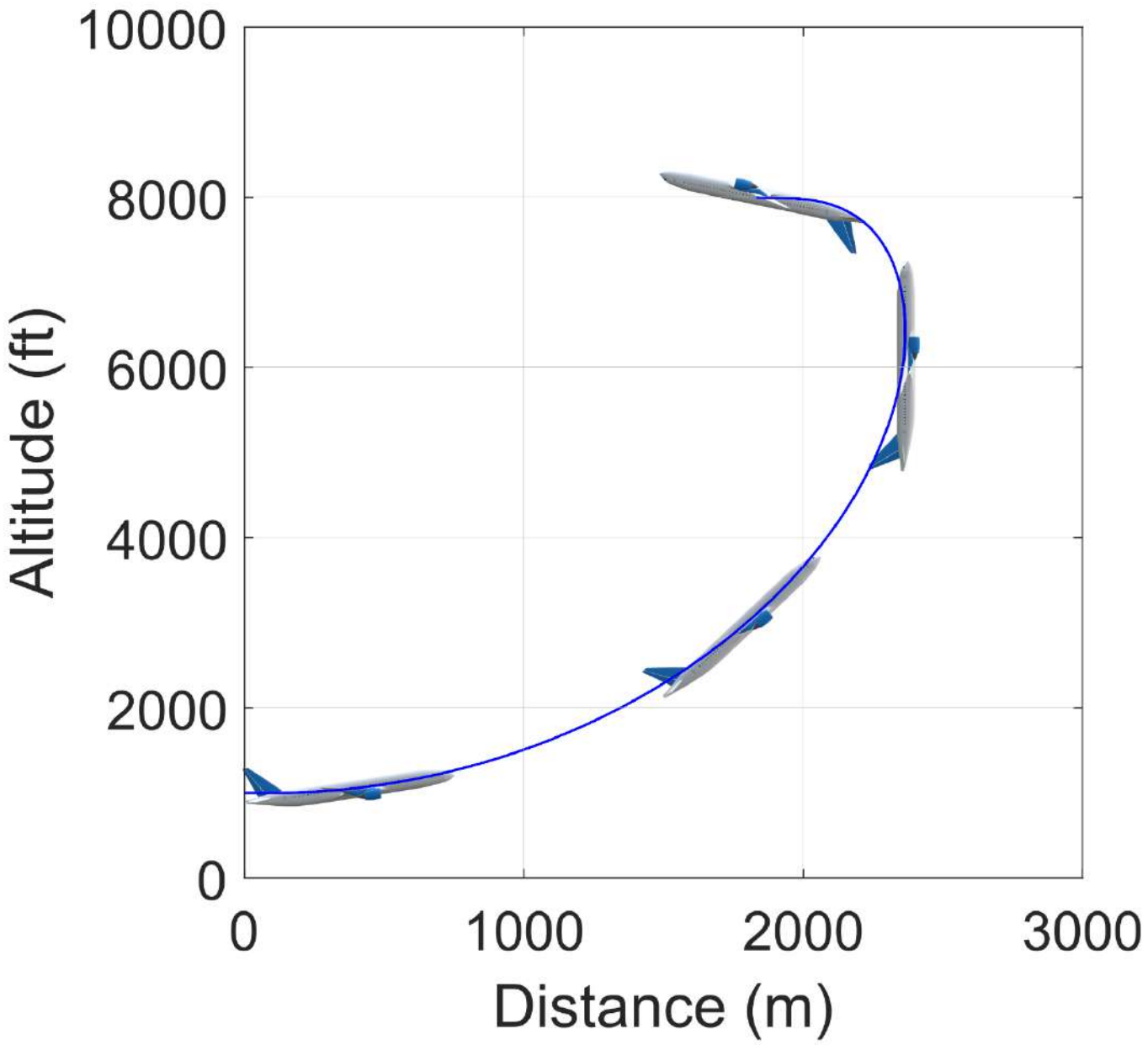


Figure 02 : *Profile of Our Plane during the Immelmann manoeuvre. The trajectory is to scale and the pitch is correct, so that the picture gives you as good an idea as possible of what things look like during an actual Immelmann turn. The plane itself is over-large as it would otherwise look like a bee and diminish rather than enhance the total effect. Note the high negative α in the last snapshot – the trajectory is almost dead horizontal but the nose is facing skywards.*

And here the most relevant flight information.

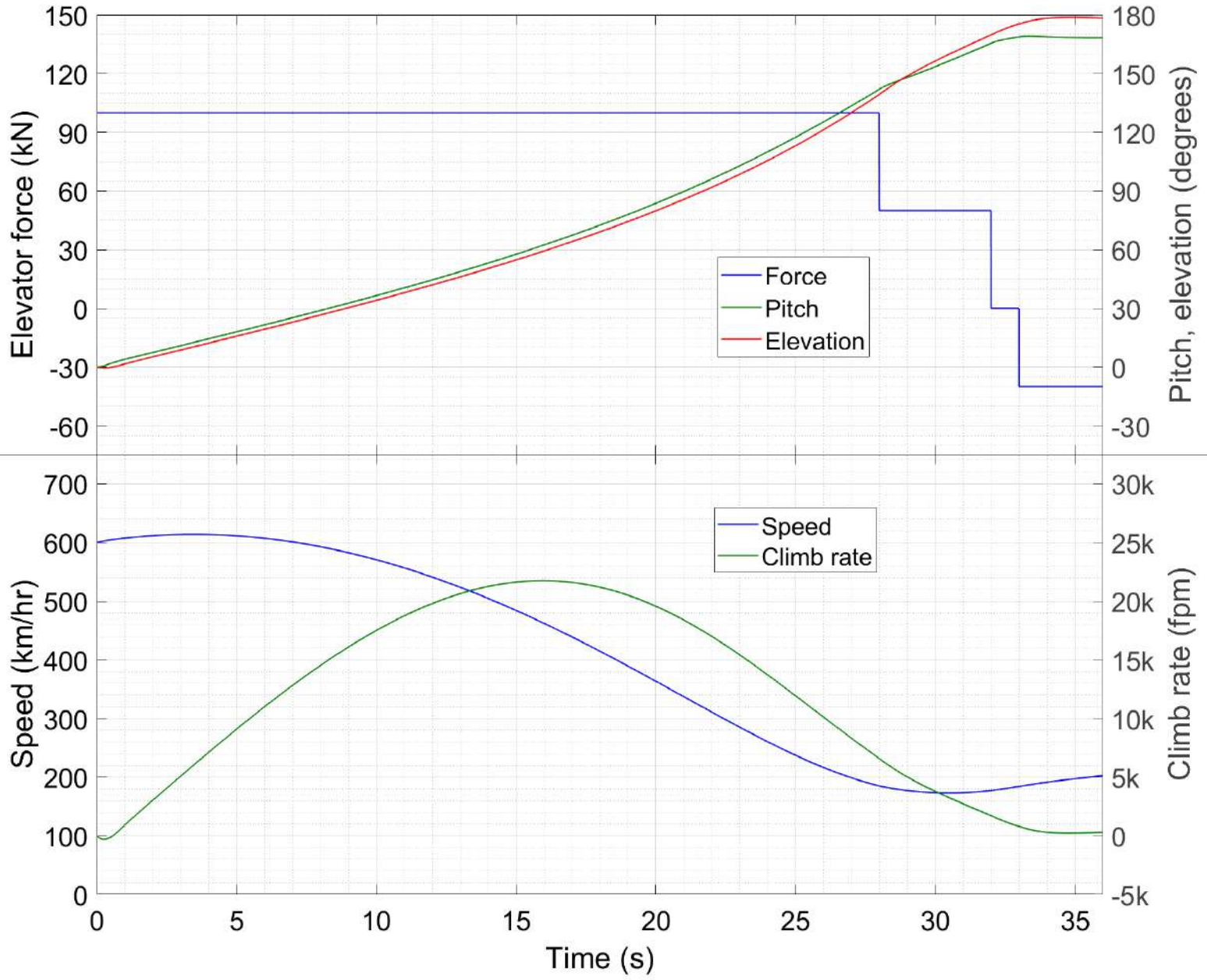


Figure 03 : *Time traces of different variables during the Immelmann manoeuvre. The symbol "k" denotes thousand.*

A high $\bar{f_p}$ causes both pitch and elevation to increase quickly. A stepped reduction when they are close to 180° halts the rise while causing the angle of attack to change sign. No stick force followed by a pushing force stabilizes the elevation at 180° (the equilibrium features a push force because the flight is inverted). The speed drops sharply as the plane climbs through a significant altitude. This is the reason why in Fig. 02 the aircraft takes a much greater distance to pitch up through the first 45 degrees than through the last almost 90 degrees.

We can see that the climb rate during much of the manoeuvre is greater than 10,000 fpm – the peak is more than double of that. The characteristics we plotted for takeoff featured nowhere near this kind of climb rate (the aircraft here is lighter but not by all that much). This is because characteristics show steady state climbs, while Immelmann features a transient climb which comes with substantial reduction of speed. Such climbs, which exchange kinetic energy for potential energy, are called **zoom climbs**. They are useful in acrobatic and military aviation but play a peripheral role in civil aviation, as the deceleration can herald the beginning of an approach to stall (see §52). A zoom climb in an airliner should be reserved for emergencies, for instance if TCAS gives an order to climb to avoid collision, or another plane declares Mayday and ATC orders everyone else in the vicinity to clear the hell out of airspace below a certain flight level.

One thing to note is that Our Plane climbs through several thousand feet in this manoeuvre, so we should ideally have used the model with K_C, k_E and C as functions of altitude. That would not have introduced any new physics though, so it's ok to use the 'incorrect' model here, as long as we are aware of it. In reality, an Immelmann manoeuvre does not take 40 seconds and climb through so many flight levels. Rather, the whole is over and done with in a moment's notice and a couple of hundred feet. It took so long in our case because a passenger airliner is designed for this type of stuff as much as a heavyweight boxer is

designed for dancing a ballet. Nevertheless, even with this plane, the manoeuvre is feasible dynamically – the Internet contains videos of lumbering planes performing vertical loops and barrel rolls, the two components of the Immelmann turn. Whether the manoeuvre is *structurally* feasible on a jetliner – i.e. whether the lift, drag, centrifugal forces and the rest during the turn might break the fuselage, wings or tail – is another matter, but that doesn't concern us here. Similarly, another issue outside our scope as modellers is the physical and mental condition of the pilot during the turn – the *g*'s pulled, the difficulty of adjusting the stick force while flying half-backwards, and the possibility of the seatbelt snapping at the worst instant. We do remember however that Immelmann is a manoeuvre which, though easy on screen, may be terribly demanding in practice.

While I could have now embarked on an analysis of redesigning the model plane to make it better suited for the manoeuvre, I think it's a good idea for this Subdivision to be over quickly. Hence Our Plane stands as is. We shall look at design aspects when we come to another manoeuvre which this plane cannot perform at all.

D. LANDING

§45 **Description.** This is the phase by which every passenger judges every pilot. Some pilots and aviation enthusiasts resent this [01-05] and advocate for 'firm' landings rather than 'smooth' ones. As we shall see however, with the proper aviation skills, it is possible under most circumstances to make a silky-smooth touchdown while being economical on runway and not having to decelerate violently as soon as the wheels are on the ground (which kind of spoils the effect anyway). In most flights (and the better so), the final few seconds are the only instant where a refined technique on the pilot's part is called for, and there is no harm if he exploits the opportunity. There are some special cases where a deliberate thud landing is the safest option, about which we shall see more later. But, those circumstances apart, there is no harm in going for the ultimate grease job.

For a detailed description of an IFR final approach, see §13. In summary, the first part of the landing consists of an approach towards the runway along the 3° (5 percent) glideslope, starting from a point directly behind the airport and 2000-3000 ft above it. Both horizontal and vertical deviation from glideslope are indicated in a cockpit instrument, like the one shown in the below Figure.

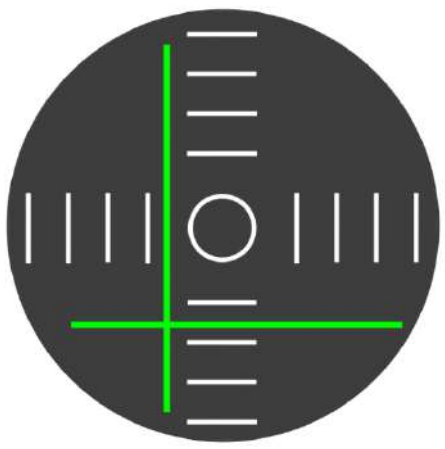


Figure 01 : *Schematic representation of a cockpit ILS display. The white circle at the centre is the aircraft itself while the intersection of the green horizontal and vertical lines (centre of the 'plus sign') denotes the target position. Horizontal and vertical separations between the circle and the plus indicate that the aircraft is horizontally, respectively vertically deviated from the glideslope. In this case, the aircraft is above the glideslope and to its right. The white dashes indicate the extent of deviation, measured in degrees of angle. The calibration depends on the aircraft and its display system.*

In our simulator, only vertical deviation is relevant since we are working in the pitch plane; I have modelled the instrument as a display of the angular deviation from glideslope, rounded to two decimal places.

In the simulation, I will let $y = 0$ denote the runway threshold. I have taken the glideslope to be exactly one foot descent for six metres forward run, which corresponds to a slope of $-2{\cdot}91^\circ$. I have also specified the threshold clearance height to be 50 ft. Note that this clearance denotes the height of the wheels above ground, while our z refers to the height of the aircraft CM. Since our CM is 3 m or 10 ft above the

wheels (at least when the undercarriage struts are neither compressed nor stretched), our glideslope equation will be

$$z_G = -0{\cdot}0508\, y_G + 18{\cdot}3 \text{ (SI Units)} \quad \text{, or} \tag{01a}$$

$$z_G \text{ (ft)} = -\frac{1}{6}\, y_G \text{ (m)} + 60 \quad . \tag{01b}$$

The decision height with CAT-1 ILS corresponds to 200 ft, which is attained about a kilometre behind the runway threshold. In the simulation I have identified this point to be 900 m behind the threshold, at which location the target altitude is 210 ft. Borrowing a railway terminology, I shall call this point the "*inner*" (the signals "distant", "inner" and "home" encountered while proceeding towards a station correspond nicely with the final approach fix, the decision point and the threshold). Although the inner has no special role in a simulation (no transition from instruments to visual), it is nevertheless a useful reference location to judge whether the approach is proceeding on track.

The 5 percent slope of the approach path corresponds to a 600-700 fpm descent for an airliner coming along it. This is way too high a speed to hit the ground. To reduce the vertical speed at touchdown, the pilot performs the **flare** shortly after crossing the runway threshold. For this, he gradually pitches up the nose to reduce the descent rate until the main wheels hit the ground; when that happens, he lets go of the stick so that the front wheels touch ground also. **Touchdown** is the process by which first the main wheels and then the nosewheel make contact with the ground. Once both wheels are on ground, the wheel brakes start retarding the aircraft; in addition the thrust reversers are also deployed as required. The landing is officially over only when the aircraft has reached a cautious speed of 30 km/hr or thereabouts.

§46 **Planning – calculation of the approach and flare.** Before planning the landing, we take the parameter values $m = 60{,}000$, $K_C = 3000$ and $C = 12$. The 60-ton landing weight is reasonable – OEW is usually half of MTOW or less (Table 2A–01), and 10 extra tons when coming in to land is reasonable. K_C and C greater than their takeoff values is also reasonable since flaps are deployed to a much greater extent for landing than for takeoff; undercarriage is also extended during the final approach. Like takeoff, landing planning begins from the characteristics. Below we redraw Fig. 5B–01 for Our Plane in landing configuration; the three climb rates this time correspond to descent along the 5 percent glideslope, level flight and 2000 fpm climb for go-around.

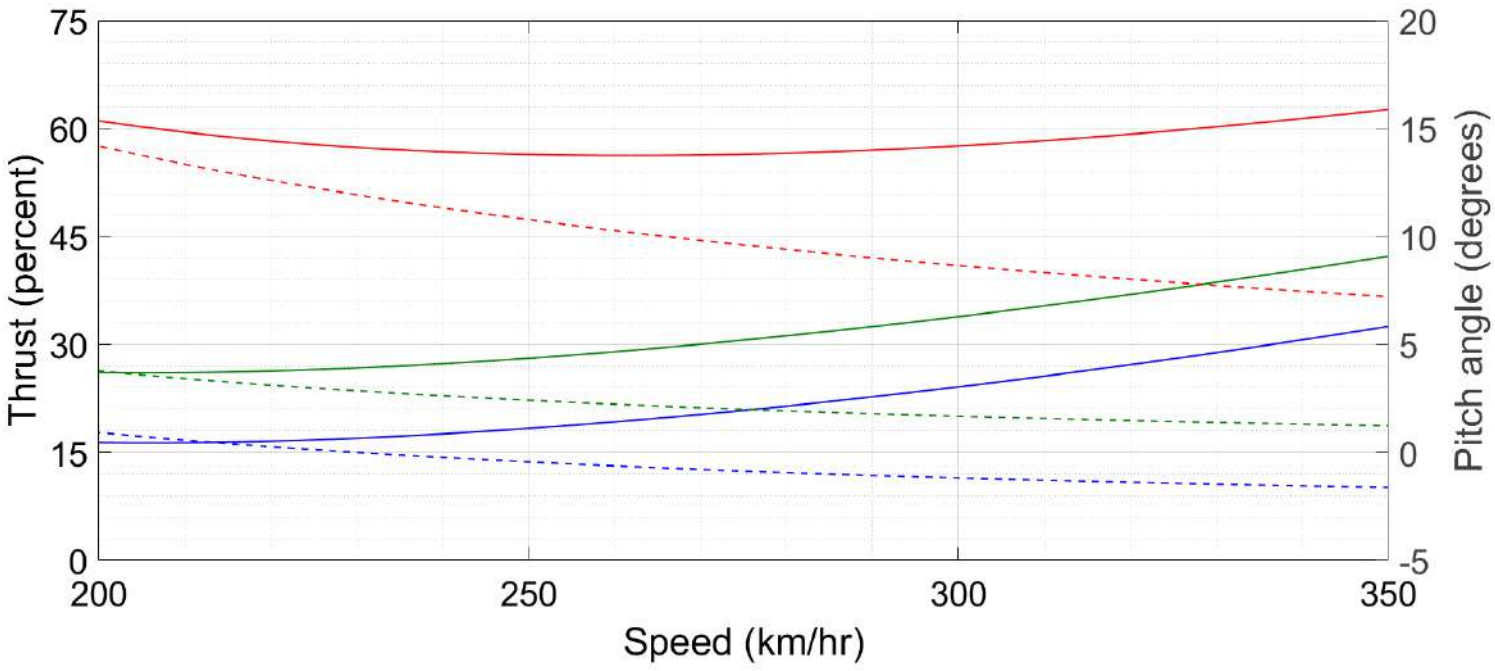


Figure 02 : *Characteristic curves for Our Plane in the landing configuration. Solid lines attach to the left hand* y*-axis and dashed lines to the right hand* y*-axis. Blue, green and red correspond to glideslope descent, level flight and 2000 fpm climb respectively.*

We can see normal command beginning at 200 km/hr or so – note that normal and reversed command are always defined with respect to level flight or flight along a given gradient. In this Figure, the blue and green curves correspond to such flights but the red one does not (see §41). Let us define the landing speed, called $\mathbf{V_{ref}}$, to be 215-220 km/hr. (The actual definition of V_{ref} is 1·3 times the stall speed at the flap

configuration being used. If we extend Fig. 02 leftwards, we will find a 15° angle of attack at less than 100 km/hr even. However, since flaps add camber to the wing, the stall α for the flapped wing is much lower than that of the clean wing (see §21). Our model treats camber to be zero, so I have just defined a landing speed with no reference to the stall speed. Note also that the factor of 1·3 in the official definition of V_{ref} is somewhat arbitrary – thus, V_{ref} is an approximate speed unlike say V_1 and V_2 which are well-defined speeds obtaining from calculations.) Then, we can see that just above 15 percent thrust and less than a half a degree of pitch are required to keep the plane on the glideslope at V_{ref} – the elevator force (not plotted) works out in the range of 23-24 kN. It is very important that the equilibrium pitch at the landing speed be positive, since a negative pitch at touchdown will cause the nosewheel to hit the ground first. The nosewheel has far less load-bearing capacity than the main wheels, so the impact of touchdown and the weight of the aircraft may cause it to collapse, leading to an immediate accident. For this reason, even though flaring increases pitch, aircraft are required to have a nose-up attitude prior to flaring (there are videos of nosewheel first landings available online, but the pilots there are flouting rules and courting risk). This constraint fixes 230 km/hr as the maximum landing speed in our case, since at that speed, the steady state descent down the glideslope corresponds to a borderline positive pitch.

While I could have simulated the entire approach at 220 km/hr, that would not be realistic. At busy airports in particular, planes are expected to begin approach at a speed higher than the landing speed and then decelerate continuously upto the inner or thereabouts. We will begin the simulation at an altitude of 600 ft, 3300 m behind the threshold. At this point, let the aircraft be established on the slope with a forward speed of 252 km/hr, and let the target speed be 220 km/hr at the inner. We need to find out the thrust required to achieve this.

Recall what we learnt in §36 about steady-state and transient motions. A decelerating motion is quintessentially time-dependent or transient and cannot be obtained from the characteristic curves. We must solve for it by going back to the model equations. In the present case, we figure out the thrust required for deceleration by using (3B–22c) in a very approximate way. For all calculations, we use SI Units – feet and what not come only at the end. First, note from Fig. 01 that the thrust required for glideslope at 250 km/hr is just above 18 percent while that for glideslope at 220 km/hr is about 16·5 percent. This variation is very small, implying that the drag remains approximately constant in this speed range (this is pure luck, achieved since 200-210 km/hr is a minima of drag, and variation of any function near an extremum is small). Now, assume that the drag is exactly constant in this speed range, and is balanced by 17·3 percent of thrust. With this assumption, every Newton of thrust above 17·3 percent generates a uniform acceleration of $(1/m)$ m/s^2 while every Newton below 17·3 percent generates a uniform deceleration of $(1/m)$ m/s^2. To slow down uniformly from 70 to 61 m/s over 2400 m (the distance from the start of simulation to the inner), we need a deceleration of 0·246 m/s^2; the mass of 60 tons gives a thrust deficit of about 14·8 kN which corresponds to 4·9 percent. Hence the total thrust required for the deceleration will be about 12·5 percent.

If the decelerated approach were within the ambit of hand-waving calculation, the flare is not. To solve for this, we shall use a more rigorous mathematical procedure. But before that, let me clearly state the objectives of the calculation. Let's say the flare begins with the plane making a steady state descent along the glideslope (about 600 fpm descent rate and 0·3° pitch in our example). During the flare, let the pilot apply a constant $\bar{f}_p$ to make the plane pitch up. Let's assume that the pilot maintains the pressure on the stick until he feels the main wheels hit ground, at which point he relaxes the stick and the flare ends. The descent rate at this instant determines the smoothness of the landing – according to one source at least [06], 100-200 fpm is considered 'very smooth', 200-300 'normal', 300-600 'firm' and above that, unacceptable. At the same time, the pitch at the instant of touchdown should also be within limits – too shallow might cause premature engagement of the front wheels while too steep will cause a tailstrike. Let us say, the desired pitch attitude for Our Plane at touchdown is 3°. Hence, the flare ends at say 100 fpm (no harm in aiming for the best!) descent and 3° pitch. What we need to find are (*a*) at what altitude should the pilot initiate the flare, and (*b*) how fast should he rotate, so that the flare ends at the desired climb rate and pitch, and on the ground.

To analyse flaring by hand (of course with approximation), the xyz model is the most suitable. This is because the objective is stated in terms of descent rate and altitude which are the base variables of that model, but not of the space vector model. Hence, for this calculation, we turn to (3B–15). To start, we assume that V_y is constant during the flare. Then, (3B–15c) becomes irrelevant. Next, we use overdamping and the accompanying approximations (see §41) on (3B–15f) to assume that at constant $\bar{f}_p$, θ increases at a constant rate. The conversion factor in this case works out to 8·04 kN excess $\bar{f}_p$ for a 1°/s pitch rate. Since its initial value is 0·3°, we write it as $\theta = 0{\cdot}0052+\omega t$ (radians!) where ω is to be determined. This gets rid of (3B–15e,f) so that the formidable (3B–15c-f) has reduced to (3B–15d) only. Moreover, the assumptions tremendously simplify this surviving equation. In the first term on the RHS, we neglect V_z^2 in comparison with V_y^2 (since $V_z << V_y$ typically) and treat θ to be small for the sines. Regarding the second term on the RHS, it is tempting to drop it altogether since that is of size V_yV_z while the first was of size V_y^2; however, this term carries cosines of θ which are much larger than the sines in the previous. The two terms actually work out to be of the same size. The permissible simplification in the second term is small θ which makes the cosines add up to 2. The next two terms in the RHS are really negligible, gravity is gravity, and the last term simplifies to CV_zV_y. Implementing all this, (3B–15d) becomes

$$\frac{\mathrm{d}V_z}{\mathrm{d}t} = \frac{1}{m}\left\{K_C V_y^2\left(0{\cdot}0052+\omega t\right) - K_C V_y V_z - mg - CV_yV_z\right\} \quad . \tag{02}$$

Since V_y is constant, this equation is linear. We use the value $V_y = 60$ m/s and take the initial condition to be $V_z(0) = -3$, which corresponds to 600 fpm descent. Along with (02), we also have the subsidiary equation $\mathrm{d}z/\mathrm{d}t = V_z$. Let $z = 0$ be the point where the flare starts, with no loss of generality.

It is not for nothing that solving linear and especially constant-coefficient differential equations is the most important mathematical technique which you ought to know [1O–45]. Equation (02) can be solved using the method of undetermined coefficients; before presenting the solution we define

$$\gamma = \frac{\left(K_C + C\right)V_y}{m}, \qquad a = -g + \frac{0{\cdot}0052K_C V_y^2}{m}, \qquad b = \frac{K_C V_y^2 \omega}{m} \quad , \tag{03}$$

so that (02) becomes

$$\dot{V}_z + \gamma V_z = a + bt \quad . \tag{04}$$

The solution is

$$V_z(t) = \left(V_z(0) - \frac{a}{\gamma} + \frac{b}{\gamma^2}\right)\mathrm{e}^{-\gamma t} + \frac{a}{\gamma} - \frac{b}{\gamma^2} + \frac{b}{\gamma}t \quad . \tag{05}$$

We can directly integrate this to find z as a function of time,

$$z(t) = -\frac{1}{\gamma}\left(V_z(0) - \frac{a}{\gamma} + \frac{b}{\gamma^2}\right)\mathrm{e}^{-\gamma t} + \left(\frac{a}{\gamma} - \frac{b}{\gamma^2}\right)t + \frac{b}{2\gamma}t^2 + \mathbb{C} \quad \text{, where} \tag{06a}$$

$$\mathbb{C} = \frac{1}{\gamma}\left(V_z(0) - \frac{a}{\gamma} + \frac{b}{\gamma^2}\right) \quad , \tag{06b}$$

the last step making use of the initial condition $z(0) = 0$.

Now, let us see the results of this calculation. We plug in the landing parameter values; the plot below is for $\omega = 1{\cdot}25°/\mathrm{s}$.

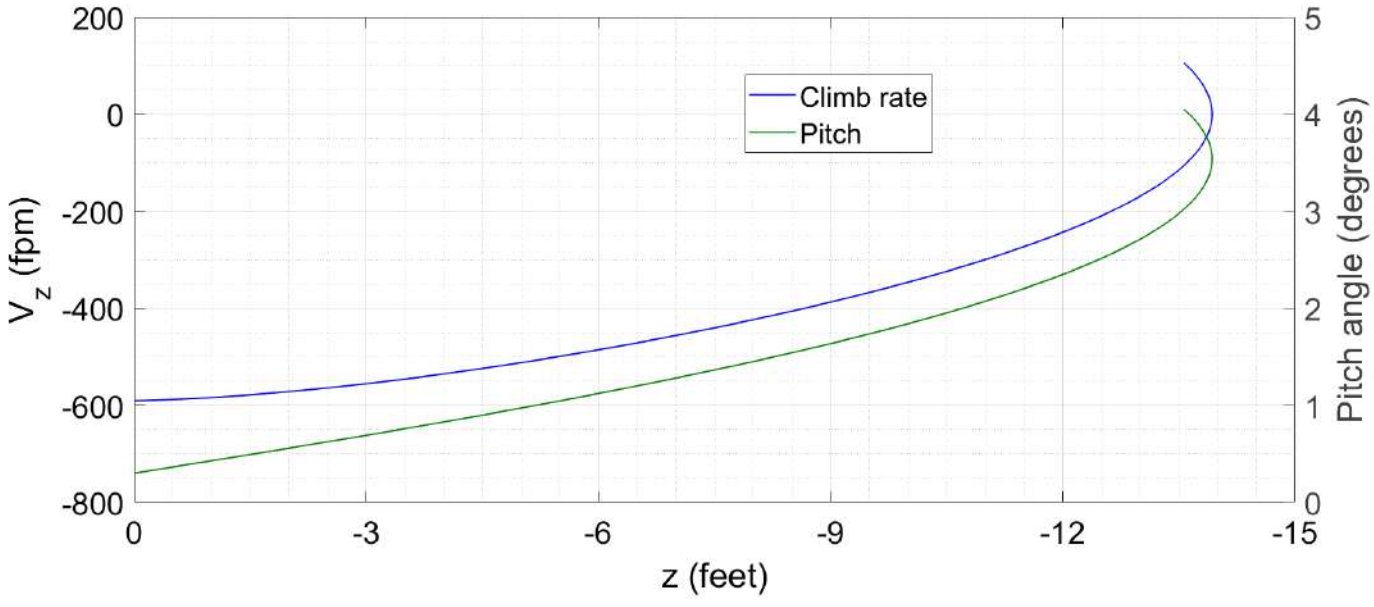


Figure 03 : *Pitch and climb rate as functions of the aircraft's vertical displacement after initiating flare, as per (06) using* $\omega = 1{\cdot}25^o/s$.

Here we can see V_z and θ as functions of z; time is implicit and evolves along both curves starting from bottom left. Focussing on the blue curve, we see the initial descent rate of 600 fpm which reduces as the plane sinks lower. 9 ft below the starting point, it is still descending at 400 fpm and 12·5 ft below, it's at 200 fpm. Now however the descent rate drops sharply with every further inch – just one more foot sees it going 100 fpm, and a hair's breadth later, the descent has changed to a climb. After this, the curve turns backwards since the plane starts rising through the heights which it earlier lost. The plot of the pitch shows that we hit 3^o exactly at 100 fpm, corresponding to the desired configuration at the end of the flare. $\omega = 1{\cdot}25^o/s$ serves to achieve this; a faster pitch rate gives a higher pitch at this instant while a slower pitch rate gives lower.

The blue line shows why achieving that grease job is so tricky. Evidently, to do 100 fpm when wheels touch ground, the pilot must start the flare exactly 13·6 ft above it. If he's a foot too late i.e. he initiates flaring at 12·5 ft, then he'll be doing double the vertical speed when the ground hits; two feet late and almost triple the speed. So we can see how easy it is to err on the side of thudding. On the other hand, should the pilot be even 5 inches early and start flaring at 14 ft, he'll not hit the runway at all, but start climbing again when the wheels still have a few millimetres clearance. So it is just as easy to err on the side of skimming. Just to remember, the plane is doing 10 ft/s when the flare is initiated, so the timing has to be precise to about 1/10 s. Of course, such precision is impossible in real life; what happens is that the pilot adjusts the pitch rate to compensate for a few dozen milliseconds of timing. While we're at it, let's also look at the distance consumed by the flare. For this, we reintroduce the time, which is absent from Fig. 03. Looking at the underlying dataset, we find an interval of 2·2 s between starting the flare and achieving 100 fpm descent; during this time, the aircraft goes 130 m forward. During the glideslope descent from 50 ft to 13·6 ft, the aircraft goes another 225 m. Hence, the touchdown occurs at about 350 m forward of threshold – very economical in terms of runway.

Our calculation thus suggests that a greased touchdown with no wastage of runway is eminently possible if the pilot has sufficient skill. The calculation however was approximate; let's now see if the simulator confirms our predictions.

§47 **Execution.** The equation is (3B–22) augmented by the ground reactions (5B–01) and (5B–02); the cycle time is 1 s from the start upto the threshold, 1/4 s from that point until the brakes are hit and 2 s thereafter. We assume that brakes can be activated only when both wheels are on the ground and bearing weight, which occurs when the pitch reaches $0{\cdot}5^o$ (this is a totally arbitrary condition but it does reflect the fact that there is a delay between touching down and applying wheel brakes). Instrument readings shown are distance from threshold, altitude, deviation from glideslope, speed, climb rate and pitch. I have also implemented (though not utilized in this simulation) the velocity ratio, which we'll see in detail in the next Section. These are precisely the quantities you need to be aware of while performing a landing.

Here's the final approach.

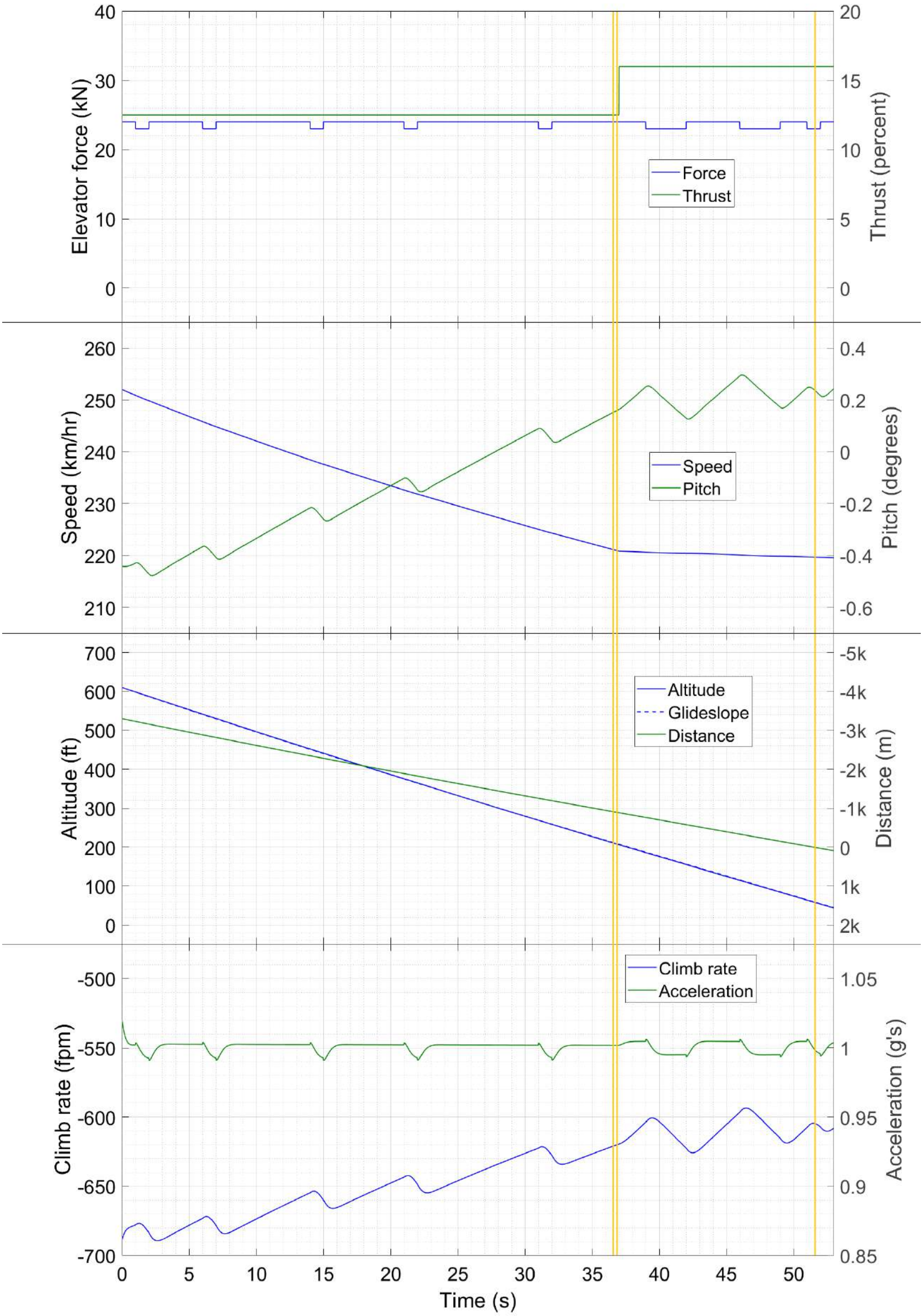


Figure 04 : *Time traces of different variables during the final approach. The symbol “k” denotes thousand.*

The two thin yellow lines at $t = 37$ s running from top to bottom indicate the inner while the single yellow line at $t = 51$ s indicates the threshold (inner double, home yellow is the expected approach configuration for those who are into railway operations as well). The thrust (top panel) is 12·5 percent upto the inner and 16 percent thereafter, while the elevator force alternates between 23 and 24 kN. The speed (second panel) has come down to 220 km/hr at the inner, thus validating our calculation regarding the thrust level. The pitch is increasing if $\bar{f}_p$ is 24 kN and decreasing if it is 23 kN, consistent with the trim state corresponding to somewhere in between. Overall, the pitch shows as increasing trend upto the inner since the speed is reducing and the angle of attack needed to maintain glideslope is increasing. After crossing the inner, the pitch oscillates about a more or less constant value of 0·2°, since we are now in a quasi-equilibrium flight. In the plot of altitude and distance (third panel), I have made the right hand axis positive downwards so that both the lines have negative slope, and their proportionality is easier to visualize. In addition to the altitude, I have also shown the glideslope as a blue dashed line attaching to the left hand axis – it is invisible since the plot of altitude overlaps with it (the approach is right along glideslope). Finally, the climb rate (bottom panel) is negative since the aircraft is descending. Since the plane's speed along a fixed gradient is decreasing with time upto the inner, the descent rate is decreasing also. Vertical acceleration, or $\mathrm{d}V_z/\mathrm{d}t$, is not really relevant for approach but is useful for calibrating the touchdown. Convention has it to measure it in g's, where one divides the $\mathrm{m/s^2}$ value by 9·8 and then adds unity to the result. Note that a value of 1g denotes no vertical acceleration with respect to the ground-fixed frame !

Figure 04 describes a clean approach, which is called a **stable** or **stabilized approach**. This means that the aircraft is in landing configuration (undercarriage extended, flaps at planned value), is within a few feet of glideslope both horizontally and vertically and is responding positively (i.e. taking corrective actions) to any deviations registering on the ILS display. Note that the word "stable" or "stabilized" is not used in its dynamical systems context here, in at least two ways. Firstly, the approach in this case (and in many realistic cases) is not an equilibrium motion and therefore cannot be stable or unstable. Secondly, an approach corresponding to equilibrium motion along a flight path touching down miles forward of the threshold will also be dynamically stable as per §34 but will be as unstabilized as it can get.

Figure 04 shows no discernible change in behaviour even after crossing the home; that comes next.

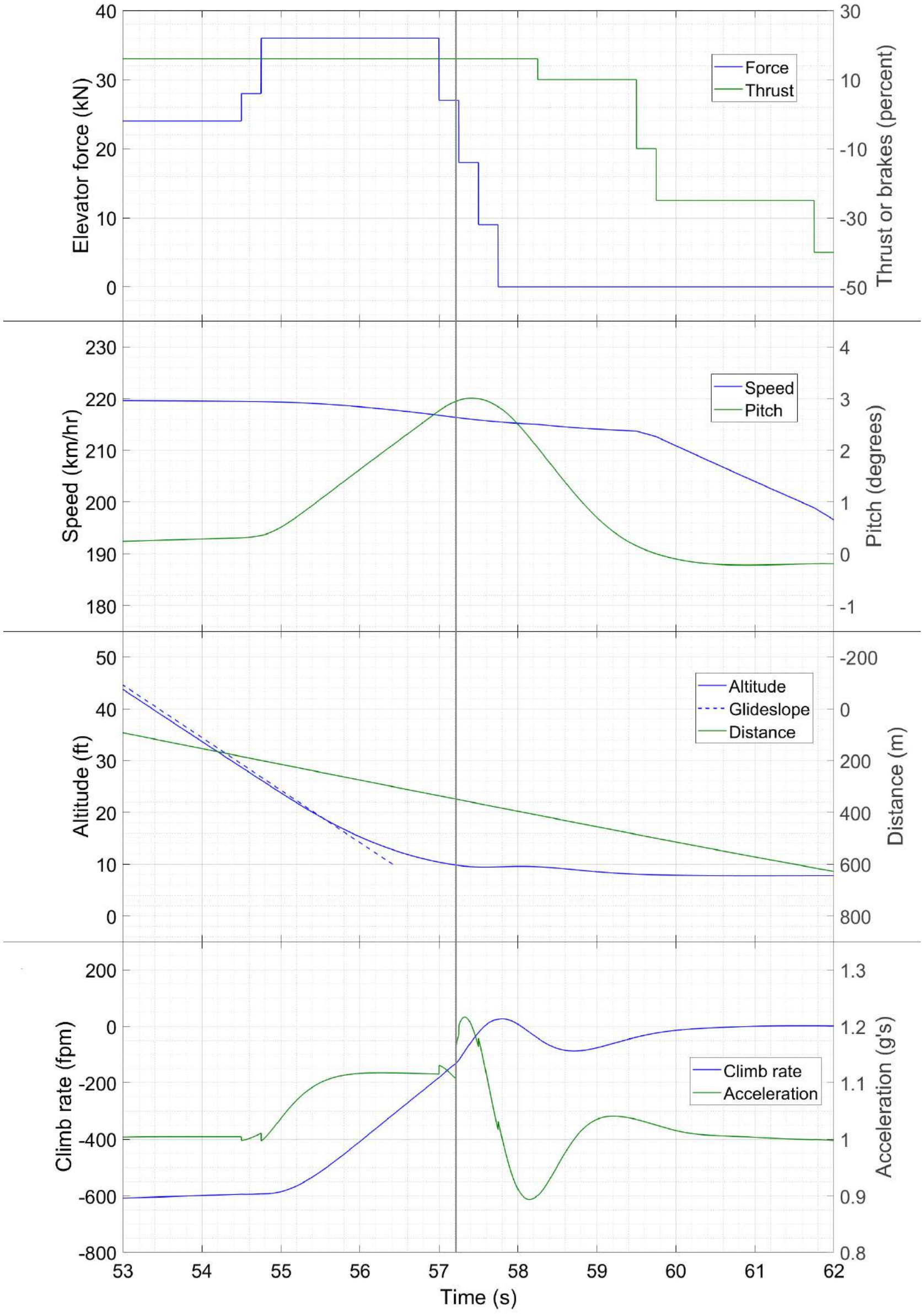


Figure 05 : *Time traces of different variables during the flare and touchdown.*

Before anything else, note again that the CM is at altitude of 9·84 ft when the wheels hit the ground – the grey* vertical line denotes this instant. To begin the flare, I increase $\bar{f}_p$ (top panel) from its glideslope 24 kN to 36 kN; the planning phase indicated a 1·25°/s pitch rate which would be attained at about 34 kN, and for takeoff we saw that a slightly higher elevator force was necessary in practice. The stepped increase from 24 to 36 is realistic and also gave me a chance to bleed off a little altitude before hitting full force – multiple practice runs had taught me that this would be necessary in this instance. The thrust remains constant at the pre-flare value since we don't have ground effect in the model and there is no reason to reduce speed until touchdown has occurred. As soon as ground is hit, I let go of the stick and then retard thrust levers to idle (which is 10 percent in this example). When pitch (second panel) becomes less than 0·5°, I initiate the braking action and the interesting part of the manoeuvre is over. The speed (second panel) shows a slow decrease during the flare because the flight path is becoming shallower – the effect is not really significant. The plot of pitch vs time is for all practical purposes a straight line, which increases from 1·58° at $t = 56$ s to 2·75° at $t = 57$ s. The rotation rate of 1·17°/s is very close to the planned value – equally close is the pitch at the instant of touchdown itself. The plot of altitude (third panel) shows that I initiated flare at an altitude of 29 ft (wheels 19 ft) and applied the full elevator force at about 26 ft (wheels 16 ft) above ground. This time, the dashed line for glideslope is visible – the aircraft is a foot below it at the home and then flies above it as the flaring starts. The distance from threshold at the instant of impact is 348 m. The descent rate (bottom panel) at this time is about 135 fpm, corresponding to a greaser (obviously, since this is a display landing and not one of dozens of practice attempts). The vertical acceleration at impact is less than 1·2g, although it comes from the ground interaction model, for which I make no great claim of accuracy. We can see that the landing parameters are in good agreement with what we had calculated in the last Section – our calculation thus acts as an excellent starting point from which to improve one's simulator performance through practice.

* After double yellow and yellow, the red is not the point of impact but the 'starter' at the far end of the runway – *that* is the line you cannot cross.

Two differences between our simulation and reality. Firstly, in the real thing, ground effect causes a significant reduction of drag when the aircraft is 20-30 ft or closer to the runway. To prevent an unwanted acceleration, the throttles must be reduced to idle before or at least during the flare. On Airbus aircraft, this is ensured by an automated callout of "retard" at a radio altitude of 20 ft – the company has clarified [07] that the callout is a reminder rather than an order or a comment on the pilot regarding his flying skills. Secondly, in real aircraft, spoilers are auto-deployed immediately after touchdown is detected, resulting in a rapid reduction of lift. In the simulator they are absent, so I have reduced lift by a large and quick reduction of the elevator force. With the spoilers present, only a gradual easing of stick and trim is sufficient after the plane hits the ground. In some aircraft, the negative torque from the undercarriage following touchdown is so high that it might even be necessary to maintain a large pull force on the stick to ensure that the nose wheel doesn't slam down onto the runway.

Approach and landing is in fact the most safety-critical phase of the entire flight. As many as half of all aviation accidents occur during this phase, at every level of aviation [08]. Hence, it behooves us to take a closer look at the dynamics of this phase and the safety lessons which we can extract from it. We consider separately the approach and the flare.

§48 **Perfecting the approach – velocity ratio.** The majority of landing accidents and incidents begin with an unstabilized approach. We have already seen in the last Section what a stabilized approach is – the unstabilized one is its logical negative. One of the key steps to prevent an unstabilized approach is the timely execution of the **approach and landing**. Each airline has its own slightly different checklist, but the key dynamical elements of this list, we can deduce ourselves. Firstly, the *undercarriage* must be extended. Next, the *flaps* must be in the correct configuration. Thirdly, the target approach and landing *speeds* must be known to both the pilot flying and the pilot monitoring. Fourthly, the *stabilizer trim* should be set for the desired speed, equal to near to the landing speed. Finally, the *automatic post-touchdown response* must be configured properly. In most aircraft, the extension of spoilers, detrimming of horizontal stabilizer, activation of disk brakes and deployment of thrust reversers all occur automatically in the correct sequence

after the computers detect weight on the undercarriage. As the pilot, you have to verify that the sequence has been configured to activate properly and that the braking settings are the ones you want (for example, you wouldn't want maximum deceleration while landing normally on a 3 km runway). The ideal time to complete these items is just before beginning final approach. Most final approach procedures have a stretch of level flight immediately preceding it, which results in interception of glideslope from below (see Fig. 2B–06 for KJFK for example); this level stretch is when you ensure that the checklist items are carried out and marked off. If your descent profile features interception of glideslope from above, then the checklist items must be completed at least within a few hundred feet above the altitude where final approach starts.

Being ready with the checklist before the approach increases the chance of your making it stable – you will be fully alert to any deviation from glideslope and will be able to take quick corrective action. Nevertheless, the checklist by itself doesn't guarantee a stable approach (obviously). At least on the simulator, I have found that the best way of ensuring adherence to glideslope is to think of it as a *proportionality of velocities* rather than of displacements. To make this proportionality more formal, let's define the **velocity ratio** (denoted $\mathbf{V_z/V}$ since the naive acronym VR may be confused with the established V_r of takeoff) as

$$V_z/V = \frac{|\text{climb rate}|}{\text{ground speed}} \quad . \tag{07}$$

Mathematically, the velocity ratio is $|V_z/V|$ which is $|\sin\eta|$. But since we measure V and V_z in different units, a conversion factor gets tacked on, which works out to 54·7 in our units. The absolute value on climb rate gives a positive number for climbs as well as descents (we all like positive numbers and pilots will not confuse between climb and descent). Using the ground speed here is essential since the glideslope is defined in the ground-fixed frame. On our –2.91° glideslope, V_z/V works out to 2·777 i.e. on the glideslope, we need to maintain 2·777 fpm descent for every km/hr of speed. Whenever V_z/V is equal or near to 2·777, we are at least tracing a flight path (almost) parallel to the slope even if not the slope itself. If the parallel path is only slightly shifted, let it be. If the deviation requires correction, then we can add a small amount to the climb or descent rate to achieve the correction.

Good aviation practice requires pilots to go around if the approach has not been stabilized by 1000 ft (in some cases 500 ft) of height. Nevertheless, the pressure on pilots to continue with a landing in violation of this guideline is quite high. "Tower, Callsign 111, going around due to unstabilized approach" is not a communication which any pilot wants to make. Even less is "Ladies and gentlemen, this is your captain speaking, we've aborted the landing because, you know, the rulebook says we were flying kinda unsafe, and safety comes first. Traffic at destination is a little busy but we should be able to get another attempt at landing within the next couple of hours. We have enough fuel as of now; should it run low, we'll divert." So much the better to proceed towards landing and pull it off isn't it – no embarrassing speeches, no irate customers. The temptation unfortunately is understandable; a good pilot, should he succumb to it, needs to be able to draw on his airmanship skills and safely bail out of trouble.

We will now see how the velocity ratio can help us stabilize a poor approach. In the upcoming simulation, the aircraft starts at a point 2 km behind the threshold in approach configuration at approach speed, descending parallel to glideslope but positioned miles high. Specifically, the initial conditions on (3B–22) are $y(0) = -2000$, $V(0) = 65$, [234 km/hr], $\eta(0) = -0{\cdot}05$ [2·87°], $\theta(0) = 0$ and $\omega(0) = 0$, and the problem variable is $z(0)$ which is 183 m or 600 ft when the slope prescribes 120 m or 393 ft. Suppose we want to get rid of the excess altitude in 1 km distance (approximately at the inner). That will require a velocity ratio of very nearly 6·0, so let this be our target V_z/V. Now, how does V_z/V depend upon the stick input ? When the aircraft is in the trim state ($\bar{f}_p$ between 23 and 24 kN), V_z/V will remain very nearly constant since it's neither pitching up nor pitching down. A pull force on the stick will reduce the descent rate and hence decrease V_z/V while a push will increase both of them. In the simulation, I have also implemented the glideslope deviation indicator in feet rather than in degrees, for a reason which will become apparent soon. The cycle time is 1 s throughout, and thrust is 10 percent (our assumed flight idle, the lowest possible since the high-speed descent will cause an undesirable acceleration anyway).

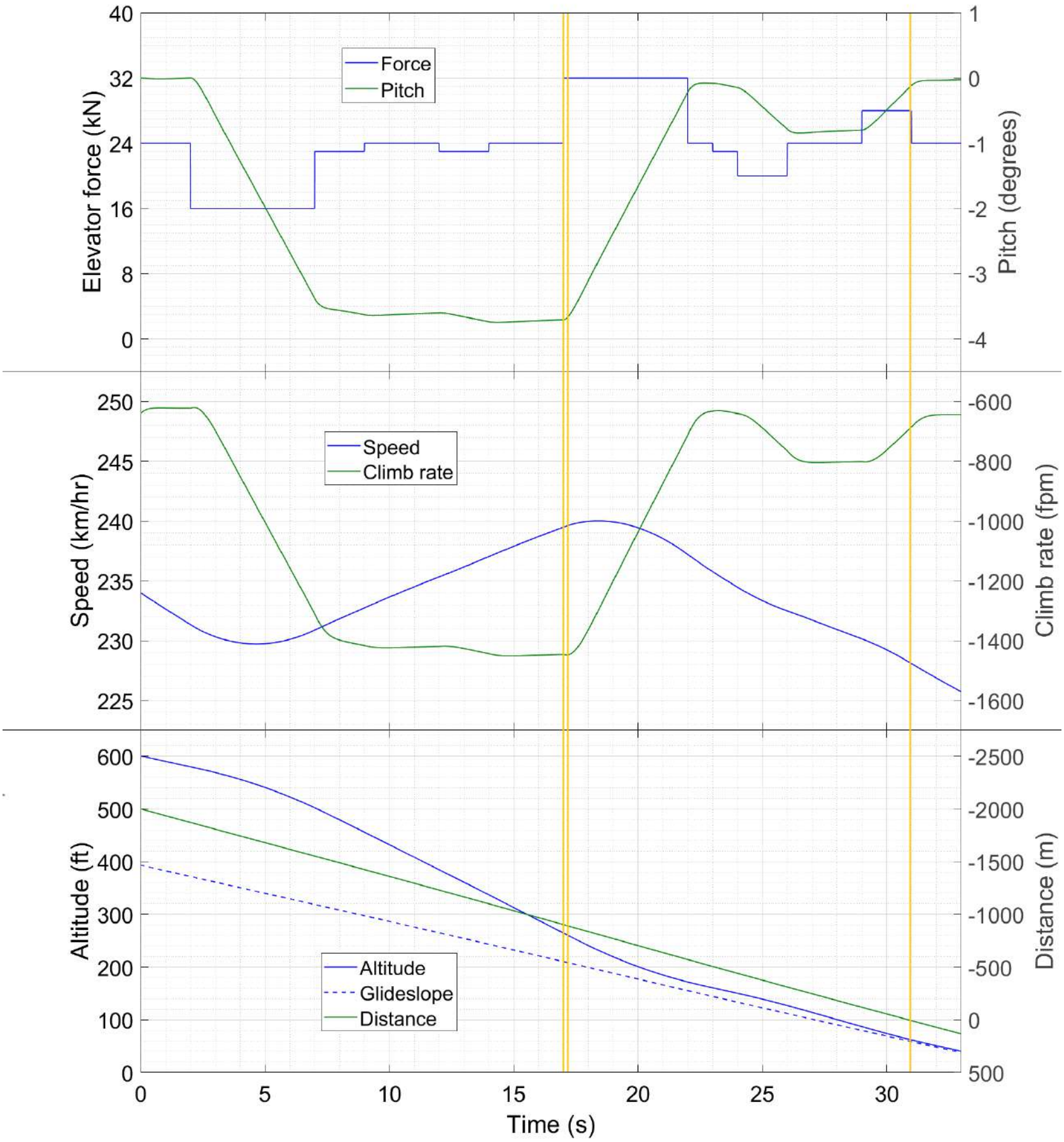


Figure 06 : *Time traces of different variables during successful correction of an initially unstable approach.*

The first two seconds see us holding $\bar{f}_p = 24$ kN (the trim state) and a velocity ratio of about 2·8. The path (bottom panel) is parallel to the glideslope, just heavily deviated. Then, I have pushed forward on the stick to increase V_z/V. The push force is pretty gradual, with $\bar{f}_p$ being 8 kN below the trim. Holding this for 5 s sees V_z/V approaching 6; thereafter returning to trim establishes it at 6 (V_z/V not shown explicitly but we can easily calculate it from the middle panel). Alternation between 23 and 24 kN keeps V_z/V between 6·0 and 6·1, and the aircraft's trajectory rapidly converges towards the glideslope. When the deviation reduces to about 50 ft (in this case, it was 54 ft at the end of one simulation cycle), I have applied nose up force to bring V_z/V back to 2·8. Five seconds at 8 kN above trim achieves this, and when trim is re-established at $t = 22$ s, we are again tracing a path parallel to glideslope but only 15 ft above it. This is an acceptable deviation, it will require less than 100 m of excess runway. But, since we still have about half a kilometre to the threshold, why not do better. So, in the time interval $t = 24$ to $t = 31$ s, I have repeated the strategy in miniature. A light nose down input (4 kN below trim) takes us to V_z/V of 3·5 while a subsequent

equally light nose up input restores us to 2·8, this time exactly on the glideslope. Thus, half a minute after being in a precarious configuration, we find ourselves on velvet at the home, all set to unleash a greaser and earn applause from the passengers who remain blissfully unaware of the approach parameters.

In addition to our reliance on the velocity ratio, our recovery strategy has a second key component. This is that that the elevator forces involved are gentle and infrequent. Even though the initial position (and my decision to continue rather than abort) will earn me a F from a flight instructor, I haven't panicked and resorted to large or frequent pushes and pulls on the stick. In the first 22 s, there's only one pushing phase and one pulling phase on top of the trim state; the excess $\bar{f_p}$ is 8 kN during both phases. As a result it has taken me 5-plus seconds to transition between the low and high velocity ratios, enough time to monitor the indicator and prevent an under- or overshoot. Only the descent rate, exceeding 1400 fpm, is high during the approach but V_z/V ensures that there's method to the madness – 6 was the number we wanted, and the number we have. This is very different from an uncontrolled scramble towards the glideslope. Seeing the deviation in feet enables me to precisely determine when the transition to the lower ratio has to be initiated – a degree value as in the indicator of Fig. 01 would necessitate a multiplication by the distance. Finally, going through the motions a second time shows that you can employ this strategy iteratively to increase the accuracy of your approach with each pass.

As a diametric opposite to the rescue strategy, here is a simulation of a pilot actively throwing his plane off the glideslope and into the newspapers. The starting horizontal displacement and velocity vector are the same as in Fig. 05 but this time the aircraft is only 5 ft above glideslope. 5 ft too high is almost negligible – it corresponds to 30 m of excess runway use. It is totally fine to let the deviation be as it is. Otherwise, the slightest of increases in descent rate can shave it off by the time one reaches the home. This pilot has other plans however – whenever the ILS display shows him a deviation from glideslope, he resorts to large stick forces. The simulator has no velocity ratio, and the pilot has no eye whatever on the speedometer or the climb rate indicator. For simplicity, thrust is set to 14 percent throughout.

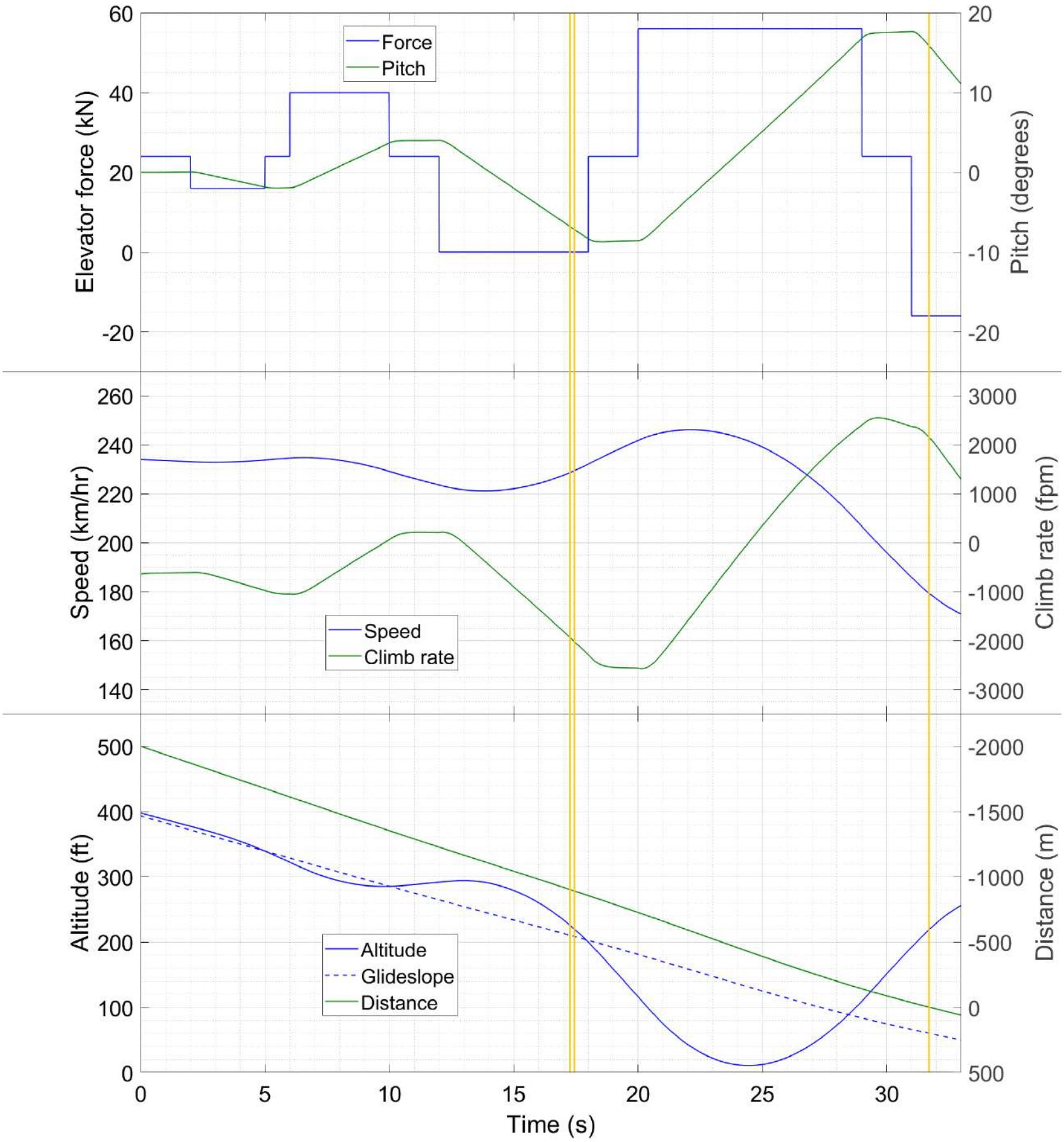


Figure 07 : *Time traces of different variables during destabilization of an initially stable approach.*

After holding the trim state for a couple of seconds, we see a reduction of $\bar{f}_p$ by 8 kN, the same as in Fig. 06. The descent rate increases rapidly and the aircraft soon crosses the glideslope, at $t = 5$ s. The descent rate has gone past 1000 fpm but, as I've already mentioned, the pilot is blissfully unaware. Seeing the crossing of slope, the pilot first returns to trim state but then, as the negative deviation increases rapidly, yanks the stick back hard, applying 16 kN of nose-up force. He keeps the back pressure on until the glideslope is crossed again, at $t = 10$ s. Again he holds trim for a couple of seconds but what good will that do, the aircraft is now climbing instead of descending. The deviation from slope, now positive, increases faster than before. Completely flustered, the pilot pushes harder than before, applying 24 kN nose-down so that the elevator is floating freely. The next slope crossing occurs at $t = 16$ s, just past the inner. The descent rate has now exceeded 2000 fpm, which manifests as an extremely rapid increase of the negative deviation despite the pilot holding trim state. Panicking, he now tries 32 kN nose-up; when the descent is arrested at $t = 24$ s, the aircraft is literally one foot away from the ground. And on it goes.

While this particular simulation is of course an exaggeration, the phenomenon is exactly the kind of thing which happens when the pilot tries aggressive elevator inputs tied to the glideslope deviation alone. This is an example of pilot-induced oscillation. If we try to represent it in the form (4O–19), then the variable x represents the deviation from glideslope while a and b are zero since the plane has no intrinsic tendency to return to the slope. k and $\mathcal{C}$ can act as stand-ins for the elevator force since that is being adjusted in response to the deviation and the deviation rate. The delay τ arises not from any instrument lag or reaction time, but from the time interval between the pilot's changing the stick force and the plane's beginning to approach closer to the slope. For example, the pilot applies $\bar{f}_p = 0$ at $t = 12$ s to correct a positive deviation, but the descent rate increases beyond 650 fpm (the slope value) only after $t = 14$ s. As you can see, our use of the equation (4O–19) to model pilot-induced oscillation is quite heuristic; nevertheless, the solution, oscillations of increasing amplitude, is pretty well in agreement with what (4O–19) predicts in an unstable case.

Since V_z/V is so useful for approach stabilization, it might help the pilots if actual aircraft are equipped with a cockpit instrument which displays its value. The requirements for such an instrument will be the ground speed and vertical speed indicators, which are already present on today's jetliners. The appearance of this instrument can be similar to the ILS display in Fig. 01 with a plus sign being centred on the instantaneous value. Pilots will use the stick to centre the aircraft at the intended target, both on and off glideslope. In the general three-dimensional case, there will also be motions perpendicular to the pitch plane. Since the velocity ratio does not account for these, the smaller they are, the more accurately will the ratio indicate conformity to glideslope. Fortunately, during a final approach, such motions are kept to a minimum anyway so that the aircraft may remain aligned with the runway centreline throughout, and land on it. The V_z/V indicator will be equally effective for non-standard approaches, like the 5·5° approach to London City Airport, UK (EGLC). Visual approaches following curved paths, for instance the Potomac-tracing approach to KDCA (see §13), can also be programmed if we take the approach slope to be the ratio of total altitude lost to total horizontal distance travelled along the curved path. In Subdivision 5J we shall see another example of stabilizing an approach by utilizing the velocity ratio.

As with the V_z/V indicator, it may also be beneficial for pilots to modify the glideslope indicator to display deviations in feet rather than degrees. While degree deviations are the fundamental input received from the ILS, they can easily be converted to feet if the ILS has a DME as well, which most major airports do. The amount of excess (or deficient) runway used for the landing depends on the feet and not the degree deviation, so this small modification to the cockpit panel might make the flying experience a lot more intuitive.

To expedite an approach or to save fuel, sometimes what the pilot does is, he does not select the landing configuration of flaps and undercarriage right at the start of the approach but instead begins with wheels up and flaps at a lower setting. Then, he extends the flaps and wheels progressively. This is more difficult to execute than the approach which begins in landing configuration because the handling characteristics of the aircraft change with every incremental flap or wheel extension and it requires quick adaptation to the new characteristics to stay on the glideslope. Hence, progressive extension is alright when you are flying a normal approach on an aircraft type with plenty of prior experience. When the situation is abnormal (say overweight or compromised aircraft) or you are new to the type, then it is safer to select the landing configuration beforehand, get the feel for the aircraft in that configuration during level flight and only then begin the descent down the slope.

The approach by itself of course doesn't get the plane on the ground – now let's look at the manoeuvre which does.

§49

Types of flare, bounce and shimmy. Our model (3B–22) describes three fundamental types of flare – transient, steady state and quasistatic. In this Section we look at each of these techniques, and their advantages and drawbacks. In addition, we can design flares which are mixtures of two or more of the techniques.

Transient flare

This is the technique we already used in Fig. 05. It is transient because the aircraft's motion during the flare is far away from equilibrium. The pitch is increasing and the descent rate decreasing continuously when the ground is hit, and the nose-up force is released. In §46 we have already seen what happens if we initiate a transient flare too late or too early. In the former case, we get a thud landing; in the latter, we run the risk of the plane not touching down at all. Moreover, the continuous increase in pitch might also result in a tailstrike if the pitch becomes too high while the wheels have not yet touched the ground. Hence, the primary drawback of the transient flare is the possibility of adverse effects if initiated too early. The advantage of this method is that the runway length used by it is the least. In the example simulation, we made a soft landing while using only 54 m more runway than we would have used in the absence of flaring (landing distance was 348 m in the simulation and would have been 294 m without flare since we were a foot below glideslope at the home). Just to reiterate, it takes 300 m of runway to slap the ground at 600 fpm and 350 m to kiss it at 135 fpm – hardly any extra space to pull off that greaser. You will get a better idea of the runway usage after seeing the other types of flaring, so let's look at those now. ■

Steady state flare

In this technique, the aircraft follows an equilibrium flight from an altitude of a few feet upto the ground. Thus, the tail end of the final approach is one equilibrium and the few seconds prior to touchdown are another; the flare represents a transition between the two. To design and execute a steady state flare let's first plot the characteristics for three climb rates : –200, –100 and 0 fpm.

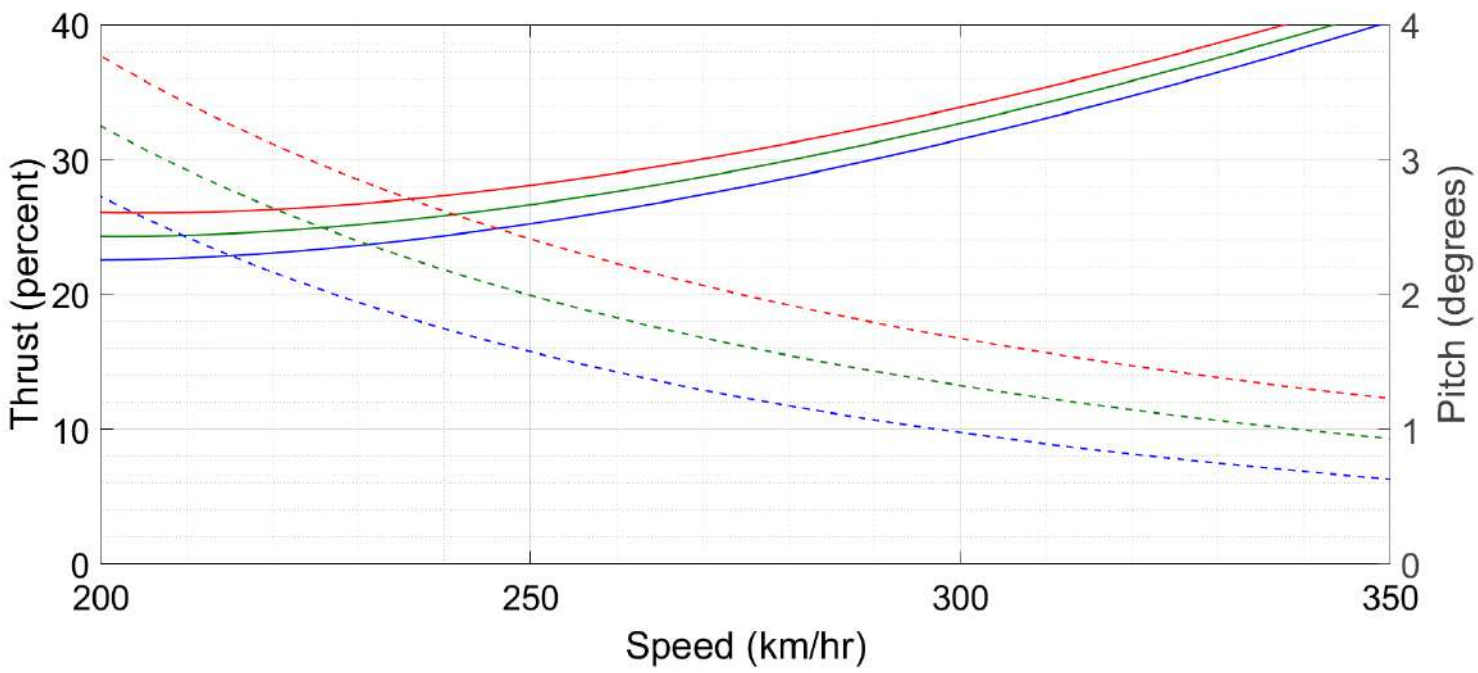


Figure 08 : *Characteristic curves for Our Plane. Solid lines attach to the left hand* y*-axis and dashed lines to the right hand* y*-axis. Blue, green and red correspond to climb rates of –200, –100 and 0 fpm (level flight) respectively.*

The red line (level flight) is of course the same as the green line of Fig. 02; the other two lines are new. We can see that a thrust of about 25 percent and a pitch of 2·4° give us an equilibrium descent rate in the 100-200 fpm range at a speed of 210-220 km/hr. So, let's define these as the target thrust and pitch at touchdown, and plan to transition to these values from approach thrust and pitch (16 percent, 0·25°) during the flare.

Here is the simulation result.

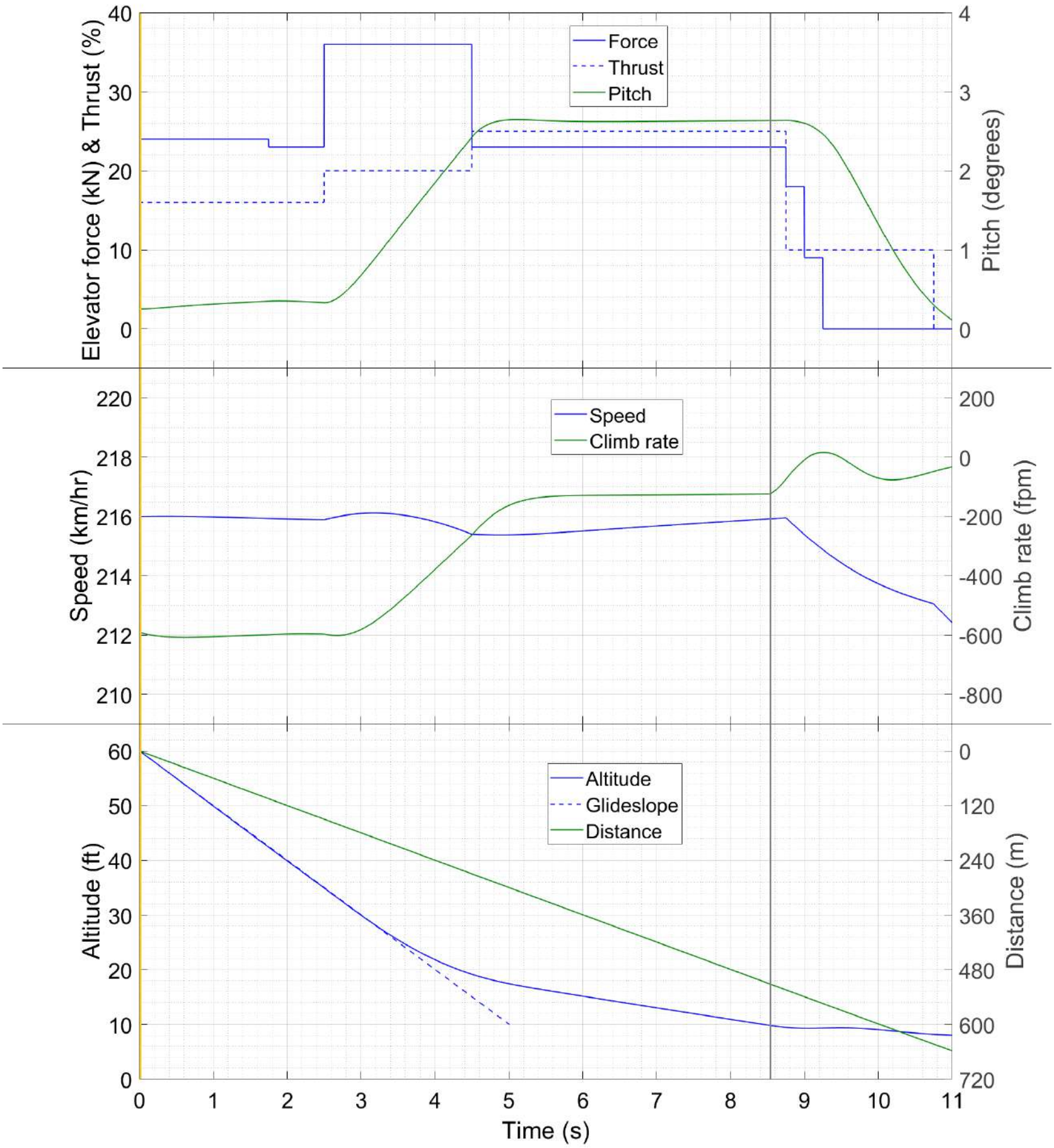


Figure 09 : *Time traces of different variables during a steady state flare and touchdown.*

It starts from the threshold, in approach configuration. I have initiated the flare at 35 ft (wheels 25 ft) above ground, using the same $\bar{f}_p = 36$ kN as in the transient flare. This time, when the pitch becomes 2·4° (top panel), I have returned to the trim state. Parallelly, I have increased thrust to 20 percent during the flare and then 25 percent when it is finished. Almost immediately, the speed becomes nearly constant (middle panel, note the scale on the left hand y-axis!). About half a second after returning to trim, the pitch stabilizes to a constant and one second after that the descent rate stabilizes to a constant as well. Thus, the flight beyond $t = 6$ s is at or very near a fixed point. The descent rate is about 130 fpm, as predicted during the planning phase. In this condition, the aircraft wafts down to the ground at $t = 8{\cdot}5$ s; thereafter I have taken down the elevator force and retarded the thrust. Note that the presence of ground effect in real aircraft will make the thrust increases during the flare unnecessary – if anything, the thrust might have to be retarded to maintain the equilibrium condition just next to the runway.

From Fig. 09 we can deduce the consequences of initiating flare too late and too early. If we're too late, then the ground will come up before the steady state is reached, and we'll get a harder landing. If we're too early, then we'll cover more and more altitude in the touchdown steady state, which gobbles runway like anything. The simulation touchdown occurs at about 515 m, with 150 m of these being used for descending the last five feet. The primary drawback of the steady state flare is the extra length as compared to the transient flare – while Fig. 09 contains an impractical 2·5 s (5 ft descent) of steady state flight for demonstration purposes, 30 horizontal metres per vertical foot is no joke. The less we have of the touchdown equilibrium flight, the shorter the landing; in the limit of no equilibrium flight at all, we get a transient flare. The advantage of the steady state flare however is that it is guaranteed to end in a touchdown, with zero risk of flotation or tailstrike. If the target descent rate is chosen for a firmer landing, say 300-400 fpm, then the drawback of excess runway use is significantly mitigated. Hence, when the landing circumstances are difficult, then a steady state flare targeting a firm landing is the safest option to go for (see also the next Section). As a flipside however, the steady state flare is possibly harder to execute in reality (as against on a simulator) than a transient flare, since it requires both an increase and a decrease of elevator force during the flare, whereas the transient one requires the increase alone. ■

Quasistatic flare

In this technique, we bring the aircraft to level or almost level flight a few feet above the runway. Then, by cutting power to idle, we let it decelerate while holding pitch. As it slows down, the lift decreases and the plane starts to descend, eventually settling down on the runway. The technique is quasistatic because during the flare the aircraft is not in one steady state but passes through (or close to) a succession of steady state configurations as the speed bleeds off slowly. Here is a simulation of it.

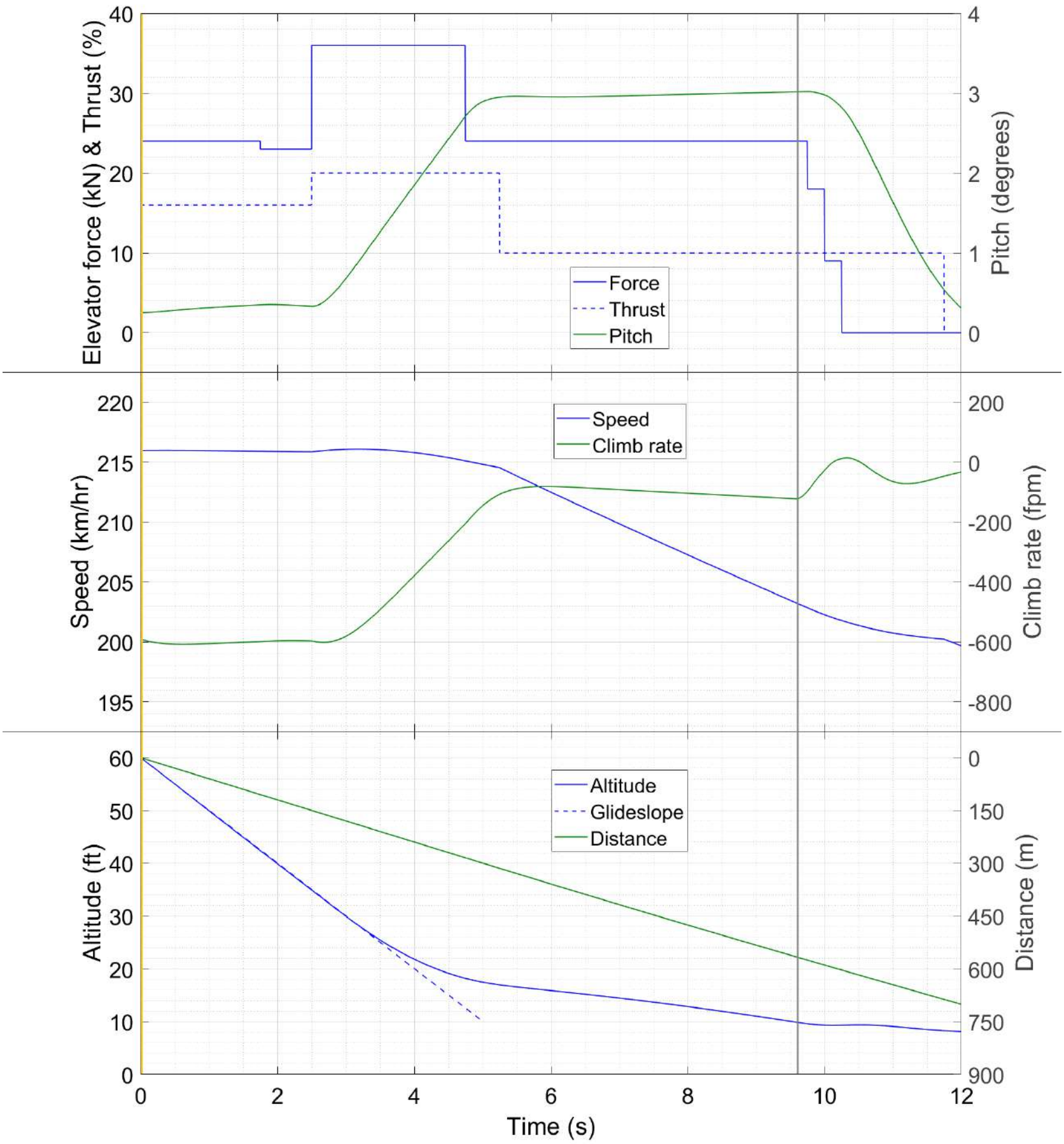


Figure 10 : *Time traces of different variables during a quasistatic flare.*

The approach and initial nose-up force are the same as in the other two cases, and the flare starts at 35 ft as in Fig. 09. The difference is that the pitch increase continues upto 3° while the thrust retards to idle. The post-flare equilibrium is established at $t = 6$ s; at this instant, the descent rate is barely 80 fpm and the altitude is 16 ft (wheels 6 ft). From this point onwards, the speed reduces continuously due to the low thrust setting and the descent rate starts increasing. Touchdown occurs at a descent rate of 120 fpm, 570 m forward of threshold. The advantage of this technique is that it is easy to implement in reality – just settle into level flight a few feet above the runway and then let things take their course. It also depends almost entirely on visual cues rather than on instrument readings, and results in a soft touchdown even if the initial settling height is off by a couple of feet. For these reasons, it is the go-to landing strategy in general aviation. The drawback is that, when applied to jetliners having twice or thrice the landing speed of GA aircraft, the runway lengths involved become excessive. Moreover, due to ground effect, idle thrust at 5 ft above the runway may cause the plane to speed up instead of slowing down. Then, the lift will increase and it will

never reach the runway. For this reason, the quasistatic flare is inapplicable to the types of aircraft which are the primary focus of this Article. ■

While we're at it, let's also look at the dynamics of the aircraft immediately following the touchdown. If we treat the undercarriage itself as massless, then we can obtain the z-directional motion by modeling the aircraft as a point mass with a vertical spring below it, as shown in the Figure below. This is exactly how our ground reaction model (5B–01) describes the aircraft. In the Figure, we also see lift and gravity acting on the mass.

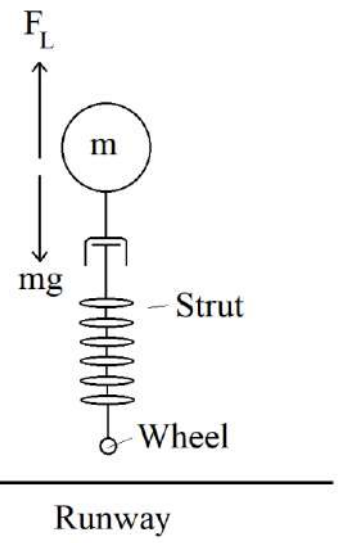


Figure 11 : *Mass-spring-damper model of the aircraft undercarriage.*

We can see that the spring can be compressed between the aircraft and the ground but not extended – as soon as its length tends to exceed the natural length, the bottom will lose contact with the ground and the spring action will cease. Hence, whenever the plane's altitude exceeds 9·84 ft, there will be a loss of contact between wheels and ground. If the landing is heavy, then the spring will compress significantly, and there is a risk of the subsequent re-expansion pushing the aircraft up out of the ground. This is a bounce, and is undesirable for obvious reasons. If the landing is very smooth however, then also there is a risk of the contact being lost almost immediately because of the lift. This is undesirable because weak or no contact can cause the wheel to **shimmy**, which is a rapid oscillation of the strut about the o-axis. Such loss of contact is mitigated by deployment of spoilers (in our simulation, by rapid neutralization of elevator) as soon as contact is detected. In the third panel of Fig. 05, we can see first a decrease and then an increase of the altitude immediately after touchdown. Because this is a model landing, the increase does not take it beyond 9·84 ft so that the contact is never lost (the spring remains compressed by 3 inches even at maximum extension post-touchdown). But, in a less-than-model landing, a momentary separation and reconnection can well occur, and that can lead to shimmy.

To better understand the contact retention dynamics, let's solve for the spring-mass-damper system of Fig. 11 with the lift being treated as constant. Our equation is

$$m\ddot{z} = -k(z-3) - C\dot{z} - mg + F_L \quad . \tag{08}$$

If we let $w = z - 3$ and substitute the parameter values from (5B–01), we get

$$\ddot{w} + 0{\cdot}833\dot{w} + 16{\cdot}7w = -g + F_L/m \quad . \tag{09}$$

The initial conditions will be $w(0) = 0$ and $\dot{w}(0) = u_0$, where u_0 is the climb rate (including the negative sign) at the instant of touchdown. We will consider two values of F_L. The first will be $1{\cdot}1mg$, which is approximately what we have for the transient flare (the bottom panel of Fig. 05 shows an acceleration of 1·1g immediately prior to touchdown). The second will be mg, which is close to what we have for the steady state flare. The equations in these two cases will be

$$\ddot{w} + 0{\cdot}833\dot{w} + 16{\cdot}7w = 0{\cdot}98 \quad \text{, and} \tag{10a}$$

$$\ddot{w} + 0{\cdot}833\dot{w} + 16{\cdot}7w = 0 \quad , \tag{10b}$$

respectively. Their respective solutions for the given initial conditions are

$$w = 0{\cdot}0587 + e^{-0{\cdot}0417t}\left[-0{\cdot}0587\cos 4{\cdot}07t + \left(\frac{u_0}{4{\cdot}07} - 0{\cdot}0060\right)\sin 4{\cdot}07t\right] \quad \text{, and} \tag{11a}$$

$$w = e^{-0{\cdot}417t}\left(\frac{u_0}{4{\cdot}07}\sin 4{\cdot}07t\right) \quad . \tag{11b}$$

In the below Figure, we will look at plots of the solutions (11a) and (11b) for four different descent rates at touchdown – 100, 200, 300 and 600 fpm*. Since the equations (11) cease to hold when w exceeds 0, i.e. when the undercarriage loses contact with the ground, we plot the solutions only until such exceedance occurs.

* To split hairs, I have used –0·5, –1·0, –1·5 and –3·0 m/s for the four cases.

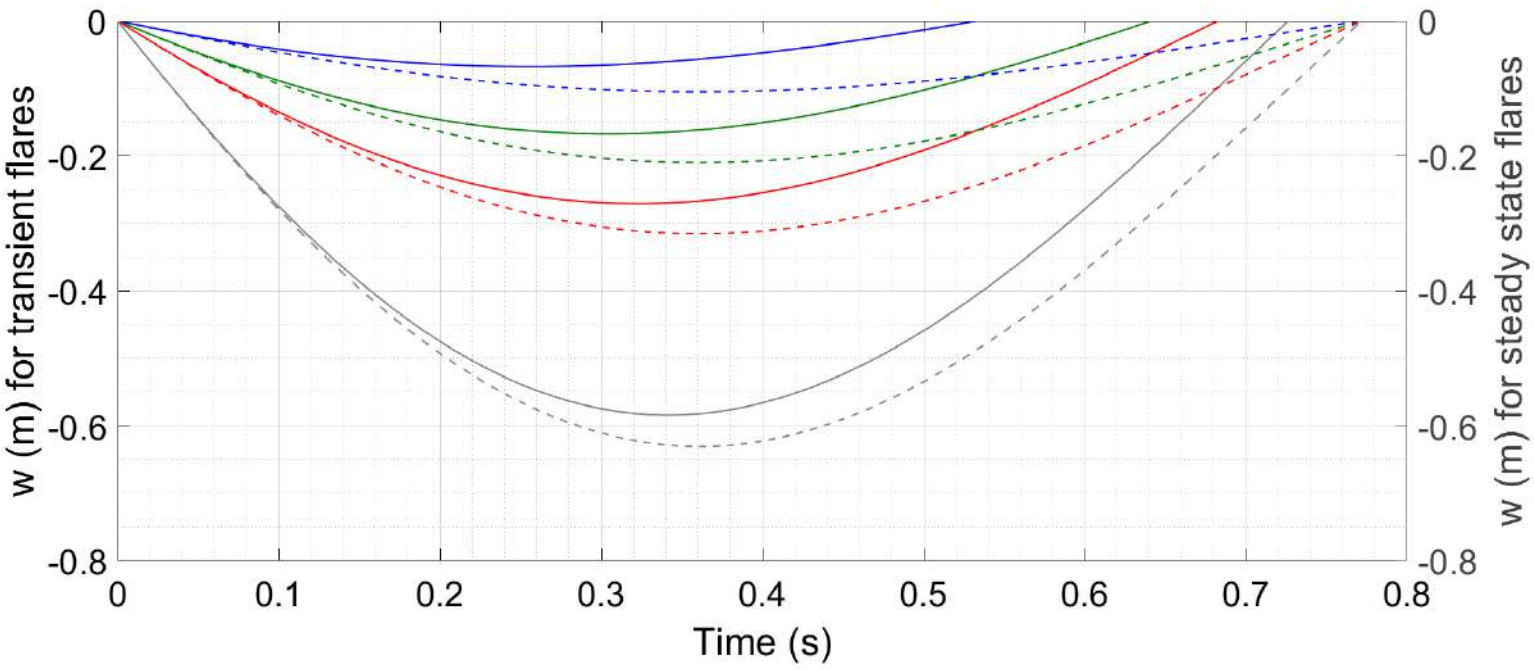


Figure 12 : *Trajectory of the aircraft CM as a function of time. Solid lines attach to the left hand* y*-axis and dashed lines to the right hand* y*-axis. Blue, green, red and grey correspond to touchdown descent rates of 100, 200, 300 and 600 fpm respectively.*

In each case, the undercarriage loses contact after a while, which is plausible since w describes the oscillation of a spring about a zero equilibrium point for the steady state flares and a positive equilibrium point for the transient ones. Evidently, reduction of lift will have to be achieved within this time frame to avoid the loss of contact, which is what we've done in all the simulations.

What is more interesting is the time it takes to lose contact. For the transient flares, the time to loss of contact increases with increase in the descent rate. From 0·53 s at 100 fpm, it goes up to 0·64 s at 200 fpm and increases more slowly thereafter. Hence, a firmer touchdown does give us more time to reduce lift before the loss of contact occurs. As the descent rate increases though, the vertical speed of the fuselage during its rebound from the lowest point becomes significantly higher. Then, even if the lift is reduced, inertia can take the aircraft past the loss of contact point i.e. result in a bounce. This suggests an optimal descent rate – neither too soft nor too hard – to minimize the chance of wheel shimmy. In particular, the anti-grease brigade appears to have scored a point here. For the steady state flares however, the time to loss of contact is the same for all the descent rates, and this is greater than the maximum obtained for the transient flares. Even at 100 fpm, we have 0·77 s to reduce lift and stay on the ground. Thus, with this technique, the grease job is back. For the quasistatic flares, F_L at touchdown is less than mg so it buys us even more time to reduce lift. Comparing Figs. 05, 09 and 10 for altitude vs time, we can see that the post-touchdown maximum altitude is visually very close to 10 ft for the transient flare, but visually some distance below 10 ft in the other two flares. In fact, in the transient flare, I had to initiate the elevator reduction a quarter second before the impact (see again Fig. 05 top panel) so as not to lose contact after touching down.

Earlier, I have deprecated our ground reaction model – why then did I use it for a calculation of shimmy ? This is because the qualitative aspects of the model are sound, even if the numbers turn out to be

implausible. It might well be the case that k and $\mathcal{C}$ of (5B–01) and the reaction torque (5B–02) are off by factors of two or five, that the springs are heavily nonlinear and can be modelled only as Duffing oscillators, etc etc. For this reason, the time window of 0·5-0·8 s of our calculation might well be 0·2 s (though unlikely) or 2 s (much more probable) in reality, and it will vary from aircraft to aircraft. But the basic principle of the undercarriage acting like a spring will remain true for all aircraft, as will the concept of a lift-reduction time window which will be higher for a steady state or quasistatic flare than a transient one.

All things considered, the ideal flare in normal conditions is perhaps the one where the elevator returns to trim and the aircraft just reaches a dynamic equilibrium when it touches the ground. That way, the descent rate at touchdown can be controlled, there is no risk of tailstrike, there is no wastage of runway and there is least probability of wheel shimmy. Timing and executing this flare on a real aircraft will of course require considerable skill and practice.

§50 **Further discussion, accidents and incidents.** Our calculated values of the height where flare is initiated are in excellent agreement with what Airbus recommends in its manuals [07] – wheels around 30 ft above ground for the narrow body aircraft and 40 ft for the wide body ones. In our simulations, the values were closer to 20 ft. As we have already seen, Our Plane is not an actual aircraft, but a fictitious one with plausible parameter values. Also, the flare height in our case was determined by our choice of 1·25°/s pitch rate – if we'd opted for a lower rate then we'd have got a greater height. The height can and does vary depending on individual pilots' preferences, to the extent that Boeing recommends a flare height of 30 ft rather than 40 ft for its largest jets [09]. It is interesting to observe that calculations of flaring height and landing distance are usually not attempted in flight dynamics Literature – two of the References cited in Chapter 1 have tried it and found numbers which are off by a factor of 2-3 in one case and almost 10 in the other.

In the approach and flaring simulations, we can again see the intuitive response of a stabilator as compared to a horizontal stabilizer plus elevator – maintain pitch by setting 24 kN, raise the nose with a higher $\bar{f}_p$ and lower the nose with a lower $\bar{f}_p$. All this is independent of speed, which is a big help. In many of the approaches, we can see considerable variation of speed, which can cause the response to become unintuitive in a two-piece tail. There, either we would have to make further stick adjustments to compensate for varying stabilizer force with change in speed, or we would have to adjust the trim wheel (not a recommended practice during approach and flare). This intuitiveness however comes with the drawback that the aircraft is more sensitive to stick input. Suppose that the maximum $\bar{f}_p$ we can command is 100 kN, and suppose this is achieved at a 60° deflection of the stick. This gives a stick sensitivity of 0·6°/kN, and the 12 kN difference between the landing trim $\bar{f}_p$ and the flare $\bar{f}_p$ corresponds to a 7° deflection of the stick. This is a small number – if the pilot makes even a 1° error in setting the position of the stick, then he will make a bad landing. With a two-piece tail on the other hand, let's apportion 60 kN to the stabilizer and 40 kN to the elevator (we need trim plus 33 kN during the takeoff, and the excess has to come from the elevator). With the same 60° full-scale stick deflection, we now get a stick sensitivity of 1·5°/kN, and the difference between landing trim and flare becomes 18°. This is far easier for the pilot to set and hold.

A best of both worlds can perhaps be obtained if we use a two-piece tail but configure the fly-by-wire to simulate a stabilator. For this, we can set two numbers A and B such that q° of stick deflection translates to $\bar{f}_p = A+qB$ kN at the tail. A will typically be the trim value while B will have to be chosen suitably depending on the aircraft weight and flight phase. Given A and B, the flight computers can adjust the elevator and stabilizer deflections so that the shifted linear relation between stick deflection and tail force holds true at all times. This implementation would be somewhat different from the auto-trim currently implemented on Boeing and Airbus aircraft. On Airbus, zero stick deflection attempts to maintain constant climb rate (1g acceleration) [10]. Boeing finds this unintuitive and configures the fly-by-wire such that zero stick input simulates an aircraft with fixed horizontal stabilizer. A shifted linear relation between stick deflection and $\bar{f}_p$ will probably retain a lot of the feel of a mechanical aircraft while using electronics to make the flying experience more intuitive.

Now let's come to the touchdown and the debate between greased and firm landings. It is undeniable that a greaser in the correct location on the runway requires greater skill on the pilot's part. Hence, in normal conditions, that should be the ideal landing to strive for. A pilot who is wafting his aircraft down onto the target is very likely not compromising safety of the flight; he is just more skilful than the one who is keeping it firm and on target. That said, there are a few circumstances where the ideal has to be a firmer, steady state landing. These are as follows.

► **The approach parameters are abnormal.** This refers to the case where you are too slow, too fast, in an improper pitch attitude etc when you cross the home. This can happen due to a malfunction of a component, an unscheduled overweight landing or a less than perfect approach made by you or your copilot. A greaser flare from such a position is unlikely to be something you have got practice with, and flotation in this case (especially overspeed) is about the worst thing you can do. Hence, we have to go for the safe option here and keep it firm.

► **There is a gusty wind.** Gusty wind means that its speed is varying rapidly and erratically with time. In this case, a sudden change in wind can cause a sudden change in airspeed. If a gust increases your airspeed right when you are two feet above the runway, then a greaser can turn into a floater. Since this is unacceptable, you have to aim for a firm, decisive touchdown. If the gust decreases your airspeed when two feet above, then the landing will become heavier still, through no fault of your own. Afterwards, you can explain to the passengers why you did as you did. A *steady* wind however, even from the worst possible direction, should not preclude a greased touchdown if you are skilful enough with the controls.

► **The runway is wet or contaminated.** Wet and contaminated both mean that the runway contains water – contaminated has more water. In this case, there is a risk of aquaplaning, in which the wheels are supported just above the runway surface by a very thin layer of compressed water. If the aircraft aquaplanes, then the efficacy of its wheel brakes becomes nil, and the landing ends in grass (or worse). To prevent aquaplaning, you have to plonk the aircraft down onto the runway so that the wheels can punch through the film of water and make contact with the asphalt. Again, you can explain the thud to the passengers while you are taxiing to the terminal building.

Just to clarify, these three conditions are when even the most proficient pilot will touch down firmly. If you are new to the job or to the aircraft type etc, then sticking to firm touchdown is the best option if the runway is short. Practising grease jobs (essential if you want to pull it off!) is best when the runway is long and you have ample space to waste through some inadvertent flotation (bound to happen while you are in the learning stages).

A good landing features both a good approach and a good flare. In popular discussion, the distinction between the two can sometimes become blurry [11-13], so let me quickly clarify the role of each. A good approach sees you crossing the home at the correct altitude and thus sets you up for a touchdown at the correct location. It also maximizes the probability of a good flare, since you are most used to initiating flare from the proper approach configuration. A bad approach sees you crossing the home at the wrong altitude. It automatically screws up your landing location and increases the probability of a poor flare since you are likely unused to initiating flare from an improper configuration. A good flare takes up minimal runway beyond the landing point in the absence of the flare. It also ensures the optimal rate of touchdown – greaser under normal conditions and firm under abnormal ones. A bad flare can eat up huge amounts of runway through flotation or result in a hard landing with bounce, which again wastes runway due to delayed application of brakes. Thus, approach and flare are complementary and inter-related aspects of landing.

Multiple aviation accidents and incidents have occurred due to ill-configured approaches and poor landings. We focus here on two of them, both involving the airline Air India Express (AXB). These two are in fact the only accidents involving an Indian airline within the past 20 years. The first accident was with AXB 812 on 22 May 2010, a Boeing 737-800 from Dubai (UAE) to Mangalore (India). The second was with AXB 1344 on 07 August 2020, another Boeing 737-800 from Dubai (UAE) to Kozhikode (India). An additional feature common to both accidents was that the airports in question were tabletop designs, implying a sharp drop in the altitude of surrounding terrain immediately outside the perimeter.

In AXB 812 of 22 May 2010, the captain was experiencing deep sleep for about 1·5 hours prior to the commencement of the descent, while the autopilot was flying and the first officer was making the radio calls. Captain awoke approximately 20 minutes prior to the crash, when the descent should already have been commenced. However, due to traffic restrictions, ATC required AXB 812 to commence descent when 140 km away from Mangalore, instead of 240 km which the first officer had requested. This necessitated a steeper descent than was planned. During parts of the descent, the captain, now the pilot flying, could be heard yawning and clearing his throat, suggesting an incomplete reversion to the wakeful state. The checklists and actions to be taken during the descent were ignored or abbreviated by both him and the first officer (pilot monitoring, working radio). As a result, the flaps and speed were deviated from planned settings when the ILS was first intercepted horizontally. At this time, the aircraft was vertically far above glideslope and was descending faster than was normal, with the spoilers extended. When Mangalore ATC queried whether AXB 812 was established on approach, the captain strongly suggested to the first officer to lie "affirmative" – the first officer complied. 4 km behind the airport, the aircraft was almost 1500 ft above the glideslope. At this point, the ILS receivers on board the aircraft caught onto a *false glideslope*, which can be generated by reflections of the radio waves emitted by the airport instruments. False glideslopes typically have inclinations which are integer multiples of the true slope – in this case, AXB 812 caught the 9^{o} slope and believed it to be the glideslope. Although the captain soon realized the error, the descent rate and speed were uncontrollable, and the aircraft passed the threshold at 200 ft altitude and 37 km/hr above the intended landing speed. Touching down 2/3 way into the 2450 m long runway at Mangalore, the aircraft was completely unable to stop in time. Crashing through the airport perimeter fence, it fell into the ravine outside, killing all but eight of the 160 passengers and all the crew.

In AXB 1344 of 07 August 2020, the initial setup was quite different. While the captain of AXB 812 had been negligent, the captain of this one was conscientious and was, at least at first, flying by the book. Weather at Kozhikode was problematic with heavy rain and high winds from West. To compound the problem, windshield wiper on the aircraft was faulty. AXB 1344 first made an approach towards Runway 28 (into the wind) at Kozhikode; however it went around when pilots were unable to establish visual contact with the runway at the decision height. While they were preparing for a second approach to Runway 28, a departing aircraft Air India Flight 425 requested permission to use Runway 10. Kozhikode ATC switched the runway immediately and asked AXB 1344 if they were prepared to make an approach to Runway 10. Despite the presence of tailwind, AXB 1344 accepted the changed runway without hesitation. While the initial approach proceeded as planned, deviation from glideslope began on final approach when the captain (pilot flying) disconnected the autopilot and prepared for manual landing. The descent rate increased to 1500 fpm and the aircraft sank below the glideslope. The first officer (pilot monitoring) called out the high descent rate. When the captain attempted to correct this, the approach became unstabilized, with the descent rate decreasing to 300 fpm while the aircraft floated up above the slope. Subsequently, the descent rate again increased to 1000 fpm. Threshold was crossed at 92 ft and descending rapidly, at which point the captain increased thrust to arrest the descent rate, resulting in an unwanted acceleration of the aircraft. In addition, the captain made frequent stick inputs of opposite signs. The descent rate oscillated wildly between 120 and 720 fpm and the aircraft eventually touched down halfway into the 2700 m long runway. Given the excessive speed, slippery conditions and the tailwind, it was unable to stop in time. Crashing through the airport perimeter fence, it fell into the ravine outside killing both the pilots and 19 out of the 184 passengers.

We can see that in both cases the captains used an incorrect or at least sub-optimal technique of approach stabilization and disturbance recovery. Both these flights, and AXB 1344 in particular*, could have been salvaged by monitoring the velocity ratio during the approach – since it is currently not available on a separate instrument, the pilots should have tracked it manually. In fact, the situation of AXB 1344 is extremely reminiscent of Fig. 07, minus the caricatured exaggerations. What should have been attempted in this case after the initial destabilization was adherence to V_z/V and a firm, steady state touchdown. In addition to the captain's technical error, there were also issues of crew resource

* For AXB 812, the amount of deviation involved might well have made any attempt at recovery hopeless. The safest option for that one would have been to go around and try the landing again.

management (see §08) in both the accident flights. In AXB 812, the first officer thrice called for go-around which the captain ignored; thereafter the first officer did not proactively initiate a go-around himself even though the operating protocol called for the same. In AXB 1344, the first officer failed to adopt a sufficiently emphatic tone while calling attention to the captain's technical inadequacies, made no calls for go-around until it was too late and again neglected to seize controls himself when the aircraft was in a precarious condition. Adding to the problems with AXB 1344 was the captain's reluctance to divert to an alternate airport even though airline procedure called for it if the destination had rainy weather and windshield wiper was fully or partially inoperative. Ironically, the captain's motivation in not diverting was grounded in duty rather than negligence. AXB 1344 was one of a series of Vande Bharat repatriation flights returning Indian citizens from foreign countries during the worst of the COVID-19 pandemic. The captain was scheduled to operate another such flight the next day; if he had diverted, then he would have exceeded his duty hours and been prohibited from working the next flight. There being no other captain available for that flight, it would have had to be cancelled. Hence the captain felt moral pressure to land within his duty hours, leading to his cutting corners regarding the choice of airport and runway. Unfortunately, his desire to serve his country, manifesting inappropriately, had the same consequences as did the actions of the captain who slept in his seat.

A further factor which can complicate an approach and landing is partial or full engagement of the autopilot during manual operation and a consequent mismatch of the intentions of the pilots and of the machine itself. For instance, as we have seen in §48, a sequence of actions to slow down the aircraft takes place automatically following touchdown, triggered by weight on wheels. If there is a question of going around after touchdown (too long, too fast, banked, bouncing etc), then this sequence has to be manually deactivated or paused. One accident related to this occurred with Emirates Flight 521 on 03 August 2016, a Boeing 777-300 from Thiruvananthapuram (India) to Dubai (UAE). After touching down at Dubai more than 1 km forward of threshold, the pilots attempted to go around. They electronically selected TOGA thrust and applied the appropriate stick inputs. However, the autopilot was configured to use low thrust settings after touchdown so it did not respond to the command for TOGA thrust – the aircraft climbed a few feet, decelerated, descended, slammed into the runway and caught fire. A firefighter was killed while trying to douse the blaze; fortunately, there were no fatalities on board the aircraft as well.

We can now answer a few more questions from the Quiz. Q10 cracks almost on autopilot; the correct answer is Choice B. The question specifies skilful execution, so the flare will be transient. For this flare type, we used about 350 m in the simulations. With a faster approach (many transport aircraft come in at approximately 250 km/hr) and a heavier plane (lower pitch rate in flare), the distance can go upto 500 m, which still remains well within the ambit of Choice B. In Q01, we see the aircraft with undercarriage extended – this automatically rules out Choice B. The aircraft is either pictured a few feet after takeoff, when the undercarriage is yet to be retracted, or in its final approach, when extended undercarriage is normal. The pitch is visually very low, and we can measure it to find 3°, see the below Figure.



Figure 13 : *The aircraft from Q01 of the Quiz. Relative to the horizontal (green line), the* d*-axis (along the windows) is raised by approximately 75 pixels for 1240 pixels' horizontal run, giving a pitch of 3°.*

Such a low pitch cannot occur at takeoff – even at the instant of separation from ground, the aircraft requires more than 3° pitch (equal to angle of attack) to generate enough lift, and thereafter the pitch only increases until it settles to its equilibrium value corresponding to a steep climb gradient plus the angle of

attack. 12° was the value in our simulation; though Our Plane isn't real, it's realistic. On the other hand, during approach and landing it is normal to see a slight positive or slight negative pitch depending on the aircraft type, weight, speed and configuration. Hence the correct answer is Choice C. Further confirmation of the answer comes from the fact that the flaps are heavily extended, which is again a normal procedure for landing. To give you a better idea of what the aircraft looks like during landing, I include below a schematic profile of Our Plane during the simulation of Figs. 04-05. The profile is schematic because the trajectory is blown up in the *z*-direction.

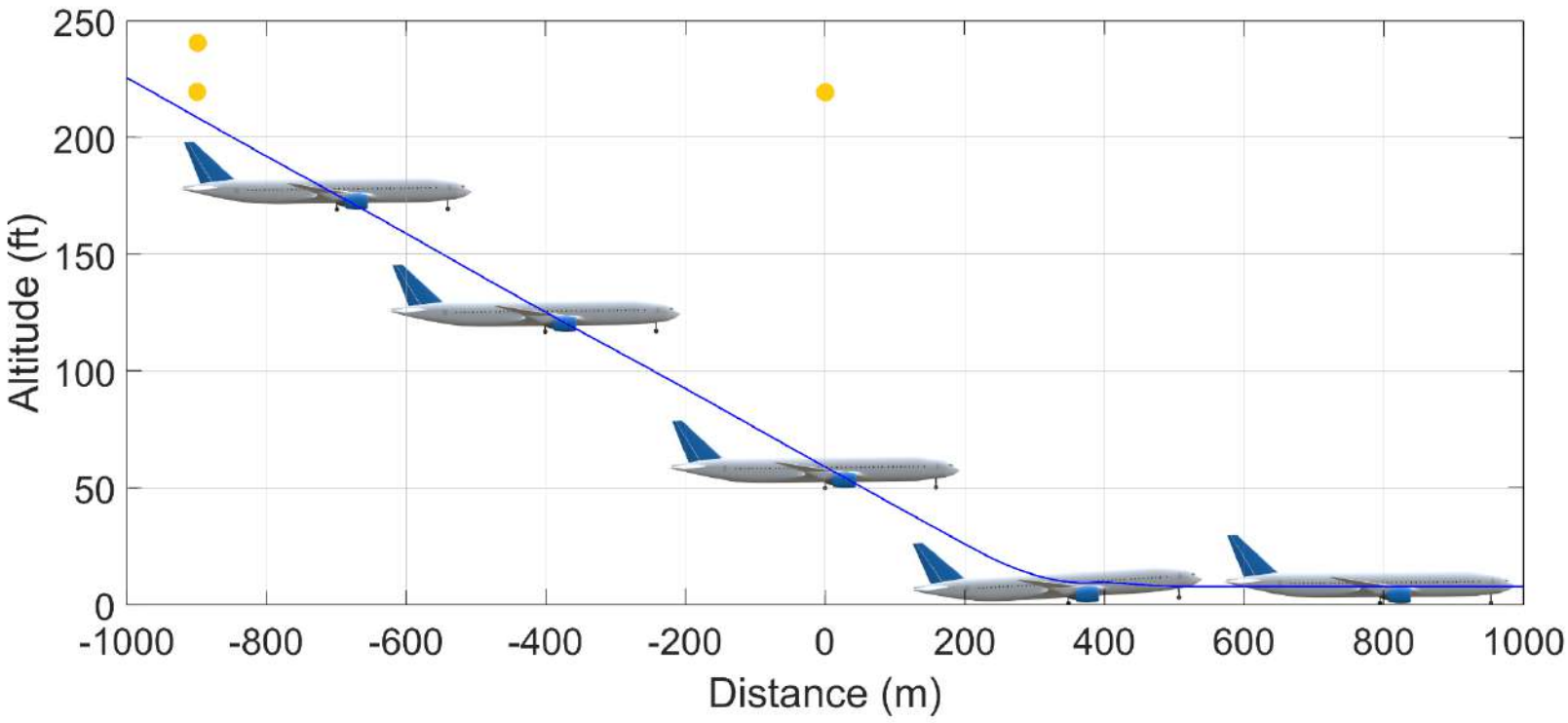


Figure 14 : *Schematic profile of Our Plane during the simulation of landing. Although the pitch is accurate, the trajectory is heavily expanded in the z-direction. Otherwise, the aspect ratio would become 20:1 for the approach alone and even more for the ground run – not a practical Figure. The plane itself is also over-large. The double-yellow and yellow dots correspond to the inner and the home; flaring begins between the third and fourth snapshots.*

Q09 is the next to crack – 10 km away from the airport corresponds to final approach for the incoming aircraft. Hence, they must be on or near the glideslope, which corresponds to an altitude of 1700 ft at that distance. Choice B is the closest to this and must be the correct answer. Q12 describes exactly the situation analysed in §46 – the decelerated approach is quintessentially time-dependent while the power curve is a characteristic. Hence the speed at the top of the approach cannot be determined using the power curve alone, making Choice D the correct answer. What will the desired top speed be ? That, starting from which, if we use flight idle thrust throughout the approach, then the aircraft will reach V_{ref} at the home. Practically, we shall have to use a lower speed at the start of the approach so that we can keep the approach thrust above idle – that way, if there's a tendency towards overspeeding, we can retard to idle and correct the deviation without having to use spoilers. Extending spoilers during approach is not a recommended practice since it changes the lift and the handling qualities of the aircraft, and may result in destabilization of the approach.

It goes without saying that the next manoeuvre will be a softie – this time we exit the pitch plane altogether.

E. COORDINATED TURNS

Turn coordination refers to the act of ensuring that during the entirety of a turn, the aircraft is facing the direction in which it is flying. This takes place in the yaw plane.

§51 **Turn coordination.** A coordinated turn is one where yaw φ equals azimuth ξ (equivalently, heading equals track), or the plane's velocity has no component along the q-axis. q-axis velocity is also called sideslip, so a coordinated turn means no sideslip. This is of course a highly desirable situation, and is achieved using

the vertical stabilizer and rudder, as we shall see here. To pull a turn we need centripetal acceleration. This comes from the term f_{ex} in (3C–03). In this equation, f_{ex} acts along the q-axis. In a real aircraft, centripetal acceleration comes from banking, as we have seen in §31. Since lift acts along the o-axis, the actual turning force has zero component along q. The banked lift does acquire a component along the n-axis where n,t,v is the basis defined in §17. However, the yaw plane model on its own has no scope to accommodate either bank or the n-axis, so we go with a stand-in f_{ex} acting along q. This is a concrete example of the limitations of yaw and banking plane models which we saw in §32.

When f_{ex} is applied, it changes the plane's azimuth. The moment the yaw differs from the azimuth, the angle of attack at the vertical stabilizer becomes nonzero and its lift generates a yawing moment which tends to make the plane face its direction of motion (this is identical to how the wings in a B-C-E aircraft tend to reduce α to zero; the vertical stabilizer is by definition at E which is behind B, so it works in the same way). So, even if the pilot commands f_{ex} but doesn't touch the rudder, the plane doesn't do too bad a job of coordinating its own turn. We see an example of rudder-free turn in the below Figures, for a turn of approximately 90° to starboard.

First comes the profile picture.

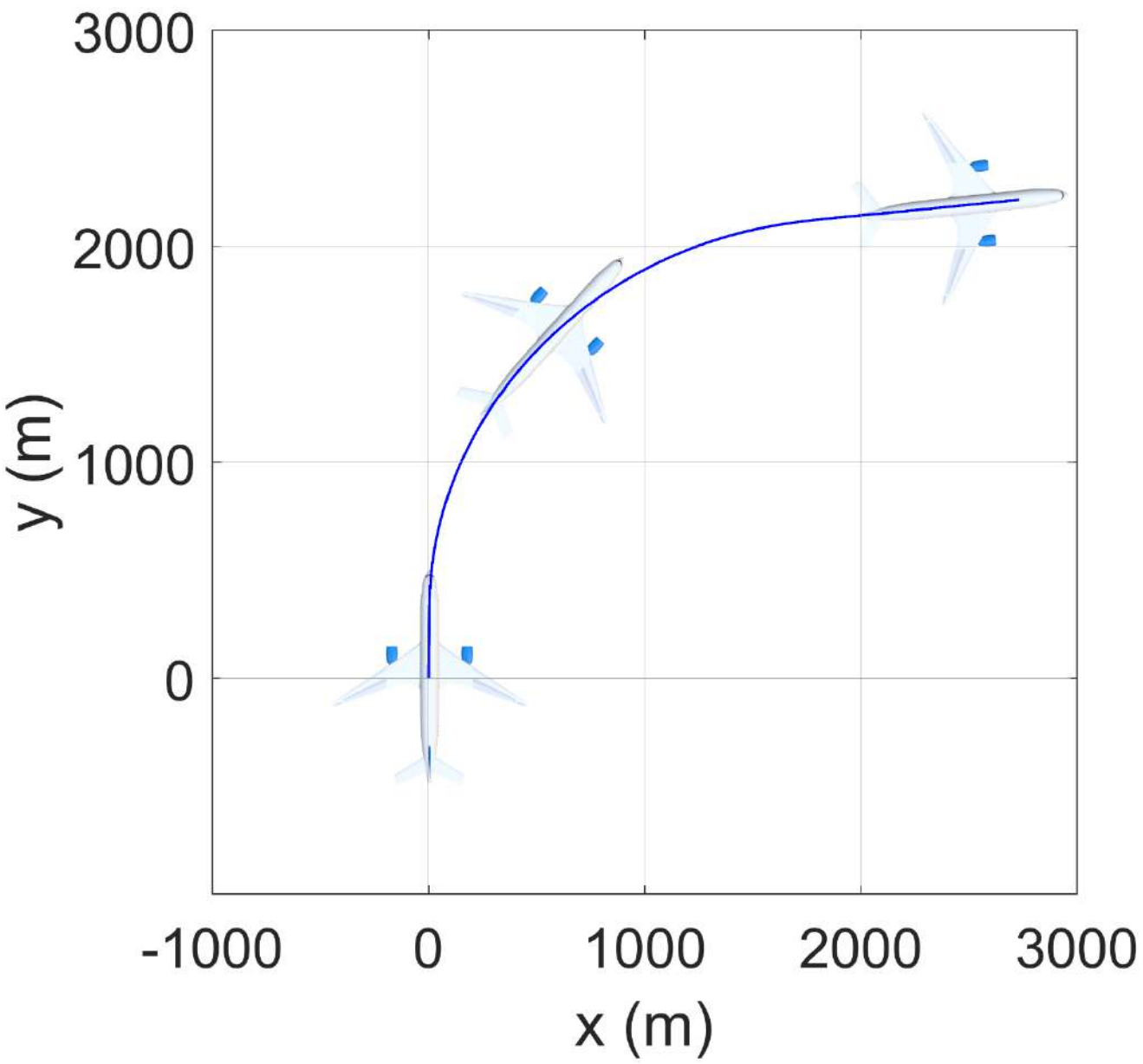


Figure 01 : *Profile of Our Plane during the uncoordinated turn. The trajectory is to scale and the yaw is correct, so that the picture gives you as good an idea as possible of what things look like during an actual uncoordinated turn. The plane itself is over-large as it would otherwise look like a bee and diminish rather than enhance the total effect.*

Next, the details of the manoeuvre.

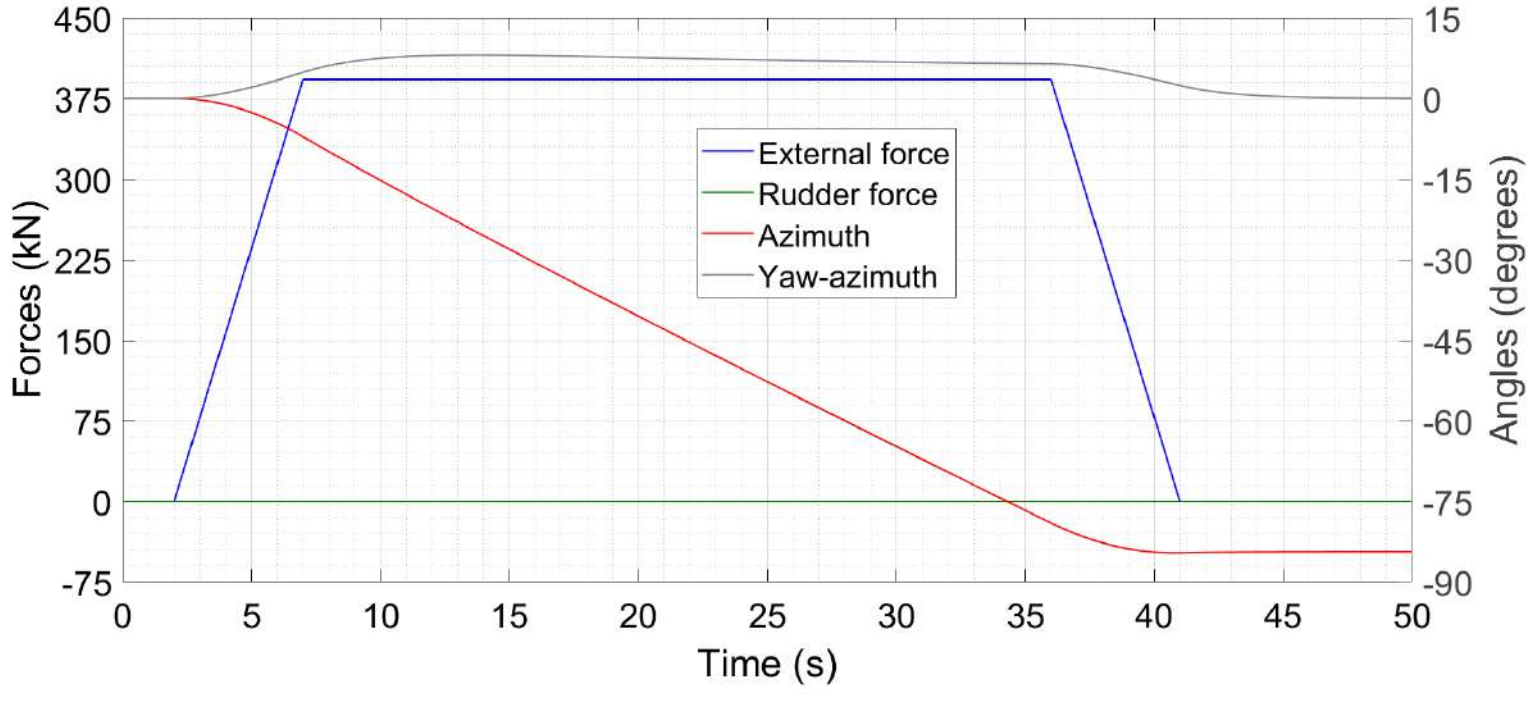


Figure 02 : *Time traces of different variables during the uncoordinated turn.*

We can see f_{ex} starting from 0 and rising to a maximum of 392·7 kN (40 percent of weight) in the time interval 2 s to 7 s, staying at 392·7 kN upto 36 s and decreasing back to zero over the next 5 s. There is no rudder input, so the control force f_w is zero throughout. The azimuth decreases uniformly while f_{ex} remains active, as we would expect. The most interesting quantity, the one which measures the degree of coordination of the turn, is the *yaw defect*, the difference $\varphi - \xi$. This difference rises to a maximum of 8° after the turn is initiated, and decreases very gradually to about 6° when the turn is complete, reducing quickly to zero thereafter. A positive difference indicates that the aircraft's nose points slightly to port side, which is what we would expect during a rudder-free starboard turn. We can see the evolving yaw defect in Fig. 01 as well – the angle between the plane and its trajectory is zero at the first and last instants shown but non-zero at the second.

While 6-8° of yaw defect isn't bad, it's also completely unnecessary. To kill it, we need to apply the rudder so that there is a finite yawing moment at zero angle of attack of the stabilizer. By the overdamped approximation, this moment, and hence the rudder force f_w, should be proportional to the turn rate i.e. to the external force. To get the sign of f_w, note that we need a clockwise or negative yaw moment for a starboard turn, which is achieved if f_w is along the negative q-axis. A few seconds on the simulator tell us that 44 kN is the best value of f_w to coordinate the turn in question. Here are the profile and the details with this force applied.

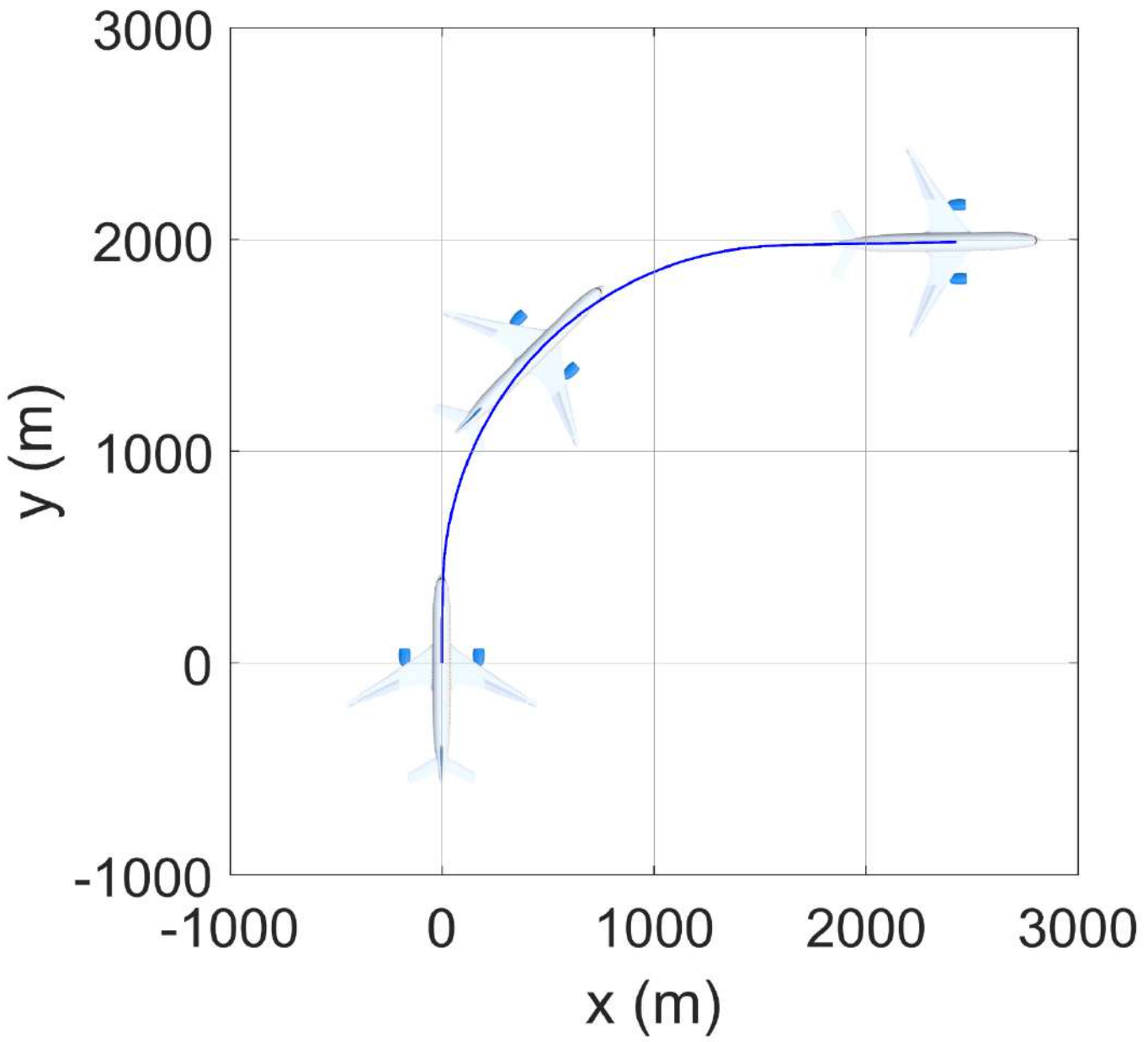


Figure 03 : *Profile of Our Plane during the coordinated turn. The trajectory is to scale and the yaw is correct, so that the picture gives you as good an idea as possible of what things look like during an actual coordinated turn. The plane itself is over-large as it would otherwise look like a bee and diminish rather than enhance the total effect.*

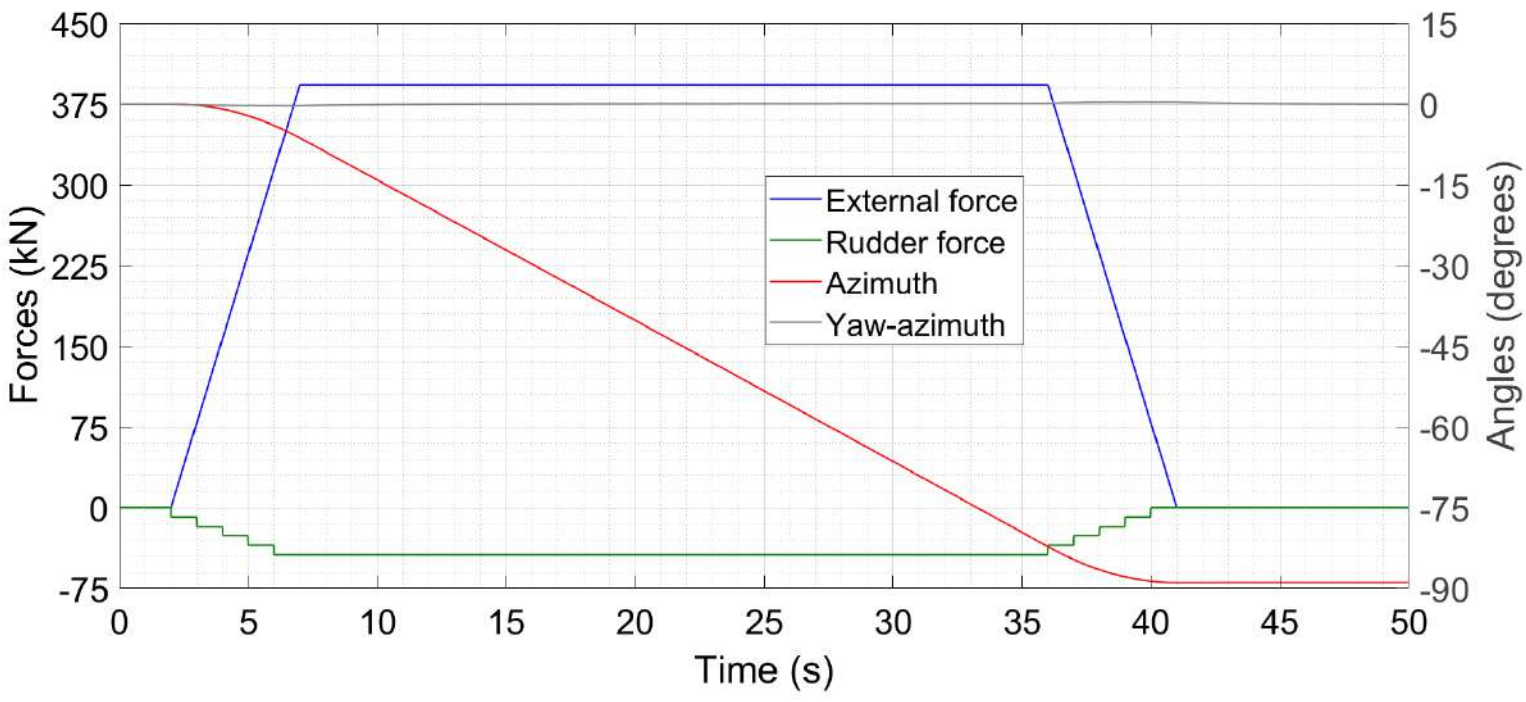


Figure 04 : *Time traces of different variables during the coordinated turn.*

The external force is the same as in Figs. 01-02 but now we have supplemented it with the appropriate rudder force. The yaw defect is zero throughout, at least to the precision of this graph. The total angle of turn is more than in Fig. 02 (almost 90° vis-a-vis 84°) because the q-axis f_{ex} goes entirely into producing centripetal acceleration here while with positive yaw defect, a (small) part of it goes into increasing the forward speed. In Fig. 03 we can see that Our Plane is parallel to its trajectory at all time-points shown.

Question Q15 of the Quiz deals with yaw plane and turn coordination. We can see immediately from Fig. 02 that the correct answer is Choice B. Just as the phenomena in the yaw and banking planes are easy, so too are the corresponding Quiz questions.

F. SIMPLE STALL

We have seen the phenomenon of aerodynamic stall in §21 and §29. In one line, stall refers to the sudden loss of lift when an airfoil exceeds a critical angle of attack. In the context of flying, a simple stall is when both wings enter a stall while the tail remains operative (nonstall). A simple stall on a fully functional aircraft is completely avoidable, and is also recoverable unless it takes place excessively close to the ground. Since a stall is most certainly not an intentional manoeuvre, I will not use the requirement-planning-execution approach this time. Rather, we will see Our Plane inadvertently approaching and experiencing a stall, and then recovering from it. For all simulations we use (3B–28) with a cycle time of 1 s. The values of C_1 and d_3 are 20 and 1 SI Units respectively. The stall angle of attack for the wings is 15°.

§52 **Approach to the stall.** A fully functional aircraft enters an unplanned stall only as a result of pilot error. A fully functional aircraft enters an unplanned stall only as a result of pilot error. A fully functional aircraft enters an unplanned stall only as a result of pilot error. The three repetitions should drum in the point that if you are flying a fully functional aircraft and you enter an inadvertent stall, then it's YOUR FAULT. What we are here to do is help you avoid this situation, both before takeoff and in flight. We will look at the erroneous procedures which can lead towards a stall, the signatures of an impending stall and the technique of correcting the situation immediately.

In the below Figure we see Our Plane at MTOW in the clean configuration (flaps retracted) progressing towards a stall. With a starting altitude of 5000 ft and a speed of 306 km/hr, the pilot is attempting a climb of 2000 fpm at a constant thrust level of 70 percent. Forty five seconds into the attempted climb, the aircraft is on the brink of stalling. Obviously, this is not what is supposed to have happened. So let's go through the failed climb step by step and analyse what the pilot could (and should) have done differently.

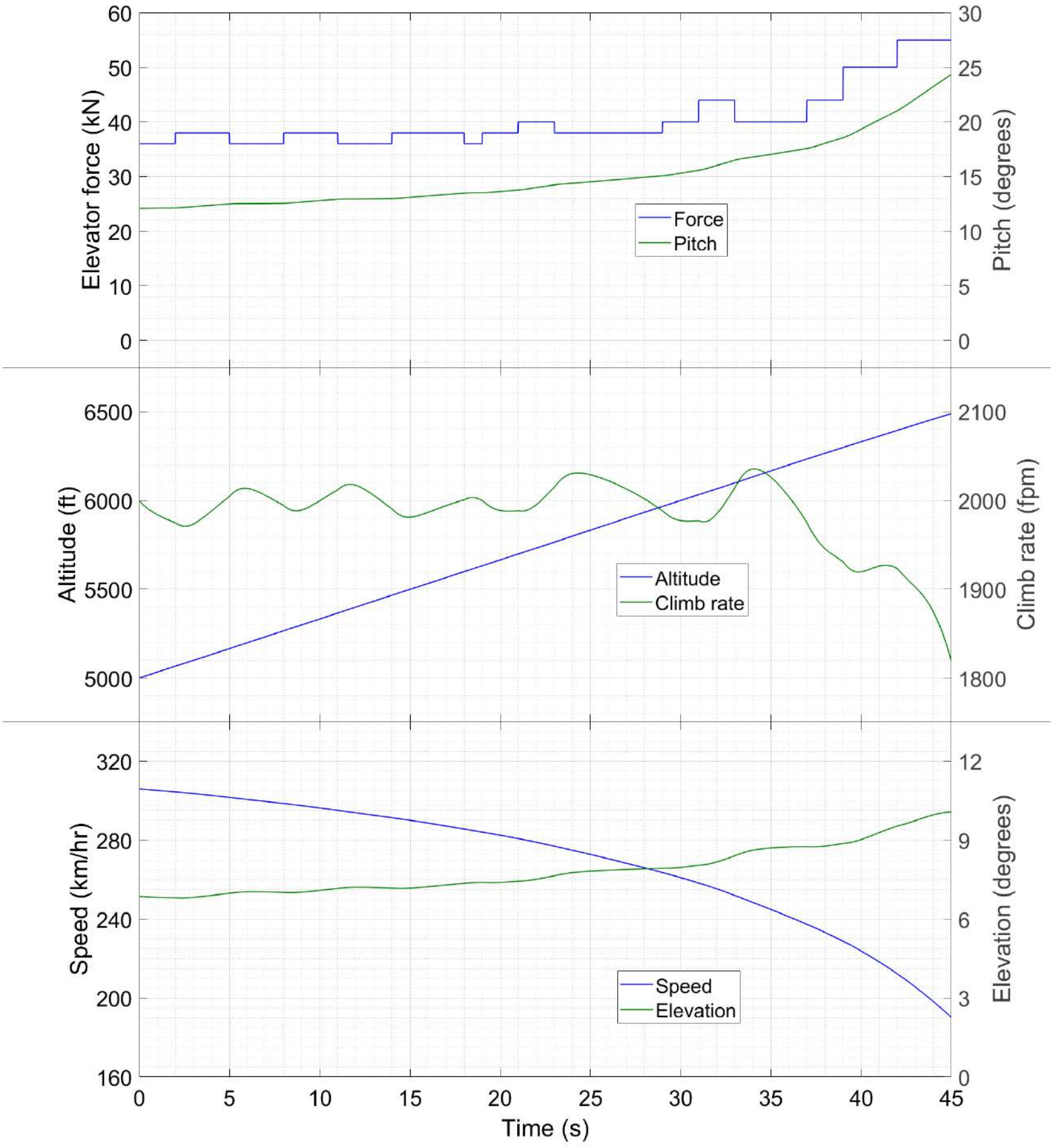


Figure 01 : *Time traces of different variables during approach to a stall.*

First off is the aircraft configuration. We have already seen in §36 and §41 that the fully loaded aircraft has reversed command upto 450 km/hr, and that flaps must be progressively deployed as the operating speed decreases. We used a moderate flap configuration for the takeoff and even then selected 320-plus km/hr for the initial climb. Yet, in this case, the beginning of the climb features the clean configuration at 306 km/hr only. This is highly contrary to procedure. Next let us look at the characteristics for the clean MTOW aircraft for climb rates of 0, 1000 and 2000 fpm. This time, I will plot the steady state angle of attack α^* on the right hand y-axis, for a reason to become clear shortly.

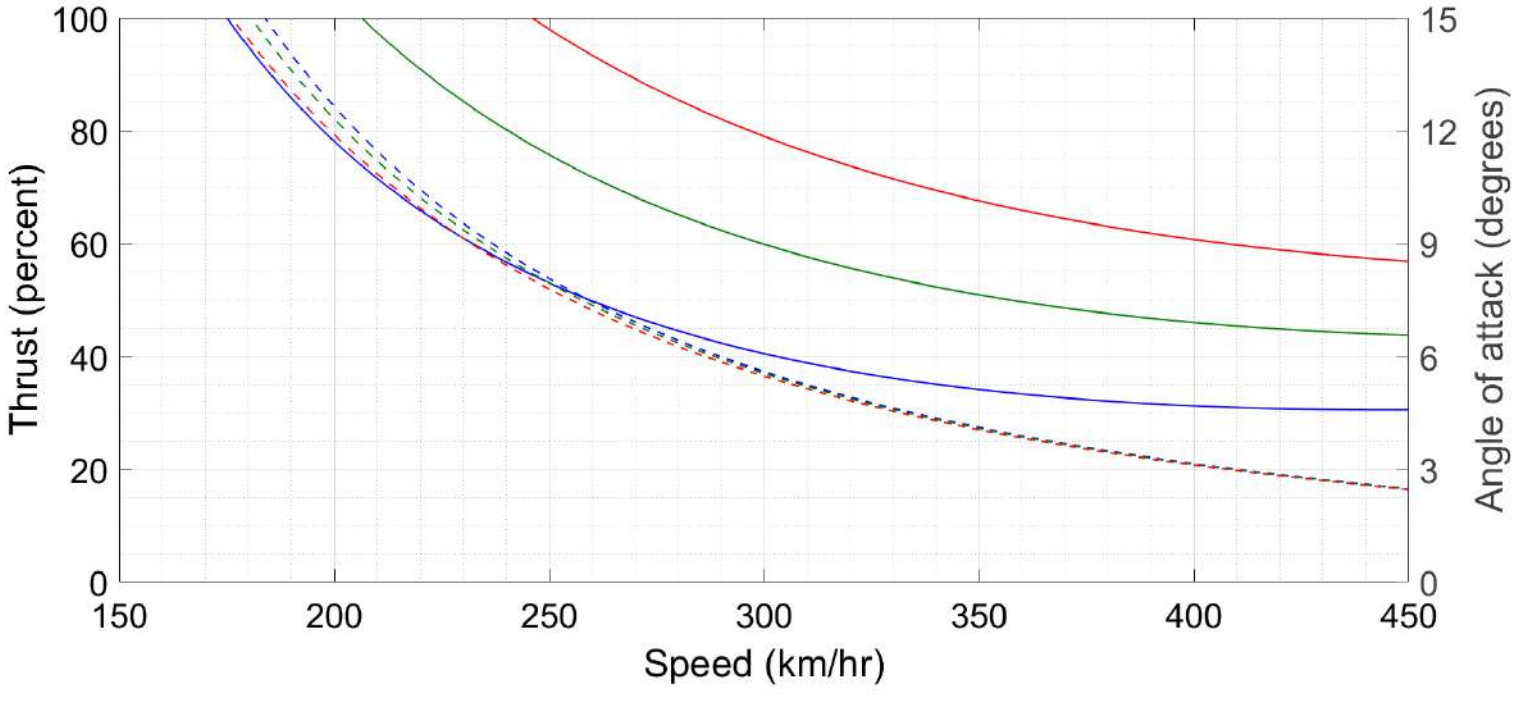


Figure 02 : *Characteristic curves for Our Plane in the clean configuration. Solid lines attach to the left hand* y*-axis and dashed lines to the right hand* y*-axis. Blue, green and red correspond to climb rates of 0, 1000 and 2000 fpm respectively.*

We can see that the power required for equilibrium 2000 fpm at 306 km/hr is about 78 percent – climbing while accelerating (as is customary) would have required still higher power. Hence, the thrust level selected by the pilot (70 percent) for the climb was inadequate. Both the flap and the thrust settings in the attempted manoeuvre show a clear lack of awareness of the aircraft's characteristics on the pilot's part. This awareness is supposed to be gained before the flight itself, so the first mistake made by the pilot is inadequate prior preparation.

If I were to stop the discussion at this point, then I would join the ranks of those sententious instructors whose motto of "do thine homework" makes them as popular as their teaching is effective. So, let us take for granted that the pilot has not done his homework in this particular instance. Then, what, if any, are the warning signs available to him in real time as the flight progresses towards stalling ? Before discussing this however, I will spend some time on the concept of **stall speed**.

There is only one parameter which determines whether the wing will stall or not, and that is the angle of attack. Nevertheless, a huge amount of aviation literature discusses stall in terms of a critical speed, called the stall speed, rather than a critical angle of attack. This speed is obtained from the critical angle of attack via the characteristics. From Fig. 02 we can see that, for level flight as well as the two climbs, the equilibrium α^* increases as the speed decreases. The speed at which α^* on the characteristics becomes equal to α_S is the stall speed. For Our Plane, $\alpha_S = 15^o$ so the stall speed is about 180 km/hr. Note that the stall speeds are slightly different for the three climb rates considered in the Figure, but are close enough. We can use the speed as a proxy for the angle because the equilibria of (3B–22) are stable and planes like to operate at or near these points. To be a little more quantitative, consider the overdamped form (5B–05) of (3B–22e,f) and subtract from it (3B–22d) to get an equation for $\mathrm{d}\alpha/\mathrm{d}t$. Then this equation looks like

$$\frac{\mathrm{d}\alpha}{\mathrm{d}t} = -\frac{K_C V}{4}\left[\frac{1}{m}\left(\sin 3\alpha + \sin\alpha\right) + \frac{2V\bar{d}_1}{\Gamma}\sin 2\alpha\right] + \frac{mg\cos\eta}{V} + \ldots\ldots \quad , \tag{01}$$

where the dots represent all the other terms in the RHS of (5B–05) – (3B–22d). These are smaller than the terms I have written out, so we can ignore them. If η and α are small, then (01) reduces to a linear constant coefficient inhomogeneous differential equation whose particular solution is the equilibrium α^* where lift balances weight and whose homogeneous solution is exponentially decaying with a large exponent. This implies that perturbations from the equilibrium die out with great rapidity, and justifies the use of the stall speed as a proxy for the stall angle of attack.

To be sure, if an external agent (storm, UFO whatever) suddenly pitches up the plane to 15° or more while flying level at 450 km/hr, it will stall immediately. However, in the course of normal operation, a 15° or higher angle of attack at that speed is so far from the equilibria that it is not likely to be encountered. Rather, high α even in transient operation is likely to occur only when the nearby steady state features this condition also. Hence, the stall speed as obtained from the characteristics gives a good indication of when the plane will actually stall. Again, just as it is possible to stall at a high speed, it will also be possible to undercut the stall speed in a suitably designed manoeuvre without actually stalling. While aerobatic (and military) pilots will need to know the details of such procedures, for the majority of us, the stall speed is an excellent indicator of when we are in trouble. That said though, we will see examples of high-speed stalls and low speed nonstalls as we progress through this Article.

Coming back to the faulty climb, the middle panel of Fig. 01 shows that the pilot is diligently maintaining the climb rate of 2000 fpm. The first warning sign which he receives, and ignores, in real time is the decrease of speed as the climb proceeds (lower panel). Within ten seconds the speed has decreased from 306 to just above 295 km/hr. Never mind the flap configuration and the region of command, decreasing speed during *any* climb is a clear indication of insufficient power for the manoeuvre – either the thrust must be raised or the climb rate reduced (unless it's a deliberate zoom climb performed in emergency circumstances – see §44). In this case, throttling the engines to 90 percent or more would have been enough to start accelerating and forestall the rest of the drama. However, the pilot either did not notice the decreasing speed or missed its implications. This is a real-time error which has nothing to do with poor pre-flight preparation.

Observation of the pitch (top panel) shows another missed warning. The angle is 12° to begin with and increases past 14° at 22 s. Now, in the hell-for-leather climb out of the airport in §42 (Fig. 5B–03), we had used a pitch of 12·5°. The present climb is far less aggressive – V_z/V for the takeoff climb is almost 9 but for this one it is 6·5 at the start. Why then is the pitch so high ? It is because of two factors : (*a*) the diminishing horizontal speed coupled to a given climb rate generates a higher η, and (*b*) the requirement of balancing the weight at low speed and with no flaps generates a higher α. Granted the mistake with the speed, if the pitch indication had struck the pilot as anomalous, then he would have received another cue that the aircraft was not in a desirable operating configuration. However, this cue too was missed, either due to inattentivity towards pitch or a lack of understanding of its implications.

The final warning comes at 30 s onwards. We can see here a progressively increasing elevator force being required to maintain the climb rate. In other words, the pilot is pulling the stick harder and harder. Near the end of the figure, the elevator force is more than 50 percent above trim. This is most certainly not how one maintains a steady climb – as we saw for the takeoff, one just raises the nose initially and then comes back close to the $\bar{f}_p$ for level flight. The increasing pull force was yet another opportunity for the pilot to figure out that something was not quite right. Although this is his last chance at self-realization, it still gives a few seconds of cushion prior to the stall – enough time to make a drastic corrective action and be on his way.

Given the number of mistakes made by the pilot during the climb, it is a small wonder that a stall is the result. Of course, the entire action takes place in less than a minute, so the errors (except for poor prep) are coming one behind the other, and not at a relaxed pace like when you are reading about them. It can be quite easy to be distracted or mentally switched off for the few seconds during which all this happens. However, good airmanship is all about awareness and quick reflexes, and the more you are familiar with anomalies and warning signs, the better a pilot you will be.

§53 **Stall.** When a plane is close to a stall, an alarm trips off inside the cockpit. This alarm is designed to draw action from even the most distracted or somnolent pilot. In general aviation aircraft it consists of a very loud horn or an automated voice screaming "STALL! STALL! STALL!" while in airliners it consists of a stick shaker, a device which rattles the stick violently while producing an infernal noise. For the simulation, we ignore the alarm and continue from where we left off in Fig. 01, with the pilot holding 70 percent thrust and 55 kN elevator force indefinitely. We see the results below; the panels are the same as in Fig. 01.

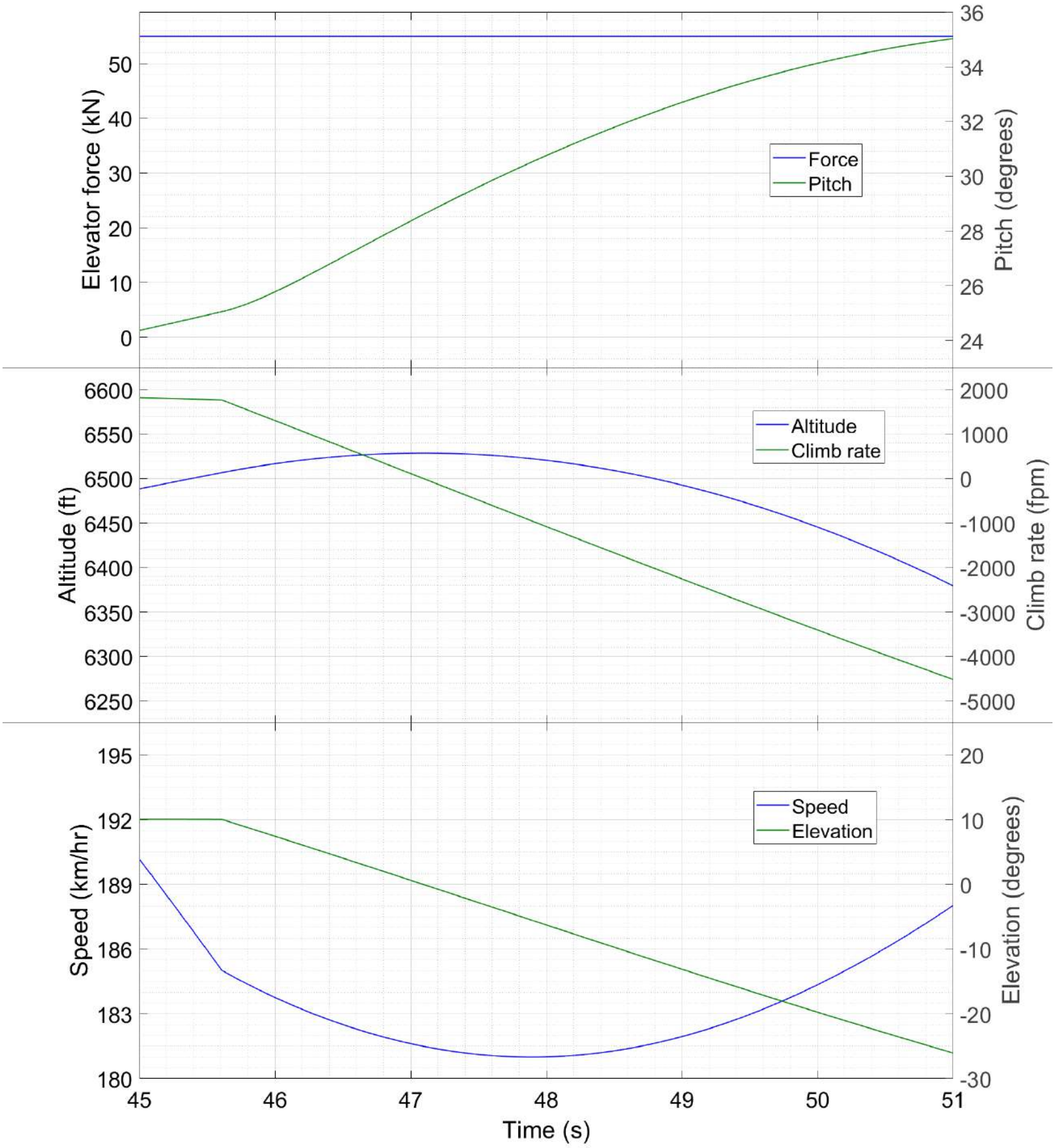


Figure 03 : *Time traces of different variables during stall. Note that the pilot is artificially holding the stall for a very long time, so that you can get a better idea of the behaviour in this condition.*

The stall proper begins at 45·6 s, characterized by the kink in the climb rate, speed and elevation. In the model, the lift just after stall is 1/3 of the lift just before stall; the latter balances the weight so the former produces a downward acceleration of $2g/3$. $1g$ is about 2000 fpm/s – no joke. Just five seconds after stall, the climb rate (middle panel) has become –5000 fpm and the elevation (bottom panel) is approaching -30^{o}. The pitch (top panel) on the other hand is increasing faster than it was before the stall, on account of the reduced lift on the wings. Mitigating the pitch rate is the fact that the angle between the elevator (which stays near to the flight path) and the fuselage is increasing, so $\bar{f_p}$ is having a smaller contribution to torque. The stall occurs at around 185 km/hr – Fig. 02 for the climb had the speed closer to 175. The difference arises because Fig. 02 is for steady state while the actual climb is a transient motion (continuously increasing pitch). Although the drag in stall is much higher than before stall, the speed (bottom panel) is actually increasing after the stall because the plane is dropping like a stone. At the end of five seconds of

stall, the aircraft is in a precarious configuration : $\eta = -25^{o}$ and $\theta = 35^{o}$, i.e. the plane is diving while pointing skywards. To better impress this configuration on your minds, I will now show the aircraft's profile during the stall.

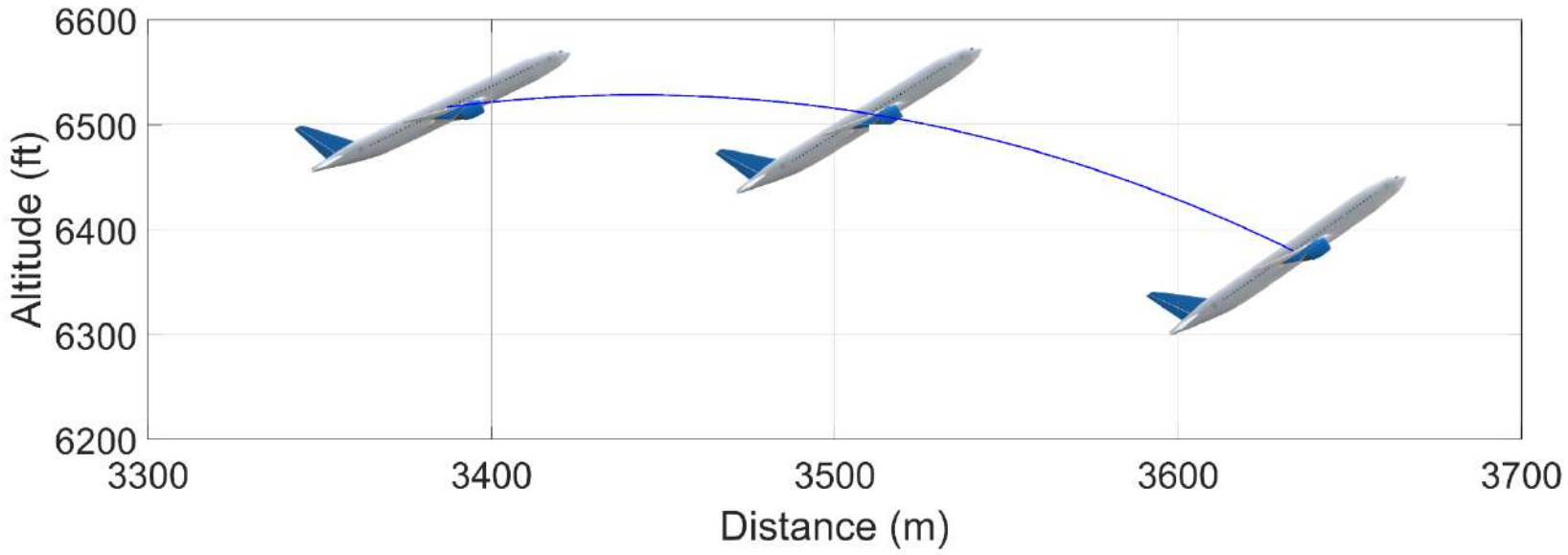


Figure 04 : *Profile of Our Plane during stall. The trajectory is to scale and the pitch is correct, so that the picture gives you as good an idea as possible of what things look like during an actual stall incident. The plane itself is over-large as it would otherwise look like a bee and diminish rather than enhance the total effect.*

This picture is the key to the stall recovery strategy, which we now consider in full detail.

§54 **Recovery from stall.** So we have the configuration of Fig. 04 – what next ? There is a very definite procedure – *and only this one procedure* – of recovering from a simple stall. We are going to see this now. You may think that learning this is unnecessary since you will never stall your plane anyway. But, with a malfunctioning aircraft or unexpected severe weather, even the best of pilots can find themselves in a stall. Then it is critical that you initiate the recovery procedure immediately and bail yourself, your passengers and your plane out of trouble.

Since stall occurs at a low speed, the first thing to do is build up speed. For that we have to increase thrust – to the max. Stall recovery on a jetliner* is always at TOGA thrust – no flex-max, climb thrust or other derates. This is an urgent situation and not the time to think of engine welfare. It takes an instant to slam the throttles against the wall; this done, we come to the stick. To plan the correct action here, we start from the stalled configuration – diving while pointing skywards. Our ultimate aim has to be to reverse the dive to a climb i.e. to increase η from negative to positive. For that however we'll need lift, and while the wing is stalled, there's no lift (so to speak). Hence, our immediate objective has to be to exit the stall and regain lift. The stall is occurring because α is huge : θ is large positive and η large negative. To end the stall, we shall have to reduce α to 15^{o} or lower. Since increasing η is out of the question, our only option is to decrease θ i.e. pitch down, push the stick forward. Common sense says that we reduce α as fast as possible so it's a full forward force on the stick until we are out of the stall.

* An exception to the full power rule may be applicable to some GA and other turboprop aircraft – see later in this Section.

With the stall nullified, we continue to have the problem of the dive. In the example simulation, η was -25^{o} when we left off and will decrease further while we are pitching the nose down. Hence, the instant of exit from stall will feature the plane diving while inclined at least 10^{o} below horizontal – still a dangerous configuration. We come out of this situation the usual way – pull the stick back to raise the nose. By this time, the high thrust will have increased the speed considerably, and the plane's preference will be for the corresponding low-α equilibrium states. Hence, pulling the stick now will pull up the nose and the trajectory along with it – it will not cause a pitch up only and send the aircraft into a second stall. Of course, if the speed at this time is still low, the pull-up will have to be gradual as you wait for the plane to accelerate.

Here's our pilot executing the recovery procedure.

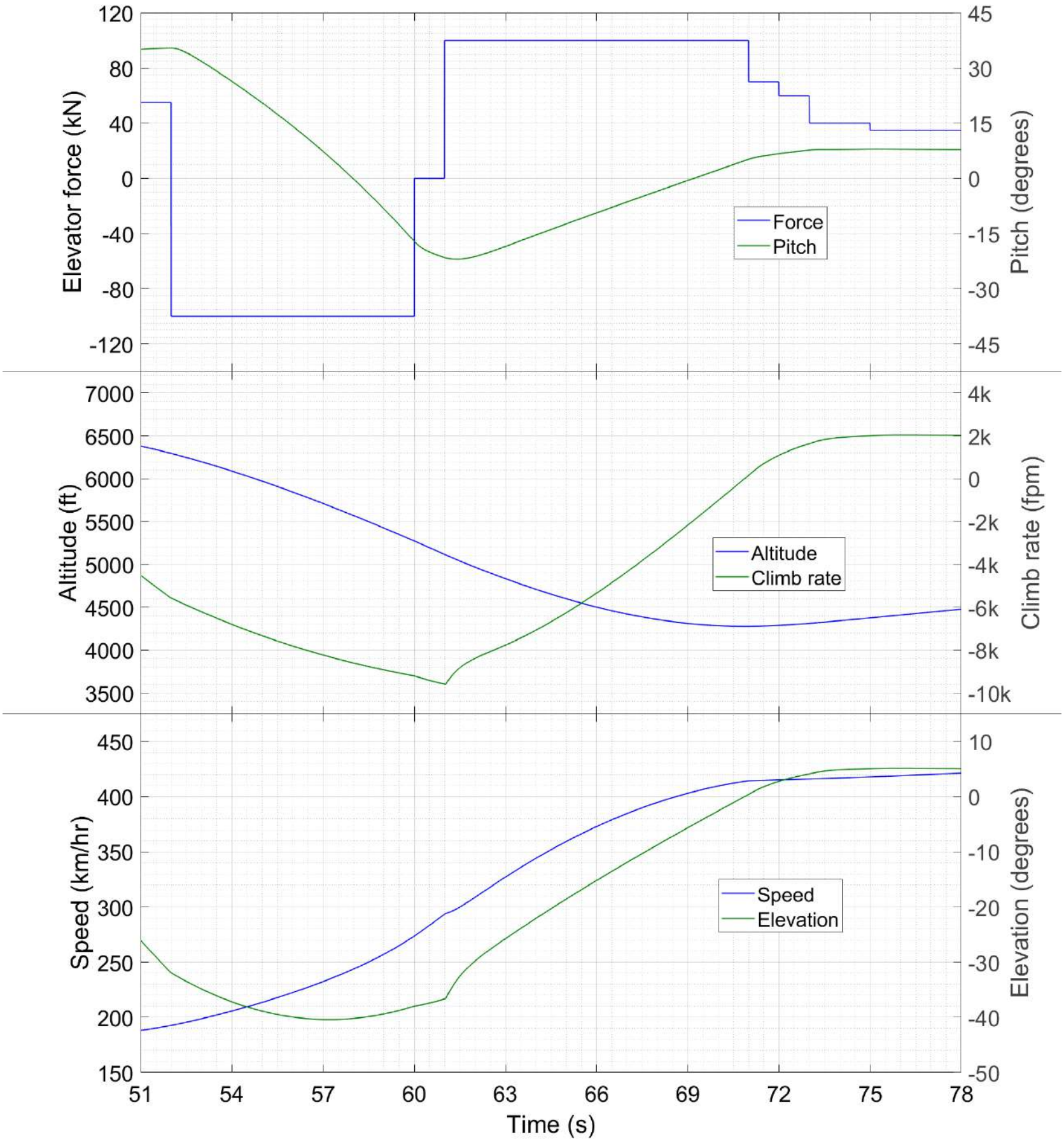


Figure 05 : *Time traces of different variables during recovery from stall. The symbol "k" denotes thousand.*

Continuing from the endpoint of Fig. 03, he holds the existing thrust and elevator force for half a second, so that we can see the change in behaviour once the recovery starts. The pilot then increases thrust to 100 percent and applies full nose down elevator force, which we assume is 100 kN (top panel; the increase in thrust is not plotted explicitly, but it occurs at the same time as the stick is pushed forward). The exit from stall occurs at $t = 61$ s, again indicated by the kinks in some of the plots; here I have implemented an angle of attack indicator among the simulator instruments which enables the pilot to anticipate the end of stall at 60 s and transition from push to pull. This indicator is present on some aircraft and absent on others; in the latter case, push has to continue until the stall warning ceases. The descent rate (middle panel), greater than 5000 fpm at the start of the recovery, increases to a peak of almost 10,000 fpm before the stall is exited. The elevation and pitch at this instant are -35^{o} and -20^{o} respectively, so there is a considerable amount of pull-up required to complete the recovery. The speed (bottom panel) is 300 km/hr, at which point the equilibrium α (Fig. 02) is about 5^{o}, considerably less than α_S. Hence the pilot

applies the maximum pull force of 100 kN for the second phase of the recovery. At $t = 71$ s, the climb rate finally passes through zero. At this time the pilot retards the throttles to 70 percent thrust and eases back on the stick to stabilize at 2000 fpm – the parameters of the initial climb configuration. The speed continues to increase even after the climb is established. The deration of thrust is perhaps a little premature – in reality we might like to accelerate still some more on high thrust – but I have implemented it to show that the original climb configuration is perfectly alright when initiated at the proper speed. The altitude (middle panel), 6500 ft at the start of the stall, drops to a minimum of 4250 ft. Note that the bulk of the altitude loss occurs during the recovery, not the stall itself ! Of course, the drop was so huge in this instance because we held the stall for whole six seconds – initiate the recovery quicker and the loss will be lower. Even so, a stall episode is costly in terms of altitude, and can become extremely dangerous if it occurs close to the ground, where there is insufficient altitude for recovery.

In summary, the stall recovery strategy is *throttle—push—pull*. Throttle the engines to full, then push the stick to exit the stall and finally pull the stick to exit the dive. Again, there's only one stall recovery strategy and that's this one. Now that you've seen the physics behind it, you should understand why we do it and remember it throughout your flying career. A special circumstance which you should be aware of is the following. In any aircraft, the engines exert a reaction torque on the fuselage, directed about the *d*-axis (banking torque). Whereas this torque is a negligible quantity on a jetliner, it can be significant on a general aviation or other turboprop aircraft. In such a case, a less aggressive throttle input might be more advisable for stall recovery, since one most certainly doesn't want a large banking moment thrown into the mix during this process. For these details, please consult the flight manual of the particular aircraft you are flying.

Also note that the strength of the push and pull will depend on how far we are into the stall. In the simulation example, we saw an extreme case, so it needed full nose down input and full nose up input as well. The earlier the recovery starts, the less drastic the inputs which will be required. The elements of the process are the same even if we recognize an approaching stall before it happens – for example, if our example pilot had cottoned onto the improper configuration during the climb itself. Again, high thrust is required to increase speed; that apart, a gentle nose down input (maybe even $\bar{f_p} = 0$ since the lift automatically pitches the plane down) to reduce the climb rate followed by maintaining $\bar{f_p}$ of level flight will be sufficient to see us running smoothly.

§55 **Further discussion, accidents and incidents.** There are three types of stall, of which simple stall is the most benign. The other two are deep stall or super stall, and stall spin. **Deep stall** is when the stall reduces or nullifies the effectivity of the horizontal tail. It occurs only on aircraft which have a *T-tail* i.e. the elevator is mounted high on the vertical stabilizer instead of on the fuselage itself. Figure 06 shows such a design – the particular aircraft here is a Bombardier Q400. Other aircraft such as ATR 72 and CRJ 200 also feature this configuration.



Figure 06 : *A Q400. Note that the horizontal tail is mounted high up on the vertical one, and not at the fuselage level as in Our Plane and most jetliners. The image [01] carries the appropriate permissions for this usage.*

When these planes enter a stall, the turbulent air from the stalled wings flows past the horizontal stabilizer and elevator and renders them partially or totally ineffective. Now, we saw that the horizontal tail is the primary means of recovering from a simple stall – in deep stall, the stall itself militates against its recovery. Hence, on T-tail aircraft, stalling must be prevented at all costs. Pilots certified for these planes require

extra training, and the flight computers are also programmed to override pilot input and pitch down automatically if the plane approaches close to a stall.

A **stall spin** is when only one wing enters the stall, at least initially, with a consequent high asymmetry in lift and drag between the two wings. It occurs when the aircraft is performing a climbing or descending turn at very close to the stall speed. While this is a fundamentally three-dimensional motion and we can defer its quantitative analysis to the sequel Article, what qualitatively happens is this. During a turn, the two wings move at different horizontal speeds, with the outer one faster. On the other hand, if the bank rate (not the bank itself) is zero, both wings have the same vertical speed, which is the climb rate of the aircraft as a whole. Same vertical and different horizontal speeds correspond to different η's. Since both wings share the pitch of the whole aircraft, the two θ's are the same. Hence the two α's are different; the one which first crosses α_S enters the stall. Which one will it be ? To find that out, let's first note that during a climb, η for both wings is positive, and that for the inner one is more positive since the horizontal speed of the inner one is lower. Hence, the outer wing makes the lesser η in this case. On the other hand, during a descent, η for both wings is negative, and that for the inner one is more negative due to the lower horizontal speed. Hence, the inner wing makes the lesser η in this case. Now, during both climb and descent, both wings are generating positive lift which means that θ is greater than both η's. The larger α is made by the wing with lesser η, and if there is to be an asymmetric stall, that one will stall first. Hence, the outboard wing will stall first during a climbing turn and the inboard wing will stall first during a descending turn.

What happens after one wing stalls ? Let's say the stall is on the starboard wing. Then, the lift of the port wing far exceeds that of the starboard wing, giving rise to a strong starboard banking moment (positive as per our convention). Simultaneously, the drag on the starboard wing far exceeds that of the port wing, causing a starboard yawing moment (negative per convention). Both of these cause the plane to enter a very rapid starboard turn. This further slows down the starboard wing relative to the port wing and exacerbates the asymmetric stall. Because the total lift is low, the plane also begins to dive while spinning rapidly. Although some recovery procedures exist, they are only partially reliable except on some ultra-manoeuvrable aircraft. As with deep stall, prevention is the only cure for a stall spin. Unlike COVID-19 however, stall spin has a fully effective vaccine – manually verify the speed prior to every climbing or descending turn and keep a watch on the speed during the whole manoeuvre. If the airspeed indicator is compromised, use pitch as proxy and go for level and shallow turns only.

The approach to stall which we saw here is one common way it happens in practice. It is in fact a conceptual re-creation of an actual incident which happened to a Boeing 777-200F cargo plane while departing KJFK on 15 November 2020 [02]. In the actual, the ground speed at the time of the stall was close to 380 km/hr, more than double of our simulations (whether there was a tailwind is unknown). Once again, remember that Our Plane is not a real plane – the physics is the same but the numerical values are different. After a somewhat slow takeoff, this 777 attempted an extremely aggressive climb (excess of 4000 fpm on a full load), decelerating and stalling in the process. Fortunately, the pilots applied the recovery procedure and it continued on its way after a 500 ft loss of altitude. Approach and landing is another flight phase where stalls are common, since the aircraft in this phase is quite slow and the stall α is reduced on account of the flaps. Ill-configured aircraft are especially prone to stall during turns since those require more lift (see §56) and also have more induced drag. The turn rate and climb rate determine whether it's a simple stall or stall spin which occurs. In all cases, the approach to stall has the three hallmarks which we saw – low speed, high pitch and progressively increasing elevator force. Three separate indicators are especially useful when our aircraft is compromised. For example, if the speedometer is lost, we can check if the pitch readings for the flight phase in progress are as they should be.

This example also shows why operation in reversed command is more dangerous than in normal command. In the botched climb, the pilot was operating in reversed command; attempting a manoeuvre beyond the aircraft's capabilities (at least, at the selected configuration), he ended at a stall. On the other hand, if the plane had been in normal command then this situation would not have arisen. For example, 70 percent thrust also corresponds to an equilibrium 2000 fpm climb at a speed of about 650 km/hr. If the

pilot had attempted the climb starting at say 700 km/hr, then the speed would have reduced until 650, at which point it would have stabilized and the rest of the climb would have proceeded smoothly.

For the stall itself, we remember that what we see here is a conceptual model. Equations (3A–09) and (3B–28) are plausible representations of what happens in a stall, but are not an actual model of stall in any particular airfoil. A real aircraft may have a different lift reduction, a different drag increase etc after stalling. What is invariant is the sudden decrease of the lift, the consequent reduction in climb rate and the decoupling of θ from η. One feature of a real stall which our model doesn't capture is the vibration of the aircraft on account of turbulence in the separated flow behind the wings. This is called **stall buffet** and acts as a sensory indication to the pilot of the stall, independent of all instrument readings. Similarly, the sudden downward acceleration caused by loss of lift is another such indication. These, together with the climb rate and pitch profiles during stall, are necessary to recognize the stall in the (howsoever unlikely) event that multiple instruments fail simultaneously including the stall warning alarm itself.

In general aviation, stalls are responsible for a large number of accidents. Most feature pilot error in some form or other – in initiating the stall and possibly in executing the recovery. In air transport, crashes due to stalls are very rare, though not non-existent. On 12 February 2009, Colgan Air Flight 3407, a Bombardier Q400 flying from Newark (USA) to Buffalo (USA), stalled during final approach and crashed less than 10 km from the airport. Less than four months later, on 01 June 2009, Air France Flight 447, an Airbus A330 from Rio de Janeiro (Brazil) to Paris (France), entered a stall at cruising altitude and crashed into the Atlantic Ocean. On 28 December 2014, Indonesia Air Asia Flight 8501, an Airbus A320 from Surabaya (Indonesia) to Singapore, entered a stall at cruising altitude and crashed into the Java Sea. All passengers and crew were killed in all three accidents. In the first of these, the aircraft was fully functional while in the other two it was slightly compromised; in both of these, the malfunction was nowhere near catastrophic. What was catastrophic, in all three accidents, was the pilot's action of *pulling the stick back as hard as he could after the aircraft stalled*. Yes, you got that right. These were ATPL pilots who made this elementary mistake in stall recovery, with such terrible consequences. It is for this reason that the recovery strategy should become second nature – the stall alarm should completely override the normal instinct of pull to climb, push to descend.

Yet another transport aviation accident has occurred as I write this – the crash of Yeti Airlines Flight 691, an ATR 72-500 from Kathmandu (Nepal) to Pokhara (Nepal), on 15 January 2023 during final approach to destination. While it is way too early to reach any conclusive diagnosis, preliminary videographic evidence suggests that a stall spin might have been responsible. Immediately prior to the crash, the flight was descending while turning left and was in a high pitch attitude; suddenly it banked 90^o to port and crashed. The directions are consistent with a stall spin, and the high pitch may indicate that α was close to α_S. Of course, this conclusion must be taken with more than a pinch of salt – *any accident analysis performed by anyone other than the appropriate investigative agency is just speculation*. Facts become available only after the investigator publishes their reports. Nevertheless, a stall spin *is* a possibility in this accident and is yet another reminder of the need to be maximally vigilant during low-speed operations. Note also that reports suggesting a simple stall rather than a spin are likely to be incorrect – simple stall does not feature a sudden, catastrophic bank to one side.

We now consider an actual stall-related incident of a different kind. From our usual territory of jetliners, we come over to the world of gliders. A glider is an unpowered aircraft which has very high L/D, achieved using long, slender wings. It gains altitude in thermals, which are pockets of rising air. Having attained altitude in one thermal, it flies a descending trajectory to the next thermal, bleeding off the gravitational potential energy to overcome drag en route. For takeoff, the glider is attached using a wire to a conventional aircraft called the tow plane, just as a railway coach is connected to the loco using a coupler. The tow plane takes off from a runway, hauling the glider behind it. They climb together and travel to a suitable location, for instance a thermal, where the glider releases the wire and the tow plane returns for landing. From a piloting viewpoint, a glider and a jetliner are poles apart; on the other hand, they both have wings, elevators, ailerons and rudder and are both governed by (3B–22). We consider the glider incident here because it yields a situation-specific recovery strategy featuring an undercut of the stall speed,

which is impossible to figure out except using a model-based approach – the very accomplished pilot in charge of the glider appears to have not considered it during or after the incident.

In an educational video made by a glider pilot – also a flight instructor – with tens of thousands of flying hours, he discusses a recent incident [03] in which he was being towed into the air by a tow plane whose pilot had been briefed to takeoff and climb at 130 km/hr. Unfortunately, the tow pilot made an error and the duo became airborne at 100 km/hr only. The stall speed of the glider was 96 km/hr, so the situation was critical for the glider. The glider pilot yelled for a higher speed, but his initial communication was drowned out by another transmission on the same frequency. Later, the demand for the proper speed was successfully transmitted to and implemented by the tow pilot, from which point onwards the flight proceeded normally. In response to the tutorial video, someone asked why didn't the glider pilot release immediately. His response was that "at the moment [he] was too afraid that the glider might stall and drop hard to the ground if [he] pulled the release".

In my opinion, this reasoning and the consequent decision reflects an over-reliance on the concept of stall as triggered by a critical speed rather than a critical angle of attack. To be sure, steady level flight at below the stall speed is impossible. But it is still possible to make a controlled descent to the ground at below stall speed without actually entering a stall. To investigate this in detail, let us use Our Plane in the clean configuration to simulate the situation. We implement the tow as level flight at 187 km/hr at 90 percent thrust and 37 kN elevator force. The angle of attack (equal to pitch since elevation is zero) is $14{\cdot}2^{\circ}$, a hair's breadth away from stalling. We implement disconnection of tow as a reduction of thrust to 60 percent at $t = 3$ s. We choose 60 rather than zero because a glider is a very low-drag aircraft and it is expected to decelerate only gradually after being released from tow. A partial reduction of thrust in our model plane captures this more accurately. We use a simulation cycle time of $1/2$ s.

First let's see what happens if $\vec{f}_p$ remains 37 kN throughout after disconnection from tow.

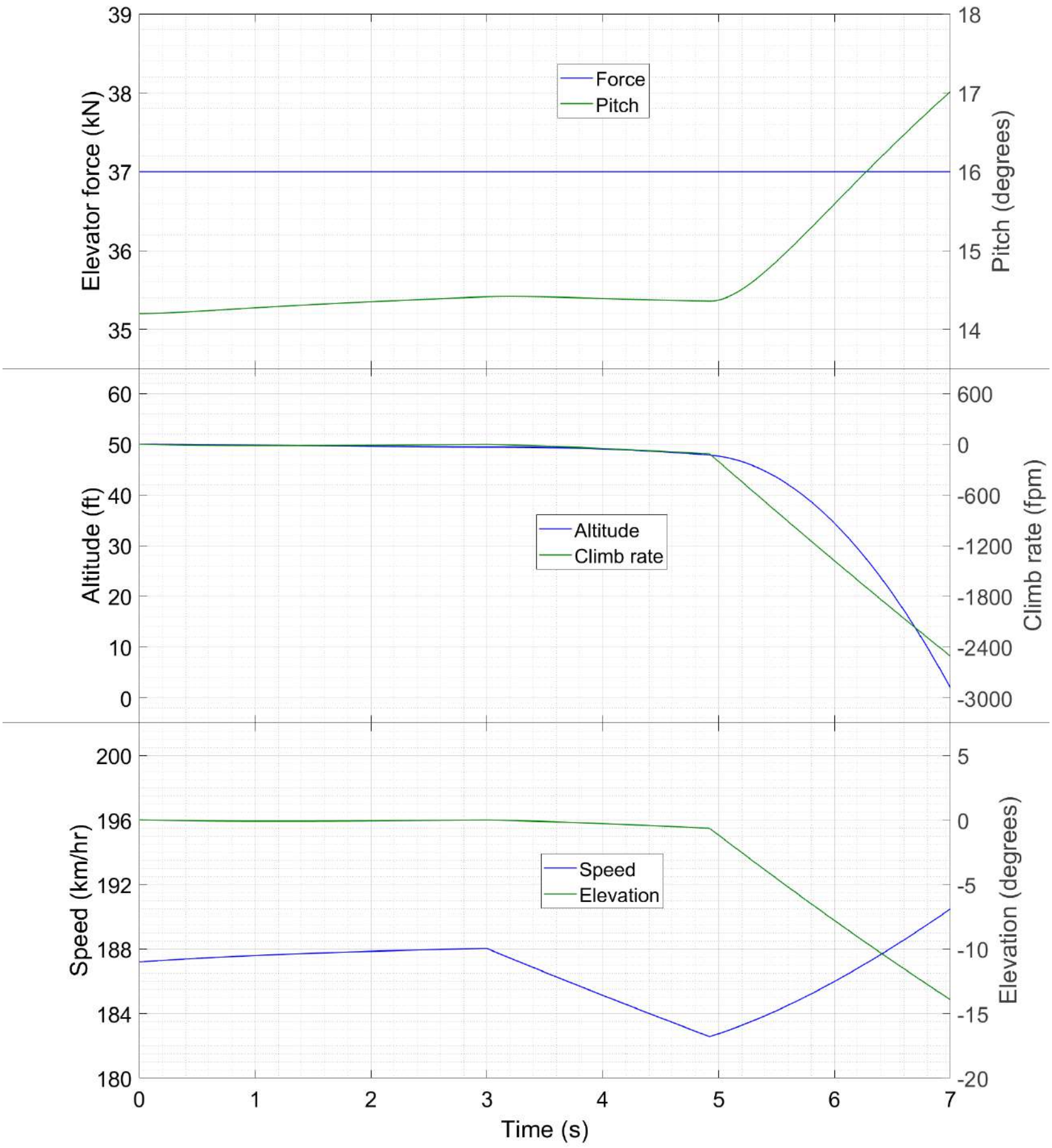


Figure 07 : *Time traces of different variables during simulation of disconnection from the tow, with no corrective action attempted by the pilot.*

Nothing good. The aircraft stalls less than 2 s after the thrust reduction, when the speed (bottom panel) decreases below 183 km/hr. As soon as the stall is encountered, the nose goes through the roof while the plane itself starts plummeting. From the middle panel, we can see a descent rate of 600 fpm being attained when the aircraft is just 5 ft below its initial altitude. 600 fpm is about the maximum descent rate which a typical airliner and its occupants can safely withstand. By the time the altitude has dropped through 10 ft, the descent rate has nearly doubled. Thus, the glider pilot was correct in reasoning that if he disconnected the tow while keeping everything else unchanged, the glider would immediately stall and crash.

What can be done however is to disconnect the tow while adjusting the elevator input so that the aircraft doesn't stall but flies down to the ground while extracting as much lift as it can. This won't be the entire weight but might still be enough to cushion the descent. The higher the nonstall angle of attack, the more will be the lift at any given speed. Hence, in the upcoming simulation I have adjusted the elevator

force so as to keep the angle of attack in the range 14·5° to 15° while the aircraft loses altitude. To simplify my task, I have varied the elevator force in steps of 5 kN only.

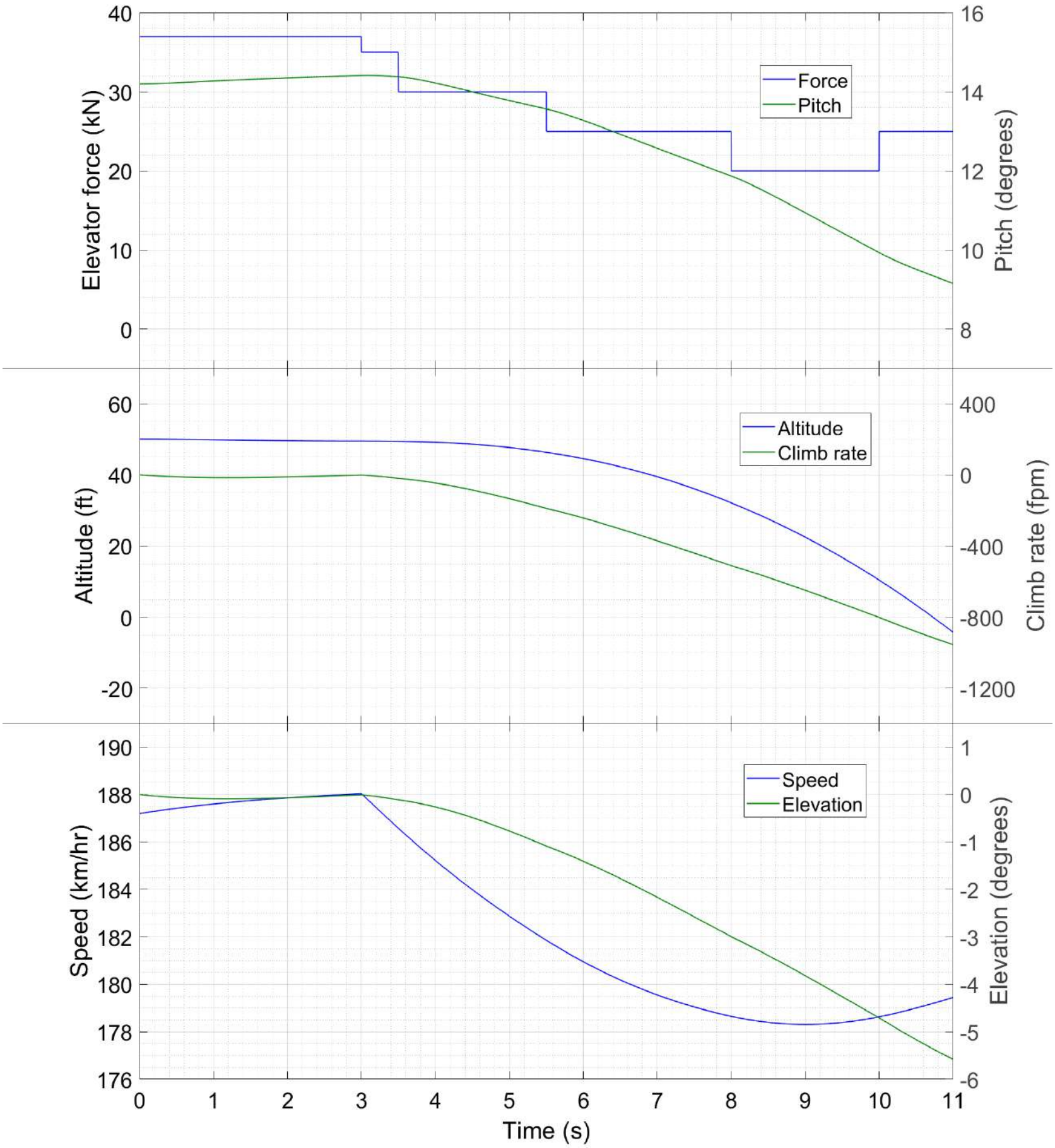


Figure 08 : *Time traces of different variables during simulation of controlled descent to ground following disconnection of the tow.*

This time we see a very different outcome. As the speed reduces, so does the lift, and the elevation decreases. Progressively easing back on the stick however allows the aircraft to pitch down as well so that α remains at the ceiling of the nonstall range. The 'stall speed' of 183 km/hr is passed at $t = 5$ s without incident; the next six seconds show controlled flight below this speed. As in Fig. 07, the descent rate increases with time but now it does so in a much more gentle manner. 600 fpm is reached when the plane has descended through 25 ft while 800 fpm occurs after 40 ft.

This simulation shows that it might have been possible for the glider pilot to disconnect immediately and fly the plane down to the ground. Indeed, if the pilot had decided to release from tow, the disconnection would have occurred just a few seconds after the premature takeoff and the glider would have been at a

low altitude, enabling this manoeuvre to be performed successfully. It does remain true that this procedure of descending while remaining just below stall α is a difficult manoeuvre to execute in real time, and even more so if the glider lacks an angle of attack indicator. Nevertheless, since slow tow appears to be a recurrent problem in glider flying (see comments to video in Ref. [03]), a controlled descent to ground at below stall speed might well be a useful trick to learn on a simulator and apply in such cases.

Finally we can take on the relevant quiz questions. Q04 has the by-now-obvious correct answer Choice C. Q16 requires a little more insight. We've seen what a gusty wind is in §50. A sudden change in wind during a climb or descent can be dangerous because it can result in a stall with no error made by the pilot. To see why this is so, note that the elevation of the plane's trajectory relative to the wind is $\eta' = \arctan V_z/(V_y - U_y)$ [see §29 and we have assumed the wind to be horizontal only], and the angle of attack is $\alpha' = \theta - \eta'$. A sudden change in U_y causes a sudden change in η'. The pitch θ on the other hand, being a dynamical variable, changes only gradually in response to the change in wind, and as a first approximation may be thought of as constant. Hence, an abrupt change in wind causes an equally abrupt change in α' – if this change takes it past α_S then the plane stalls with no prior warning. For this reason, a gusty wind condition during climb or descent can result in a stall unless the pilot is extremely careful or skilful – Ref. [04] gives an example of an experienced and rule-abiding glider pilot who crashed in exactly these circumstances*. This is the safety risk lying at the heart of Q16. Although an aircraft prefers to takeoff and land into a headwind (see §43), Choices A and C do not pose a risk unless the pilot makes an error, a contingency explicitly ruled out in the question – the fact that he has opted to perform the takeoff and landing despite the tailwind certifies the operation as safe. Choices B and D are the ones involving risk. Now which of the two is riskier ? The one where the jumps in α are likelier to be of greater magnitude. Now, the smaller V_y is in comparison with U_y, the larger the effect which a given change in U_y will have on η' and hence on α'. Thus, the greater the risk of stalling arises from the phase with smaller V_y, which is landing. Hence the correct answer is Choice D. It follows that if you have to land at an airport with gusty wind, then safety is increased by deliberately opting for a higher airspeed during the approach. Further, since less extended flaps allow a higher α_S and hence a greater margin of error in these circumstances, a flap setting less than that for a normal landing is the optimal choice in this case. Hence, the mantra for gusty landing is lower flaps, higher speed. Even so, pulling it off requires some skill and experience – if you are faced with it and don't feel confident about it, then diversion to an alternate airport is the safest option.

* Remember, a glider is unpowered, so the pilot did not have the option of applying full thrust and accelerating and/or climbing out of the gust.

G. BANKING PLANE DYNAMICS

The Subdivision title itself makes clear that this is our second excursion from the pitch plane, and once again we have a lollipop.

§56 **Why don't we feel a banked turn ?** When a bus or a car with us in it negotiates a corner at speed, the experience is quite uncomfortable. Why then when a plane turns at a much greater speed do we not feel much ? A possible explanation may have been that the radius of curvature is so high as to make the centrifugal force negligible and hence the turn imperceptible. This however is absolutely not true. Rather, the forces during a banked turn work out in just such a manner as to make the experience comfortable for the people inside.

To see this, let's again look at the free body diagram of the forces on the banked aircraft. This is basically Fig. 3C–02 again but with the two wing lifts and the tail lift merged into one overall lift force F. To restrict ourselves to two-dimensional motions, we must consider zero pitch and assume that the lift is somehow getting generated.

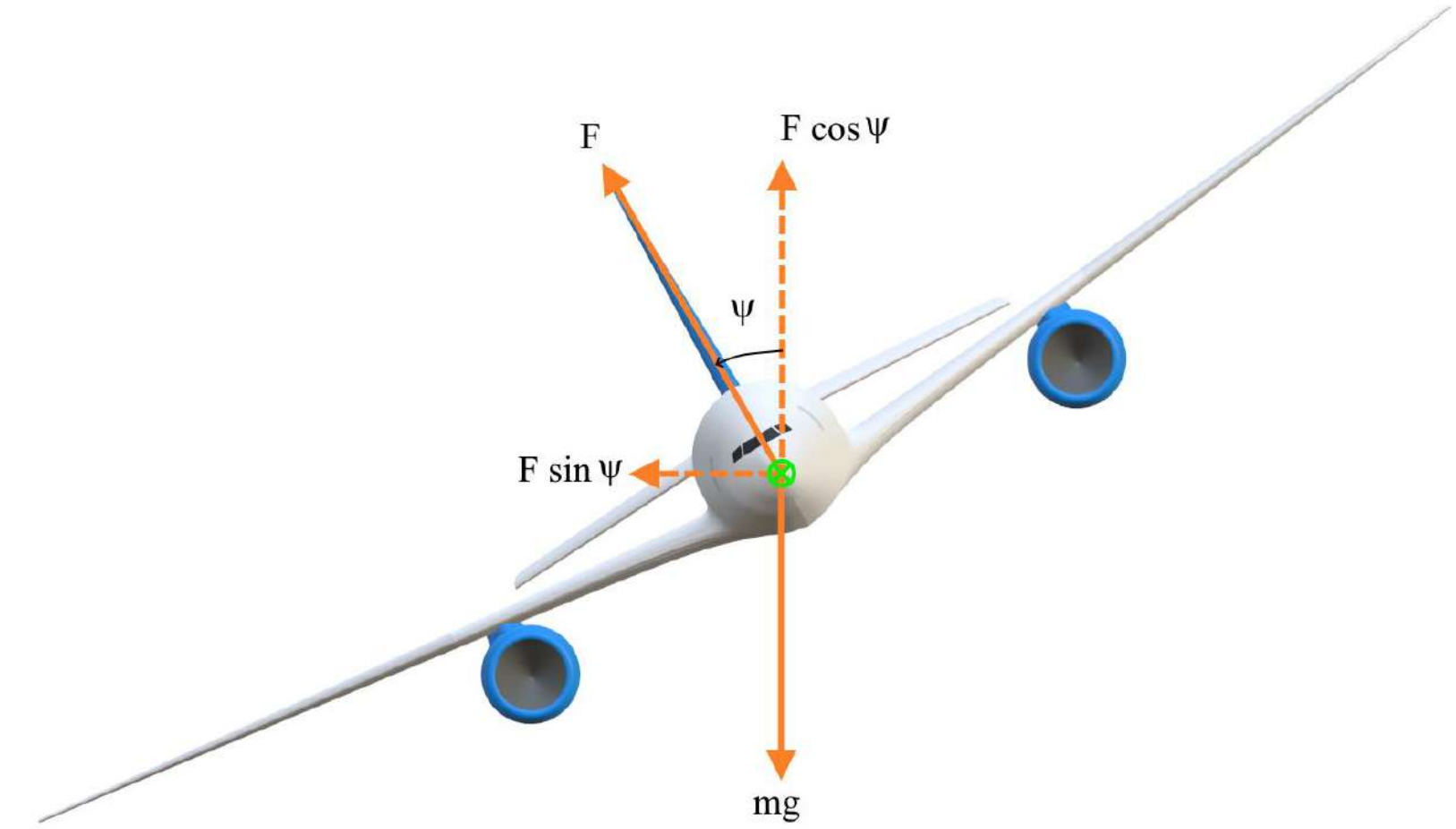


Figure 01 : *Free body diagram of Our Plane performing a starboard turn.*

From this figure we can see that the $\sin\psi$ component of lift goes into providing the centripetal acceleration while the $\cos\psi$ component balances the weight. Hence, more lift – by a factor of $\sec\psi$ –is required during a turn than in straight flight to prevent the aircraft from beginning a descent. This has to be generated by pulling the stick appropriately. A typical banking angle is 30^{o} or more, so the required increase in lift is around 15 percent, not at all insignificant. Increased lift means increased α, which is why there is increased risk of a stall during turns. Moreover, as we saw in the last Section, a stall in a turn can become stall spin rather than simple stall. To avoid this, verify the speed explicitly before initiating a turn. If it's anywhere close to the stall speed for the turn (which is higher than that for straight), then don't pull the turn until you have increased your speed. As regards the radius of curvature of the turn, we have

$$F\cos\psi = mg \quad \text{, and} \tag{01a}$$

$$F\sin\psi = \frac{mV^2}{R} \quad , \tag{01b}$$

where R is the turning radius, so that

$$\psi = \arctan\frac{V^2}{gR} \quad , \tag{02}$$

a formula which is covered during competitive examination prep as well as in almost every classical mechanics course in the context of a car turning on a banked road.

Now consider again Fig. 01 together with the free body diagram of a person inside the aircraft (mass μ) sitting in his seat (the person may be either the pilot or a passenger). We show the two simultaneously in Fig. 02. This time, we draw the diagrams in the non-inertial frame which rotates with the aircraft and has its origin at the centre of the turn. In this frame, the centrifugal force acts on both the plane and the person, and both are in equilibrium. The forces on the passenger are gravity, normal reaction N_1 from the seat of the chair and a lateral reaction N_2 from the armrest of the chair. This reaction may be directed to starboard or port as appropriate, so we have shown it as a dashed line at both armrests. N_2 will determine how uncomfortable the turn will be for the person – in a rashly driven bus, it has a high value, equal and opposite to the centrifugal force.

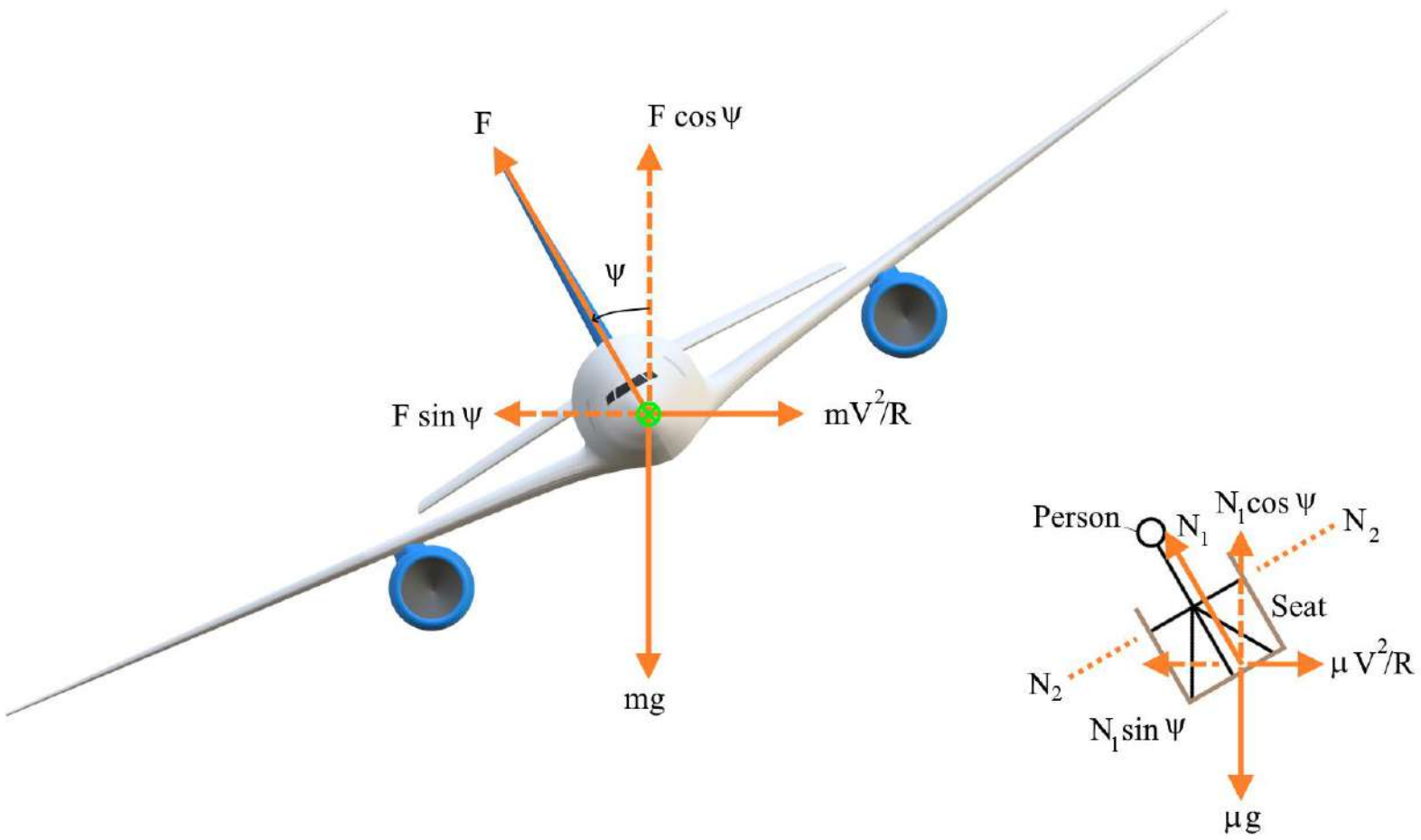


Figure 02 : *Free body diagram of the plane as well as of a person inside it, drawn in the non-inertial frame in which the aircraft is stationary.*

Now however we can see that if $N_1 = \mu g/\cos\psi$ and $N_2 = 0$ then the free body diagram of the person will become identical to that of the aircraft. Since this corresponds to equilibrium for the aircraft, it must also correspond to equilibrium for the person. In other words, the nuisance lateral reaction which makes the turn uncomfortable is identically zero. This is why we don't feel the turn at all despite the high acceleration involved. The banking ensures that the relevant component of gravity cancels off the centrifugal force. A 30° bank generates a centrifugal acceleration of 5 m/s^2; if the plane had attempted such a turn without banking, then very likely the passengers would have ended up first in the aisles and then in the hospital.

§57 **Further discussion.** That the banked turn is imperceptible also means that if the flight instruments fail and there is no visual reference, then the pilot is unable to determine whether the plane is flying straight or is in a turn. In the latter case, if the pilot believes he is flying straight, then he will not command the excess lift required, and the plane will begin to descend. As soon as it acquires some vertical velocity, the angle of attack will increase and the requisite lift will get generated, so the descent rate will stabilize. The trajectory described will be a descending helix, called **spiral dive**. Since the flight path can lead only to the ground, it is also called graveyard spiral*. The phenomenon in which the pilot flies a turn believing straight is called **spatial disorientation**. On 01 January 1978, Air India Flight 855, a Boeing 747-200 from Mumbai (India) to Dubai (UAE), experienced a malfunction of the attitude indicator on the captain's side shortly after takeoff. The first officer's attitude indicator was still functional but the crew were unable to resolve the disagreement between the two readings. They mistakenly believed the aircraft to be flying straight when in fact it was in a steep left bank. 1 min 40 s after takeoff, AIC 855 crashed into the Arabian Sea, killing all passengers and crew*. Nowadays, with improved safety standards, total instrument failure does not occur at the air transport level. In lower level aviation such as recreational and business

* Both spiral dive and stall spin feature a combination of turn and descent, but the similarities end there.

* A spate of avoidable accidents as well as an abysmal punctuality record during the 1970's and 80's resulted in the state-owned AIC brand suffering irreversible damage. By the 2010's, AIC was a completely different airline, offering safe (no accident after 1990) and punctual domestic and international flights, the latter with excellent timings. Despite sterling service during the 2019 Pakistan airspace crisis and the 2020-onwards COVID-19 crisis, AIC was unable to turn a steady profit and was disinvested by the Government of India in 2022. As of yet, the airline appears to be undergoing some teething troubles following the ownership transition; let us hope that these get sorted out at the earliest.

flying, spatial disorientation is still a cause of accidents. A high-profile case involved the death of JOHN F KENNEDY Junior, son of the US President, on 16 July 1999.

A couple of the Quiz questions are now up for grabs. For Q13, the correct answer is Choice B. Since the aircraft is given as performing the first turn after departure, its weight is very close to the takeoff weight, i.e. the maximum at any stage of the flight. A 120^{o} turn right after takeoff is invariably taken at a rapid rate and features a fair amount of banking; we just saw that banking requires more lift. Choice A features a steady climb, where the lift just balances the weight. The value of 3000 fpm is a red herring, designed to impress you with its size and trap you into selecting this choice. Choice C features another turn so again we'll have the banking effect. However, in a long-haul flight, the weight at landing is significantly less than the weight at takeoff, since the fuel has been burnt off. Hence, the lift required for the turn onto final approach will be lower than that for the turn onto departure track.

For Q18, with all instruments except airspeed indicator failed in IMC, spatial disorientation and spiral dive is the most likely mechanism of a potential crash, as we saw above. Hence the correct answer is Choice C. Let us also rule out the other options. Fuel exhaustion is next to nonsensical since the pilots will have a good idea of how long they can fly before fuel becomes an issue. Unless they voluntarily continue for so long as to run short of fuel, the absence of the fuel gauge will not matter. Uncontrollability is also out because the failure is of instruments and not of control surfaces. Finally, the functioning airspeed indicator rules out a stall – the pilot simply has to keep the aircraft well clear of the stall speed. An option we didn't include was a straight dive, arising from failure of altimeter and climb rate indicator. That too is an unlikely crash mode however since the plane will accelerate if it enters a straight dive. When the pilot sees the speed going up and staying up despite no change in throttle, he will realize that a loss of altitude is taking place, and will take corrective action. In spiral dive however, the extra lift also means extra induced drag so there will not be a significant change in speed in the transition from level flight to dive.

A quantitative estimate of this change in speed, as well as an analysis of the design considerations which can cause an aircraft to spontaneously exit a spiral dive, will require the full three-dimensional model and we defer it to the sequel to this Article. For now, back to the pitch plane for the final build-up.

H. PUGACHEV COBRA

§58 **Description.** Pugachev cobra, named for the Russian test pilot VIKTOR PUGACHEV though it had been discovered by others*, is a dramatic 90^{o} or more pitch up and back during quasi-level flight. It can be performed only by the most sophisticated fighter jets, for reasons we shall see shortly. In brief, the manoeuvre proceeds as follows. Starting from fast, level flight, the pilot pitches up the nose rapidly, going past the 90^{o} mark, before pitching down again to nearly horizontal. The aircraft stalls immediately after the pitch starts rising, and this prevents a rapid climb from being developed. During the pitch down phase, a descent takes place which counteracts the climb during pitch up, so that the manoeuvre ends at more or less the same altitude at which it began. Because the aircraft is in stall for most of the time, the cobra also features huge drag and a significant loss of speed. We show a schematic of the manoeuvre below, taken from Wikipedia [04].

* Exactly who discovered this manoeuvre isn't clear. Potential contenders are fighter pilots of the Swedish Air Force [01], Syrian Air Force [02] and another Russian pilot, IGOR VOLK [03].

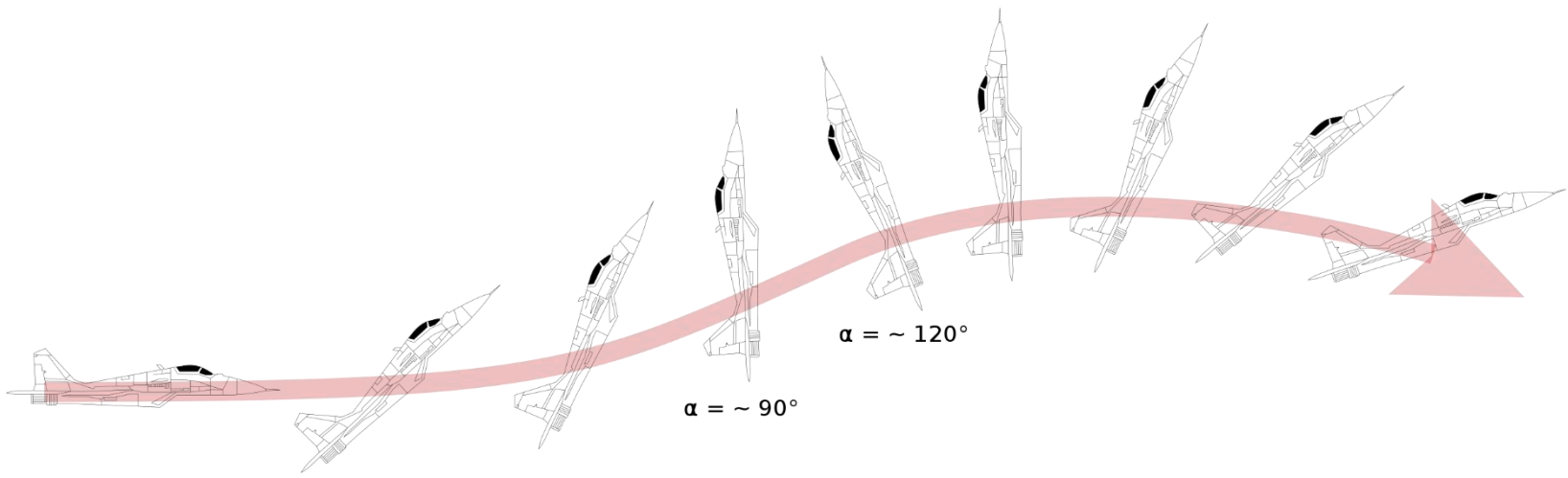


Figure 01 : *Schematic representation of an aircraft performing a Pugachev cobra. The image [04] carries the appropriate permissions for this usage.*

Note that in the image (which I haven't edited), the angle which is identified as α should in fact have been θ. Since the notation α for angle of attack is universal, the image is not just using a different notational convention but is expressing a technical confusion between pitch and angle of attack – this is just the kind of confusion which our Article hopes to eliminate. Technically, the pitch of 90° should be crossed for the cobra to have been achieved successfully. Videos of the manoeuvre are also linked in Ref. [03].

The cobra is one of a class of **post-stall manoeuvres**, in which a stall, rather than being an unwanted phenomenon, is planned into the manoeuvre and assists in accomplishing its objective. In this case, it is the speed loss which is aided by the stall – bleeding off hundreds of km/hr's over a couple of horizontal kilometres with no change in altitude is next to impossible otherwise. While the utility of such manoeuvres in combat is not known, they certainly make for thrilling displays at airshows.

§59 **Design of the aircraft.** Let us try to make Our Plane perform the cobra. The first part of the manoeuvre features a rapid pitch-up starting from high speed. To achieve this, we must apply full nose up input on the stick while cruising at speed. But this is exactly how the Immelmann manoeuvre was initiated and the result was a five-figure fpm climb instead of a stall. As we saw in §52, at high speed the aircraft automatically operates at or near the corresponding low-α steady state so the nose drags up the trajectory along with it*. How to prevent this from happening in the cobra ?

* Which is why we could blithely pull off the Immelmann in §44 without having to worry about a stall.

§52 also tells us that it is the pitch stability of the aircraft [via the overdamped approximation and (5F–01)] which makes it fond of the equilibrium states – to neutralize this preference, we must kill the pitch stability. Hence, the first criterion for a successful Pugachev is that the aircraft must be C-B-E i.e. CP must be forward of CM. In other words, $\bar{d_1}$ must be negative and the aircraft stability must be relaxed. Such aircraft typically cannot be flown by pilots alone without the aid of the onboard computers, which apply control inputs multiple times per second to keep the plane on the desired trajectory. Next, since a climb is undesirable, the faster we pitch up in the initial phase, the less altitude we are going to gain in this phase. To achieve this, the elevator must be capable of exerting a high force when needed, much more so than in the airliner. Thirdly, the angle between the flight path (approximately horizontal) and the fuselage (sometimes near vertical) may be huge, and the aircraft must be controllable in such a configuration. A horizontal stabilizer fixed to the fuselage will serve no purpose in such a state. Hence, the elevator must really be a pivoted stabilator, capable of making an arbitrary deflection with the fuselage.

The question now arises as to how to return the aircraft to normal flight from a 90° pitch configuration. Even if the stabilator is functioning, its influence will be very limited because its lift will be approximately normal to the flight path and hence almost parallel to the fuselage; the torque of this lift will be small. Even in the stalled state, the wings will be generating some lift and, in a C-B-E plane, this will give rise to a positive torque. To achieve the return to zero pitch, we must have sources of negative torque when the pitch is high. Other than lift, the only forces on the aircraft are thrust and drag; we must leverage both of them for this torque. For the model cobra-plane, we keep the nonstall fuselage drag to act through

the CM, and take the stall drag to act through a point aft of it. In other words, d_3 must be negative. In Our Plane, the engines are mounted below the fuselage and give rise to a positive torque; here we reverse the configuration so that they too have a negative torque. Finally, to retain safety of the manoeuvre, it must be possible for the aircraft to balance its weight even in the 90° pitched up configuration. This balance can be achieved only by the thrust, so we need the full thrust to be approximately equal to the weight. Relaxed stability, fully rotating stabilators, restoring torque in stall and high thrust are all characteristic of military aircraft rather than jetliners.

We keep unchanged as many parameter values as possible from Our Plane. Using a mass of 80 tons, we now alter $\bar{d_1}$ to –1·5 m, $\bar{h}$ to –0·5 m and the elevator lift constant k_E to 300 SI Units (it was 150 before). Keeping the wing stall angle at 15° from Subdivision 5F, we use $C_1 = 10$ SI Units and $d_3 = -3$ m. Two caveats are important here. The first is that we do not consider the issue of whether these parameter values are feasible to design. For example, CP forward of CM and centre of stall drag aft of CM might not be possible for the wings. In this case, the fuselage itself will have to be designed so that the drag acts aft of CM in the stalled (and especially high-α) state. The second issue is that, as with the Immelmann turn, we again ignore structural feasibility of the manoeuvre. A real plane capable of a Pugachev cobra will certainly not be 80 ft from CM to tail – it will be much smaller so that the stresses on the airframe are lower. These considerations are however fit for aircraft design, which is a different subject. Here, our only concern is with the dynamics, and the moment we arrive at a parameter set which permits the cobra, we are happy.

§60 **Execution.** We simulate the stall model (3B–28) with a cycle time of 1/4 s throughout. To facilitate my own task, I have used only three different thrust levels – 0, 100 and 200 percent. Recall that 100 percent is 30 kN which is 37·5 percent of the aircraft's weight. I have also used a few discrete $\bar{f_p}$ values – plus and minus 500, 300, 200, 100 and 50 kN, and zero. I have implemented an elevator stall warning when the magnitude of α_E exceeds 22·5°; whenever the warning activates, I have reduced the tail force.

Here is the profile of the manoeuvre.

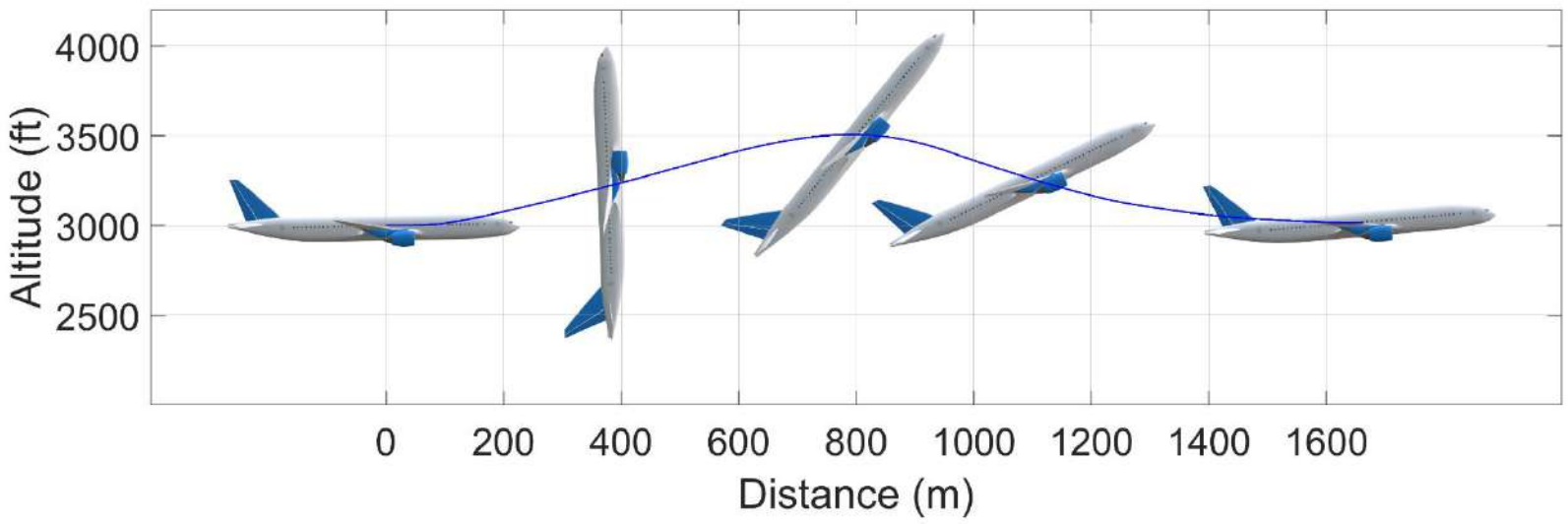


Figure 02 : *Profile of the aircraft during Pugachev cobra. The trajectory is to scale and the pitch is correct, so that the picture gives you as good an idea as possible of what things look like during an actual cobra manoeuvre. The plane itself is over-large as it would otherwise look like a bee and diminish rather than enhance the total effect. The second snapshot captures the instant of maximum pitch, just above 92°. Unlike Fig. 01, we can see a high degree of asymmetry between the pitch up and pitch down phases. Here I have shown Our Plane and not a modified one, even though it is a different model aircraft which actually performs this particular simulation. If you think I am going to prepare a second CAD model just for this one picture, then that will not be the case.*

And here are the details.

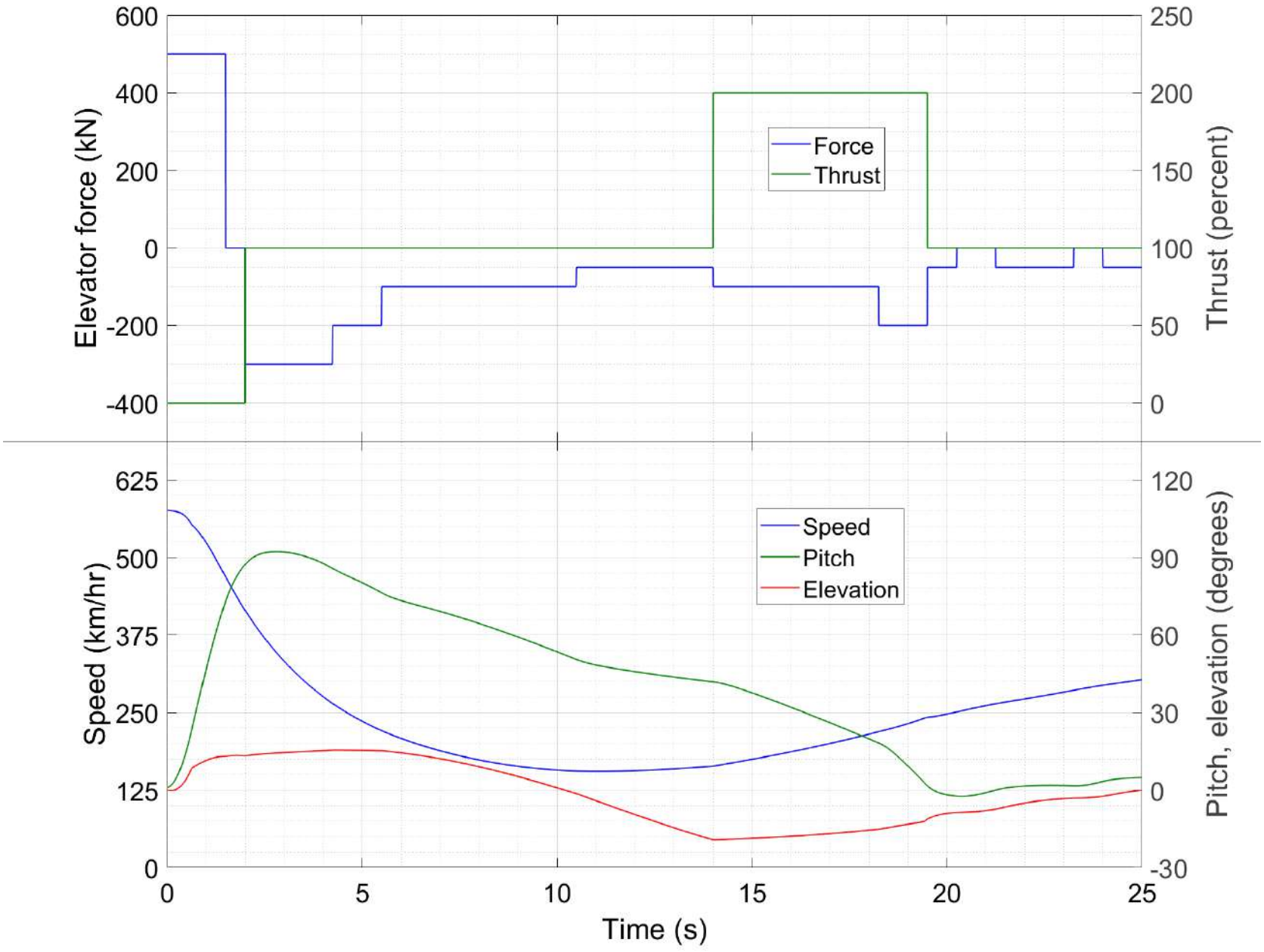


Figure 03 : *Time traces of different variables during the Pugachev cobra.*

I have started from zero thrust and $\bar{f}_p = 500$ kN (top panel), so that the plane pitches up and stalls as fast as possible with minimal tendency of climbing. The kink in the elevation (bottom panel) at about 0·5 s indicates the stall. Even so, the climb rate (not shown in the plot but calculable as $V \sin \eta$) exceeds 5000 fpm. As the pitch approaches 90° I have let go of the stick and then transitioned to push, while simultaneously activating 100 percent thrust. The pitch exceeds 90° for a couple of seconds, thus ensuring that the cobra is technically accomplished. By the time the peak pitch is reached, the speed has already dropped by more than half. The thrust setting of 100 percent facilitates the lowering of the nose while not balancing the weight and allowing the climb to transition to a descent. 300 kN is the maximum push force which is permissible at this instant without the elevator stalling; as the speed reduces, the force has to be progressively reduced. We can see that the decrease of pitch is much slower than the increase because of the positive contribution of the wings to the torque, and the reduced elevator force which we are constrained to use on account of the lower speed. This is responsible for the asymmetry in Fig. 02 – the plane takes thrice the distance to pitch down from 90° to 0 as it does to pitch up from 0 to 90°. As the elevation passes through 0°, the speed starts increasing on account of gravity. When a 3000 fpm descent is established, I have selected 200 percent thrust, which keeps the descent rate approximately constant while accelerating the pitch down rate. Taking advantage of the increasing speed, I have also progressively increased the tail force to hasten the end of the manoeuvre. The kink in the elevation at 19·5 s indicates the exit from stall. At this point, the plane is in a dive so a brief pull-up is necessary, which I have achieved using zero elevator force. Note that steady level flight for a C-B-E plane corresponds to a push and not a pull on the stick !

Overall, the manoeuvre has reduced the speed from 575 km/hr at the start to 250 km/hr at the point of exit from stall. The distance covered has been only 1·7 km while the altitude gained and lost has been about 500 ft. As with the Immelmann turn, I have gone for a primarily qualitative approach with the cobra

manoeuvre instead of performing a detailed analysis and optimizing its execution. This is reasonable because manoeuvres from civil aviation require lots of analysis and prior prep to achieve the best and safest results, while quickfire manoeuvres like this one are executed by the pilots in split seconds using their instincts alone. One feature I observed during practice simulation runs (and there were many!) was that an extended hold of 90°-plus pitch was very difficult or impossible to recover from. In such a run, the aircraft entered the configuration where the elevator was 90° to the fuselage, and the lift (such as it was) overpowered the thrust to keep increasing the pitch. To rectify this, a huge thrust had to be selected to achieve the pitch down, and the manoeuvre ended at considerably higher than the starting altitude. Even in the simulation trace, we can see the germ of this phenomenon – in the time interval from $t = 11$ s to $t = 14$ s, when the elevator force is at its weakest, the angle of attack (pitch minus elevation) is actually increasing. In this case, we can increase both thrust and elevator force soon enough to exit this state and still end the manoeuvre gracefully. Most real aircraft which perform Pugachev manoeuvres are also equipped with **thrust vectoring**, which enables the engines to produce thrust at an angle to the *d*-axis instead of parallel to it. With vectored thrust, recovering from a precarious pitch state is much easier than using aerodynamics alone. Both the aircraft in the video [03] are using thrust vectoring to pull off the stunt; nevertheless, aircraft without this feature are also capable of performing it. In the opening seconds of the video, we can also see a pronounced asymmetry between the pitch up and pitch down phases, as in Fig. 02.

The purported advantage of stall-assisted deceleration in close combat is as follows. If aircraft Alfa is pursuing aircraft Bravo, then Bravo can pull a Pugachev and get behind Alfa, thus reversing roles. In practice however, I am not sure of whether getting into a precarious pitch configuration, even for a short time, will be advantageous to Bravo. Seeing him begin the manoeuvre, Alfa can simply pull a hard turn while shooting continuously and cop the cobra in the belly. In any case, most air-to-air combat today occurs beyond visual range, where the precision of the missiles is far more important than the manoeuvrability of the planes. In airshows however, a plane flying horizontally while pointed vertically is sure to garner plaudits from the audience, and this is perhaps the most significant application of the Pugachev cobra.

J. ELEVATOR FAULT

So far we have been looking at planes which are fully functional. Fortunately, almost all transport flights are of this type. Once in a blue moon however, we have an aircraft which develops a technical snag en route. Here we take a look at one of the worst (and fortunately one of the rarest) of these situations. When it happens in the real thing, it pushes the pilot to the limit of his technique; on the simulator, it will take our model to the limit of its descriptive and predictive capacity.

§61 **Description.** Unfortunately this is not an elevator outage on the Washington DC Metro – there is no shuttle to the destination available from the nearest airport. Or maybe there is – if at all one gets there. In airliners with separate elevator and horizontal stabilizer, the fault can be of two types : either (*a*) the elevator alone is lost, or (*b*) both elements are lost. A "loss" in this context may mean that the component has been shorn off, it is floating freely and exerting zero force, or it is jammed in a particular position. In Case (*a*), it is possible to control the aircraft using the trim wheel; while it still requires some pilot skill to return to earth, a safe landing is manageable and expected. In Case (*b*), the aircraft becomes quasi-uncontrollable in pitch*. Achieving a safe return from this situation requires enormous pilot skill as well as good luck. Since Our Plane merges the stabilizer and elevator into a stabilator, the loss of this element automatically corresponds to Case (*b*).

* In GA and other aircraft where the horizontal stabilizer is fixed to the fuselage, Case (*a*) has the same disastrous effect as Case (*b*) in a jetliner.

Here is a quick simulation of Our Plane (not the Pugachev cobra aircraft of the last Subdivision) with an elevator fault and no intervention being attempted by the pilot. Taking the mass as 80 tons, the initial condition features level flight at 500 km/hr, 5000 ft above ground. Thrust is 33 percent throughout, approximately the steady state requirement for level flight at that speed. Here is the aircraft profile during the subsequent half a minute of flight.

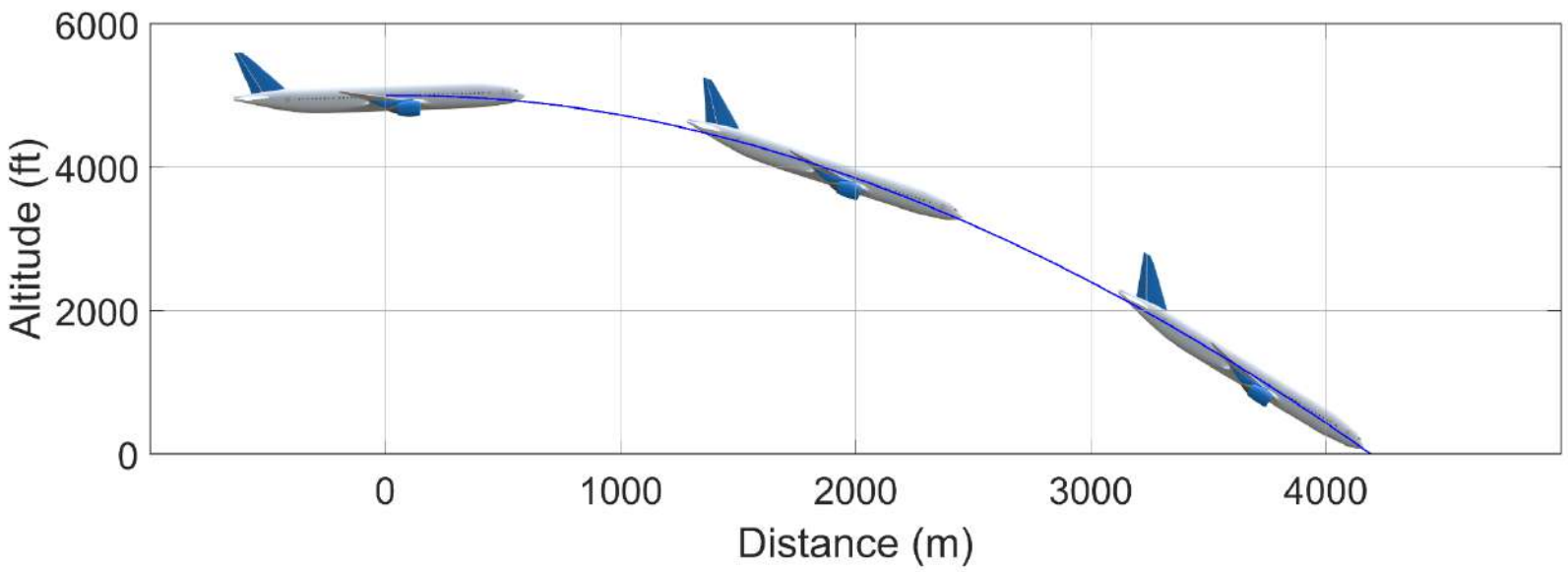


Figure 01 : *Profile of Our Plane with no elevator and no accident-avoidance measures being attempted. The trajectory is to scale and the pitch is correct. The plane itself is over-large as it would otherwise look like a bee and diminish rather than enhance the total effect. In the Figure, I have not changed Our Plane to account for a missing elevator – a hydraulic failure would not be externally manifest but would cause the elevator to exert zero force.*

Suffice it to say that this Figure depicts an aviation accident. Our task now is to figure out why this happened, and what can be done to achieve a happier outcome.

§62 **Planning – basics of approach and flare.** Understanding the accident is easy enough. In a fully functional airliner, the wing torque is negative and the tail torque is positive. When the elevator is lost, the latter becomes zero. The torque of the wing lift causes the nose to pitch down and sends the plane into a dive.

To start planning the recovery strategy, we note that the thrust has a positive contribution to torque on account of the engines' being mounted below the CM. Without the elevator, this is the only source of positive torque we can harness to counter the negative effect of the wing lift. Furthermore, the thrust being in our control, we can also use it to achieve some measure of pitch adjustment. In the typical parameter values, $\bar{h} = 0{\cdot}5$ m and $\bar{d_1} = 1$ m. For the 80 ton plane, the torque of thrust even at full throttle ($T\bar{h} = 150$ kNm) comes nowhere close to balancing the torque of the lift ($mg\bar{d_1} = 784$ kNm). To remedy this situation, we shall have to reduce $\bar{d_1}$ i.e. move the CM backwards, closer to the CP of the wings. This is easier said than done – on a passenger plane, we should try to move the passengers back while in a cargo plane we should try to relocate the freights. Fuel may also be pumped aft if the plane design allows for this. Whatever the logistics, if CM cannot be relocated to a point where thrust achieves balance and pitch control, then the situation is unrecoverable. If CM can be relocated to such a point (or was in such a point to begin with), then at least there is hope. This binarity is where luck enters the picture for the first time if the elevator fault occurs in a real plane*; in what follows we assume that luck is on our side.

* If the plane has a two-piece tail then the loss of elevator and trim but not the stabilizer itself (i.e. stabilizer jammed but not shorn off) at least does not cause an immediate earthward plummet. Hence, the dual-tail provides an extra layer of security. It can happen though that the trimmed airspeed is very high, and CM repositioning is necessary to bring it down by reducing d1 XXXX BAR XXXX, as per (4O–08).

Let us say that we have managed to reposition the CM such that $\bar{d_1}$ is now 7·5 cm. Then, a thrust level of 39·2 percent achieves pitch equilibrium with the lift. Equilibrium at a midrange thrust is good because we can then use a higher thrust to pitch up and a lower thrust to pitch down. So, at least in theory, the flight is now safe – power up to climb, power down to descend and hold approximately 40 percent thrust to maintain level flight. I say in theory because thrust-based control is harder to implement than it sounds. Firstly, the speed gets tied to the pitch, so the two are no longer decoupled from each other. Secondly, the rate of change of pitch becomes vastly slower – in the presence of the elevator, the maximum pitching torque we can apply on the plane (assuming max elevator force of 100 kN) is more than 2000 kNm while in its absence, the excess torque at full thrust is about 90 kNm only.

To demonstrate operation of the crippled aircraft, I will focus on the manoeuvre which is most difficult under the circumstances – approach and landing. Let us say we have managed to establish steady level flight at 1000 ft and are proceeding towards the airport from directly behind. Under normal circumstances, we would simply push down the nose when the glideslope is intercepted, follow the slope upto and past the runway threshold and flare out at the end, as in Subdivision 5D. Without the elevator, every step will introduce a complication. Firstly, since the achievable pitch rate is low, interception of the slope will have to start at some point behind it, by retarding thrust to idle. As the nose gradually pitches down, we will have to ensure that the desired pitch attitude is attained when the plane is on the slope. Exit from the slope will be even more difficult. To maintain pitch equilibrium, the slope will have to be flown at approximately 40 percent thrust – triple the approach thrust of Fig. 5D–04. Hence, when it's time to flare, we shall be at considerable speed, descending extremely fast, and in a nose-down attitude. If we wait to flare until the usual 20-30 ft altitude, then, with the slow pitch rate, we shall still be in nearly the approach configuration when we hit the ground. Nosewheel first at high vertical and horizontal velocity is not a landing but a crash. While nobody is expecting a greased touchdown in this situation, a bouncer will be undesirable as it will delay the application of wheel brakes and squander precious hundreds of metres of runway (remember, we are at elevated speed to begin with). To prevent this, we shall have to initiate the flare long before the threshold so that the plane pitches up and the descent rate is arrested before the ground is hit. A flattening trajectory starting from far behind the runway has its own risks however – it can lead to a touchdown point way ahead of the threshold, after which the high forward speed will carry us out of the runway and into the grave. Take a moment to ponder the situation – it's almost literally आगे कुआँ पीछे खाई (aage kuan peeche khai)*. Now add in the fact that, unlike a normal landing, this has no go-around option – full or at least high thrust is what achieves the flare anyway, and we can't do more. So, our first chance at the landing will also be our last. At some point on the glideslope, miles behind the airport, we must make our fixed and final commitment to land – technique and fortune will determine what happens after.

* Translates approximately as "between a rock and a hard place" though no idiom can ever be translated without changing some of the underlying meaning or imagery.

To shift the balance in favour of technique, we transition from words to numbers – obtain (or at least try to obtain) the thrust as a function of time, which, when implemented starting from a point 1000 ft above ground and at a location to be determined, will culminate in a safe landing on a target zone of the runway. This is a typical inverse problem – instead of finding the trajectory given the thrust, we are instead trying to find the thrust which leads to a given trajectory. The system involved here, (3B–22), is sixth order and nonlinear. While we can find the thrust by hit and trial on the simulator itself, such an exercise is likely to require dozens or even hundreds of tries and take inordinate time. Practically, what is necessary here is a calculation for the unknown thrust which is feasible to be executed by engineers in the time span while the pilot of the stricken plane approaches the airport (and optionally circles round it once or twice). Once the calculation is over, the engineers can relay the results to the cockpit to be used as appropriate. Hence, we will now embark on an approximate but deterministic solution of (3B–22) with $\bar{f}_p = 0$ which will at least give the pilot an approximate strategy to use for the landing.

As always, we start from the characteristics. For this step, we assume that the elevator is present, since it will be impossible to draw characteristics otherwise. In addition to $\bar{d}_1 = 0{\cdot}075$, we use the parameter values $K_C = 2250$ and $C = 12$, which corresponds approximately to the takeoff flap configuration with the undercarriage extended. We assume that due to the high thrust requirement and the consequent elevated speed of operation, the maximum flap setting which we used in Subdivision 5D is no longer a safe option (a reasonable assumption which is likely to hold true in practice). We plot the characteristics for three flight profiles – descent along glideslope, descent at 600 fpm and level flight. The second choice is motivated by the fact that 600 fpm is usually the maximum descent rate which the undercarriage is certified to withstand.

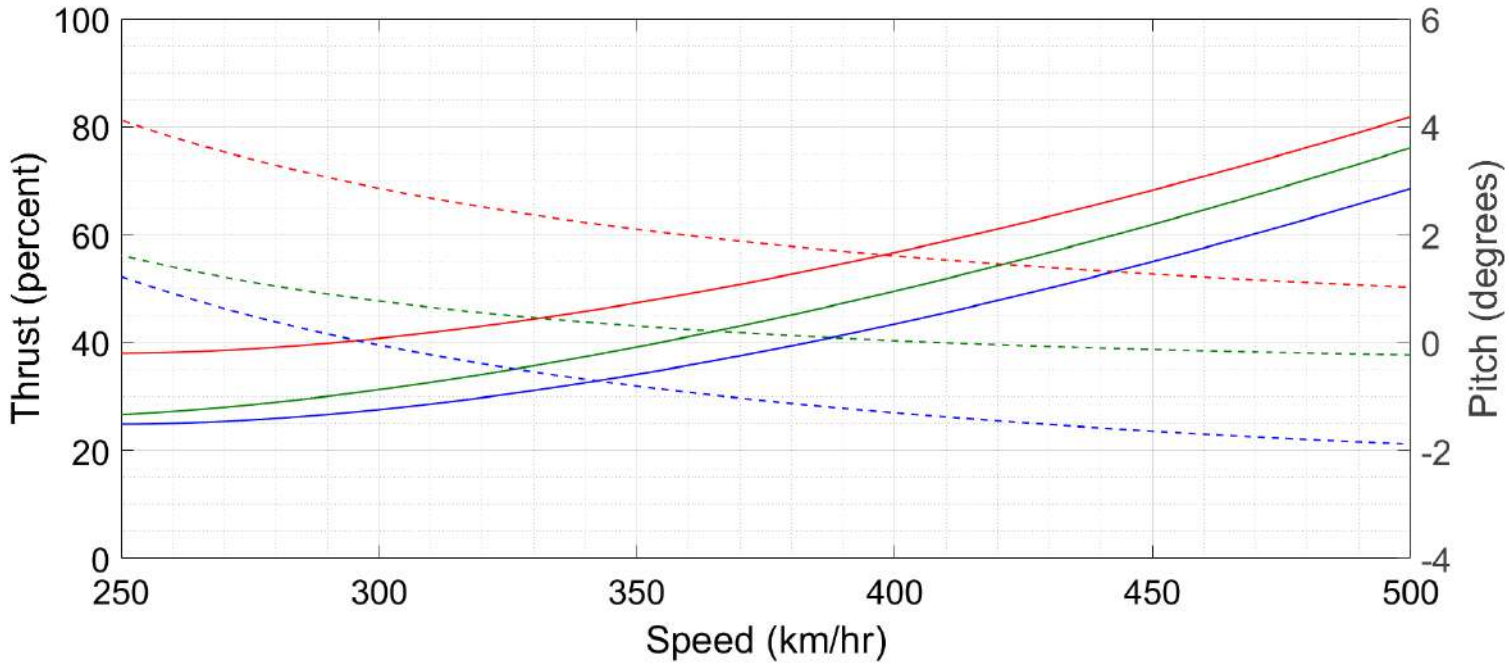


Figure 02 : *Characteristic curves for Our Plane with the elevator in place. Solid lines attach to the left hand* y*-axis and dashed lines to the right hand* y*-axis. Blue, green and red correspond to descent along glideslope, descent at 600 fpm and level flight respectively.*

As we have discussed in §50, the best flare to use in this situation will be a steady state flare with a firm but not heavy touchdown. To design this flare, let us assume that the plane is in the equilibrium configuration on the glideslope when the flare starts. This assumption has little basis except for providing a starting point for the calculation – we shall refine it iteratively as we proceed. The steady state configuration must be the point corresponding to 40 percent thrust; the speed here is about 380 km/hr (!) and the pitch is about $-1{\cdot}2^{o}$. Next, we note from §52 that the angle of attack α always gravitates towards its equilibrium value. Since pitch changes are slow, let us assume that α is always in steady state, i.e. given V and θ at any instant, the corresponding α and hence η at that instant are the ones corresponding to a fixed point in the plane with elevator. Then, in the 400 km/hr range, a pitch of zero corresponds to a 600 fpm descent while a pitch of $1{\cdot}5^{o}$ corresponds to level flight. During the flare, if we hold a steady pitch intermediate to these two values, then we shall achieve ground contact at a steady descent rate between 0 and 600 fpm, a safe landing. Hence, let us fix (for now) $0{\cdot}7^{o}$ as the target pitch attitude to maintain during flare.

Next, we need some idea of where to start the flare. For this, the overdamped dynamics (5B–05) shows that, with the given parameter values, a 10 percent deviation in thrust from the equilibrium corresponds to a pitch rate of $0{\cdot}056^{o}$/s. So, if we use 90 percent thrust for the flare, corresponding to 50 percent excess thrust, then we'll get a pitch rate of $0{\cdot}28^{o}$/s and the change from $-1{\cdot}2^{o}$ to $0{\cdot}7^{o}$ pitch will take about 7 s. But there is another issue to be taken care of here. Jet engines cannot change their power level instantly – they take a few seconds to ramp up and down between low and high settings. Normally, this time isn't significant but in an emergency, where we're reliant on thrust to control pitch, we can ignore it no longer. For the purpose of the calculation, we assume that the thrust can change at a maximum rate of 25 percent per second. Then, it will take two seconds for the thrust to ramp up from 40 to 90 percent at the start of the flare, and two more seconds to ramp down to 40 for the steady state flight upto the touchdown. During these four seconds, we shall get an approximate average pitch rate of half the maximum i.e. $0{\cdot}14^{o}$/s, and the pitch change from glideslope to flare will actually take 9 s instead of 7 s ($0{\cdot}28^{o}$ change in each of the first and last two seconds and $1{\cdot}4^{o}$ in the middle five). At 380+ km/hr, the plane will fly about 1 km during these 9 seconds, so the approximate start of flaring will have to be about that far behind the airport, i.e. approximately at the inner.

So at this point, we have some crude numbers – fly the glideslope upto the inner at 40 percent thrust and then initiate flaring using 90 percent thrust, aiming for a target pitch of $0{\cdot}7^{o}$. While this is better than what we started from, it is still unsatisfactory for two reasons. First is the assumption of steady state on the glideslope. Intercepting it at 1000 ft and about 270 km/hr (the steady state speed for level flight at 40 percent thrust), we may not have enough distance upto the inner to attain steady state on slope. This will be good

for us, since it will mean we are flying slower. However, it will result in alteration of the flare parameters. The second weakness of our calculation so far is that it makes no reference to where on the runway we'll land – a protracted flare starting on slope at the inner is likely to see us kilometres forward of home at touchdown. To compensate for this, we must deliberately be a few feet below glideslope when we start to flare. At this point we have no estimate of how many feet this will be.

In what follows, we shall use the above crude result as a starting point for a more sophisticated calculation which will give us the y and z coordinates of the point where the flare must be initiated to achieve an adequately soft landing at a target point on the runway. This will be perhaps the most involved mathematical process in the entire Article – if you want the results only, skip to the last paragraph of the next Section.

§63 **Planning – calculation of waypoints on the flight path.** Since this Section features calculation, we use SI Units throughout, with the exception of the degree in some cases. Let the runway threshold correspond to $(y,z) = (0,0)$. We start from the very beginning – interception of glideslope. Having established steady state level flight at 308 m (1010 ft, thousand altitude plus ten from wheels to CM) above ground and a speed of 75 m/s, we are proceeding horizontally towards the airport. The pitch at this point (see Fig. 02) is $3{\cdot}5^{o}$. On the slope at that speed, the pitch required is about $0{\cdot}5^{o}$. The decrease in pitch will be achieved by retarding thrust to 10 percent (our assumed flight idle), which will also cause the speed to reduce while the nose pitches down. Our initial task is to find y^* and a time τ^* such that, starting from level flight at the point (y^*, 308), holding 10 percent thrust for τ^* seconds leads to the elevation η becoming $-2{\cdot}91^{o}$ (glideslope angle) at a point exactly on the glideslope.

We do this using the simulator itself – it's a straightforward single run of the simulator and not a hit and trial. Using initial conditions corresponding to level flight at 75 m/s and accounting for maximum 25 percent change in thrust per second, we find that it takes 14 s to reduce thrust from 40 to 10 percent, maintain the latter to achieve the desired reduction in pitch and elevation, and then ramp back up to 40 percent when $\eta = -2{\cdot}9^{o}$. During these 14 s, the aircraft travels 980 m forwards and 22·6 m downwards, and decelerates to a speed of 66 m/s. So, if we initiate the interception from the point (y^*, 308), then we'll attain the glideslope η at (y^*+1050, 285·4). Now, stipulating that this point lies on the glideslope itself and using the glideslope equation (5D–01a), we find $y^* = -6240$ m. The point of entry into the slope then becomes (–5260, 285). Let's call this point P.

At the other end of the manoeuvre, we can easily fix the point where the flare ends. Since our intended flaring technique is steady state, we should return to 40 percent thrust at the end of the flare and maintain that level until touchdown. It is reasonable to stipulate that the flare conclude when the wheels are 3 m above ground, i.e. the CM is 6 m above it. While in a normal landing, this point would be attained about 250 m forward of threshold, we want to reduce the length in this instance because of our excessive landing speed. Hence, let's aim to reach the 6 m altitude at 100 m forward of threshold. Then, we get a second reference point, R (100, 6) through which the aircraft must pass. Between P and R is Q, the point where the flare is initiated. As yet, Q is at an unknown distance behind the airport and an unknown height below the glideslope; what follows is a determination of its coordinates.

We approach this task as follows. First, an assumption : since the gradient of PQ will be only slightly different from that of the true glideslope, we shall interchange the two as necessary. Now, let the unknown V_0 be the aircraft speed at Q; by our assumptions, the pitch θ_0 at this point is given by the dashed blue curve in Fig. 02. Let the thrust during flare consist of a 2 s uniform ramp-up from 40 to 90 percent, τ^+ s holding at 90 percent where τ^+ gets determined by the target pitch at R, followed by a 2 s uniform ramp-down to 40 percent. Then, for different values of V_0, we will solve [a simplified form and/or subset of] (3B–22) with the thrust $T(t)$ being given by the flare function we just defined. For each V_0, we will find a horizontal distance y^+ and a vertical distance z^+ which the plane travels during the flare. Since the flare is constrained to end at point R (100, 6), the coordinates of Q for this V_0 should be ($-y^+$+100, $-z^+$+6). Of course, we still don't have Q uniquely, since it's tied up with this unknown V_0. So now, we use the known velocity of the aircraft at point P together with the fact that PQ is a straight line. For each candidate Q, we will solve [a

simplified form and/or subset of] (3B–22) for the velocity along the path PQ, using as initial condition the known velocity at P. Then we will evaluate this velocity at the candidate Q – the true Q will be the point at which this velocity equals V_0. This condition will imply a consistent trajectory from 66 m/s at P to V_0 at Q followed by the corresponding flare from Q to R. In other words, we find Q by separately calculating many different trajectories PQ and QR and then stipulating that the two match up. The technique is similar to the method of matched boundary conditions used to obtain periodic solutions to ordinary and partial differential equations [01].

Before starting the boundary matching proper, we obtain a suitable form of (3B–22) on the slope PQ. The relevant equation is (3A–22c); the catch is the presence of the unknown thrust function T and the extra variable θ in the drag term. We sneak around these hurdles as follows : for the thrust, we assume that it is constant on the slope, and for the drag, we replace it by a parabola which depends on V alone. Figure 02 shows that the thrust required to maintain constant speed along the slope, and hence the drag encountered at that speed, indeed looks like a parabola – moreover, the drags at two different slopes (glideslope and zero) are parallel, implying that the same parabola holds over many slopes. With these approximations, (3A–22c) reduces to

$$\frac{\mathrm{d}V}{\mathrm{d}t} = \frac{1}{m}\left\{T - mg\sin\eta - \left(c_1 + c_2 V + c_3 V^2\right)\right\} \quad , \tag{01}$$

where c_1, c_2 and c_3 are obtained from fitting. We find their values by fitting the curve for level flight at $V = 70$ and $V = 110$; the specific numbers I have used here are $c_1 = 2{,}79{,}375$, $c_2 = -4725$ and $c_3 = 33{\cdot}75$ SI Units.

This equation allows us to obtain a preliminary estimate of the speed at Q based on transient dynamics (recall that in the last Section we only had a steady state value), and in turn an estimate of the target pitch θ^+ we will need at R for a safe landing. Without this estimate, we cannot do the boundary matching. To find the speed at Q, we first need the thrust T to be used. As the plane accelerates along the slope, its angle of attack and hence its pitch must reduce, so T must be less than the 40 percent which produces constant pitch. The speed at P is 66 m/s; at Q it will definitely not exceed 100 m/s. If we take the average speed on the slope to be 80 m/s and assume that the slope runs from P to the inner (since we don't have an updated estimate yet), then it will take about 50 s to do the run PQ. Of course this is an approximate number, but it works. Then, during these 50 s, we'll have to reduce pitch from approximately $1{\cdot}5^\circ$ to approximately $-0{\cdot}5^\circ$ (the pitch at a speed of 90-plus m/s on the glideslope as per Fig. 02), which corresponds to a rotation rate of $-0{\cdot}04^\circ$/s, and 7 percent thrust defect. Hence we can use 33 percent thrust as the equivalent constant value in (01). Of course, these numbers are all obtained from hand-waving arguments and during the actual simulation we'll have to adjust thrust in real time depending on our deviation from the intended trajectory and pitch. But the approximate numbers serve two important purposes : (*a*) they give us a general idea of the thrust to use, and (*b*) they allow us to proceed with the analytical determination of Q. For η we now use $-0{\cdot}0508$ radians, which is the gradient of the true glideslope.

Having set $T = 100$ kN and $\eta = -0{\cdot}0508$ in (01), we now recast it in terms of V and the distance S along the slope; the Chain Rule gives $\mathrm{d}V/\mathrm{d}t = V\,(\mathrm{d}V/\mathrm{d}S)$. Using this and plugging the numbers into (01) yields

$$\frac{\mathrm{d}V}{\mathrm{d}S} = \frac{a}{V} - b - cV \quad , \text{ where} \tag{02a}$$

$$a = -1{\cdot}745, \quad b = -0{\cdot}059, \quad c = 0{\cdot}000422 \quad . \tag{02b}$$

This equation is separable so we solve by transferring the variables; we have

$$\frac{V\,\mathrm{d}V}{a - bV - cV^2} = \mathrm{d}S \quad , \tag{03}$$

so that

$$S = \int \frac{V \, \mathrm{d}V}{a - bV - cV^2} + \mathbb{C} \quad , \tag{04}$$

where fancy $\mathbb{C}$ is a constant of integration. Any website of integrals worth its salt has the one on the LHS listed in its formula database; copying the formula we have

$$S = -\frac{1}{2c}\left[\log\left(a - bV - cV^2\right) - \frac{2b}{\sqrt{-b^2 - 4ac}} \arctan\left(\frac{b + 2cV}{\sqrt{-b^2 - 4ac}} \right) \right] + \mathbb{C} \quad . \tag{05}$$

The initial condition $S(0) = 66$ shows that $\mathbb{C}$ is the negative of the above RHS evaluated at $V = 66$, completing the solution of (02).

Using this solution, we find that the plane attains a speed of 80 m/s after travelling about 3·3 km and a speed of 85 m/s after travelling about 4·9 km. Since the distance from P to Q will be approximately 4·3 km (still assuming Q to be at the inner for want of an updated estimate), the speed at this point will be between these two as well. At this speed, Fig. 02 shows that our initial flaring pitch target of 0·7° is insufficient for achieving an acceptable touchdown; while the flare will increase speed somewhat, 0·7° will still be too close to the maximum permitted descent rate, while leaving an unnecessarily high margin from level flight. Hence we now revise the flaring pitch target to 1·2°, which is comfortably between the 600 fpm and level flight curves in Fig. 02 over a wide range of speed centred at the estimated speed at Q.

The flaring pitch target obtained, we formally begin our boundary matching calculation for the determination of Q. For the first half of this calculation, we need the horizontal and vertical distances travelled during the flare. For this, we will have to solve (3B–22) with the thrust being given by the flare function, which we recall consists of a ramp-up, a plateau and a ramp-down. To simplify the calculation, we replace this by a three-steps function which is constant at 65 percent for 2 s, constant at 90 percent for τ^+ s and again constant at 65 percent for 2 s. Using the overdamped assumption, this allows us to have a transparent form for ω :

$$\omega(t) = \begin{cases} 0{\cdot}14° / \mathrm{s} \;\; \text{if} \;\; 0 < t \le 2 \\ 0{\cdot}28° / \mathrm{s} \;\; \text{if} \;\; 2 < t \le \tau^+ + 2 \\ 0{\cdot}14° / \mathrm{s} \;\; \text{if} \;\; \tau^+ + 2 < t \le \tau^+ + 4 \\ 0 \;\; \text{otherwise} \end{cases} \quad , \tag{06}$$

($t = 0$ being the start of the flare). This leads to a transparent form for θ, which is the time integral of ω. By our assumptions, the initial value θ_0 is the pitch corresponding to V_0 on the glideslope in Fig. 02. Then, $\theta(t)$ is the function (expressed in degrees)

$$\theta(t) = \begin{cases} \theta_0 + 0{\cdot}14t \quad \text{if} \quad 0 < t \le 2 \\ \theta_0 + 0{\cdot}28 + 0{\cdot}28\left(t - 2\right) \quad \text{if} \quad 2 < t \le \tau^+ + 2 \\ \theta_0 + 0{\cdot}28 + 0{\cdot}28\tau^+ + 0{\cdot}14\left(t - \tau^+ - 2\right) \quad \text{if} \quad \tau^+ + 2 < t \le \tau^+ + 4 \\ \theta_0 + 0{\cdot}56 + 0{\cdot}28\tau^+ \quad \text{otherwise} \end{cases} \quad . \tag{07}$$

We can see at once that, to achieve the target pitch of 1·2° at R, τ^+ must be given by

$$\tau^+ = \frac{1{\cdot}2 - \theta_0 - 0{\cdot}56}{0{\cdot}28} \quad . \tag{08}$$

For $\theta_0 = 0$, the pitch corresponding to 83 m/s on the glideslope, τ^+ is about 2·3 s so that the whole flare takes 6·3 s.

Equation (3B–22c), the most important of the six equations of (3B–22) for our present purposes, contains dependences on α and η which couple it to the rest of the system. While (07) takes care of θ, we are yet to do anything about α and η. It is the duration of the flare which shows us the way out of the mess. At 83 m/s, the drag on the glideslope corresponds to more than 25 percent thrust; the flare thus consists of 2 s at 65 percent excess thrust and 4 s of 40 percent excess thrust. The accelerations in these two phases are 2·4 m/s^2 and 1·5 m/s^2 respectively, for a total speed increment of 10·8 m/s. Over such a small range of

speed, we can treat α to be constant, equal to its value α_0 at point Q. Since we already have θ as a known function of time, this immediately makes η a known function of time as well. With this, (3A–22c) breaks off from the others; we have

$$\frac{\mathrm{d}V}{\mathrm{d}t} = \frac{1}{m}\left\{\frac{K_C V^2}{4}\left(\cos 3\alpha_0 - \cos\alpha_0\right) + T(t)\cos\alpha_0 - mg\sin\eta(t) - CV^2\right\} \quad , \qquad (09)$$

with $\eta(t) = \theta(t) - \alpha_0$ where $\theta(t)$ is given by (07). The initial condition is $V(0) = V_0$.

Equation (09) is a textbook differential equation called the Ricatti equation. It can be solved analytically, though in the present case I have elected to do it numerically, using EULER's method*. Given $V(t)$ and the pre-determined $\eta\,(t)$, we can find V_y and V_z as $V\cos\eta$ and $V\sin\eta$ respectively, and then integrate these in time to obtain the total horizontal and vertical distances travelled during the flare. Below we plot these two quantities for various values of V_0 in the range 75 to 100 m/s.

* The extra precision arising from a more sophisticated numerical integration method is completely unnecessary here.

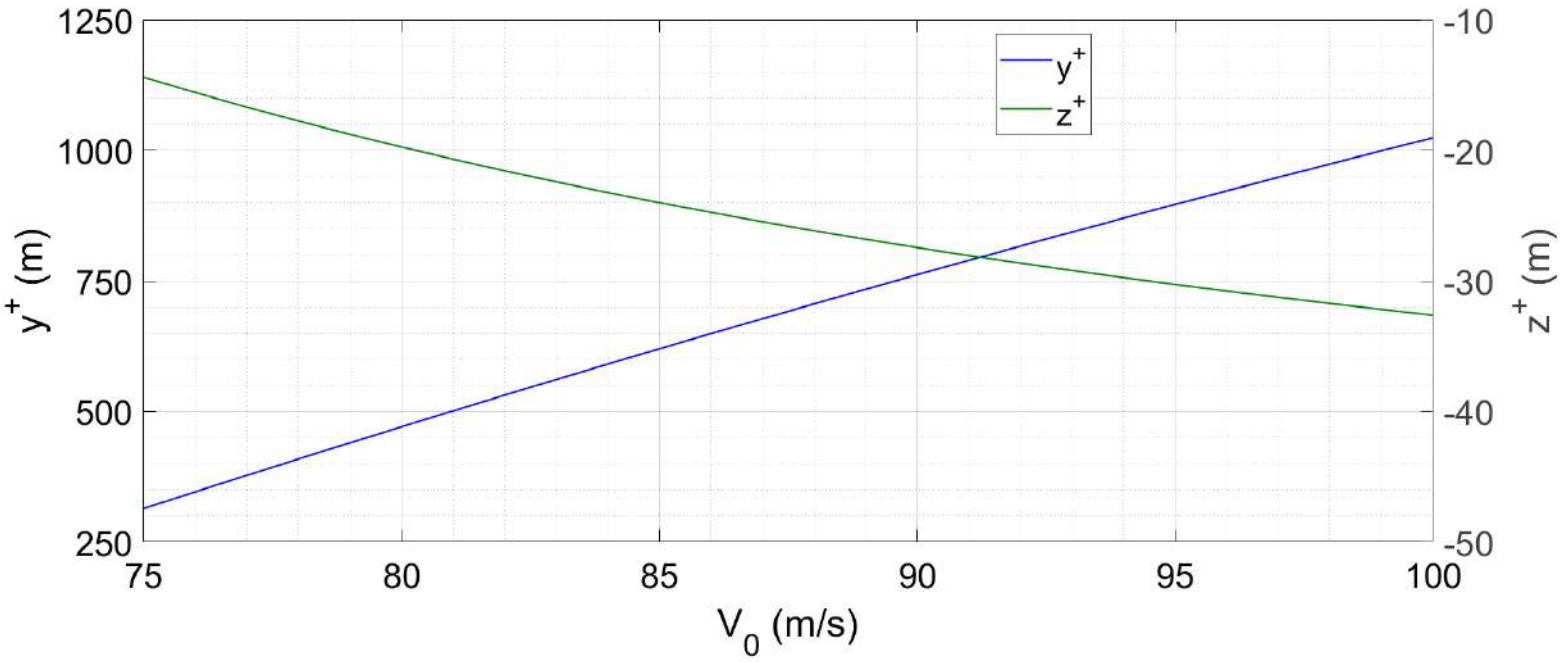


Figure 03 : *Horizontal and vertical distances travelled by the aircraft during flare, for different values of the unknown parameter* V_0.

Here, y^+ is positive and z^+ is negative because the aircraft moves forward and loses height during the flare. Both increase in size with increasing speed, which is very plausible. Thus, we have obtained y^+ and z^+ for each V_0, and hence we can get the corresponding candidate Q as $(-y^+ + 100, -z^+ + 6)$. This completes the first part of the boundary matching process.

For the second part – computation of trajectory from P to the candidate Q – we already have the equation (01) into which we substitute 33 percent thrust as before. Now, for η, we use the inverse tangent of the slope from P to the candidate Q. Recasting (01) as (02a) and using the initial condition $V = 66$ at point P, we solve (02a) to find the velocity at candidate Q. Since each candidate Q is linked to a definite V_0, we plot the results as "V at candidate Q" as a function of V_0. Since the true Q is given by $V = V_0$, we also plot the identity function, as below.

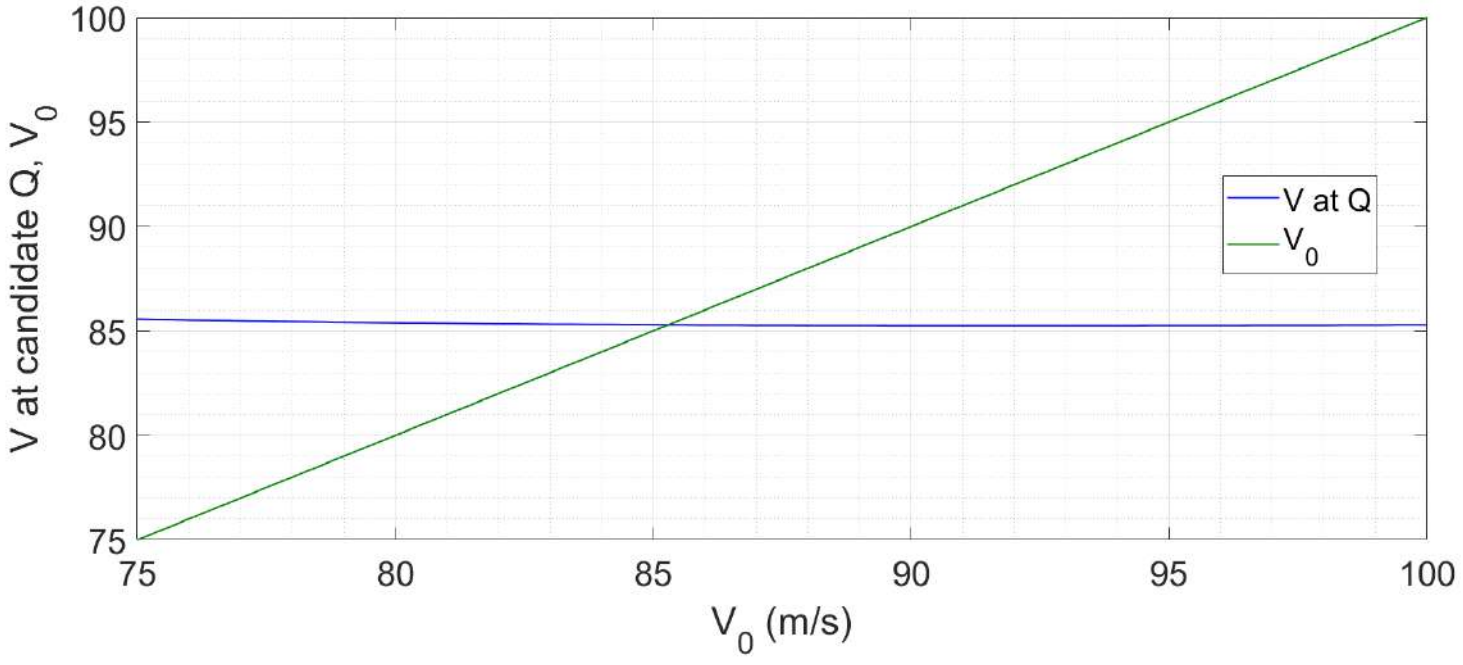


Figure 04 : *The speed at the candidate Q as a function of* V_0*, together with the identity function.*

Equality is achieved at $V_0 = 85{\cdot}15$ m/s; the corresponding Q is at (–525, 30). This completes the calculation.

Now let us interpret what we have got. The flare initiation point has turned out to be 525 m behind the airport, at an altitude of 98 ft. The true glideslope at that distance would have the altitude 148 ft, so our target flaring point is 50 ft below it. About half of these feet have a trivial origin – our desire to have the wheels 10 ft instead of 33 ft above ground at 100 m forward of threshold. The remaining half are non-trivial and are the correction we must implement to account for the extended flare. The slope of PQ is $-3{\cdot}08^o$, $-0{\cdot}17^o$ more than that of the true glideslope. The speed at touchdown will be of the order of 345 km/hr (85 m/s at Q plus 11 m/s added during flare), and with a flaring pitch of $1{\cdot}2^o$, the descent rate as extrapolated from Fig. 02, will be slightly upwards of 300 fpm.

If we had wanted – we *don't* want but still – we could have now refined the estimate for Q by iterating the process once more. In what we did, we simulated the flare by starting from the true glideslope and then matched it to the approach to find the point Q (which we now call Q_0) and an updated approach slope PQ_0. To improve accuracy, we can now start the flare from the calculated PQ_0, match it to the approach and end up with Q_1. Several rounds of this will give a more accurate Q_n. Likewise, we can improve accuracy by relaxing the assumptions inherent in the reductions of (3B–22) used for the two phases. The point of this exercise however is not to demonstrate four-decimal place precision via a mathematical tour de force. Rather, as I have already stated, our aim here is to generate a guideline which the pilot can use, within the time frame realistically occurring between the elevator fault and the attempted landing. This objective has been accomplished.

We now present the results of the calculation in a form suitable for practical use. Approaching at 1000 ft of altitude, slope interception should begin at about 6·25 km behind the airport. To achieve this step, we should retard throttles to idle until the slope is intercepted on the instruments. Then, we should advance the throttles to perform the approach along a straight line which is slightly steeper than the true glideslope. The slope of this approach should be $-3{\cdot}08^o$ and the velocity ratio V_z/V (see §48) should be 2·940. Flare should be initiated at a point 525 m behind the airport and an altitude of 98 ft. For the flare, we must advance throttles to 90 percent thrust and hold until pitch just crosses $0{\cdot}9^o$, then retard to 40 percent and maintain pitch $1{\cdot}2^o$ upto touchdown. Note that the calculation assumes the flare to begin from a pitch of $-0{\cdot}25^o$ which is the steady state pitch corresponding to V_0 on the glideslope; if the actual pitch during approach is different, then we shall have to compensate for that. Of course, all these numbers are guidelines; now, let us head over to the simulator and see how good or bad our guidelines are.

§64 **Execution.** The simulated system is of course (3B–22), cycle time is 1 s upto –800 m, 1/4 s from that point until brakes are applied and 2 s thereafter. Displayed readings are distance, altitude, deviation from actual glideslope, speed, climb rate, velocity ratio and pitch. As in §48, I have implemented the glideslope deviation as feet rather than degrees. To model the finite rate of change of thrust, I have imposed a

maximum change through 25 percent in a 1 s simulation cycle and 6 percent in a 1/4 s cycle. Like §47, we have the constraint that after touchdown, brakes can't be applied until the pitch becomes 0·5° or lower. For the final braking, I have used a deceleration of 3 m/s^2 which is achieved at a 'thrust level' of –80 percent (the simulator has only the one source of *d*-axis force; it makes no claims to an accurate representation of on-ground dynamics).

To fly the approach while maintaining the target V_z/V of 2·940, we need a qualitative relation between velocity ratio and thrust. If the thrust is 40 percent, then the pitch remains constant. If we are on the slope and below the steady state speed (which will be the case in this simulation), then that thrust will also cause the aircraft to accelerate, and its α will decrease. Hence, η will increase, leading to a lower descent rate for a higher speed and V_z/V will go down. If on the other hand the thrust is idle, then the speed will decrease while the pitch decreases also, dragging the elevation with it. In other words, the aircraft will enter a dive while slowing down, and so V_z/V will go up. Hence, if Vz/V is above target then we'll need to apply more thrust while if it is below target then we'll need to apply less thrust.

Here's the approach, starting from steady state level flight at 40 percent thrust 7 km behind the airport and at 1010 ft of altitude, and going all the way upto the start of the flare (note the increase of thrust right at the end). The end time is 86·5 s. The glideslope in the third panel is the true one and not the intentionally deviated PQ.

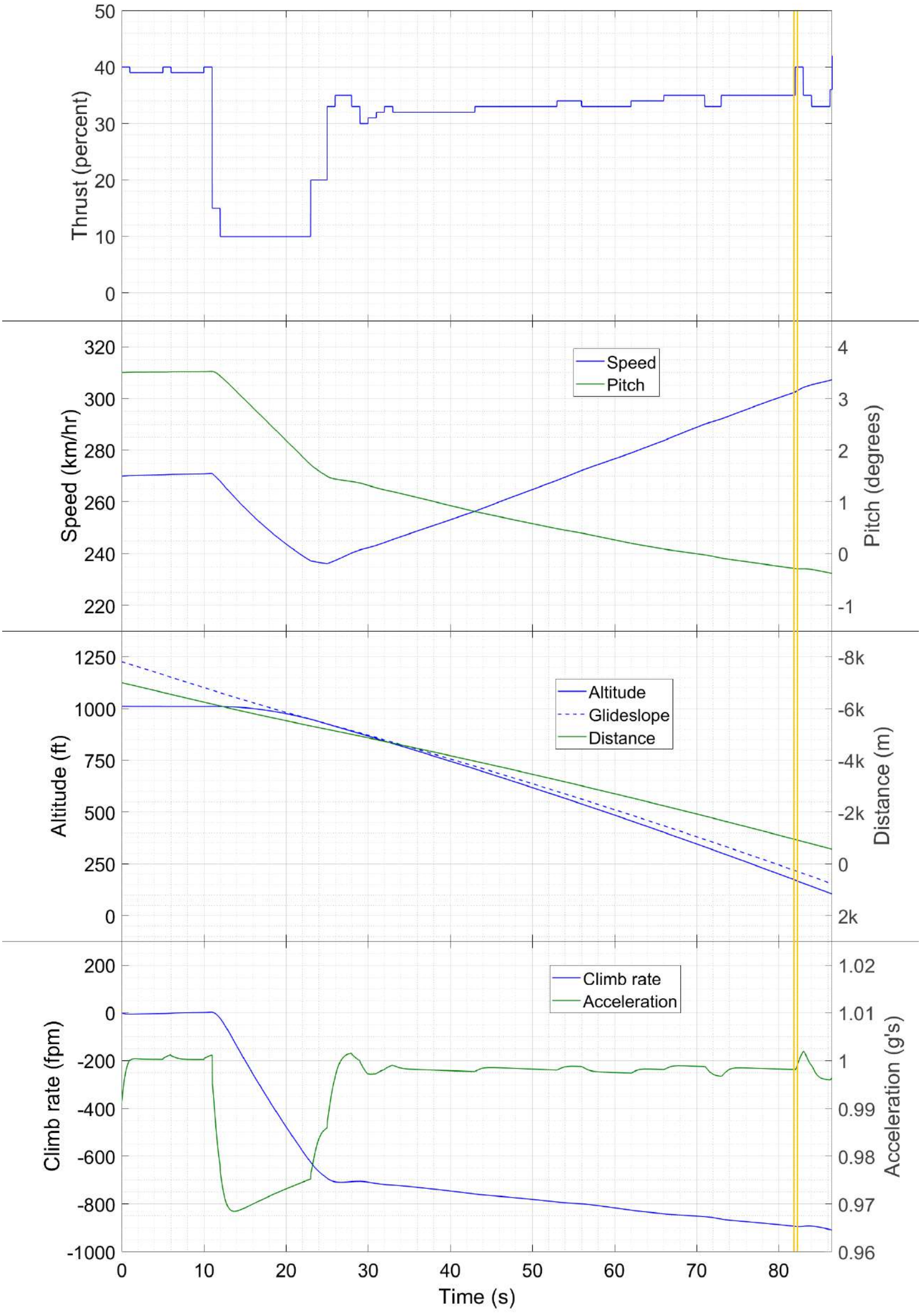


Figure 05 : *Time traces of different variables during the final approach. The symbol “k” denotes thousand.*

In this Figure we can see interception of glideslope at 5280 m behind the airport, followed by a progressive downward deviation upto a point 563 m behind the airport, at an altitude of 104 ft (the significant figures don't come from the graph but the underlying dataset). At this point the pitch is –0·38°, which is about 0·15° below the calculated value. Since the pitch rate during flare is 0·28°/s, I must initiate the flare about half a second before reaching Q; since our speed at this point is about 85 m/s, I have chosen $y = -563$ m* as the point for flare initiation. During the approach, the thrust remains in the 32-35 percent range, consistent with our estimate of 33 percent. The speed, decreasing to 236 km/hr at P, increases almost monotonically to 307 km/hr at the end of the time trace. Pitch and climb rate decrease smoothly throughout the approach, the latter just crossing –900 fpm, consistent with our forced extra-fast descent. The flare must take of this; let's see how good a job it does.

* The exact number gets determined by the discrete character of the simulation cycles. The plane goes forward by approximately 20-25 m per cycle.

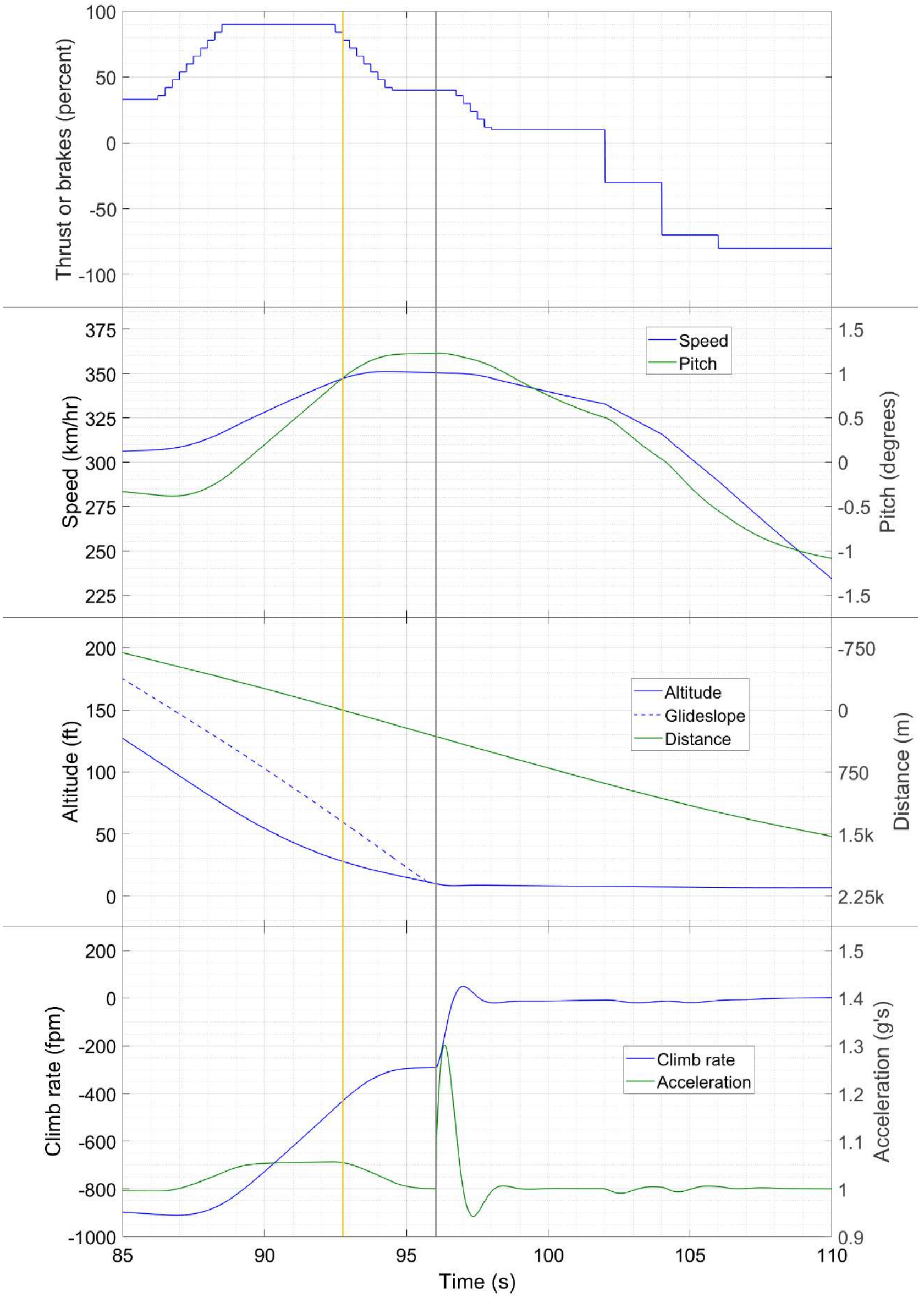


Figure 06 : *Time traces of different variables during flare and touchdown. The symbol “k” denotes thousand.*

I have backed up by 1·5 seconds and started the Figure from 85 s rather than 86·5 s, to achieve a visually smoother transition between approach and flare. At $y = -525$ m, the corresponding z is 97·8 ft, showing that we pass almost exactly through the calculated Q. For the flare we ramp up to 90 percent thrust and hold it for 4 s, initiating the rampdown when the pitch approaches $0{\cdot}9^{o}$. Threshold is cleared at 28 ft, and the plane passes $y = 100$ m at 21 ft, showing almost exact adherence to the point R. The flare at this point however is still a little bit from over; it officially concludes (i.e. we return to 40 percent thrust) at 172 m and 17·5 ft. Touchdown occurs at 324 m forward of threshold at 350 km/hr and 291 fpm – just the landing we'd wanted. After verifying that there's no bounce, I've started the thrust retardation and braking process, and the interesting part of the manoeuvre is over. We reach a cautious speed of 30 km/hr at 2170 m forward of threshold. This fits into all but the shortest runways at major airports (which would not be attempted for a landing in such circumstances anyway).

In summary, the guidelines provided by the calculation have proved to be very effective. Passing through P, Q and R, we have made a highly stabilized approach followed by an on-target, firm touchdown. Thus, our heavy mathematics has enabled the pilot to pull off the one-chance landing on the first try itself. Here is a schematic profile of this feat. For comparison, we show it together with the schematic profile of the normal landing, Figs. 5D–04,05. This time, we show the trajectory as well as Our Plane itself to scale, so that the distances and heights involved become apparent. For visual clarity however, we multiply the pitch by a factor of three for the normal landing and a factor of seven for the landing without elevator.

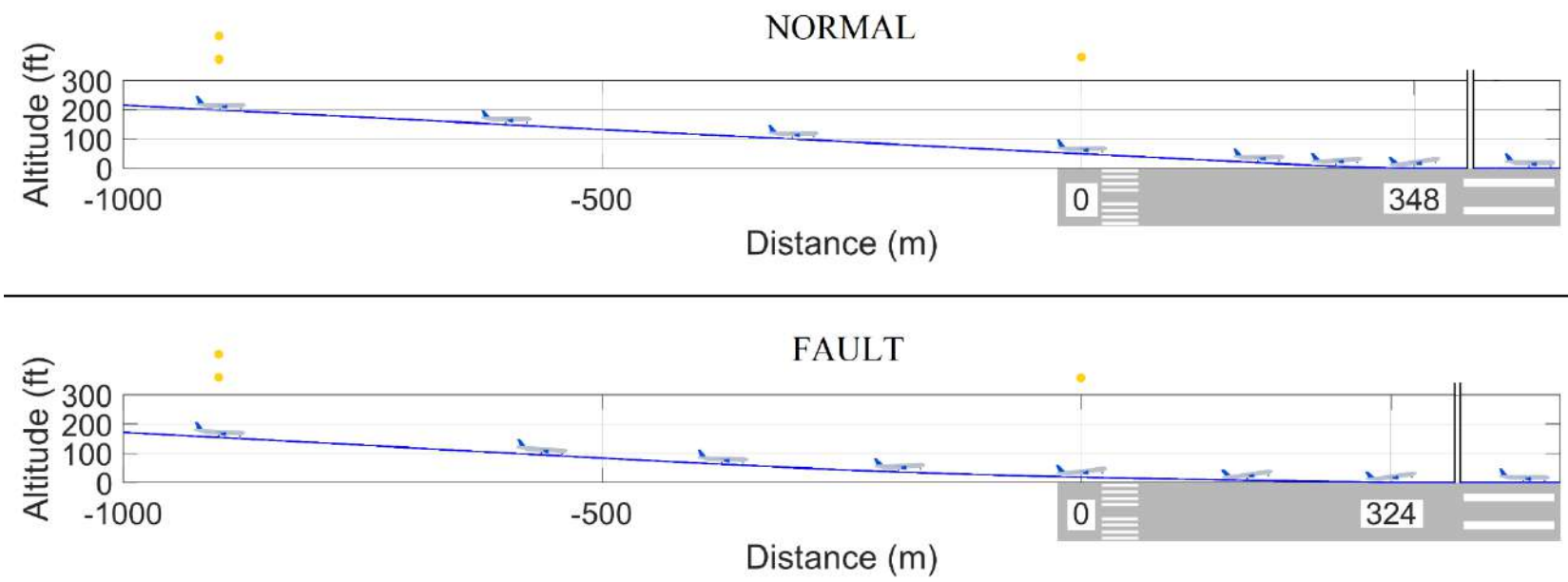


Figure 07 : *Schematic profile of Our Plane during the simulation of landing with (top panel) and without (bottom panel) elevator. The trajectory as well as the aircraft itself are to scale, while the pitch is amplified by a factor of 3 in the top and 7 in the bottom. The double yellow and yellow indicate the inner and the home. We can also see a schematic representation of the runway with threshold and aiming point markings. In the normal landing, flaring begins at the fifth snapshot and continues upto the seventh (touchdown). In the abnormal landing, flaring begins at the second snapshot (Point Q) and ends at the sixth (return to 40 percent thrust), with touchdown occurring at the seventh. A cut in the graph beyond the touchdown indicates a removal of material – the restoration to pitch zero occurs farther forward of the point shown. Inclusion of that part in full scale would further distort the already grotesque aspect ratio of this Figure. On the other hand, not showing a final snapshot at zero pitch would make the Figure look incomplete.*

If the normal greased landing is difficult, then the landing with fault is nightmarish. Just look at the flaring distance in the two cases. One begins on top of the runway and pitches up in a single fluid motion; the other begins more than half a kilometre behind the runway and raises the nose inch by inch upto the moment of reckoning. The regular one can be pulled off by eyesight alone; this special manoeuvre can be achieved only by either miraculous instinct or rigorous analysis.

§65 **Further discussion, accidents and incidents.** The control elements of the aircraft are the engines, elevators, ailerons and rudder. If any one of these is lost in flight, the situation is serious. When the first two elements are involved, the situation becomes very very serious. This is because the engines generate motion, and the elevators operate in the plane where lift is actually produced. In this context only, let's despatch Q07 of the Quiz. The correct answer is Choice B, which we just saw is a hell for the pilot. Choice A is a minor

deviation from routine circumstance – twinjets are designed to fly for extended durations with one engine out, and flight plans must be constructed so as to always remain within this duration of an airport. An engine out just after V_1 during a MTOW takeoff is another matter, especially if we throw some winds into the mix, but Choice A explicitly does NOT refer to this case. Choice C is the equivalent of elevator fault in the yaw plane. Ipso facto the situation becomes less grave since there's no risk of the plane falling out of the sky. It will tend to wibble-wobble in flight, but that can be corrected using asymmetric thrusts from the two engines. The CM will not need to be in a lucky position for asymmetric thrusting to be effective. Finally, Choice D will be harrowing for the passengers, with the oxygen masks coming out and the icy wind rushing in, but the hole will not threaten the integrity of the flight. After an emergency descent and deceleration, the pilots will be able to continue to the nearest airport without difficulty.

For Q14 we need to consider the case where the horizontal stabilizer and elevator are separate. When one is frozen and the other floating, let's look at the various options to see whether they will hold true or not. Choice A is unwanted coupling of speed and pitch. This will definitely occur. To raise the nose, the pilot will have to increase thrust, both to leverage the torque of the engines and to generate more torque from the fixed stabilizer by going above the trimmed speed. Similarly, to lower the nose, he will have to retard thrust. At once, we have a nuisance coupling between speed and pitch. Choice B is low pitch rate. This too was there in our simulation, and the two-piece tail won't change it. The torque of thrust will remain low, and a change in pitch brought about by acceleration or deceleration will also be slow. Choice C is excessive speed near ground. This is where the information about 465 km/hr climb becomes relevant. We would expect the climb to be undertaken with the trim set for a speed of 465 km/hr or thereabouts. With the stabilizer jammed at that position, the plane will tend to seek that speed near the ground as well, just as Our Plane kept gravitating towards the speed corresponding to 40 percent thrust. Even if CM is relocated, a significant reduction of the trimmed speed is highly unlikely. Hence, high speed near ground will be a problem as well, and the correct answer is Choice D.

If an elevator fault does occur, the target airport for the emergency landing will have to be selected carefully. Among the essential requirements are long runway, dry runway, no wind or steady headwind and visual meteorological conditions. Strongly desirable are maximum category ILS*, professional and cooperative ATC who are trained to deal with these kinds of situations, and highest grade firefighting and emergency medical services in the event that those are required. For this reason, once steady flight without the elevator is established, a better airport farther away might prove a superior diversion point to one which is closer but has less facilities.

* VMC will enable the pilot to sight the runway from afar and aim for it. ILS will guide him towards it in a different way. The more aids the pilot has for this approach, the better it will be.

On the simulator, I personally found that V_z/V was the easiest metric to use for stabilizing the approach. With thrust controlling speed and elevation both, the approach is not at all an easy one to fly. During earlier attempts on the approach, I had not incorporated V_z/V but instead tried to synchronize the horizontal and vertical displacements, or the speed and the pitch. In both cases, it needed a lot of tries before the plane passed satisfactorily close to Q. Even then, the approach was somewhat messy with the descent rate showing some fluctuations rather than a smooth increase. After introducing V_z/V however, I got the approach you see here on only the second try. This further indicates the utility of this quantity as an approach-stabilizing parameter.

Elevator fault has occurred a number of times in air transport in the past 50 years, with varying results. On 12 August 1985, Japan Airlines (JAL) Flight 123, a Boeing 747 flying from Tokyo (Japan) to Osaka (Japan), experienced a catastrophic failure of the aft pressure bulkhead. The explosive decompression resulted in severance of all hydraulic lines to the control surfaces, as a result of which the elevators, stabilizer trim, ailerons and rudder were lost. In addition, the vertical stabilizer was shorn off the fuselage. Working the four engines independently of each other, the crew were able to keep the aircraft aloft for 32 minutes following the loss of control. Ultimately however, their efforts proved to be in vain and JAL 123 became the deadliest single-aircraft accident* in aviation history. Fifteen years later, on 31

January 2000, Alaska Airlines (ASA) Flight 261, a McDonnell Douglas MD-83 from Puerto Vallarta (Mexico) to San Francisco (USA), suffered a partial jam, then a total jam and finally a shearing off of its horizontal stabilizer. The CM was far forward of CP and the aircraft entered an uncontrolled dive, crashing into the sea. Just fifteen days after this, on 16 February 2000, Emery Worldwide Airlines Flight 17, a Douglas DC-8 from Reno (USA) to Dayton (USA), lost mobility of the starboard elevator and crashed immediately after takeoff. The flight was carrying cargo and not passengers; the crew were killed.

* Collisions between two aircraft have resulted in higher-fatality aviation accidents, the historical worst being the crash of two Boeing 747s on the runway at Tenerife Airport, Spain on 27 March 1977.

On 19 July 1989, United Airlines (UAL) Flight 232, a McDonnell Douglas DC-10 from Stapleton (USA) to Chicago (USA), experienced an uncontained failure (explosion) of the tail-mounted engine no. 2*. All hydraulic lines were severed, leading to inoperability of elevators, stabilizer trim, ailerons and rudder. Despite the heavily compromised aircraft, the crew achieved a measure of control using the remaining two engines alone, ultimately making an approach towards Runway 22 of Sioux City at 410 km/hr. At the last moment however, the plane banked heavily to starboard and crashed onto the runway. 112 people died while 184 survived, including the three flight crew. Despite the fatalities, UAL 232 is generally considered a success story of airmanship and crew resource management. The catastrophic malfunction was expected to result in everyone on board being killed, and only the crew's excellent performance resulted in so many survivals. It says much for the flying ethics of the crew that they themselves viewed the flight as a failure, on account of the lives that were lost.

* As we've seen in §43, the DC-10 has three engines.

On 12 April 1977, Delta Airlines (DAL) Flight 1080 from San Diego to Los Angeles (USA), a Lockheed L-1011 Tristar, suffered a jam of its port elevator at maximal negative deflection (full nose-up torque) shortly after takeoff. While the starboard elevator and horizontal stabilizers were unable to counter the pitch-up torque, the pilots managed to harness the differential between the wing- and tail-mounted engines to generate a negative pitching moment. Moreover, they shifted the passengers as far forward as possible to move the CM forward and get the maximum negative torque from the wing lift. These measures paid off and DAL 1080 flew to Los Angeles (deemed the most suitable airport for the emergency landing) for a stable approach followed by a safe landing. The captain's recollection of the incident [02] makes for illuminating reading – having read this Article, you not only can understand everything he did but might also do a couple of things differently if faced with the situation in the cockpit. For one, you will probably be faster at initiating thrust-based pitch control, and for another, you will likely extend flaps and undercarriage prior to beginning the final approach instead of being surprised by the changed handling characteristics midway. One wonders if the passenger relocation technique might also have worked on the ill-starred ASA 261. On 22 November 2003, a DHL cargo flight from Baghdad (Iraq) to Muharraq (Bahrain), an Airbus A300, was hit by a surface to air missile. All hydraulic lines were severed, resulting in loss of elevators, ailerons and rudder. In a first of its kind incident, the crew were able to steer the crippled plane back to Baghdad and perform an approach and safe landing. Excellent airmanship, both in flying technique and crew resource management, as well as nerves of steel are the primary components of all these success stories. For future incidents of this nature, may they be rarest of rare, let's hope we've added one more element to the success mixture – mathematical calculation.

K. CHAPTER CONCLUSION

§66 **Concluding remarks to Chapter 5.** This was of course the most consequential Chapter in the entire Article, the one in which force and moment balances prised open the gateway to the skies. Mathematical equations held a light to the stuff involved in manoeuvres from takeoff to touchdown and all the soaring, wheeling, swooping and loop-the-looping which come in between. Free body diagrams showed us how to recover from a vertical dive and matched boundary conditions enabled us to thread a trajectory from level to slope

and slope to runway. From the broadest overview to the finest detail, our model has told us all we need to know about aircraft and their dynamics.

Did I say, all ? No ! Motions on a sheet of paper cannot account for everything. Just for a mere turn we had to resort to an artifice. And then there are single-engine operation, stall spin and recovery, barrel roll, crosswind landing and a dozen other manoeuvres which we can't even begin to describe unless we embrace all of space. Let these be the rewards that motivate us to undertake the study of flight dynamics in three dimensions as soon as the time is right.

---- o ----

6

CONCLUSION AND FUTURE DIRECTIONS

As in Chapter 1, in this Chapter we use the first person plural to denote the authors as a group. This style is more conducive for the content at hand.

§67 **Summary of contributions.** Flight dynamics and control is an ancient subject, the problem having been created and solved when the first archaeopteryx took to the air. Manmade applications of flight dynamics also have a long history, beginning when cavemen ensured that arrows remained oriented along their direction of travel at all times by adding feathers to the back of the shaft (doubtless the feathers would have been called "stabilizers" if that word had been around then). Nevertheless, human aviation is quite a recent subject, and academic flight dynamics even more so – the vast majority of work on this subject dates from the past 50 years. This Literature contains a gap between the design and operational aspects of the subject, and we have tried to bridge this gap using our explicit nonlinear model. In terms of the top down and bottom up classification of §01, our treatment is top down in two pieces, in the sense that we start with the equations and derive everything from those, but do so separately in two and three spatial dimensions.

Although we have derived the equations of motion in the pitch, yaw and banking planes, the first one is by far the most significant since the motions there are standalone. The elements which enable our model to be closed-form are the adoption of a particular theory of lift and drag, and the detailed treatment of the forces on the elevator. The stability analysis with short period and phugoid modes establishes quantitative agreement between the new model and the existing models. Thereafter, the characteristic curves and the extensive flight simulations generate mathematical insight into aspects of flying hitherto explored only qualitatively. As we have mentioned in §05, our equations of motion [(3B–21,22) and their generalizations for stall and wind] are applicable to a fixed wing aircraft with conventional geometry (wings and tail). Equations for aircraft having unconventional geometries, such as those of Concorde, certain military aircraft and fixed wing drones, can also be written following the same modeling principles.

Our primary research contribution is a rigorous dynamical understanding of the motions of a passenger airliner with a human pilot during typical flight phases as well as in control emergencies. We hope that this understanding will have a beneficial impact on pilot training and hence improve aviation safety. Accidents and incidents which can be averted by good airmanship are rare at the ATPL level but become progressively more common at the CPL and PPL levels. A knock-on contribution is our use of the aircraft's characteristic curves for manoeuvre planning, and our proposal of new cockpit instruments to display the velocity ratio and indicate glideslope deviation as a distance rather than an angle. We have also proposed an alternative control law between stick and tail for a fly-by-wire aircraft, which we feel may be more intuitive than either of the existing laws. Our secondary research contribution is the statement of closed-form nonlinear equations of motion, which can lead to fixed wing aircraft becoming an archetypal system in nonlinear science. Its dynamics and bifurcations are quite different from those of canonical models like Duffing, van der Pol and related mechanical or electrical oscillators, chemical reaction systems, multi-body gravitating systems and other setups commonly studied in this field. The reason for its not getting attention in this community appears to be the absence of an equation of motion which can be written down without invoking a data table. A tertiary research contribution is the DDE-based mathematical model of pilot-induced oscillations – incorporation of delay into aircraft dynamics, though not without precedent (see for example Ref. [01]), is rare in the Literature.

From the educational viewpoint, our primary contribution is an overhaul of the subject of flight dynamics as it appears in the university curriculum. A course on this topic often seems to introduce a

considerable amount of mathematics without giving the students an idea of the motions which the equations describe, or teaching them how to use the maths to actually fly an aircraft. Indeed, an isolated handful of students who had excelled in flight dynamics courses at premier universities were tested on the Quiz and found wanting. A recent freshers' welcome event at the University of Maryland featured a contest where incoming graduate students of aerospace engineering were shown a picture of an airplane and asked to label its parts – many students made incomplete or incorrect identifications. With our new, straight-in approach to flight dynamics, we hope to impart to our students a broad as well as deep understanding of aircraft and their behaviour. Our absence of specialized prerequisites makes this content appropriate for an elective course for which almost any science or engineering major can register; at the same time, the level of detail and rigour will prepare the most specialized student of aircraft dynamics for a career in research or in industry. Our secondary pedagogical contribution is again the statement of explicit nonlinear equations of motion, which can be incorporated into the curriculum and evaluations of a typical course on dynamical systems or nonlinear oscillations.

§68 **Future directions.** Let us now look at the future possibilities with our work. The need to write the three-dimensional sequel is by now obvious, and we won't spend more time on it except to say that it will be done as and when we have available the requisite time, manpower and computing power. Rather, in this Section we will address the limitations of the model in its present form and discuss some future directions while staying within the two-dimensional framework. We focus only on the pitch plane equations since the models in the other two planes possess very obvious shortcomings.

In the below Table, we give all the assumptions which have been made, both in model derivation and in simulations, and the expected consequences of making or relaxing them.

Assumption	**Consequence**
Modified Newtonian theory of lift used.	The aerodynamic force is given by (3A–05) or (3A–07). With a different theory, the expressions may change to include lower powers of U, higher order trigonometric functions of α etc. These changes will be small since (3A–05) or (3A–07) are known to show good agreement with experiments. A significant limitation of the modified Newtonian theory is that it is not expected to yield a realistic picture of the airflow behind the aircraft. However, that is not a quantity of interest while studying the dynamics of a single aircraft (as against say the dynamics of formation flying).
The parameter ε in (3A–07) set to unity while deriving (3B–22).	With nonzero ε, we will get a different L/D and hence the location and value of minima in characteristic curves will be different. There will be no qualitative change in aircraft behaviour.
The camber γ in (3A–07) set to zero while deriving (3B–22).	The behaviour of a camberless wing at angle of attack α will equal that of a cambered wing at angle of attack $\alpha-\gamma$. Hence, camber will cause a shift of characteristic curves with respect to α.
Horizontal stabilizer plus elevator replaced by stabilator.	With a two-piece tail, (3B–21) will have to be replaced by two similar equations, one for each piece. The total $\bar{f}_p$ will be given by the sum of the

	two forces. We have discussed in detail the implications of this, throughout the Article.
Elevator downwash, i.e. effect on the tail of downward airflow aft of wings, neglected.	Downwash will cause a change in the effective angle of elevation of the tail, replacing η in (3B–21) by some η'.
Pitch rate terms excluded while proceeding from (3B–06) to (3B–07) and from (3B–09) to (3B–10).	There will be a correction to wing lift and tail pitch θ_E if pitch rate terms are included. Since $\omega d_{1,2} << V_{y,z}$ the corrections will be small.
Changes in location of CP of wings and tail with change in V and α neglected.	$\bar{d_1}$ and $\bar{d_2}$ in (3B–22) will become functions of V and α instead of constants.
An ad hoc parameter Γ assumed for rotational drag instead of accounting for variations with V, α and other parameters.	Time constant for damping of rotational motions as well as overdamped pitch rate for given $\bar{f_p}$ may vary between different flight phases.
Fixed maximum of 100 percent thrust assumed instead of relating thrust to N1, EPR or other significant parameter.	At higher speeds, the maximum thrust available might not be the TOGA rating of the engine, requiring rescaling of thrust in simulations.
A simple model (5B–01,02) used for ground reactions.	A more realistic model will yield more accurate estimates of g's pulled during touchdown, time to spoiler activation to prevent wheel shimmy, pitch rate on the ground after touchdown, etc. It will also enable more accurate calculation of tail clearance and V_{mu} during takeoff.
Undercarriage drag neglected during takeoff run.	With the drag included, the acceleration will be slower and the run longer.
Ground effect neglected.	With ground effect included, there will be less induced drag when the aircraft is close to the ground, requiring lower thrust settings during flare and touchdown.

Table 01 : *List of assumptions made in the pitch plane equations of motion, together with the consequences of making or relaxing them.*

As you can see, the list is long but the effect in each case is a detail – shift of characteristic curves, insertion of additional dependences in the equations etc. None of these assumptions threatens the integrity of the fundamental equations (3B–22) and of the discussion which follows from these equations. Since Our Plane is a fictitious aircraft anyway, the numerical details are currently irrelevant. They *will* become relevant when attempting to write the model equations for specific aircraft such as Airbus A320 and Boeing 777. This is a concrete future work associated with the present Article. When embarking on this study, one will first have to address as many of the assumptions from Table 01 as are necessary, and only then set about the task of determining the best fit parameter values from experimental results.

Upgrades to the peripheral aspects of the flight simulator will also be welcome. Currently, even though the core of the simulator – i.e. the equations, the numerical integration routine, the plotter etc. – is cutting-edge, the user interface is rather basic, as you can see from Fig. 5A–01. It will be nice to get a version of the simulator which is operated more like a computer game, using various keys to increment and decrement thrust and elevator force, extend and retract flaps and so on. A version where pitch and

bank are controlled by a joystick, as in Airbus aircraft, will be especially desirable. A ‘gamified’ form of the simulator, using real aircraft models as in the last paragraph and this Article as the training manual, should be as educative as it will be entertaining. Currently, our simulator is written in Matlab, a proprietary software, since that is the only computer language in which we have the requisite proficiency. Translation into an open-source language will enable it to be more freely accessible, and we eagerly welcome such an effort.

There are some calculations which we have deliberately left out in this Article despite being within the scope of the model. These pertain to maximizing range, endurance, climb performance etc, and require us to factor in the variation of air density with altitude. For instance, we can use the suitably modified (3B–22) to find the altitude as a function of distance on an extended flight which yields the maximum range for a given fuel load. The answer should work out to a flight path which continuously climbs as it burns fuel. You will observe (if you do not know already) that long-haul flights typically start off at a lower altitude and every few hours add on 2000 ft, finishing at a higher altitude. This is called step climb; it achieves the objective of increasing height with distance while remaining within the RVSM constraints. Concorde, which flew above all other traffic and hence was free of these constraints, climbed continuously during cruise. Similar considerations can yield the trajectory which the aircraft should follow from flaps retraction at a given altitude and speed to cruising altitude and speed, so as to perform the climb while achieving different objectives such as minimizing fuel, minimizing time to altitude or maximizing average horizontal speed during climb. We have excluded these from the Article as we wanted to focus only on short-duration manoeuvres and their dynamics. When adapting the Article to a university course on flight dynamics however, these supplementations may be desirable.

Currently, the stability analysis of Chapter 4 is quite basic. We have identified the modes of motion and their stabilities, but have neither constructed their analytical approximations [1O–19-21] nor related the eigenvalues to the various parameters in the model. With a heavily nonlinear equation like (3B–22) and a large set of parameters, the aircraft will surely have a rich bifuraction structure. Analysis of this structure should be a rewarding exercise in nonlinear science, with potential utility to aircraft designers as well.

The focus in this Article is on passenger aircraft with human pilots. It won’t take much effort to adapt our simulator to describe an autopilot and hence use our model for the design, testing and validation of autopilots. Nowadays, completely autonomous aircraft i.e. UAV are all the rage, and represent a growing field of research and development. Drone pilots are a new class of professional, whose number is expected to increase rapidly over the coming years. A nonlinear equation of motion should be of signal assistance in modeling the dynamics of these vehicles, programming their flight paths and intervening manually in the event of a problem. In Subdivision 5J we saw one example of a non-trivial path-planning problem for Our Plane; similar considerations should apply to the path-planning of autonomous flight vehicles as well.

§69 **Conclusion.** We’ve said all we wanted to say, so we’ll keep this brief. By now you (should) have an excellent idea of what makes an aircraft go. You also know what more can be done with our model and simulator. We cordially invite you to try your hand at it, and let us know if you do. And of course, we will be more than happy to get your feedbacks on our Article, whether positive or negative. We’ll make periodic updates in response to the suggestions we receive from you. Finally, whether you are a passenger or a pilot, we hope that reading our Article will make your next flight more enjoyable. If it does, then writing it has been worth the effort.

---- o ---- o ---- o ---- ---- o ---- o ---- o ----

ANSWERS TO THE QUIZ QUESTIONS

Q01 – C
Q02 – A
Q03 – A
Q04 – C
Q05 – D
Q06 – B
Q07 – B
Q08 – D
Q09 – B
Q10 – B
Q11 – C
Q12 – D
Q13 – B
Q14 – D
Q15 – B
Q16 – D
Q17 – B
Q18 – C
Q19 – B
Q20 – A

REFERENCES

In most cases we give the first and last names of all the authors, with exceptions if the information is not fully available or a different nomenclature style is commensurate with the authors' cultural or personal preferences.

[1O–01] GEORGE BRYAN, "*Stability in Aviation*", Macmillan, London, UK (1911)

[1O–02] BERNARD ETKIN, "*Dynamics of Atmospheric Flight*", Second Edition, Dover Publications, New York City, USA (1971)

[1O–03] DUANE MCRUER, IRVING ASHKENAS and DUNSTAN GRAHAM, "*Aircraft Dynamics and Automatic Control*", Princeton University Press, Princeton, USA (1971)

[1O–04] HOLT ASHLEY, "*Engineering Analysis of Flight Vehicles*", Addison Wesley, Reading, USA (1974)

[1O–05] ROBERT NELSON, "*Flight Stability and Automatic Control*", Second Edition, McGraw Hill, New York City, USA (1998)

[1O–06] ROBERT STENGEL, "*Flight Dynamics*", Princeton University Press, Princeton, USA (2004)

[1O–07] JONATHAN HOW, "*Aircraft Stability and Control*", MIT OpenCourseWare (2004). Available at https://ocw.mit.edu/courses/16-333-aircraft-stability-and-control-fall-2004/

[1O–08] MICHAEL COOK, "*Flight Dynamics Principles*", Second Edition, Elsevier, Amsterdam, Netherlands (2007)

[1O–09] DAVID CAUGHEY, "*Introduction to Aircraft Stability and Control*", ebook (2011). Available at https://courses.cit.cornell.edu/mae5070/Caughey_2011_04.pdf

[1O–10] DANIEL DOMMASCH, SYDNEY SHERBY and THOMAS CONNOLLY, "*Airplane Aerodynamics*", Fourth Edition, Pitman, New York City, USA (1967)

[1O–11] L J CLANCY, "*Aerodynamics*", Pitman, London, UK (1975)

[1O–12] BARNES MCCORMICK, "*Aerodynamics, Aeronautics and Flight Mechanics*", Wiley Interscience, New York City, USA (1979)

[1O–13] JOHN ANDERSON, "*Introduction to Flight*", Third Edition, McGraw Hill, New York City, USA (1989)

[1O–14] RICHARD SHEVELL, "*Fundamentals of Flight*", Second Edition, Prentice Hall, Hoboken, USA (1989)

[1O–15] W N HUBIN, "*The Science of Flight : Pilot-oriented Aerodynamics*", Iowa State University Press, Ames, USA (1992)

[1O–16] G J HANCOCK, "*An Introduction to the Flight Dynamics of Rigid Aeroplanes*", Ellis Horwood, Hertfordshire, UK (1995)

[1O–17] BANDU PAMADI, "*Performance, Stability, Dynamics and Control of Airplanes*", AIAA, Reston, USA (1998)

[1O–18] WARREN PHILLIPS, "*Mechanics of Flight*", Wiley, Hoboken, USA (2004)

[1O–19] NANDAN SINHA and N ANANTHKRISHNAN, "*Elementary Flight Dynamics with an Introduction to Bifuraction and Continuation Methods*", CRC Press, Boca Raton, USA (2014)

[1O–20] NANDAN SINHA and N ANANTHKRISHNAN, "*Advanced Flight Dynamics with Elements of Flight Control*", CRC Press, Boca Raton, USA (2017)

[1O–21] N ANANTHKRISHNAN and S UNNIKRISHNAN, "Literal approximations to aircraft dynamic modes", **AIAA Journal of Guidance, Control and Dynamics** 24 (6), 1196-1203 (2001)

[1O–22] WOLFGANG LANGEWIESCHE, "*Stick and Rudder*", McGraw Hill, New York City, USA (1944)

[1O–23] HARRY HURT, "*Aerodynamics for Naval Aviators*", US Naval Air Systems Command, Washington DC, USA (1959)

[1O–24] CHARLES DOLE, "*Flight Theory and Aerodynamics*", Wiley, New York City, USA (1981)

[1O–25] PAUL CRAIG, "*Stalls and Spins*", Tab Books, Blue Ridge Summit, USA (1993)

[1O–26] CHRIS CARPENTER, "*Flightwise*", Airlife Publishing, Shrewsbury, UK (1996)

[1O–27] R H BARNARD and D R PHILPOTT, “*Aircraft Flight*”, Fourth Edition, Pearson, Upper Saddle River, USA (2010)

[1O–28] CAE Oxford Aviation Academy, “*Principles of Flight*”, KHL Printing Company, Singapore (2014)

[1O–29] JOHN WATKINSON, “*The Art of Flight*”, AIAA Publishing, Reston, USA (2016)

[1O–30] NASA Glenn Research Center, “*Beginner’s Guide to Aeronautics*”, online (2023). Available at https://www1.grc.nasa.gov/beginners-guide-to-aeronautics/

[1O–31] F B J MACMILLEN, “Nonlinear flight dynamics analysis”, **Philosophical Transactions of the Royal Society A** 356 (1745), 2167-2180 (1998)

[1O–32] PHILIPPE GUICHETEAU, “Bifurcation theory : a tool for nonlinear flight dynamics”, **Philosophical Transactions of the Royal Society A** 356 (1745), 2181-2201(1998)

[1O–33] YOGI PATEL and DARREN LITTLEBOY, “Piloted simulation tools for aircraft departure analysis”, **Philosophical Transactions of the Royal Society A** 356 (1745), 2203-2221 (1998)

[1O–34] CRAIG JAHNKE, “On the Roll-coupling instabilities of high-performance aircraft”, **Philosophical Transactions of the Royal Society A** 356 (1745), 2223-2239 (1998)

[1O–35] MARK LOWENBERG and ALAN CHAMPNEYS, “Shilnikov homoclinic dynamics and escape from roll autorotation in an F4 model”, **Philosophical Transactions of the Royal Society A** 356 (1745), 2241-2256 (1998)

[1O–36] BRAD LIEBST, “The Dynamics, prediction and control of wing rock in a high-performance aircraft”, **Philosophical Transactions of the Royal Society A** 356 (1745), 2257-2276 (1998)

[1O–37] M G GOMAN and A V KRAMTSOVSKY, “Application of continuation and bifuraction methods to the design of control systems”, **Philosophical Transactions of the Royal Society A** 356 (1745), 2277-2295 (1998)

[1O–38] MARK LOWENBERG, “Bifurcation analysis of multiple-attractor flight dynamics”, **Philosophical Transactions of the Royal Society A** 356 (1745), 2297-2319 (1998)

[1O–39] F B J MACMILLEN and MICHAEL THOMPSON, “Bifurcation analysis in the flight dynamics design process – a view from the aircraft industry”, **Philosophical Transactions of the Royal Society A** 356 (1745), 2321-2333 (1998)

[1O–40] CRAIG JAHNKE, “*Application of dynamical systems theory to nonlinear aircraft dynamics*”, Doctoral thesis, California Institute of Technology, Pasadena, USA (1990)

[1O–41] UMBERTO SAETTI and JOSEPH HORN, “Flight simulation and control using the Julia language”, **AIAA Scitech Forum 2022**

[1O–42] DANIEL KLEPPNER and ROBERT KOLENKOW, “*An Introduction to Mechanics*”, McGraw Hill, New York City, USA (1973)

[1O–43] DAVID MORIN, “*Introductory Classical Mechanics with Problems and Solutions*”, Cambridge University Press, Cambridge, UK (2005)

[1O–44] JOHN TAYLOR, “*Classical Mechanics*”, University Science Books, USA (2005)

[1O–45] B SHAYAK, “*Differential Equations – Linear Theory and Applications*”, ebook (2020). Available at www.shayak2.in/Shayakpapers/DELTA/DELTA.pdf

[1O–46] WILLIAM BOYCE and RICHARD DIPRIMA, “*Elementary Differential Equations and Boundary Value Problems*”, Tenth Edition, Wiley, Hoboken, USA (2012)

[1O–47] HENRY EDWARDS and DAVID PENNEY, “*Differential Equations and Boundary Value Problems*”, Fifth Edition, Pearson, Upper Saddle River, USA (2015)

[1O–48] Sir BRIAN PIPPARD, “*The Physics of Vibration*”, Cambridge University Press, Cambridge, UK (1989)

[2A–01] Photograph by JOERG MANGELSEN, taken from www.pexels.com

[2A–02] VINCENZO MADONNA, PAOLO GIANGRANDE and MICHAEL GALEA, “Electrical power generation in aircraft : review, challenges and opportunities”, **IEEE Transactions on Transportation Electrification** 4 (3), 646-659 (2018)

[2A–03] www.wikipedia.org/

[2A–04] International Civil Aviation Organization, “*Units of Measurement to be Used in Air and Ground Operations*”, Annexe 5 to the Convention on International Civil Aviation (2010)

[2A–05] European Aviation Safety Agency, Type Certificate Data Sheets (2023). Available at https://www.easa.europa.eu/en/document-library/type-certificates

[2A–06] https://i.imgur.com/CcsquvM.jpg

[2A–07] https://swarajyamag.com/news-brief/at-15-per-cent-share-of-women-pilots-in-india-significantly-higher-than-international-average-of-5-per-cent-govt

[2A–08] https://www.iea.org/data-and-statistics/charts/ghg-intensity-of-passenger-transport-modes-2019

[2B–01] https://skybrary.aero/articles/aerodrome-traffic-circuit

[2B–02] https://skyvector.com/

[3A–01] HERBERT GOLDSTEIN, "*Classical Mechanics*", Third Edition, Addison Wesley, Reading, USA (2002)

[3A–02] DONALD GREENWOOD, "*Principles of Dynamics*", Prentice Hall, Hoboken, USA (1988)

[3A–03] R KRISHNAN, "*Electric Motor Drives – Modeling, Analysis and Control*", PHI Learning Private Limited, New Delhi, India (2010)

[3A–04] LEV DAVIDOVICH LANDAU and EVGENY MIKHAILOVICH LIFSHITZ, "*Fluid Mechanics*", Second Edition, Pergammon Press, Oxford, UK (1984)

[3A–05] PIJUSH KUNDU and IRA COHEN, "*Fluid Mechanics*", Second Edition, Academic Press, San Diego, USA (2002)

[3A–06] CLAES JOHNSON, "Kutta-Zhukovsky lift theory", online. Available at https://secretofflight.wordpress.com/kutta-zhukovsky/

[3A–07] GEORGE BATCHELOR, "*An Introduction to Fluid Dynamics*", Cambridge University Press, Cambridge, UK (1967)

[3A–08] ED REGIS, "No one can explain why planes stay in the air", **Scientific American** (2020). Available at https://www.scientificamerican.com/article/no-one-can-explain-why-planes-stay-in-the-air/

[3A–09] CODY GONZALEZ and HAITHEM TAHA, "A Variational theory of lift", **Journal of Fluid Mechanics** 941, #A58 (2022)

[3A–10] TIANSHU LIU, "Can lift be generated in a steady inviscid flow ?" **Advances in Aerodynamics** 5, #6 (2023)

[3A–11] ROBERT SHELDAHL and PAUL KLIMAS, "Aerodynamic characteristics of seven symmetrical airfoil sections through 180-degree angle of attack for use in aerodynamic analysis of vertical axis wind turbines", **Sandia National Laboratories Technical Report** #SAND80-2114 (1981)

[3D–01] JON KLEINBERG and EVA TARDOS, "*Algorithm Design*", Pearson, Upper Saddle River, USA (2005)

[4O–01] FREDERICK LANCHESTER, "*Aerodonetics*", Archibald Constable, London, UK (1908)

[4O–02] ROD DRIVER, "*Ordinary and Delay Differential Equations*", Springer Verlag, Heidelberg, Germany (1976)

[4O–03] RICHARD RAND, "*Lecture Notes on Nonlinear Vibrations*", ebook (2012). Available at https://ecommons.cornell.edu/handle/1813/28989

[4O–04] https://skybrary.aero/articles/pilot-induced-oscillation

[4O–05] https://engineering.purdue.edu/~propulsi/propulsion/jets/tfans.html

[4O–06] http://large.stanford.edu/courses/2011/ph240/nguyen1/docs/cfm-technical-data.pdf

[4O–07] https://safetyfirst.airbus.com/control-your-speed-during-climb/#:~:text=For%20example%2C%20an%20A320%20at,the%20Flaps%20Auto%2Dretraction%20speed.

[4O–08] https://www.pprune.org/archive/index.php/t-467918.html#:~:text=The%20B777%2D300ER%20at%20MTOW,KIAS%20for%20heavy%20weight%20Takeoffs.

[5B–01] Airbus Industries, "*Flight Operations Briefing Notes*", online (2004). Available at https://skybrary.aero/sites/default/files/bookshelf/493.pdf

[5B–02] https://www.wikipedia.org/

[5B–03] https://www.skybrary.aero/

[5B–04] https://avherald.com/

[5B–05] www.flightradar24.com/

[5C–01] https://en.wikipedia.org/wiki/Immelmann_turn#/media/File:Immelmann_turn.svg

[5D–01] https://www.aerotime.aero/articles/24376-is-a-smooth-landing-the-measure-of-a-good-pilot

[5D–02] https://www.travelinsightpedia.com/why-smooth-landings-are-worse-than-hard-ones

[5D–03] https://blog.boomsupersonic.com/is-a-smooth-airplane-touchdown-always-a-safe-landing-ccb65b54b718#:~:text=A%20soft%2C%20smooth%20landing%20is,of%20learning%20how%20to%20fly.

[5D–04] https://www.travelagentcentral.com/transportation/a-smooth-landing-test-a-good-pilot-and-should-we-clap-upon-touchdown

[5D–05] https://thepointsguy.com/news/hard-airplane-landings/

[5D–06] https://aviation.stackexchange.com/questions/47422/what-is-the-typical-touchdown-vertical-speed-of-a-large-airliner

[5D–07] RAIMUND GEUTER, SANDEEP GUPTA, THOMAS LEPAGNOT and MARC LE-LOUER, “A Focus on the Landing Flare”, online (2020). Available at https://safetyfirst.airbus.com/a-focus-on-the-landing-flare/

[5D–08] https://www.skybrary.aero/articles/approach-and-landing-accidents-ala

[5D–09] JAMES ALBRIGHT, “Landing Flare”, online (2020). Available at https://code7700.com/landing_flare.htm

[5D–10] DOMINIK NIEDERMEIER and ANTHONY ALBREGTS, “Fly-by-wire augmented manual control – basic design considerations”, **28th International Congress of the Aeronautical Sciences** (2012)

[5D–11] https://www.quora.com/How-do-pilots-achieve-smooth-landing

[5D–12] https://pilotworkshop.com/tips/landing_airplane_safely/

[5D–13] CATHERINE CAVAGNARO, “Technique : Landing Like a Pro”, online (2020). Available at https://www.aopa.org/news-and-media/all-news/2020/april/pilot/technique-landing-like-a-pro

[5F–01] https://commons.wikimedia.org/wiki/File:Bombardier_Dash_8-Q402NextGen,_SpiceJet_JP7322500.jpg

[5F–02] https://onemileatatime.com/southern-air-777-stall-takeoff-jfk/

[5F–03] https://chessintheair.com/tow-plane-flies-too-slow-glider-heavy-with-water-ballast/

[5F–04] https://chessintheair.com/invisible-microburst-kills-expert-glider-pilot/

[5H–01] https://en.wikipedia.org/wiki/Cobra_maneuver

[5H–02] TOM COOPER, “The Unknown Story of the Syrian MiG-21 Pilot who Developed the Cobra Manoeuvre: i.e. Pugachev Wasn’t the First to Perform the Cobra”, online (2019). Available at https://theaviationgeekclub.com/the-unknown-story-of-the-syrian-mig-21-pilot-who-developed-the-cobra-manoeuvre-i-e-pugachev-wasnt-the-first-to-perform-the-cobra/

[5H–03] https://migflug.com/jetflights/the-incredible-pugachevs-cobra-maneuvre/

[5H–04] https://en.wikipedia.org/wiki/Cobra_maneuver#/media/File:Pugachev_Cobra.svg

[5J–01] Unit N^{o}. 15 of Ref. [1O–45]

[5J–02] JACK MCMAHON, “Flight 1080”, **Airline Pilot**, 182-186 (1978)

[6O–01] TIBERIUS HACKER, “Flight Stability and Control”, American Elsevier Publishing Company, New York City, USA (1970)